



HAL
open science

Study of iron-sulfur cluster biogenesis in environmental and metabolic stress conditions

Soufyan Fakroun

► **To cite this version:**

Soufyan Fakroun. Study of iron-sulfur cluster biogenesis in environmental and metabolic stress conditions. Microbiology and Parasitology. Université Paris Cité, 2023. English. NNT : 2023UNIP5059 . tel-04914252

HAL Id: tel-04914252

<https://theses.hal.science/tel-04914252v1>

Submitted on 27 Jan 2025

HAL is a multi-disciplinary open access archive for the deposit and dissemination of scientific research documents, whether they are published or not. The documents may come from teaching and research institutions in France or abroad, or from public or private research centers.

L'archive ouverte pluridisciplinaire **HAL**, est destinée au dépôt et à la diffusion de documents scientifiques de niveau recherche, publiés ou non, émanant des établissements d'enseignement et de recherche français ou étrangers, des laboratoires publics ou privés.



Université
Paris Cité



INSTITUT
PASTEUR

Université Paris Cité
École doctorale Bio Sorbonne Paris Cité (ED562)

Institut Pasteur
Département de Microbiologie
Équipe Adaptation au Stress et Métabolisme chez les entérobactéries
(CNRS – UMR 6047)

Study of Iron-Sulfur cluster biogenesis in environmental and metabolic stress conditions

Par **Soufyan FAKROUN**

Thèse de doctorat de Microbiologie
Dirigée par Sarah DUBRAC

Présentée et soutenue publiquement le 3 juillet 2023
Devant un jury composé de :

Rapporteurs :

Pierre MANDIN, CR-HDR, LCB, Marseille, Aix-Marseille Université

Benoît D'AUTREAUX, CR-HDR, I2BC, Gif-sur-Yvette, Université Paris Saclay

Examineurs :

Alexandra GRUSS, DR, INRAE, Jouy-en-Josas, Université Paris Saclay

Maude GUILLER, DR, IBPC, Paris, Université Paris Cité

Sandrine OLLAGNIER DE CHOUDENS, DR, CEA, Grenoble, Université de Grenoble Alpes

Frédéric BARRAS, PU, Institut Pasteur, Paris, Université Paris Cité

Directrice de Thèse :

Sarah DUBRAC, CR-HDR, Institut Pasteur, Paris, Université Paris Cité

Title: Study of Iron-sulfur cluster biogenesis in environmental and metabolic stress conditions

Abstract: Iron-sulfur (Fe-S) clusters are essential metallic cofactors present in most living organisms. In *Escherichia coli*, Fe-S clusters are involved in the activity of over 180 proteins, while in humans, dysfunctions in Fe-S cluster homeostasis are the root of many diseases. Fe-S cluster-containing proteins participate in major processes including respiration, central metabolism, DNA replication, and repair. In *E. coli*, Fe-S cluster biosynthesis is catalyzed by two multi-protein complexes, ISC under optimal conditions, and SUF under stress conditions (oxidative stress, low iron bioavailability). My PhD project focused on the relationship between Fe-S cluster metabolism and fatty acid metabolism, as well as the characterization of an Fe-S cluster regulator.

An unexpected link between fatty acid and Fe-S biogenesis has been reported in eukaryotes. The first objective of this thesis was to test this link and study the mechanisms in prokaryotes using *E. coli* as a model. A bacterial two-hybrid approach showed specific interactions between Acyl Carrier Protein (ACP) and three members of the ISC pathway (IscS, Fdx, and HscB). We used the CRISPRi tool to decrease the expression of the essential *acpP* gene encoding ACP. The study of the effect of ACP decrease on various Fe-S cluster reporters, regulators and enzymes activities, allowed us to show that ACP has a positive effect on the ISC-dependent Fe-S biogenesis.

The second objective of my thesis was to characterize an Fe-S cluster regulator whose function is still unknown, YeiL. As the expression of this gene was undetectable under tested conditions, we studied the effect of the overexpression of *yeiL*, both its wild-type form and a mutated form that cannot bind the Fe-S cluster. Transcriptomic analysis showed that the production of these two forms modifies the expression of hundreds of genes. Ontological analysis revealed that anaerobic nitrate respiration, nitric stress response, and the use of oxidized sugars, aldaric acids, are amongst the functions regulated by YeiL. Furthermore, these three functions are all related to nitric oxide, NO, which originates from nitrate respiration, induces a specific adaptive response, and promotes the formation of aldaric acids. By studying the expression of *hcp*, which encodes a NO reductase, we have shown a link between YeiL and OxyR, two transcriptional regulators in competition for the control of *hcp* expression. Our study of the transcriptional regulation of aldaric acids metabolism genes has allowed us to demonstrate that YeiL interferes with the dedicated activation pathway via the regulator CdaR. Thus, it appears that in both pathways studied, YeiL regulates gene expression by competing with other previously identified regulators. NO is an effector of the innate immune response, it displays a bactericidal effect but also promotes aldaric acids formation. Using a mice gut colonization model, we have shown that the YeiL regulator has a positive effect on long-term colonization.

Keywords: Iron-Sulfur clusters, Fatty acids, Transcriptional regulation, Nitric oxide

Titre: Étude de la biogénèse des centres fer-Soufre en conditions de stress métaboliques et environnementaux

Résumé : Les centres fer-soufre (Fe-S) sont des cofacteurs métalliques essentiels dans la plupart des systèmes vivants. Chez *Escherichia coli*, les centres Fe-S sont impliqués dans l'activité de plus de 180 protéines tandis que chez l'Homme, des dysfonctionnements dans l'homéostasie des centres Fe-S sont à la base de nombreuses pathologies. Les protéines à centres Fe-S participent à des processus majeurs incluant la respiration, le métabolisme central, la réplication et la réparation de l'ADN. Chez *E. coli*, la biosynthèse des centres Fe-S est catalysée par l'activité de complexes multi-protéiques, ISC en conditions optimales, et SUF en conditions de stress (stress oxydant, faible biodisponibilité en fer). Mon projet de thèse s'est focalisé sur la relation entre le métabolisme des centres Fe-S et celui des acides gras, ainsi que sur la caractérisation d'un régulateur à centre Fe-S.

Un lien inattendu entre la biogénèse des acides gras et celle des centres Fe-S a été rapporté chez les eucaryotes. Le premier objectif de cette thèse a été de tester ce lien et d'étudier les mécanismes chez les procaryotes en étudiant *E. coli* comme modèle. Une approche de double hybride bactérien a montré des interactions spécifiques entre l'ACP (Acyl Carrier Protein) et trois membres de la voie ISC (IscS, Fdx, et HscB). Nous avons utilisé l'outil CRISPRi pour diminuer l'expression du gène essentiel *acpP* codant l'ACP. L'étude de l'effet de la diminution d'ACP dans la cellule sur différents rapporteurs, activité de régulateurs et d'enzymes à centres Fe-S, nous a permis de montrer que l'ACP a un effet positif sur la biogénèse ISC-dépendante des centres Fe-S.

Le second objectif de ma thèse a été la caractérisation d'un régulateur à centre Fe-S dont la fonction est encore inconnue, YeiL. L'expression de ce gène étant indétectable dans les conditions classiques testées, nous avons étudié l'effet de la surexpression de *yeiL* sous sa forme sauvage et sous une forme mutée ne pouvant plus lier le centre Fe-S. Une approche transcriptomique a montré que la production de ces deux formes modifie l'expression de centaines de gènes. L'analyse ontologique a révélé que la respiration anaérobie du nitrate, la réponse au stress nitrique, et l'utilisation de sucres oxydées, les acides aldariques, sont parmi les fonctions régulées par YeiL. De plus, ces trois fonctions ont comme point commun l'oxide nitrique, NO. Le NO est un produit de la respiration du nitrate, il induit une réponse adaptative spécifique, et favorise la formation d'acides aldariques. En étudiant les modalités d'expression de *hcp*, codant une NO réductase, nous avons montré un lien entre YeiL et OxyR, deux régulateurs transcriptionnels en compétition pour le contrôle de l'expression de *hcp*. L'étude de la voie de régulation des gènes du métabolisme des acides aldariques nous a permis de montrer que YeiL interfère avec la voie d'activation dédiée, via le régulateur CdaR. Il apparaît donc que dans les deux voies étudiées, YeiL régule l'expression de gènes par compétition avec d'autres régulateurs précédemment identifiés. Le NO est un effecteur de la réponse immunitaire innée, il a un effet bactéricide mais favorise aussi la formation d'acides aldariques. En utilisant un modèle de colonisation de l'intestin de souris, nous avons pu montrer que le régulateur YeiL a un effet positif sur la colonisation à long terme.

Mots-clés : Centres Fer-Soufre, Acides gras, Régulation transcriptionnelle, Oxyde nitrique

Remerciements

J'ai effectué cette thèse au sein de l'unité Adaptation au Stress et Métabolisme chez les entérobactéries à l'Institut Pasteur. Je tiens à remercier un certain nombre de personnes clés qui ont été d'un grand soutien, qui m'ont permis de me développer aussi bien sur un plan scientifique que personnel. Je tiens à remercier en premier lieu le Pr. Frédéric Barras de m'avoir accueilli au sein de son laboratoire. J'ai énormément appris auprès de Fred, notamment sur la réflexion scientifique, la didactique et la communication scientifique. Je tiens également à le remercier pour sa bonne humeur. Je tiens également à remercier Sarah Dubrac, ma directrice de thèse, mon mentor, ma coéquipière dans cette aventure, mais avant tout mon amie. Sarah a été pour moi la personne la plus importante du laboratoire depuis mon arrivée. Elle a été d'un soutien sans faille. Présente dans les moments les plus heureux et les plus tristes de ma vie personnelle et professionnelle. Sarah a été un mentor exceptionnel, elle a su me guider dans cette aventure tout en m'inspirant beaucoup de confiance afin de m'appropriier pleinement ce projet. Merci à toi Sarah et félicitation pour cette thèse.

J'ai eu la chance d'effectuer ma thèse dans une unité comptant des personnes aussi bien formidables d'un point de vue scientifique qu'humain. Merci à l'ensemble de l'unité SAME. Merci à Emmanuelle Bouveret pour son aide et ses conseils qui m'ont permis de naviguer dans le monde fascinant et complexe des acides gras. Merci également à Jean-Michel Betton de m'avoir permis de profiter de son savoir encyclopédique en biochimie mais également pour avoir été un super compagnon de bureau et d'avoir rendu si amusant tous ces lab meetings. Un grand merci à Rodrigo, Manu, Francesca, Macha, Jessica, Oliver et Viola pour leur gentillesse, leur aide et leur bonne humeur. Je tiens également à remercier tout particulièrement Veronica pour son soutien lors de la dernière ligne droite. Enfin j'aimerais remercier Marine, une personne d'une grande authenticité dotée d'une profonde gentillesse et enfin une très grande source d'inspiration.

J'aimerais naturellement remercier ma famille pour leur soutien sans faille. Mes parents, sans les très grands sacrifices qu'ils ont effectués je ne serais pas là où je suis actuellement. Mes sœurs qui ont toujours été présentes dans toutes les étapes de ma vie. Je suis très reconnaissant d'avoir une famille aussi soudée, nous avons ensemble traversé de nombreuses épreuves sans faiblir. Je ne saurais jamais vous remercier assez.

J'aimerais enfin remercier mes innombrables amis pour avoir été à mes côtés et qui ont toujours su me redonner le sourire. Un grand merci à Quentin pour avoir été présent jusqu'à la dernière ligne droite et grâce à qui j'ai pu percer tous les secrets culinaires de la rue Oberkampf.

Je tiens à remercier chaleureusement Pierre Mandin et Benoît D'Autréaux d'avoir accepté d'être mes rapporteurs. Je suis également très honoré de pouvoir accueillir comme examinatrices Maude Guiller, j'ai pu avoir le privilège de passer un court séjour très enrichissant au sein de son laboratoire, Sandrine Ollagnier De Choudens et Alexandra Gruss. Je vous remercie très sincèrement d'avoir accepté de participer à ma formation de chercheur.

"الوقت كالسيف ان لم تقطعه قطعك"

Résumé substantiel

Les centres fer-soufre (Fe-S) sont des cofacteurs métalliques essentiels dans la quasi-totalité des organismes vivants. Les centres Fe-S sont composés de fer ferreux (Fe^{2+}) ou ferrique (Fe^{3+}) lié à du sulfure (S^{2-}). Ils existent sous différentes configurations, notamment les structures rhombiques [2Fe-2S], cubiques [3Fe-4S] ou cubanes [4Fe-4S], et dépendent de machineries spécialisées pour leur production. Les propriétés physico-chimiques des centres Fe-S permettent une diversité de réactions, du transfert d'électrons à la catalyse chimique redox et non redox. Chez *Escherichia coli*, il a été prédit que les protéines Fe-S représentent 4% du protéome (181 protéines) et pour environ la moitié d'entre elles, cela a été validé par des données expérimentales (Lenon *et al.* 2022). La biogenèse des centres Fe-S est réalisée par des machineries multiprotéiques. On en décompte actuellement 5, MIS et SMS chez les bactéries et les archées, NIF chez les bactéries, ISC et SUF chez les bactéries et les eucaryotes. *E. coli* possède les machineries ISC et SUF. La biogenèse des centres Fe-S implique trois étapes majeures : l'acquisition de fer et de soufre, l'assemblage du centre Fe-S et enfin le transfert du centre aux protéines clientes. Chez *E. coli*, la machinerie ISC est utilisée en conditions optimales tandis que SUF prend le relais en cas de stress. Différents types de stress peuvent affecter la biogenèse des centres Fe-S tels que le stress oxydant, le stress nitrosatif ou la carence en fer. La machinerie ISC contient 9 protéines, dont 8 codées dans un seul opéron. Le système ISC contient un régulateur transcriptionnel, IscR, une désulfurase de cystéine, IscS, une protéine d'assemblage, IscU, un transporteur, IscA, deux chaperons dédiés, HscA et HscB, une ferrédoxine Fdx, une protéine accessoire, IscX, et la frataxine CyaY.

Chez les eucaryotes, le système ISC se trouve dans les mitochondries et contient des composants fonctionnellement et structuralement homologues à ceux de la machinerie ISC bactérienne. Cependant, une protéine supplémentaire, ISD11, absente chez les procaryotes, participe également à la production de centres Fe-S par son interaction avec la cystéine désulfurase NFS1 (homologue de IscS). ISD11 appartient à la famille LYRM, une classe de protéines caractérisées par un motif leucine-tyrosine-arginine que l'on trouve uniquement dans les mitochondries. En 2016, une interaction entre la protéine ISD11 et ACP a été rapportée. ACP est une protéine essentielle impliquée dans la biogenèse des acides gras. Des structures cristallographiques du complexe ACP-ISD11-NFS1 ont été obtenues et des études

sur l'interaction tripartite suggèrent un rôle positif de ACP dans la biogenèse des centres Fe-S (Van Vranken *et al.* 2016). Il a été suggéré que l'interaction du complexe ACP-ISD11 avec NFS1 stabilise cette dernière (Herrera *et al.* 2018). Chez les procaryotes, malgré l'absence de la protéine ISD11, une interaction entre ACP et IscS dès 1996, avec la co-purification de ACP et IscS issues de *E. coli* (Flint 1996). De plus, en 2003, Gully et collaborateurs ont rapporté que chez *E. coli*, IscS co-immunoprécipite avec ACP (Gully *et al.* 2003). Dans le premier chapitre de résultats de cette thèse, j'ai décrit l'étude du rôle d'ACP dans la biogénèse des centres Fe-S chez *E. coli*. Nous avons montré, par double hybride bactérien, que ACP interagit non seulement avec IscS, mais aussi avec la ferrédoxine Fdx et la chaperonne HscB du système ISC. Nous avons étudié l'effet de ACP sur la biogenèse des centres Fe-S en utilisant l'outil CRISPRi pour diminuer l'expression de *acpP*. En suivant l'activité des protéines Fe-S telles que les régulateurs transcriptionnels ou des enzymes, nous avons démontré que ACP joue un rôle positif dans la biogenèse des centres Fe-S via la machinerie ISC.

Dans le second chapitre nous avons étudié la fonction du dernier régulateur à centre Fe-S de fonction inconnu, YeiL, chez *E. coli*. Les régulateurs transcriptionnels à centres Fe-S utilisent ces derniers comme senseurs de stress. Les centres Fe-S sont très sensibles à l'oxydation. L'oxygène moléculaire, O₂, peut directement endommager ces centres. De plus, le fer réduit, Fe²⁺, peut réagir avec le peroxyde d'hydrogène par le biais de la réaction de Fenton pour produire des espèces réactives de l'oxygène (ROS) qui endommagent les centres Fe-S. Les espèces réactives de l'azote qui peuvent induire la nitrosylation des atomes de fer exposés des centres Fe-S et ainsi altérer leurs propriétés. Enfin, une faible disponibilité en fer peut réduire l'assemblage des centres Fe-S. *E. coli* possède 5 régulateurs transcriptionnels à centres Fe-S. Quatre d'entre eux FNR, IscR, SoxR et NsrR sont bien caractérisés. Les centres Fe-S de ces régulateurs, leur état d'oxydation, ainsi que les modifications dont ils peuvent être la cible jouent un rôle clé dans leur activité (Crack *et al.* 2012). Le cinquième régulateur à centre Fe-S, YeiL, restait encore non caractérisé. YeiL appartient à la famille CRP-FNR et présente une identité de séquence de 22 % et une similarité de 42 % avec FNR, ainsi qu'une identité de séquence de 17 % et une similarité de 45 % avec CRP. La principale caractéristique de cette famille est la présence d'un motif de liaison à l'ADN hélice-tour-hélice (HTH) dans leur partie C-terminale et un domaine putatif de liaison aux nucléotides dans leur partie N-terminale. La forte similarité avec le domaine de dimérisation CRP/FNR suggère que YeiL est

également susceptible de se dimériser. YeiL possède cinq résidus de cystéine. La seule étude publiée sur YeiL montre qu'il possède un centre [4Fe-4S] (Anjum *et al.* 2000). Dans cette même étude, aucun phénotype majeur a été lié à l'absence de *yeiL*, sinon une légère réduction de la densité bactérienne en phase stationnaire lors de la croissance aérobie. Le gène *yeiL* semble être principalement exprimé pendant la phase stationnaire. De plus, il a été suggéré que l'activité du promoteur *yeiL* était réprimée par FNR mais activée par RpoS, Lrp et YeiL lui-même, bien que l'effet de ces régulateurs sur l'expression de *yeiL* soit modeste (Anjum *et al.* 2000). Un rôle de YeiL dans la survie en conditions limitantes en azote a également été proposé. Ces conclusions tirées d'un article publié par Anjum et collaborateurs en 2000 étaient les seules informations disponibles, et l'absence de toute autre donnée nous a incité à caractériser YeiL. L'objectif de ce projet était de caractériser le rôle de YeiL en identifiant son régulon, de tester le rôle de son centre Fe-S pour son activité, et enfin d'identifier les conditions physiologiques et environnementales de son expression. Dans cette étude, nous avons montré que la production de YeiL affecte l'expression de centaines de gènes, impliqués des fonctions clés telles que la respiration anaérobie, le métabolisme des sucres et la réponse au stress causé par l'oxyde nitrique (NO). Nous avons étudié le mécanisme par lequel YeiL est capable de réprimer l'expression des gènes du métabolisme des acides aldariques, des sucres oxydés, et avons montré qu'il s'agit d'un effet indirect qui passe par le contrôle de l'expression du régulateur de cette voie, CdaR. Nous avons démontré une interférence entre YeiL et OxyR dans le contrôle de l'expression de *hcp*, une réductase impliquée dans la réponse au stress NO. Nous avons également identifié la région 3' de la séquence codante de *yeiL* comme étant responsable de sa faible expression.

Preamble

I did my PhD in the Stress Adaptation and Metabolism in enterobacteria Unit led by Pr. Frederic Barras at the Institut Pasteur. The main thematic of the lab is the study of *Escherichia coli* adaptation to stress and more specifically stresses affecting iron-sulfur (Fe-S) clusters. Fe-S clusters are metallic co-factors essential in most of the living organisms. My thesis is subdivided in two parts, one focusing on the interplay between fatty acids biogenesis and Fe-S cluster biogenesis and the other on the study of the last uncharacterized Fe-S transcriptional regulator. These two studies were performed using a combination of genetics, omics, biomolecular, and biochemical approaches.

In 2003 a study published by Emmanuelle Bouveret demonstrated an interaction between ACP, the acyl carrier protein, crucial for fatty acid biogenesis and IscS the cysteine desulfurase of the ISC machinery of Fe-S cluster biogenesis. This link between fatty acids and Fe-S clusters homeostasis was further assessed since 2016 in a series of paper that demonstrated a physical and functional link between ACP and the ISC machinery in eukaryotes. The objective of my thesis was to characterize the interaction between ACP and the biogenesis of Fe-S clusters in *E. coli*. While some major differences exist between Fe-S cluster biogenesis in eukaryotes and prokaryotes, we have demonstrated that nonetheless the positive impact of ACP is conserved.

I have also during my thesis studied an Fe-S transcriptional regulator of unknown function, YeiL. A study in 2000 demonstrated that YeiL, a regulator belonging to the FNR-CRP family, contains a 4Fe-4S cluster. Additionally, their findings suggest conditions of expression of YeiL that we were unable to replicate. Thanks to a transcriptomic approach, utilizing both an overexpression of the wild type regulator as well as a form unable to bind its cluster, we have identified a large set of genes that are affected by YeiL. We have studied YeiL regulation of three different pathways that are aldaric acid metabolism, nitrate respiration, and nitric oxide stress resistance.

This thesis contains a general introduction on the subjects being discussed in the two parts, mainly Fe-S clusters biogenesis, Fe-S-dependent regulators, nitric oxide stress response, and fatty acids biogenesis with a focus on ACP. It contains a review published in *Advances in Microbiology* that I participated in the writing of, which discusses the ISC-dependent Fe-S

biogenesis in *E. coli*. As these two parts are independent, I have chosen to present them separately in the form of two draft-like articles. Each part contains therefore an introduction, a material and methods, results, and a discussion. Additionally, a concluding remarks part is included at the end of this thesis containing a general discussion of the two subjects.

Table of contents

INTRODUCTION	1
I - Iron-Sulfur Clusters biogenesis	2
I - 1 - Emergence of the Fe-S cluster biogenesis machineries	2
I - 2 - The ISC machinery	3
I - 3 - The SUF machinery	42
I - 3 - 1 - Fe-S assembly	42
I - 3 - 2 - Physiological role of SUF in <i>E. coli</i>	43
I - 3 - 3 - Two machineries, for what purpose?	45
I - 4 - Fe-S carriers	46
I - 5 - The other Fe-S biogenesis machineries	47
I - 5 - 1 - The NIF machinery	47
I - 5 - 2 - MIS and SMS	48
II - Fe-S regulators of <i>E. coli</i>	48
II - 1 - Description of the Fe-S proteome of <i>E. coli</i>	48
II - 2 - Diversity of Fe-S regulators in <i>E. coli</i>	50
II - 2 - 1 - FNR, the regulator of anaerobic adaptation	51
II - 2 - 2 - IscR and Fe-S cluster homeostasis	53
II - 2 - 3 - SoxR, a determinant regulator for oxidative stress response	54
II - 2 - 4 - NsrR, a nitrosative stress sensitive regulator	56
III - Nitric oxide stress	58
III - 1 - Damage caused by NO to Fe-S clusters	58
III - 2 - NO sources	59
III - 2 - 1 - Host mediated NO production	59
III - 2 - 2 - Endogenous NO production by <i>E. coli</i>	61
III - 3 - Defense systems against NO	62
III - 3 - 1 - Hcp, the first line of nitric oxide detoxification	62
III - 3 - 2 - HmpA and NO detoxification in aerobiosis	63
III - 3 - 3 - NorV a NO reductase	64
III - 3 - 4 - YtfE, an ambiguous role	64
III - 4 - Transcriptional regulations involved in NO defense	65
III - 4 - 1 - <i>hcp-hcr</i> regulation	65
III - 4 - 1 - 1 - FNR and anaerobic induction of <i>hcp</i>	65
III - 4 - 1 - 2 - The NarXL and NarPQ nitrate-responsive two-component systems	65
III - 4 - 1 - 3 - NsrR, the <i>ad hoc</i> NO responsive transcriptional repressor	66
III - 4 - 1 - 4 - OxyR, a NO-stimulated activator	66
III - 4 - 2 - Regulation of <i>hmpA</i> and <i>norVW</i>	67
IV - The Acyl Carrier Protein	69
IV - 1 - The role of ACP in the type II biogenesis of Fatty acids (FasII)	69
IV - 1 - 1 - The initiation step	69
IV - 1 - 2 - The fatty acid biogenesis cycle	70
IV - 2 - Acyl-ACP is important for the biosynthesis of fatty-acid derived compounds	71
IV - 2 - 1 - Phospholipid biosynthesis	71
IV - 2 - 2 - Lipopolysaccharide biosynthesis	71
IV - 2 - 3 - Lipoate Synthesis	72
IV - 2 - 4 - Biotin Synthesis	72
IV - 3 - ACP's unexpected partners	74
IV - 3 - 1 - SpoT and the stringent response	74
IV - 3 - 2 - The structural Maintenance of Chromosomes complex	74
IV - 4 - ACP and Fe-S biogenesis	75

IV - 4 - 1 - Mitochondrial ACP impacts Fe-S biogenesis.....	75
IV - 4 - 2 - Structure of the mitochondrial ACP-ISD11-NFS1 complex.....	75
IV - 4 - 3 - ACP and IscS in <i>E. coli</i>	77
RESULTS	78
Chapter I: Cross-talk between fatty acid biogenesis and Iron-Sulfur cluster biogenesis	79
Chapter I - Introduction	80
Chapter I - Materials and Methods.....	81
Chapter I - Results.....	87
I - Study of the interactions between ACP and the ISC machinery	87
I - 1 - ACP interacts with three members of the ISC system	87
I - 2 - Modelisation of the molecular interactions between ACP and IscS.....	89
I - 3 - Impact of ACP maturation in the interactions with the ISC system.....	91
II - ACP involvement in Fe-S phenotypes.....	91
II - 1 - Setting up the CRISPRi tool to repress <i>acpP</i> expression	91
II - 2 - ACP decrease leads to Fe-S dependent growth defect.....	95
II - 3 - ACP plays a role in gentamycin sensitivity.....	97
III - The role of ACP in the activity of Fe-S proteins	98
III - 1 - Study of Fe-S regulators	98
III - 2 - Study of Fe-S enzymes: the aconitases	104
IV - Interaction between ACP and IscS <i>in vitro</i>	106
IV - 1 - Does ACP impact IscS cysteine desulfurase activity?	106
IV - 2 - Characterization of the interaction by analytical ultracentrifugation	107
Chapter I - Discussion	109
Chapter II: Study of YeiL, the last uncharacterized Fe-S regulator in <i>E. coli</i>	112
Chapter II - Introduction	113
Chapter II - Material and Methods	117
Chapter II - Results.....	127
I - Identification of the YeiL-regulated genes.....	127
I - 1 - Global analysis of the YeiL regulon	127
I - 2 - Overproduction of YeiL leads to a general stress response	130
I - 3 - YeiL regulates anaerobic nitrate respiration	133
I - 4 - Connection between YeiL and OxyR in regulation of nitric oxide stress response	134
I - 5 - Aldaric acid metabolism is repressed by YeiL	137
I - 6 - Study of the YeiL direct regulon	141
I - 7 - Looking for the YeiL binding motif.....	142
I - 8 - YeiL has a positive impact on mice gut colonization	144
II - Study of the <i>yeiL</i> gene expression.....	146
II - 1 - <i>yeiL</i> is poorly expressed despite its active promoter.....	146
II - 2 - Set up of a suppressor approach to identify factors involved in <i>yeiL</i> expression control.....	149
II - 3 - Screening of conditions for YeiL production.....	151
Chapter II - Discussion	153
Chapter II - Supplementary data.....	156
CONCLUDING REMARKS.....	172
BIBLIOGRAPHY.....	179

List of figures:

Figures of the introduction

- Figure 1: Fe-S cluster assembly and delivery by the SUF machinery in *E. coli*
Figure 2: Regulation of Fe-S cluster synthesis in *Escherichia coli*.
Figure 3: Schematic representation of the Fe-S carrier network in *E. coli*.
Figure 4: The Fe-S proteome of *E. coli*.
Figure 5: Crystallographic structure of [4Fe-4S]-FNR.
Figure 6: Crystallographic structure of Apo-IscR dimer bound to *hyA* promoter DNA.
Figure 7: Crystallographic structure of Holo-SoxR.
Figure 8: Crystallographic structure of Holo-NsrR.
Figure 9: Structures of iron-nitrosyl species.
Figure 10: Fisher projection of ribose and ribaric acid.
Figure 11: Representation of the nitrate respiratory chain in *E. coli*.
Figure 12: Representation of the proposed mode of action of HCP depending on its redox state.
Figure 13: Genetic regulation of the NO defense systems in presence of endogenous or exogenous NO sources.
Figure 14: Maturation of ACP by ACPS and FabD.
Figure 15: Fatty acid biogenesis (FasII) in *E. coli*.
Figure 16: Lipoate biosynthesis pathway in *E. coli*.
Figure 17: Biotin biosynthesis pathway.
Figure 18: Crystallographic structure of the (ACP-ISD11-NFS1)².

Figures of Chapter I

- Figure 1: ACP interacts with three members of the ISC machinery.
Figure 2: Alphafold2 predicts an interaction between ACP and IscS.
Figure 3: The negative patch of ACP contains critical residues for its interaction with IscS, Fdx and HscB.
Figure 4: The guide RNAs target the 5'UTR region of *acpP*.
Figure 5: Different gRNA length leads to differential growth defect.
Figure 6: CRISPRi system is efficient in repressing *acpP* expression.
Figure 7: Decreasing ACP level in a Δ *sufBCD* strain leads to growth defects.
Figure 8: Decreasing ACP leads to a better survival to gentamycin treatment.
Figure 9: ACP positively affects IscR activity.
Figure 10: ACP positively affects FNR activity.
Figure 11: ACP positively affects NsrR activity in an ISC-dependent fashion.
Figure 12: ACP does not affect SoxR activity.
Figure 13: ACP does not affect the activity of the Beta-galactosidase.
Figure 14: ACP affects positively the activity of the aconitase enzymes.
Figure 15: ACP does not enhance IscS desulfurase activity *in vitro*.
Figure 16: 6His-ACP and 6His-IscS do not form a complex *in vitro*.

Figures of Chapter II

Introduction

Figure 1: Alphafold prediction of the structure of YeilL.

Results

Figure 1: Overview of the YeilL- and YeilL*-regulated genes.

Figure 2: Overlap of YeiL and YeiL* regulon.
Figure 3: Analysis of the most regulated functions.
Figure 4: YeiL and YeiL* production induce a stress response.
Figure 5: YeiL* regulates expression of genes involved in nitrate respiration.
Figure 6: YeiL* activates expression of cytoplasmic nitrate reductase gene.
Figure 7: YeiL and OxyR cross-regulations of *hcp* under nitrate respiration.
Figure 8: Study of *hcp* expression under NO exposure.
Figure 9: Aldaric acid metabolism is repressed by both YeiL and YeiL*.
Figure 10: YeiL and YeiL* down-regulate *cdaR* expression.
Figure 11: YeiL and YeiL* prevent aldaric acid induction.
Figure 12: MBP-YeiL/YeiL* purification and EMSA experiments.
Figure 13: Identification of the YeiL and CdaR binding sites in the *cdaR* promoter region.
Figure 14: YeiL plays a role in gut colonization.
Figure 15: YeiL down-regulates its own expression.
Figure 16: The determinant for *yeiL* low expression is present in its distal coding region.
Figure 17: A palindromic sequence inside the *yeiL* coding sequence is involved in *yeiL* expression.
Figure 18: Screen of suppressors for *yeiL* expression determinants.
Figure 19: The SPA tag leads to increased *yeiL* mRNA steady state.
Figure 20: YeiL production is not changed upon exposure to Fe-S related stress or galactarate.
Figure 21: Expression of *yeiL* is not regulated by OxyR and nitric oxide.

Figures of Concluding remarks

Figure 1: Proposed molecular mechanism for YeiL and OxyR regulation of *hcp-hcr* expression.
Figure 2: Proposed mechanism for CdaR and YeiL regulation of *cdaR* expression.

List of tables:

Tables of results Chapter I

Table 1: Strains used in this study

Table 2: Plasmids used in this study

Table 3: Primers used in this study

Tables of results Chapter II

Table 1: Strains used in this study

Table 2: Plasmids used in this study

Table 3: Primers used in this study

Table 4: YeiL- and YeiL*-regulated genes

Abbreviations

aTc: anhydroTetracyclin

BACTH: Bacterial Adenylate Cyclase-based Two Hybrid

β-Gal: β-Galactosidase

bp: base pair

CFU: Colony Forming Unit

CRISPR: Clustered Regularly Interspaced Short Palindromic Repeats

CRISPRi: CRISPR interference

Dip: 2,2'-Dipyridyl

EMSA: Electrophoretic Mobility Shift Assay

ETC: Electron Transport Chain

Fe-S: Iron-Sulfur

IPTG: IsoPropyl β-D-1-ThioGalactopyranoside

LB: Lysogeny Broth

MBP: Maltose Binding Protein

NO: Nitric Oxide

nt: nucleotide

PCR: Polymerase Chain Reaction

PLP: Pyridoxal Phosphate

PMF: Proton Motive Force

qRT-PCR: quantitative Real Time PCR

RNS: Reactive Nitrogen Species

ROS: Reactive Oxygen Species

SAM: S-adenosylmethionine

X-gal: 5-bromo-4-chloro-3-indolyl-β-D-galactopyranoside

Introduction

I - Iron-Sulfur Clusters biogenesis

I - 1 - Emergence of the Fe-S cluster biogenesis machineries

Iron-Sulfur (Fe-S) clusters are metallic cofactors essential in all living organisms. Fe-S clusters are composed of ferrous (Fe^{2+}) or ferric (Fe^{3+}) iron bound to sulfide (S^{2-}). They exist in a number of arrangements including, but not limited to, rhombic [2Fe-2S], cuboidal [3Fe-4S] or cubane [4Fe-4S] and rely on dedicated machineries for their production. Formation of Fe-S aggregates arose spontaneously in early geological times and they were instrumental in life evolution. For long was thought that Fe-S cluster assembly remained spontaneous in living organisms as the environment was favorable for their synthesis, *i.e.* anaerobiosis and abundance of iron and sulfur (Wächtershäuser 1992, Meyer 2008). Earth oxidation following the emergence of photosynthesis would have led to unfavorable conditions for Fe-S based biology, as potentially damaging reactive oxygen species appeared and oxidized iron and sulfur elements became more difficult to assimilate. The emergence of dedicated machineries for the production of Fe-S clusters would allow to mitigate such unfavorable conditions (Imlay 2006, Andreini *et al.* 2017, Gao 2020). While this view was the most accepted, a recent study demonstrated that the emergence of the Fe-S cluster biosynthetic machineries predates Earth great oxidation event (Garcia *et al.* 2022). Indeed, Garcia and collaborators phylogenetic approach suggests that Fe-S biogenesis machinery were already present in LUCA, the last universal common ancestor.

There are 5 different machineries for the biogenesis of Fe-S clusters, NIF, ISC, SUF, SMS and MIS. The ISC and SUF systems can be found in bacteria and eukaryotes whereas the MIS and SMS systems can be found in both bacteria and archaea. As for the NIF system, it is usually found in nitrogen fixing bacteria (Yuvaniyama *et al.* 2000). As the model organism used in my thesis is *Escherichia coli* (*E. coli*), I will mainly focus on the two machineries present in this organism, ISC and SUF. It is however noticeable that while *E. coli* serves a model organism for the characterization of Fe-S cluster biogenesis, it is however rather an exception than a model. Indeed, most bacteria possess one Fe-S cluster machinery, and most of them have the SUF system (Garcia *et al.* 2022). This discrepancy in the distribution of Fe-S machineries in bacteria is intriguing regarding the presence of both systems in *E. coli*.

I - 2 - The ISC machinery

During my thesis, I have been asked to participate in the writing of a review on the bacterial ISC (Iron Sulfur Cluster) system. This review covers all the steps of the biogenesis of Fe-S through the bacterial ISC system. As no major advance have been published on this topic since the publication of the review, I have decided to include this review in my thesis.

Making iron-sulfur cluster: structure, regulation and evolution of the bacterial ISC system

Corentin Baussier^{a,1}, Soufyan Fakroun^{b,c,d,1}, Corinne Aubert^a, Sarah Dubrac^{b,c}, Pierre Mandin^a, Béatrice Py^{a,*} and Frédéric Barras^{b,c,*}

^aLaboratoire de Chimie Bactérienne, CNRS-Aix Marseille Université, UMR 7283, Institut de Microbiologie de la Méditerranée, Institut de Microbiologie, Bioénergies et Biotechnologies, Marseille, France ^bStress Adaptation and Metabolism Unit, Department of Microbiology, Institut Pasteur, Paris, France ^cERL CNRS 6002, CNRS, Paris, France

^dUniversité Paris Diderot, Sorbonne Paris Cité, Paris, France

*Corresponding authors: E-mail: py@imm.cnrs.fr and fbarras@pasteur.fr

Published in *Advances in Microbiology* in 2020



Making iron-sulfur cluster: structure, regulation and evolution of the bacterial ISC system

Corentin Baussier^{a,1}, Soufyan Fakroun^{b,c,d,1}, Corinne Aubert^a, Sarah Dubrac^{b,c}, Pierre Mandin^a, Béatrice Py^{a,*} and Frédéric Barras^{b,c,*}

^aLaboratoire de Chimie Bactérienne, CNRS-Aix Marseille Université, UMR 7283, Institut de Microbiologie de la Méditerranée, Institut de Microbiologie, Bioénergies et Biotechnologies, Marseille, France

^bStress Adaptation and Metabolism Unit, Department of Microbiology, Institut Pasteur, Paris, France

^cERL CNRS 6002, CNRS, Paris, France

^dUniversité Paris Diderot, Sorbonne Paris Cité, Paris, France

*Corresponding authors: E-mail: py@imm.cnrs.fr and fbarras@pasteur.fr

Contents

1. Introduction	2
2. Overview of the ISC assembly line	5
3. The assembly step	5
3.1 Role of individual ISC components	5
3.1.1 <i>The cysteine desulfurase IscS</i>	5
3.1.2 <i>The scaffold protein IscU</i>	7
3.1.3 <i>The ferredoxin Fdx</i>	9
3.1.4 <i>The bacterial frataxin CyaY</i>	10
3.1.5 <i>IscX</i>	13
3.1.6 <i>The acyl carrier protein ACP</i>	13
3.2 Global architecture of the cysteine desulfurase/scaffold core assembly complex	15
4. Fe-S cluster delivery step	16
4.1 Chaperones to release Fe-S cluster from the ISC scaffold	16
4.2 Multiplicity of carriers to deliver Fe-S clusters	18
5. Regulation of Fe-S cluster biogenesis	20
5.1 IscR, master and commander of Fe-S cluster biogenesis systems usage	20
5.2 New roles for IscR beyond Fe-S cluster biogenesis regulation	21

¹ Co-first authors.

6. Evolution	25
7. Conclusion	27
Acknowledgments	28
References	28

Abstract

Iron sulfur (Fe-S) clusters rank among the most ancient and conserved prosthetic groups. Fe-S clusters containing proteins are present in most, if not all, organisms. Fe-S clusters containing proteins are involved in a wide range of cellular processes, from gene regulation to central metabolism, *via* gene expression, RNA modification or bioenergetics. Fe-S clusters are built by biogenesis machineries conserved throughout both prokaryotes and eukaryotes. We focus mostly on bacterial ISC machinery, but not exclusively, as we refer to eukaryotic ISC system when it brings significant complementary information. Besides covering the structural and regulatory aspects of Fe-S biogenesis, this review aims to highlight Fe-S biogenesis facets remaining matters of discussion, such as the role of frataxin, or the link between fatty acid metabolism and Fe-S homeostasis. Last, we discuss recent advances on strategies used by different species to make and use Fe-S clusters in changing redox environmental conditions.



1. Introduction

Fe-S clusters are ubiquitous prosthetic groups that life exploited very early during evolution. Present living organisms are all dependent upon Fe-S cluster-based biology. The evolutionary success of these cofactors stems from chemical properties of both iron and sulfur, which come under different oxidation states and can confer or broaden physico-chemical properties of hosting polypeptides. It is reasonable to think that the fact that life made use of iron early, relates to its then high availability, as Fe²⁺ is soluble under anaerobic conditions. Subsequently, photosynthesis, which ironically depends on Fe-S cluster proteins, emerged in an anaerobic atmosphere and produced molecular oxygen that oxidized iron to its insoluble Fe³⁺ state. From then, Fe-S cluster-based biology had to compromise with both a shortage in bioavailable, soluble, ferrous iron and production of Fe-S cluster damaging reactive oxygen species (ROS). It is believed that such new unfavorable conditions selected for the emergence of Fe-S cluster biogenesis systems to build Fe-S clusters and protect them from ROS.

The hypothesis of the existence of Fe-S cluster biogenesis system was put forward in the late 90's by seminal studies from the Dean group when examining how *Azotobacter vinelandii* nitrogenase acquired its cofactors, among

which are Fe-S clusters (Jacobson et al., 1989). The hypothesis was that despite iron and sulfur being able to spontaneously associate to form clusters *in vitro*, dedicated assisting factors ought to exist to meet with *in vivo* kinetic and specificity constraints. This proved to be a formidable prediction and for the last twenty years, research in multiple labs around the world focused on the identification and the nature of the contribution of such assisting factors within Fe-S cluster biogenesis.

This wealth of research led to a great understanding of Fe-S cluster biogenesis *in vivo*. Basically, biogenesis of Fe-S proteins involves two major steps: assembly of the cluster on a scaffold protein and delivery of the cluster to client proteins (Fig. 1). The first step involves enzymes and proteins that

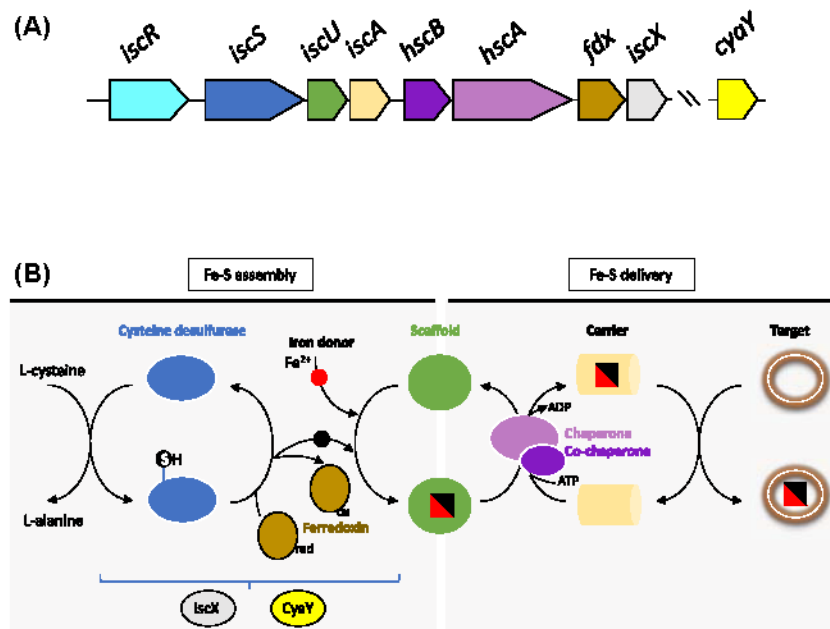


Fig. 1 The *E. coli* ISC Fe-S cluster biogenesis system. (A) Genetic organization of the *E. coli* *isc* operon. The *cyaY* gene is not part of the *isc* operon, which, respectively, locate at centisome 86 and 57. Transcription starts are indicated by black arrows. (B) Schematic representation of Fe-S cluster biogenesis by the ISC system. Persulfide (S-SH) formed on catalytic cysteine of IscS (orange dot) is indicated. The iron (red) and sulfur (black) elements are represented by dots in their free (Fe²⁺) or in persulfide (S²⁻) form, and by triangles when they are part of Fe-S clusters. The two main steps, *i. e.* assembly and delivery of the Fe-S clusters are indicated. Genes and corresponding proteins are color-coded depending on the function ensured: the IscR transcriptional regulator (turquoise blue), the IscS cysteine desulfurase (blue), the IscU Fe-S cluster assembly scaffold (green), the IscA Fe-S cluster carrier (beige), the HscA/B chaperone/co-chaperone (light and dark purple), the Fdx ferredoxin (brown). The *cyaY* and *iscX* genes whose role is still debated are in yellow and gray, respectively.

mobilize iron and sulfur, donates electrons and build Fe-S clusters, while the second step includes a series of proteins that enable targeting of Fe-S clusters to a wide array of structurally and functionally diverse client proteins. A remarkable conclusion reached by three decades of work is that both the nature of the biogenesis factors and the mechanism they use to assist Fe-S cluster-based biology are for most part conserved throughout prokaryotes and eukaryotes. In fact, three machineries were described, NIF, ISC and SUF. NIF is predicted to be specific for the maturation of nitrogenase, whereas ISC and SUF are thought to mature the bulk of cellular Fe-S proteins in both prokaryotic and eukaryotic cells. Bacteria can have one, two or all three machineries. In eukaryotes, ISC is mitochondrial, while existence of a cytosolic version received experimental support but remains a discussed issue. SUF locates within the chloroplast.

Our current knowledge on Fe-S cluster biogenesis systems largely comes from *Escherichia coli* and the mitochondrial systems, inherited from bacteria, of human and *Saccharomyces cerevisiae*. We already know that this led to the wrong perception of ISC being the archetypical Fe-S cluster biogenesis system, SUF being considered as a secondary back-up system in bacteria and restricted to plastid-containing eukaryotes. Rather, recent in-depth phylogenetic analyses revealed that ISC is limited to eukaryotes and proteobacteria, whereas SUF is likely to be both the ancestral system and the most widespread one. Nevertheless, deciphering how the ISC machinery works is of crucial importance. Hence, it is an essential process for ISC only-containing bacteria, it modulates *E. coli* tolerance to antibiotics, and its malfunction in human gives rise to severe neurological, metabolic, or hematological disorders, often with fatal outcome (Ezraty et al., 2013; Rouault, 2012; Schmucker & Puccio, 2010; Stehling, Wilbrecht, & Lill, 2014). Therefore, the present review is dedicated to the ISC system in prokaryotes and whenever it will help to shed light on the mechanism under consideration, we will also include information derived from work on eukaryotic systems. Also, because several excellent reviews and books taking stock of issues and current knowledge of Fe-S cluster biology have appeared in the recent years, hereafter we will take the liberty to address uncertainties and speculative topics, which might, or might not, be part of main stream research in Fe-S cluster biology in the future. For an in-depth coverage of eukaryotic ISC systems, the reader is invited to look at excellent recent reviews by Lill and Rouault and their collaborators (Braymer & Lill, 2017; Rouault & Maio, 2017). Regarding the SUF system, it was very recently covered by Przybyla-Toscano, Roland, Gaymard, Couturier, and Rouhier (2018)

and by Garcia, Gribaldo, Py, and Barras (2019) (Garcia et al., 2019; Przybyla-Toscano et al., 2018).

2. Overview of the ISC assembly line

Basic principles and key molecular actors of the ISC pathway are depicted in Fig. 1. Both prokaryotic and eukaryotic names are given in this order and separated by a slash. A cysteine desulfurase, IscS/Nfs1, allows to mobilize sulfur from the lateral chain of L-cysteine, through persulfide formation and transfer. The nature and identity of the iron donor remains largely uncertain and multiple origins have been proposed such as CyaY (resp. FXN in human and Yfh1 in yeast) and IscX protein (no counterpart in eukaryote). Electrons are then needed to reduce persulfide, to produce Fe-S clusters, and they will be supplied by the Fdx ferredoxin (resp. FDX in human and Yah1 in yeast). The IscU/Isu scaffold provides a molecular platform allowing to combine iron, sulfur and electrons to form an Fe-S cluster. The HscA/B chaperone/co-chaperone system is thought to help release of the cluster from the IscU/Isu scaffold. The cluster is subsequently handed over to IscA/Isa carrier that eventually delivers the cluster to the terminal apo-target. Additional carriers might be collaborating with the ISC system and they will be described in dedicated sections. In *E. coli* and several other bacteria, the ISC system is encoded by the *isc* operon, the structure of which is depicted in Fig. 1. Expression of the *isc* operon is under the control of the proximal *iscR* gene product.

3. The assembly step

3.1 Role of individual ISC components

3.1.1 The cysteine desulfurase IscS

From L-cysteine as a substrate, IscS abstracts sulfur and releases L-alanine. The catalytic reaction requires a pyridoxal phosphate (PLP) cofactor and a conserved cysteine residue (Cys328 in *E. coli*) (Mihara, Kurihara, Yoshimura, & Esaki, 2000; Schwartz, Djaman, Imlay, & Kiley, 2000). The reaction mechanism involves formation of an enzyme-bound cysteine-persulfide (R-S-SH) intermediate and was initially elucidated in studies on NifS from *A. vinelandii* (Zheng, White, Cash, Jack, & Dean, 1993, 1994). Recently, results obtained by using X-ray crystallographic snap-shot analysis suggested a new detailed model of the catalytic

mechanism in which a conserved histidine stabilizes an intermediate of the reaction (Blahut et al., 2019; Nakamura, Hikita, Ogawa, Takahashi, & Fujishiro, 2019). Once formed on IscS, the persulfide is then transferred either to the Fe-S cluster building scaffold protein IscU, or to sulfur transferases, which provide sulfur for thio-cofactors such as thiamine and molybdenum cofactor, and for thiolation of tRNAs (Fig. 2A). Therefore, *iscS* mutation, but not mutations in other *isc* genes, is pleiotropic and leads to alteration of both Fe-S cluster-dependent and Fe-S cluster-independent phenotypes (Johnson, Unciuleac, & Dean, 2006; Lauhon, 2002; Lauhon, Skovran, Urbina, Downs, & Vickery, 2004; Schwartz et al., 2000; Takahashi & Nakamura, 1999). Comparison of crystal structures of IscS in complex with either IscU or TusA, a sulfur acceptor protein required for tRNA modifications, showed that IscU and TusA binding surfaces on IscS do not overlap (Shi et al., 2010). Pull-down experiments indicated that TusA and IscU cannot bind to IscS simultaneously, and that IscU is able to displace

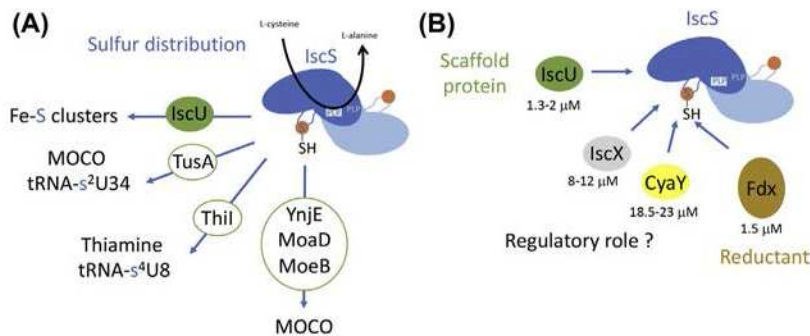


Fig. 2 *IscS* has multiple partners. (A) *E. coli* IscS homodimer (light and dark blue) is able to interact and distribute sulfur, via persulfide transfer, to sulfur acceptor proteins involved in Fe-S cluster assembly, molybdenum cofactor (MOCO) biosynthesis, tRNA thiolation, thiamine biosynthesis (Dahl et al., 2011, 2013; Ikeucchi et al., 2006; Kambampati & Lauhon, 2000, 1999; Shi et al., 2010). YnjE, a three-domain rhodanese-like protein, interacts with IscS to possibly participate to MOCO synthesis together with MoeD and MoeB (Dahl et al., 2011). The catalytic loop of IscS with the Cys328 (orange dot) residue are represented as well as the PLP cofactor necessary for the persulfuration of IscS. (B) IscS-partners in the ISC Fe-S cluster biogenesis pathway of *E. coli*. The binding affinity constants (K_d) of the pairwise protein-protein interactions are given. Pairwise affinities can be modulated by the presence of a third partner. For example, in the case of the IscS-IscU and IscS-CyaY interactions, the binding affinity constants were appreciably lower in the presence of CyaY and IscU, with K_d of 400 nM and 35 nM, respectively (Prischi et al., 2010). Cases of competition for the binding of IscS have been described between Fdx and CyaY, as well that between IscX and CyaY (Adinolfi et al., 2018; Yan et al., 2013).

TusA from IscS, suggesting that the IscS-dependent pathways are organized in a hierarchical manner giving the priority to Fe-S building. (Shi et al., 2010). IscS appears as a major protein interaction hub since in addition to sulfur acceptors, IscS interacts with several Fe-S cluster biogenesis factors Fdx, CyaY and IscX (Fig. 2B) (see below). The human and yeast homologs (NFS1/Nfs1) have an additional partner (ISD11/Isd11) that is exclusively present in eukaryotes (Adam, Bomhövd, Prokisch, Neupert, & Hell, 2006; Richards & van der Giezen, 2006; Shi, Ghosh, Tong, & Rouault, 2009; Wiedemann et al., 2006). Functional complementation studies showed that human NFS1 in conjunction with ISD11 can replace *E. coli* IscS for Fe-S cluster biogenesis, but not for tRNA thio-modifications or molybdenum cofactor biosynthesis (Bühning, Friemel, & Leimkühler, 2017). In the absence of Isd11, Nfs1 is prone to aggregate and a consecutive partial loss of Nfs1 activity leads to a dramatic decrease in the activity of Fe-S cluster-containing enzymes such as aconitase and succinate dehydrogenase (Adam et al., 2006; Wiedemann et al., 2006). Structural data showed that ISD11 binds to NFS1 distal to the desulfurase active site and does not directly participate in catalysis (Boniecki, Freibert, Mühlhoff, Lill, & Cygler, 2017). Surprisingly, other crystallographic and electron microscopy structures revealed a different architecture of the NFS1 homodimer compared with all previously determined cysteine desulfurase structures. In this architecture, contacts between NFS1 subunits were limited to only weak hydrophobic interactions, and ISD11 role was proposed to facilitate NFS1 dimerization (Cory et al., 2017). No ISD11 homolog exists in prokaryote and whether a functional equivalent arises to substitute for ISD11 remains to be investigated.

3.1.2 The scaffold protein IscU

IscU is at the heart of the ISC Fe-S cluster biogenesis machinery, because it serves as a platform to assemble *de novo* Fe-S clusters (Agar, Zheng, Cash, Dean, & Johnson, 2000; Chandramouli et al., 2007; Smith et al., 2001). IscU receives sulfur from its partner, the cysteine desulfurase IscS (Agar, Zheng, et al., 2000; Kurihara, Mihara, Kato, Yoshimura, & Esaki, 2003; Smith et al., 2001; Urbina, Silberg, Hoff, & Vickery, 2001). *In vitro*, IscS transfers directly sulfur from L-cysteine to IscU, as shown by ³⁵S transfer assay and mass spectrometry (Smith et al., 2001; Urbina et al., 2001). Whether an iron ion can directly enter the Fe-S cluster assembly site in IscU or needs a delivery component is still an open question (see below paragraph 2.1.4).

NMR methods pointed out that the apo-IscU-IscS complex is a highly dynamic structure with IscU existing in two slowly inter-converting conformational states: one disordered (D) and one structured (S) (Kim et al., 2009). Remarkably, the D state of IscU was found to be the preferential partner of IscS, and mutations that favored the S state (substitution Asp39 to Ala in IscU) allowed occupancy of the IscU Fe-S cluster assembly site (Cai, Frederick, Tonelli, & Markley, 2018; Kim, Tonelli, & Markley, 2012). These results suggest that IscS would preferentially act on the D-state populated IscU forms that would be subsequently converted to Fe-S cluster bound S-state forms.

A hallmark of the IscU scaffold is the presence of three strictly conserved cysteine residues (Cys37, Cys63 and Cys106 in *E. coli* IscU). Cys37 and Cys63 are solvent exposed, while Cys106 is mostly buried inside the structure. At these positions, Cys residues are strictly required as indicated by the loss of function of IscU variants in which Cys residues were substituted with Ala, Asp, Ser or His residues (Johnson et al., 2006; Tanaka et al., 2019). Studies by electrospray-ionization mass spectrometry of the *A. vinelandii* IscU variants containing individual Cys-to-Ala substitutions, indicated that IscS can transfer sulfur to each of the three alanine-substituted forms of IscU to yield persulfide or polysulfide species (Smith, Frazzon, Dean, & Johnson, 2005). It was then concluded that S transfer, from IscS to IscU, did not involve a specific Cys residue in IscU. However, semi-quantitative analysis of persulfide formation on mammalian IscU (ISCU) indicated that some specificity might occur since Cys104 (equivalent to Cys106 of *E. coli* IscU) appeared as a major sink of persulfide (Parent et al., 2015).

Spectroscopic and structural analyses indicated that IscU binds a [2Fe-2S] cluster using the three conserved Cys residues (Agar, Krebs, et al., 2000; Shimomura, Wada, Fukuyama, & Takahashi, 2008). The nature of the fourth ligand of the cluster is still uncertain. First, Asp39 (using *E. coli* as a reference) was proposed for this role, since it was observed that its substitution with alanine prevented the release of the [2Fe-2S] cluster of IscU variants from *Aquifex aeolicus*, *A. vinelandii*, *Homo sapiens*, and *Schizosaccharomyces pombe* (Foster et al., 2000; Raulfs, O'Carroll, Dos Santos, Unciuleac, & Dean, 2008; Shimomura et al., 2008; Unciuleac et al., 2007; Wu et al., 2002). However, the crystal structure of *A. aeolicus* holo-IscU variant containing the Asp39 to Ala substitution showed histidine (His105) to be the fourth ligand (Shimomura et al., 2008). *A. vinelandii* and *E. coli* IscU variants in which His105 or Asp39 were substituted by amino acids such as Ala, Cys, Ser, Glu, or Gln, were not functional, underlying the functional importance

of both of these residues (Raulfs et al., 2008; Tanaka et al., 2019). Last, the fourth ligand could be the catalytic Cys residue of IscS as it was observed to ligand the [2Fe-2S] cluster in the structure of the IscS/IscU(D37A) *Archaeoglobus fulgidus* complex (Marinoni et al., 2012; Pagnier, Nicolet, & Fontecilla-Camps, 2015). In conclusion, several candidate residues have been proposed to act as the fourth ligand for the Fe-S cluster of IscU. It might be worth noting that IscU His105 (using *E. coli* as a reference) and IscS Cys catalytic residue were proposed to act as ligands in studies using an IscU variant and this might have uncovered non native secondary arrangement. Nevertheless, given that by essence the role of IscU is to build a cluster in a transient way, it might well be that several residues contribute to Fe-S cluster assembly by acting as short-lived ligands.

Early *in vitro* studies of the time course of IscS-mediated cluster assembly revealed that IscU was able to sequentially assemble [2Fe-2S] clusters and then [4Fe-4S] clusters (Agar, Krebs, et al., 2000). Hence, a [4Fe-4S] cluster at the IscU dimer interface was obtained by reductive coupling of an IscU dimer containing two [2Fe-2S] clusters, one cluster within each monomer (Agar, Krebs, et al., 2000; Chandramouli et al., 2007). *In vitro*, the [2Fe-2S]- and [4Fe-4S]-bound forms of IscU are able to mature apo-client proteins (Unciuleac et al., 2007). However, the *in vivo* physiological relevance of the [4Fe-4S] bound form of IscU is questioned. Indeed, in eukaryotes, the formation of [4Fe-4S] clusters was proposed to occur at a step downstream IscU (Mühlenhoff, Richter, Pines, Pierik, & Lill, 2011; Sheftel et al., 2012). Similarly, genetic studies in *E. coli* suggested that [4Fe-4S] assembly takes place on late-acting ISC components (Vinella, Loiseau, Ollagnier de Choudens, Fontecave, & Barras, 2013).

Zinc was repeatedly found associated with purified IscU, and was located in the site of Fe-S cluster assembly (Fox et al., 2019; Gervason et al., 2019; Ramelot et al., 2004). *In vitro* studies converged to conclude that the Zn-bound form is unproductive to assemble Fe-S clusters (Fox et al., 2019; Gervason et al., 2019). These results are fully consistent with *in vivo* studies showing that intracellular zinc excess inhibits Fe-S cluster biogenesis by inhibiting activity of Fe-S proteins maturation such as IscU (Li et al., 2019). In contrast, zinc does not appear to be destabilizing clusters already present in holo-proteins.

3.1.3 The ferredoxin Fdx

In vivo studies, both in prokaryotes and eukaryotes, demonstrated the involvement of a [2Fe-2S] ferredoxin in the ISC Fe-S cluster biogenesis

process (Lange, Kaut, Kispal, & Lill, 2000; Mühlenhoff, Gerber, Richhardt, & Lill, 2003; Sheftel et al., 2010; Shi, Ghosh, Kovtunovych, Crooks, & Rouault, 2012; Tokumoto & Takahashi, 2001). A possibility was that Fdx ensures the reductive coupling of two $[2\text{Fe-2S}]^{2+}$ clusters into a single $[4\text{Fe-4S}]^{2+}$ cluster on homodimeric IscU as described above (Chandramouli et al., 2007). More recently, implication of the ferredoxin Fdx at an earlier step in Fe-S cluster biogenesis was supported by the fact that *E. coli* Fdx interacts directly with IscS, and that $[2\text{Fe-2S}]$ cluster assembly on the yeast scaffold was drastically impaired when the ferredoxin Yah1 was depleted (Kim, Frederick, Reinen, Troupis, & Markley, 2013; Tokumoto et al., 2002; Webert et al., 2014; Yan et al., 2013). Thanks to the development of a time-resolved Fe-S cluster reconstitution assay using the yeast Yah1 ferredoxin instead of the commonly used artificial reductant DTT, it was established that Yah1 was necessary for $[2\text{Fe-2S}]$ cluster formation on the Isu scaffold protein (Webert et al., 2014). Biochemical studies with *E. coli* Fdx also concluded that reduced Fdx donates its electron for IscU-mediated Fe-S cluster reconstitution (Kim et al., 2013). Last, using an *in vitro* protein persulfidation assay and human ferredoxin, FDX2, it was possible to assign more precisely at which step ferredoxin acted. Hence, persulfide transfer from the IscS cysteine desulfurase to IscU was found unaffected by FDX2, while reduction of the persulfurated form of IscU and concomitant Fe-S cluster formation required FDX2 (Gervason et al., 2019) (Fig. 3). Interestingly, the effect of FDX2 was dependent on the binding of iron on the ISCU scaffold protein, likely to allow instantaneous binding of the nascent sulfide to the nearby iron (Gervason et al., 2019).

3.1.4 The bacterial frataxin CyaY

The frataxin protein has attracted a large attention because that alteration of the cognate gene causes Friedrich ataxia (FRDA), an autosomal recessive neurodegenerative disease (Campuzano et al., 1997, 1996; Koutnikova et al., 1997; Schmucker & Puccio, 2010). Nevertheless, the actual role of FXN is still a matter of debate. Very early, Fe-S cluster defects were reported in eukaryotic cells lacking FXN, but it is only in the 2000' that FXN was described as part of the Fe-S cluster biogenesis process. This was concluded from studies showing that the bacterial frataxin (CyaY) and the eukaryotic FXN interact with the ISC assembly complex (IscS/IscU in *E. coli*; NFS1/ISD11/ACP/ISCU in human Nfs1/Isd11/ACP/Isu1 in yeast; see above) (Adinolfi et al., 2009; Gerber, Mühlenhoff, & Lill, 2003; Prischi et al., 2010; Schmucker et al., 2011; Tsai & Barondeau, 2010; Wang &

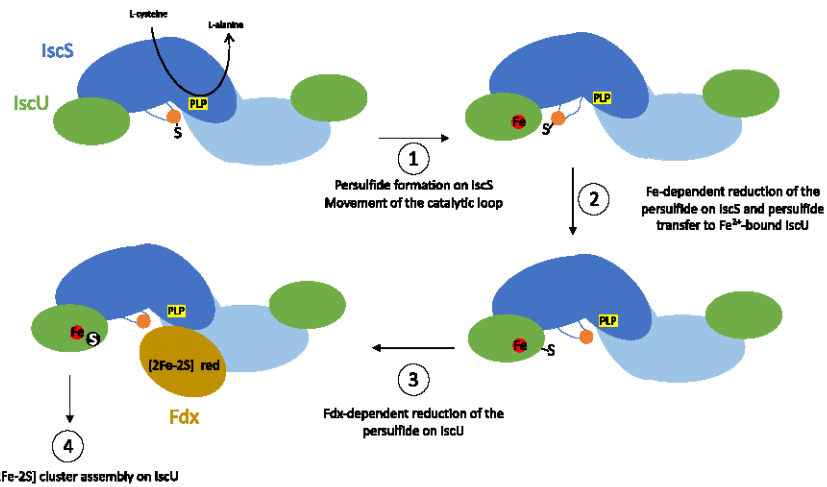


Fig. 3 Model of Fe-S cluster assembly by the ISC components. 1: PLP-dependent persulfide formation on Cys328 (orange dot) of *E. coli* IscS homodimer (the two monomers are represented in light and dark blue) by mobilization of the sulfur from L-cysteine and release of L-alanine. Movement of the catalytic loop occurs in order to be positioned in the vicinity of the conserved cysteine residues of monomeric IscU (green). 2: Fe-dependent persulfide reduction and transfer to Cys106 of the Fe²⁺-bound IscU. In this model iron comes first onto IscU. 3: Reduced holo-Fdx joins the IscS-IscU complex and reduces the persulfide into sulfide (black dot). 4: Assembly of a [2Fe-2S] cluster either after IscU dimerization or by a new round of reactions 1–3, onto monomeric IscU. For sake of clarity, Fe-S cluster assembly is depicted on only one of the two assembly sites of the (IscS-IscU)₂ complex.

Craig, 2008). CyaY and the eukaryotic FXN exhibit low level of sequence identity but are structural homologs (Cho et al., 2000; Dhe-Paganon, Shigeta, Chi, Ristow, & Shoelson, 2000; Musco et al., 2000). Moreover, CyaY was shown to rescue a yeast frataxin (Yfh1) deletion mutant (Bedekovics, Gajdos, Kispal, & Isaya, 2007). Structural analysis of the *E. coli* and human FXN-containing assembly complex showed that FXN is in close vicinity of the IscS (resp. NFS1) catalytic Cys-containing loop. Precisely, CyaY (resp. FXN) fits in the cavity delimited by the IscS (resp. NFS1) cysteine desulfurase dimer interface and the IscU (resp. ISCU) scaffold binding site (Boniecki et al., 2017; Fox et al., 2019; Prischi et al., 2010). Thus CyaY/FXN appears to locate at a key place for intervening in Fe-S cluster assembly.

Strikingly, *E. coli* lacking *cyaY* gene showed only very weak phenotypes as compared with eukaryotes lacking FXN (Li, Ohshima, Jiralerspong,

Bojanowski, & Pandolfo, 1999; Pohl et al., 2007; Roche, Huguenot, Barras, & Py, 2015; Velayudhan et al., 2014). The source of such difference was traced back to the scaffold component IscU and more precisely to the nature of the residue at position 108, which is an Ile in most prokaryotic IscU, and a Met in eukaryotic IscU. Hence, in IscU of *E. coli*, the substitution of Ile108 by a Met residue, was sufficient to drastically compromise the ISC pathway in the absence of CyaY (Roche, Agrebi, et al., 2015). Reciprocally, substitution of Met by Ile at the equivalent position in *S. cerevisiae* IscU allowed the ISC pathway to function in the absence of FXN (Yoon et al., 2012, 2015). While pointing out the subtle differences between the two homologous ISC systems, these studies also established CyaY/FXN as positive effectors of the ISC Fe-S assembly process in both prokaryotic and eukaryotic organisms.

Cells can manage to assemble Fe-S clusters in the absence of FXN provided that they have an appropriate IscU (Ile at position 108). Consistent with the location of FXN in proximity of the Fe-S cluster assembly site within the IscS-IscU complex, current belief is that FXN plays a regulatory role (Boniecki et al., 2017; Cai, Frederick, Dashti, & Markley, 2018; Fox et al., 2019; Prischi et al., 2010). Hence, it was proposed that frataxin (i) decreases the dissociation rate constants between IscU scaffold and IscS cysteine desulfurase, (ii) inhibits the interaction of IscU with IscS, (iii) relieves zinc inhibition of the Fe-S cluster assembly on IscU, (iv) favors iron entry into the IscS/IscU assembly complex, (v) increases the rate of substrate binding to the PLP cofactor onto IscS, or (vi) enhances sulfur transfer reaction from IscS to IscU (Das, Patra, Bridwell-Rabb, & Barondeau, 2019; Kim et al., 2013; Pandey et al., 2013; Patra & Barondeau, 2019; Prischi et al., 2010). All of these proposals derived from *in vitro* reconstitution assays that are highly sensitive to reactions conditions (reductant used, metal “contamination” of the proteins, stoichiometry of the components ...) and read-outs used (cysteine desulfurase activities, Fe-S cluster formation ...). Hence, despite a wealth of information stemming from genetic, biochemistry, spectroscopy and structural analyses, the actual role of FXN in Fe-S cluster biogenesis remains to be fully deciphered. Before to close, one might recall that CyaY was first thought to act as an iron donor. Over the years very few evidences were gathered to sustain such a role *in vivo*. However, a recent study revealed that CyaY from *Vibrio cholerae* has the ability to bind heme as well as iron (Uchida, Kobayashi, Muneta, & Ishimori, 2017). Whether this is calling for a new possible role and whether this would hold true for any organism or is specific to *V. cholerae* is a new exciting avenue in the saga of the *in vivo* role of frataxin.

3.1.5 *IscX*

IscX is encoded by the last gene of the *isc* operon. Homologs of *iscX* are only found in bacteria, especially in the β - and γ -proteobacteria for which the gene order in the *isc* operon is highly conserved (Shimomura, Takahashi, Kakuta, & Fukuyama, 2005). Studies in *E. coli* showed that in contrast to other *isc* genes (i) mutants lacking *iscX* showed virtually no differences from wild-type cells, (ii) *iscX* was dispensable for the maturation of three Fe-S containing hydrogenases, and (iii) the $\Delta iscX \Delta suf$ mutant was viable, grew normally and did not show any phenotypic deficit (Jaroschinsky, Pinske, & Sawers, 2017; Tanaka et al., 2016; Tokumoto & Takahashi, 2001). Results above suggested that IscX was not necessary for an optimal efficiency of the ISC system. Nevertheless, *iscX* contributes to cell physiology in iron replete conditions, as evidenced by fitness assays (Roche, Huguenot et al., 2015). Interestingly, transposon insertion in *iscX* of *Edwardsiella ictaluri*, the etiologic agent of enteric septicemia of channel catfish, led to growth delay, and this attenuated strain could be used as a vaccine to activate fish immune system (Kalindamar et al., 2019). Further investigation in *E. coli* indicated that lack of IscX caused a mild defect on IscR repressor (1.8-fold), FNR activator (1.2-fold), Sdh (1.3-fold) and Nuo (1.5-fold) activities (Giel et al., 2013; Roche, Huguenot et al., 2015). Altogether these data indicate that IscX modestly but significantly favors maturation of Fe-S proteins *in vivo*.

CyaY and IscX shared biochemical properties as they both bind iron with low affinity and form a ternary complex with IscS and IscU, yet they might carry on distinct specific function since an additive effect on maturation of Fe-S proteins was observed when combining both $\Delta iscX$ and $\Delta cyaY$ mutations (Bou-Abdallah, Adinolfi, Pastore, Laue, & Chasteen, 2004; Kim, Bothe, Frederick, Holder, & Markley, 2014; Pastore et al., 2006; Roche, Huguenot et al., 2015; Shi et al., 2010; Tokumoto et al., 2002). Recent biochemical studies suggested IscX can bind to two adjacent sites on IscS (Adinolfi et al., 2018). A first high affinity site would be bound by IscX at low concentration and would prevent CyaY binding. At high concentration, IscX would bind its second site and could mimic CyaY (Adinolfi et al., 2018).

3.1.6 *The acyl carrier protein ACP*

In eukaryotic cells, both iron-sulfur clusters biogenesis and the FASII pathway of fatty acids biosynthesis are hosted in the mitochondria. Recently, an unexpected link has been established between Fe-S cluster biogenesis and

fatty acids metabolism through an interaction between the Nfs1-Isd11 complex and the acyl carrier protein (ACP). ACP covalently binds the nascent acyl chain *via* a phosphopantetheine moiety, thus distributing acyl chains to Fas proteins responsible for maturation and elongation of fatty acids (for review, see [Nowinski, Van Vranken, Dove, & Rutter, 2018](#)). The link between Fe-S biogenesis and fatty acids biosynthesis has been discovered by immunoprecipitation of mitochondrial ACP and identification of the interacting proteins ([Van Vranken et al., 2016](#)). Interestingly, this link was also pointed out by serendipity when endogenous *E. coli* ACP was found to copurify with Nfs1 and Isd11 over expressed in *E. coli* ([Cai, Frederick, Tonelli, & Markley, 2017](#)). Further functional studies performed in *S. cerevisiae* have reinforced this link showing that partial depletion of ACP leads to a defect in maturation of Fe-S cluster-containing enzymes such as aconitase ([Van Vranken et al., 2016](#)). Structural characterization of the complex has shown that a quaternary complex is formed with two Isd11 units at the interface between a Nfs1 dimer and two acylated ACP units ([Boniecki et al., 2017](#); [Cory et al., 2017](#)). The Isd11 protein, also known as LYRM4, belongs to the large family of LYRM (Tyrosine-Lysine-Arginine Motif) proteins mainly located into mitochondria and associated with the OXPHOS complexes ([Adam et al., 2006](#), for review see; [Angerer, 2015](#)). Interestingly, interaction was observed between acylated ACP and most others members of the LYRM proteins (for review see [Masud, Kastaniotis, Rahman, Autio, & Hiltunen, 2019](#)).

Very few lines of evidence regarding a potential link between Fe-S cluster biogenesis and fatty acid metabolism exist in bacteria. In *E. coli*, a wide screening of ACP interactants by TAP purification method and a MALDI peptide mapping has revealed an interaction between ACP and IscS ([Gully, Moinier, Loiseau, & Bouveret, 2003](#)). This interaction requires the presence of the invariant serine of ACP (Ser36), on which the phosphopantetheine acyl binding module is bound, and the presence of the cysteine 328 of the IscS active site. It is interesting to recall that there is no Isd11 homolog in bacteria. Whether another yet unknown protein could act as a linker between IscS and ACP remains to be tested. Alternatively, a direct interaction between IscS and ACP could be thought of. Indeed, Nfs1 and IscS share 60% of sequence identity, but some structural differences have been highlighted ([Boniecki et al., 2017](#); [Cory et al., 2017](#)). In particular the region of Nfs1 interacting with Isd11 is composed of hydrophobic side chains whereas in IscS this same region is hydrophilic. Knowing that the interaction between Isd11 and ACP is mainly through hydrophilic side chains, we could

envision that in bacteria the interaction between ACP and IscS is direct and does not require any connecting protein.

The biological significance of a cross-talk between Fe-S cluster biogenesis and fatty acids metabolism is mysterious. The pool of acylated ACP is dependent on the availability of acetyl-CoA that also reflects the energetic status of the cell. Maturation of Fe-S proteins is crucial for major metabolic pathways and cell bioenergetics. Thus, a potential lead would be that the cell uses the level of acylated ACP as a nutrient sensor for Fe-S cluster production to fit to cell's metabolic needs and demands.

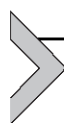
3.2 Global architecture of the cysteine desulfurase/scaffold core assembly complex

Structures of *E. coli* apo-(IscS-IscU)₂ and *A. fulgidus* ([2Fe-2S]-(IscS-IscU_{D35A}))₂ complexes were obtained by X-ray crystallography. In both cases, a homodimer of IscS interacts with IscU monomers forming an elongated S-shaped hetero-tetrameric protein complex (Marinoni et al., 2012; Prischi et al., 2010; Shi et al., 2010). In the IscS homodimer, each protomer has an active site close to the surface near the dimer interface and contains the PLP group at the base of a pocket (Cupp-Vickery, Urbina, & Vickery, 2003). Structures of IscU from *Haemophilus influenzae* and *Aquifex aeolicus*, determined both by NMR and X-ray crystallography, consist in an α - β sandwich architecture with a three-stranded antiparallel β -sheet and five α -helices (Ramelot et al., 2004; Shimomura et al., 2008). Crystal structure and cryo-electron microscopy of the human (NFS1-ISD11-ACP-ISU)₂ complex confirmed that two ISU scaffold monomers are bound at opposite tips of the NFS1 cysteine desulfurase dimer (Boniecki et al., 2017; Fox et al., 2019). Therefore, the cysteine desulfurase/scaffold core complex contains two structurally distant Fe-S cluster assembly sites.

In the *E. coli* IscS/IscU and human NFS1/ISCU complexes, the catalytic Cys residue of the cysteine desulfurase is located in a disordered region (Cys loop), but was estimated to be too far from any of the three Fe-S cluster ligands of the scaffold for sulfur transfer, unless movement of the loop occurred (Boniecki et al., 2017; Shi et al., 2010). Such movement was probably hampered in the structure of the complex when either a [2Fe-2S] cluster or a zinc ion occupies the Fe-S cluster assembly site in the IscU/ISCU scaffold (Boniecki et al., 2017; Fox et al., 2019; Marinoni et al., 2012). Thus, during Fe-S cluster assembly, the Cys loop is predicted to move from the PLP cofactor binding site to the Fe-S cluster building site, with a trajectory estimated to be 14 and 27 Å in the *A. fulgidus* and human

complexes, respectively (Fox et al., 2019; Marinoni et al., 2012). Recently, the catalytic loop of a type I cysteine desulfurase (NifS of *Hydrogenimonas thermophila*) was crystallized (Nakamura et al., 2019). Interestingly, this revealed that conformational and topological change of the Cys catalytic loop may take place in a stepwise manner through the transition of a β -sheet to a random-coiled state of the loop (Nakamura et al., 2019). Given the sequence and structural similarities between type I cysteine desulfurase, rearrangement might also occur in IscS but this remains to be demonstrated.

Very recently, the cryo-electron microscopy structure of the FXN-bound human ISC assembly complex showed that FXN binds simultaneously with both NFS1 subunits of the complex, in agreement with previous predictions from crosslinking, SAXS and NMR studies (Boniecki et al., 2017; Cai, Frederick, et al., 2018; Fox et al., 2019; Prischi et al., 2010). Importantly, this requires NFS1 to be in a homodimeric arrangement as described in the structure reported by Boniecki et al. (2017), but is incompatible with the structure proposed by Cory et al., wherein an extensive NFS1 homodimer interface was not observed (Boniecki et al., 2017; Cory et al., 2017).



4. Fe-S cluster delivery step

4.1 Chaperones to release Fe-S cluster from the ISC scaffold

The *E. coli isc* operon encodes a chaperone/co-chaperone duo, HscA and HscB, which belongs to the Hsp70 and J-protein families, respectively (Mayer & Gierasch, 2019). The ISC machinery is dependent on these Hsp70/J-protein chaperones for cluster transfer to recipient apo-proteins (Fig. 4). Hence, the activity of Fe-S proteins is drastically impaired upon depletion of the *S. cerevisiae* HscA and HscB counterpart, despite that Fe-S cluster is still formed on the IscU scaffold (Dong et al., 2017; Mühlenhoff et al., 2003). These results indicated that HscAB act downstream from IscU in the ISC pathway. *In vitro* kinetic studies of Fe-S cluster transfer from holo-IscU to apo-client reported that *E. coli* and *A. vinelandii* HscAB increased the rate of transfer from [2Fe-2S]-IscU to apo-Fdx and apo-Grx5, respectively (Chandramouli & Johnson, 2006; Dutkiewicz et al., 2006; Shakamuri, Zhang, & Johnson, 2012; Vickery & Cupp-Vickery, 2007; Wu, Mansy, & Cowan, 2005).

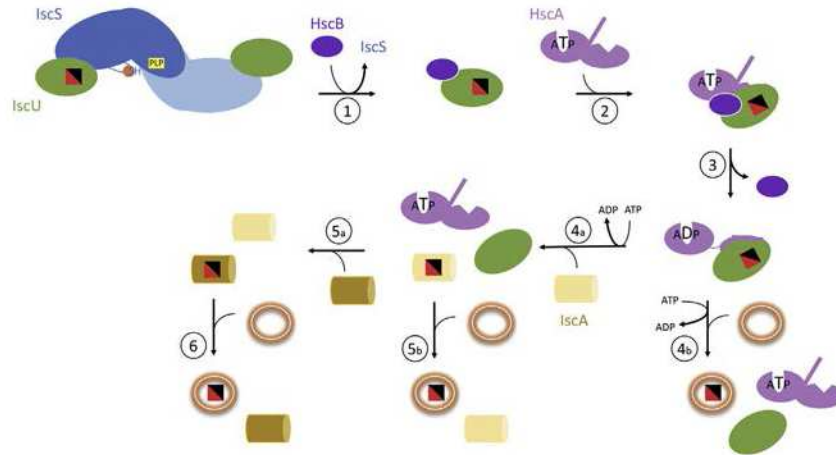


Fig. 4. Model for the chaperone-mediated Fe-S cluster transfer from IscU and delivery to targets. (1) HscB binds to holo-IscU that dissociates from IscS. (2) HscB targets holo-IscU to the ATP-bound form of HscA. When ATP is bound to HscA, holo-IscU has an easy access to the peptide binding pocket of HscA that recognizes the LPPVK sequence. ATP bound-HscA is defined as an open state because the lid of HscA, which traps the substrate, is open. This led to a temporary holo-IscU/ATP-HscA/HscB complex in which ATP hydrolysis occurs. (3) Following ATP hydrolysis, the resulting conformational change is transmitted to the lid of HscA, a closed state is formed which stabilizes IscU-HscA interaction, and HscB is released. (4a, b) Consequently to ATP hydrolysis, the Fe-S cluster is transferred to a late acting factor, such as the Fe-S cluster carrier IscA (a) or directly to target proteins (b). IscU is released from HscA upon rebinding of ATP, and it can again interact with IscS to assemble another Fe-S cluster. (5a, b) The carrier, such as IscA can deliver its cluster to another late acting factor (a) or directly to target proteins (b). (6) Last, after Fe-S cluster relay between late acting factors which might also include a [2Fe-2S] to [4Fe-4S] clusters convertor (see main text) the cluster is eventually transferred to the targets.

The Hsp70 chaperones fulfill their physiological role thanks to cyclic interaction with short hydrophobic stretches of their substrates. As a matter of fact, HscA binding to the LPPVK sequence motif of IscU has been thoroughly demonstrated using techniques such as pull-down assay and peptide array (Cupp-Vickery, Peterson, Ta, & Vickery, 2004; Dutkiewicz et al., 2004; Hoff, Ta, Tapley, Silberg, & Vickery, 2002; Tapley & Vickery, 2004). Actually, the LPPVK sequence resembles the substrate recognition consensus motif of DnaK (Rüdiger, Buchberger, & Bukau, 1997). The interaction of HscA with IscU is transient and regulated by a sophisticated allosteric mechanism that couples ATP hydrolysis and ATP rebinding in their nucleotide-binding domain (NBD) with binding and release of

substrate polypeptides. A distinctive feature of HscA from members of the Hsp70 family is that the IscU-binding cycle of HscA is independent of nucleotide-exchange factors.

Despite extensive studies on the HscA binding cycle on IscU, how HscA allows the release of the cluster is still an open question. Hence it could be envisioned that through the cycle, the conformation of holo-IscU is “remodeled” in a way that it can no longer bind the Fe-S cluster. Alternatively, among the conformational isomers of holo-IscU having different affinity for its Fe-S cluster, HscA might stabilize an isomer with low Fe-S cluster affinity, thereby favoring the release of the Fe-S cluster from IscU (Bonomi, Iametti, Morleo, Ta, & Vickery, 2011).

The HscB protein does not have intrinsic chaperone activity but it binds and delivers IscU to HscA, and it stimulates HscA ATPase activity (Hoff, Silberg, & Vickery, 2000; Silberg, Tapley, Hoff, & Vickery, 2004). In HscB, the HscB-IscU binding interface involves a large interface with hydrophobic and electrostatics interactions that is distinct of its HscA recognition site (Dutkiewicz, Nowak, Craig, & Marszalek, 2017). In IscU, the HscB binding site contains residues that are also critical for the interaction with IscS (Majewska et al., 2013; Prischi et al., 2010). These results suggest that IscS and HscB might act sequentially on IscU, with IscS first and HscB after Fe-S cluster formation on IscU. Consistent with this hypothesis, IscS and HscB bind preferentially to the D state and S state of IscU, respectively (Cai et al., 2013; Hoff et al., 2000; Kampinga & Craig, 2010; Kim et al., 2009). More recently, a direct interaction was shown between the HscB protein and the cysteine desulfurase suggesting that the HscB protein/scaffold interaction might be initiated while the scaffold was still in complex with cysteine desulfurase, (Majewska et al., 2013; Puglisi, Yan, Adinolfi, & Pastore, 2016). Thus, an attractive hypothesis is that HscB protein is a key actor in the transition between Fe-S cluster assembly and transfer steps.

4.2 Multiplicity of carriers to deliver Fe-S clusters

Once built within the machinery core, Fe-S clusters are targeted to apo-protein clients by so-called carriers. Conceptually, they serve as intermediates and were not defined as modifying the clusters they received. However, a series of experiments, mostly in eukaryotic systems, lend credence to the idea that carriers would not only transport but transform [2Fe-2S] clusters into [4Fe-4S] clusters. It might be that not all carriers behave the same. In particular Grx5 in eukaryotes was spotted as a [2Fe-2S] to [4Fe-4S] clusters convertor (for review see Braymer & Lill, 2017). But it might also be that it

depends upon the final apo-target. For instance, in *E. coli*, a carrier independent delivery route exists for maturing IscR, which hosts a [2Fe-2S] cluster, whereas maturation of the [4Fe-4S] cluster containing NsrR depends strictly on carriers (Vinella et al., 2013).

The number of carriers varies with the different bacterial species. *E. coli* for instance synthesizes 6 of them, *i.e.* IscA, SufA, ErpA, NfuA, GrxD and Mrp, while *Bacillus subtilis* is predicted to have only one, *i.e.* YutM (for review see Roche et al., 2013). The fact is that the number of apo-targets clients (ca. 150 in *E. coli*) always exceeds by far the number of carriers and this sets the question of the dynamic of the delivery network. Are all carriers able to transfer clusters to all apo-targets or is there some sort of privileged partnership? While *in vitro* transfer assays provided evidences that all carriers listed above were actually able to transfer clusters, they did not reveal much difference among them in terms of substrate specificity. In *E. coli*, regulation studies showed that the 6 carriers are not synthesized within the same conditions and genetic control was proposed to orchestrate the use of carriers. The best illustration of genetic control of redundancy is to be given by A-type carriers IscA, SufA, ErpA, which are synthesized under different iron concentration. IscA would be used for balanced iron concentration, SufA for low iron concentration and ErpA would intervene within the transition from low to high (Mandin, Chareyre, & Barras, 2016). The *nfuA* gene is under holo-IscR repression (see below) and is predicted to be synthesized under the same conditions as ErpA (Angelini et al., 2008). Like *sufA*, the *grxD* gene is increased upon iron depletion and thus GrxD is expected to intervene in these conditions (Fernandes et al., 2005). Phenotypic characterization of mutants of each carrier failed to reveal specificity, yet some trend could be observed. For instance, a *nfuA* mutation appeared to affect both complex I activity and complex II, whereas the *mrp* mutant was affected for complex I activity but not for complex II (Burschel et al., 2019; Py et al., 2012, 2018). However, in most cases, the absence of a single carrier failed to yield a total loss of maturation of any of the Fe-S protein tested. This indicated that carriers exhibit to some extent functional redundancy. Alternatively, this might point out existence of a carrier-free by-pass permitting transfer to apo-targets like it was mentioned above in the case of IscR maturation.

The case of ErpA illuminates the complexity of the *in vivo* situation. ErpA was identified as being absolutely essential for *E. coli* to grow under aerobiosis and this essentiality was attributed to the role of ErpA in maturing the essential IspG/H proteins within the iso-pentenyl-phosphate

(IPP) biosynthesis pathway (Loiseau et al., 2007). This created some confusion in the community in giving the idea that ErpA was specific for the maturation of IspG/H and conversely, IspG/H strictly dependent upon ErpA. This is wrong in two ways. First, ErpA was found to be important for the maturation of most Fe-S enzymes tested, ruling out the idea of ErpA as a specific dedicated carrier for IspG/H (Loiseau et al., 2007; Py et al., 2018; Vinella et al., 2013). Second, under anaerobiosis, IscA can substitute to ErpA for IspG/H maturation, showing that biochemically IscA and ErpA share similar capacity (Loiseau et al., 2007; Vinella, Brochier-Armanet, Loiseau, Talla, & Barras, 2009). Recently, ErpA was found to interact with NfuA such as to optimize transfer under oxidative stress (Py et al., 2018). This in-depth analysis of ErpA points out the paramount influence of growth conditions in the choice of the circuits used by Fe-S clusters to reach their apo-targets. Growth conditions can influence different levels of the overall delivery process (or any Fe-S cluster biogenesis step as a matter of fact). First, stability of Fe-S cluster varies in face of O₂, depending upon which carriers it is bound to. Likewise, we recently found that NfuA provided a very high Fe-S cluster stability whereas IscA provided the lowest. The high stability conferred by NfuA - as compared with the others carriers - revealed intrinsic biochemical differences between carriers, which could help to understand why the cell will choose one over the other as a function of oxygen tension level. Second, number of Fe-S cluster utilizing proteins being synthesized will vary depending upon growth conditions. These changes in the cellular demand will have to be met by the cell which will select which carrier(s) to use accordingly. To conclude, current available information suggests that apo-clients can benefit from most, if not all, carriers for getting their cluster and that there is no substrate specificity in the biochemical sense. However, intrinsic feature and genetic control of synthesis orchestrate this potential redundancy such that cells respond to cellular Fe-S cluster demand in the most appropriate and economic way within a given environmental condition.



5. Regulation of Fe-S cluster biogenesis

5.1 IscR, master and commander of Fe-S cluster biogenesis systems usage

In several bacteria, the master regulator of Fe-S cluster homeostasis is the transcriptional factor (TF) IscR. Our understanding of IscR function

stems mainly from genetic, molecular, biochemical and structural analyses on the *E. coli* IscR. IscR belongs to the Rrf2 family of winged helix-turn-helix TF. It contains a [2Fe-2S] cluster, which allows sensing aerobiosis, oxidative stress, iron limitation and possibly nitrous stress (Rajagopalan et al., 2013; Schwartz et al., 2001; Yeo, Lee, Lee, & Roe, 2006). Mutagenesis and structural studies have identified residues Cys92, Cys98, Cys104 and His107 as ligands for the cluster (Fleischhacker et al., 2012). A His ligand is quite uncommon and this might render the cluster labile, hence sensitive to the stress signals cited above. Both apo- and holo-forms of IscR bind DNA and have regulatory functions. Two types of binding sites, Type 1 and 2, can be found within IscR-regulated promoters (Giel, Rodionov, Liu, Blattner, & Kiley, 2006; Nesbit, Giel, Rose, & Kiley, 2009). Type 1 site is only bound by the holo-form of IscR whereas Type 2 site can be bound by both the holo- and apo-forms (Mettert & Kiley, 2014).

In *E. coli*, the *iscR* gene is the first gene of the *isc* operon and is separated from the following gene, *iscS*, by a relatively large intergenic region (111 bp). This region contains a binding site for RyhB, a small regulatory RNA (sRNA) repressed by Fur, allowing down regulation of the downstream *iscSUA* genes of the *isc* operon when iron is limiting (Desnoyers, Morissette, Prévost, & Massé, 2009). Holo-IscR acts as a repressor of the *isc* operon, which results in lowering expression of the *isc* operon to the point where IscR is under its apo-form and its levels are reduced (Giel et al., 2006; Schwartz et al., 2001). At this point, the repression is alleviated, more IscR is synthesized that gets its cluster from the ISC system and the homeostatic negative feedback loop operates again (Fig. 5). Expression of the operon encoding the second Fe-S cluster biogenesis machinery of *E. coli*, *suf*, is also under IscR control. As a matter of fact, IscR has been shown to be essential for SUF expression through its binding to a Type 2 site found in the *suf* promoter (Giel et al., 2013; Mettert & Kiley, 2014; Yeo et al., 2006). Interestingly, this regulation does not require the cluster bound form of IscR (Nesbit et al., 2009; Yeo et al., 2006). The IscR-dependent activation of *suf* benefits of the increase in IscR protein levels that arises under environmental conditions that cause the loss of its [2Fe-2S] cluster and alleviate *isc* repression.

5.2 New roles for IscR beyond Fe-S cluster biogenesis regulation

IscR regulatory function goes beyond Fe-S cluster biogenesis machineries usage. In fact, IscR was shown to regulate more than 40 genes in *E. coli*,

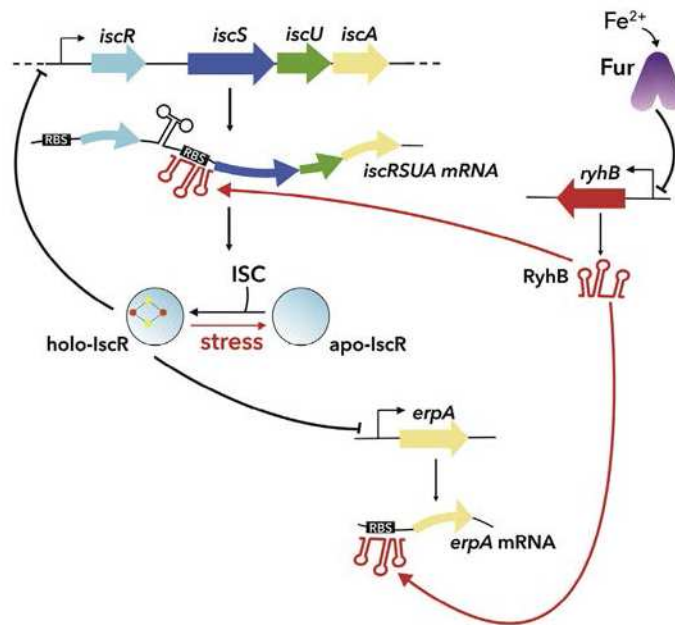


Fig. 5 Regulation of the *E. coli* *isc* operon. Under optimal growth conditions, IscR is matured by the ISC machinery. Holo-IscR represses *isc* expression, resulting in an homeostatic circuit that senses the cellular Fe-S cluster demand. Under iron limitation, Fur repression of *ryhB* expression is alleviated. RyhB targets the *iscSUA* mRNA for degradation and consequently IscR accumulates in its apo-form that no longer represses *isc* expression. The expression of the A-type carrier *ErpA* is repressed under high iron conditions by holo-IscR and under low iron conditions by RyhB. At intermediate iron concentration, both repressions are alleviated and *erpA* is maximally expressed.

among which the ATCs *erpA* and *nfuA*, Fe-S enzymes and other genes ending functions not directly related to Fe-S cluster biology such as bio-film formation or RNA metabolism (Giel et al., 2006; Martin & Imlay, 2011; Otsuka et al., 2010; Wu & Outten, 2009). Apart from *E. coli*, IscR is widely conserved and was studied in several bacteria, including pathogens such as *Erwinia chrysanthemi*, *Pseudomonas aeruginosa*, *Vibrio vulnificus*, *Xanthomonas campestris*, *Salmonella enterica* and *Yersinia pseudotuberculosis* (Choi et al., 2007; Fuangthong et al., 2015; Jones-Carson et al., 2008; Lim & Choi, 2014; Miller et al., 2014; Rincon-Enriquez, Cr  te, Barras, & Py, 2008; Zbell, Benoit, & Maier, 2007). Because it is so central to cellular bioenergetics and metabolism, Fe-S cluster-based biology is expected to be important in bacterial fitness and multiplication within its host. Moreover, both iron limitation and oxidative stress are hallmarks of conditions met by

pathogens during the invading process, and it was thus foreseeable that IscR be instrumental in coordinating adaptation to such conditions.

Less expected however was that IscR would directly control synthesis of key virulence determinants as it was reported in *S. enterica* and *Y. pseudotuberculosis*. Both pathogens rely on Type 3 secretion systems (T3SS) devices to inject effectors in the host cells. IscR was found to control synthesis of both T3SS in the two bacterial species. *S. enterica* synthesizes two T3SS, encoded by the so called pathogenicity island SPI1 and SPI2. SPI1 is required for passage of the bacterium across the epithelial border while SPI2 is required for *S. enterica* to establish a Salmonella-containing vacuole into macrophages. SPI1 carries *hilD*, which controls its own synthesis and that of effectors (Ellermeier, Ellermeier, & Slauch, 2005). A Type 2 IscR binding site arises upstream of the *hilD* gene and IscR binding was proposed to interfere with HilD positive autoregulation, lowering virulence (Vergnes et al., 2017). Consistently, an *iscU* mutant, which has high level of IscR, exhibited reduced invasion capacity in epithelial cells and virulence attenuation in mice. Conversely, an *iscR* mutant was hyper-invasive in HeLa cells.

In *Y. pseudotuberculosis*, like in Salmonella, IscR was shown to bind a Type 2 motif within the promoter of a master TF, *lcrF*, located within a T3SS (Miller et al., 2014). LcrF regulates T3SS contained effectors and thereby virulence (Miller et al., 2014). IscR is required for full expression of *lcrF*, and thereby full synthesis of T3SS encoded effectors. Consistently, IscR was found to be essential for T3SS-dependent secretion and an *iscR* mutant was deficient in colonization of the Peyer's patches, spleen and liver in mice. Thus, these two human pathogens recruited IscR to orchestrate their virulence program in targeting TTSS regulation although in opposite ways, *i.e.* an activator in *Yersinia* and a repressor in *Salmonella*. Interestingly in both cases, it seems to be the amount of IscR that matters rather than its actual maturation state, as one would have expected if *iscR* was to signal iron limitation and/or ROS directly to T3SS expression. However, the actual maturation state of IscR might still have indirect influence on T3SS effectors synthesis as IscR expression is under its own autoregulatory control.

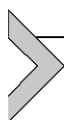
From what has been observed in *E. coli* it is likely that IscR regulon in pathogen bacteria will extend beyond T3SS. Contribution to pathogenicity of other targets is expected, to begin with the whole series of Fe-S cluster biogenesis and carrier systems but also anti-ROS defenses. As a matter of fact, IscR contribution to *P. aeruginosa* virulence and oxidative stress resistance was attributed to its control of the KatA catalase and to its negative regulation of the peroxydase Tpx expression (Kim et al., 2009;

Saninjuk, Romsang, Duang-Nkem, Vattanaviboon, & Mongkolsuk, 2019; Somprasong et al., 2012). IscR was also shown to bind upstream of *afaA* to activate CFA/I fimbriae production in response to iron starvation (Fuangthong et al., 2015; Haines et al., 2015). In *V. vulnificus*, disruption of *iscR* resulted in a reduction in motility and adhesion to epithelial cells, as well as resistance to ROS (Lim & Choi, 2014).

Gene expression regulation often involves multiple transcriptional regulators, which may compete (or synergize) for closely located operator sites. IscR was suggested to counteract activation by HilD as stated above (Vergnes et al., 2017) (see above) and was found to be counteracted by Fur in several cases (Lee, Yeo, & Roe, 2008; Seo et al., 2014). Other multifactorial situations involving IscR were recently described. The first one unearthed an unexpected role of IscR in cell-to-cell variability providing fitness advantage during shift from aerobiosis to anaerobic trimethyl amine oxide (TMAO) respiration in *E. coli* (Carey et al., 2018). TMAO reductase synthesis is under the control of the two-component system, TorR/S. In the presence of O₂, the level of TorR/S is so low that stochastic effect prevails yielding to cell-to-cell variability in TMAO reductase synthesis. IscR was found to be determining in this «regulated stochasticity» by acting upstream in the cascade, controlling the level of TorT and TorS proteins, hence mediating the oxygen regulation of cell-to-cell variability. The proposed mechanism is that IscR repression allows only for very limited production of TorT/S and consequently of TMAO reductase. Given that the promoters of *torS* and *torT* are Type 2 promoters is likely that environmental condition affecting the cluster bound state and the amounts of IscR (such as oxidative stress or iron limitation) will influence stochasticity of expression of *torS* and *torT*, but this remains to be evaluated. The second study revealed how acting at both transcription and translation initiation permits to express a gene within a narrow iron concentration range. *E. coli* synthesizes multiple Fe-S cluster carriers and the question of the redundancy has been a matter of debate for long. The *erpA* gene expression is negatively regulated by holo-IscR, *i.e.* under high iron conditions, and also negatively regulated by RyhB, *i.e.* under iron limitation, yielding to the prediction that ErpA synthesis would always be repressed. In fact, there is a window of iron concentration, referred to as intermediate, at which both IscR and RyhB repressions are alleviated (Mandin et al., 2016). The added value of this double control is that it limits redundancy by synthesizing each of the three carriers at different iron concentration range, *i.e.* SufA at low, ErpA at intermediate

and IscA at high iron concentration, yet it insures a continuing presence of at least one carrier throughout fluctuating iron concentrations.

Finally, IscR functional homologs (*i.e.*, Fe-S cluster-containing TFs that control at least the expression of one Fe-S cluster biogenesis systems) have been identified in other bacterial species. In *Rhodobacter sphaeroides*, an IscR homolog binds an Fe-S cluster through an atypical motif with only one Cys residue (Remes, Eisenhardt, Srinivasan, & Klug, 2015). In its cluster bound form, it represses genes involved in iron metabolism, including that of the operon encoding its own gene as well as a hybrid IscS-Suf system. In *Agrobacterium tumefaciens*, another Rrf2 TF, RirA, controls the expression of a *suf* operon in response to iron concentration (Bhubhanil, Niamyim, Sukchawalit, & Mongkolsuk, 2014). Another regulator named SufR is conserved in cyanobacteria and regulates the expression of a SUF biogenesis machinery which is the only system in these bacteria (Seki et al., 2006; Shen et al., 2007; Wang et al., 2004; Willemse et al., 2018). SufR has been shown to have other direct and indirect functions in the cells, including photosynthesis and central metabolism, again demonstrating that Fe-S cluster biogenesis has a central role in a wide diversity of pathways (Vuorijoki, Tiwari, Kallio, & Aro, 2017). Recently, a SufR homolog has also been identified in *Mycobacterium tuberculosis*, displaying apparently similar functions (Willemse et al., 2018). Further studies on such Fe-S cluster biogenesis regulator will surely shed some light on Fe-S cluster biogenesis control and beyond.



6. Evolution

Fe-S clusters are present in the three domains of life. The use of Fe-S clusters to catalyze biological processes can be traced back to the last common ancestor (Weiss et al., 2016). Phylogenetic analyses established that Fe-S proteins were among the most ancient and widely distributed (David & Alm, 2011; Dupont, Butcher, Valas, Bourne, & Caetano-Anollés, 2010). Prior to the widespread oxidation of Earth's atmosphere by photosynthetic organisms about 2.5 billion years ago, organisms lived in anoxic atmosphere in which iron and sulfur were plentiful and then were recruited in the formation in Fe-S clusters. The appearance of an O₂-enriched atmosphere decreased the bioavailability of metal such ferric iron and exposed microorganisms to potentially deleterious reactive oxygen species (David & Alm, 2011; Touati, 2000). Life forms have evolved various strategies for

coping with increased oxygen, such as employing protein scaffolds to shield Fe-S clusters from oxygen, expressing oxygen scavenging enzymes to keep oxygen levels low, using alternative oxygen-stable cofactors or generating altogether new pathways that are free of Fe-S clusters (Andreini, Rosato, & Banci, 2017; Imlay, 2006).

Recently, the theory that Fe-S proteins is a variable under evolutionary pressure depending on O₂ level has received support from a bioinformatic analysis that compared the usage of Fe-S clusters in 400 prokaryotic organisms with different life styles, and in particular with different O₂ requirements (Andreini et al., 2017). It was shown that the number of Fe-S proteins of a given organism depends on its genome size and on its capacity to use (or not) O₂ for growth. Hence, the fraction of Fe-S proteins is clearly lower for the genomes of aerobic bacteria than anaerobic ones. The most common Fe-S proteins in both groups of organisms are those involved in energy production and conversion, amino acid metabolism and Fe-S cluster biogenesis and are mainly composed of [4Fe-4S] type cluster (Andreini et al., 2017). However, anaerobes exhibit more than twice Fe-S proteins involved in specific energy production and conversion linked to the nature of the final electron acceptor(s) in the respiratory processes. The oxygenation of earth induced the use of oxygen as a terminal oxidant requiring only the creation of a cytochrome oxidase for all aerobes. On the contrary, electron acceptors used in anaerobic respiration are various and necessitate to adapt anaerobic chain components to highly reduced substrates. The Fe-S protein families that are specific to aerobes are involved in various functional processes, but the striking feature is that these families are mainly composed of [2Fe-2S] proteins (Andreini et al., 2017). Aerobes probably favored this strategy to use more stable and less Fe demanding [2Fe-2S] cluster in an oxygenic atmosphere (Andreini et al., 2017).

Depending on aerobic versus anaerobic metabolic status, Fe-S cluster biogenesis systems have to face two distinct problematics: mature a large number of Fe-S proteins in a reducing environment conducive to the assemblage of Fe-S clusters, or mature less Fe-S proteins in low Fe availability and oxidative Fe-S cluster damaging conditions. Interestingly, we have found that the two δ -proteobacteria, *D. vulgaris* Hildenborough, a strict anaerobe, and *M. xanthus*, a strict aerobe, exhibit widely different Fe-S cluster biogenesis factors. The percentage of number of putative Fe-S proteins is 4,4% for *D. vulgaris* Hildenborough and 1,3% for *M. xanthus* (Andreini et al., 2017). Hence, to mature about 154 predicted Fe-S proteins, *D. vulgaris* Hildenborough possesses solely a reduced version of the ISC system, containing only a

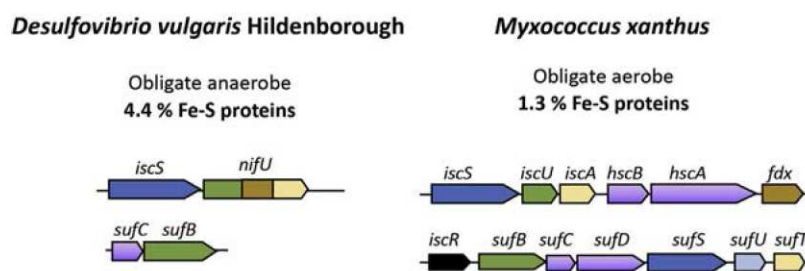
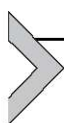


Fig. 6 Fe-S proteins and Fe-S cluster biogenesis components in *Desulfovibrio vulgaris* Hildenborough and *Myxococcus xanthus*. The percentage of putative Fe-S cluster-containing proteins as a function of the genome size in the obligate anaerobe, *D. vulgaris* Hildenborough, and the obligate aerobe *M. xanthus* is indicated. Schematic organization of the *isc* and *suf* locus in *D. vulgaris* Hildenborough and *M. xanthus*. Genes having similar functions are color-coded for their encoding domain; cysteine desulfurase (blue) sulfur relay (pale blue), ferredoxin (brown), scaffold protein (green), co-/chaperone components (purple), carrier (beige), transcriptional regulator (black). The *M. xanthus* ISC system is identical to *E. coli* except that it lacks *iscX* and that *iscR* locates upstream the *suf* operon. Such as previously described in *Helicobacter pylori*, the ISC system in *D. vulgaris* Hildenborough is constituted by a cysteine desulfurase (IscS) and a modular NifU protein that contains an IscU-type scaffold domain, a Fdx-type ferredoxin domain and an Nfu-type Fe-S cluster carrier domain (Olson, Agar, Johnson, & Maier, 2000). The *D. vulgaris* Hildenborough SUF system is only composed of the minimal functional core SufB and SufC that constitute the simplest *suf* operon (Boyd, Thomas, Dai, Boyd, & Outten, 2014; Garcia et al., 2019; Takahashi & Tokumoto, 2002; Tokumoto, Kitamura, Fukuyama, & Takahashi, 2004).

cysteine desulfurase and a scaffold, and a putative degenerated Suf system (Fig. 6). In contrast, to mature 94 predicted Fe-S proteins, *M. xanthus* has a full version of ISC, and a full version of SUF (Fig. 6). One should be cautious as additional Fe-S cluster biogenesis factors, which cannot be identified based upon current knowledge, might arise. But this comparison illustrates quite convincingly how organisms invested in a different number of biogenesis factors as a function of the level of oxygen occurring in different niches.



7. Conclusion

In 2005, we were invited to write a chapter in the same Advances in Microbial Physiology series on “How *Escherichia coli* and *Saccharomyces cerevisiae* build Fe-S proteins”. At the time this was an emerging topic, at least for what concerned the *in vivo* side. It is an undisputable fact that these last two decades, a lot has been learned on how living organisms make, and use Fe-S

clusters and, conversely, how not to do it can breed dreadful consequences, as illustrated by the increasing number of pathologies recognized to be caused by Fe-S deficiencies. Yet, it is surprising to see how many issues thought to be of primary importance at the time have remained unsolved. In our own words “The most important theme emerging from the current research relates to iron metabolism. What are the iron sources used for Fe-S biogenesis? (...) As an intracellular source, frataxin clearly appears as an iron donor to the ISC system in eukaryotes”. As we stated it in the present review, and as it was pointed out in multiple reviews, we are still totally ignorant of where iron comes from. The idea of a dedicated unique source is clearly the least likely as no mutant has ever been obtained that would exhibit the expected phenotype. Is this telling us that many redundant iron sources arise? Next years of research might give us this answer. Regarding frataxin, a role as a regulator rather than an iron donor, is the privileged hypothesis. Progress achieved by cry-electron microscopy in elucidating structure of the ISC assembly complex process will undoubtedly help to confirm and/or decipher the frataxin role but also those of ferredoxin and IscX. Complexes trapped at different steps in the Fe-S assembly provided by genetic approaches will certainly help toward this goal. Another new exciting perspective mentioned in this review is the unexpected cross-talk between Fe-S biogenesis and fatty acid biosynthesis. Deciphering its biological significance, its evolutionary advantage and its mechanistic basis will be exciting issues to entertain.

Acknowledgments

Thanks are due to members of the Barras and the Py groups for help with the manuscript and discussion. Work in our laboratories was supported by grants from the Center National de la Recherche Scientifique, Aix-Marseille Université, Institut Pasteur, Agence Nationale de la Recherche (JPAIMR «Combinatorial», Blanc «FRACOL»), Agence Nationale de la Recherche Investissement d’Avenir Program (10-LABX-62-IBRID), ERACoBioTech « Iron Plug’n Play », Association Française de l’Ataxie de Friedreich.

References

- Adam, A. C., Bornhövd, C., Prokisch, H., Neupert, W., & Hell, K. (2006). The N61 interacting protein Isd11 has an essential role in Fe/S cluster biogenesis in mitochondria. *The EMBO Journal*, 25(1), 174–183.
- Adinolfi, S., Iannuzzi, C., Prisci, F., Pastore, C., Iametti, S., Martin, S. R., et al. (2009). Bacterial frataxin CyaY is the gatekeeper of iron-sulfur cluster formation catalyzed by IscS. *Nature Structural & Molecular Biology*, 16(4), 390–396.
- Adinolfi, S., Puglisi, R., Crack, J. C., Iannuzzi, C., Dal Piaz, F., Konarev, P. V., et al. (2018). The molecular bases of the dual regulation of bacterial iron sulfur cluster biogenesis by CyaY and IscX. *Frontiers in Molecular Biosciences*, 4, 97.

- Agar, J. N., Krebs, C., Frazzon, J., Huynh, B. H., Dean, D. R., & Johnson, M. K. (2000a). IscU as a scaffold for iron-sulfur cluster biosynthesis: Sequential assembly of [2Fe-2S] and [4Fe-4S] clusters in IscU. *Biochemistry*, *39*(27), 7856–7862.
- Agar, J. N., Zheng, L., Cash, V. L., Dean, D. R., & Johnson, M. K. (2000b). Role of the IscU protein in Iron-Sulfur cluster Biosynthesis: IscS-mediated assembly of a [Fe₂S₂] cluster in IscU. *Journal of the American Chemical Society*, *122*(9), 2136–2137.
- Andreini, C., Rosato, A., & Banci, L. (2017). The relationship between environmental dioxygen and iron-sulfur proteins explored at the genome level. *PLoS One*, *12*(1), e0171279.
- Angelini, S., Gerez, C., Ollagnier-de Choudens, S., Sanakis, Y., Fontecave, M., Barras, F., et al. (2008). NfuA, a new factor required for maturing Fe/S proteins in *Escherichia coli* under oxidative stress and iron starvation conditions. *The Journal of Biological Chemistry*, *283*(20), 14084–14091.
- Angerer, H. (2015). Eukaryotic LYR proteins interact with mitochondrial protein complexes. *Biology*, *4*(1), 133–150.
- Bedeckovics, T., Gajdos, G. B., Kisfal, G., & Isaya, G. (2007). Partial conservation of functions between eukaryotic frataxin and the *Escherichia coli* frataxin homolog CyaY. *FEMS Yeast Research*, *7*(8), 1276–1284.
- Bhubhanil, S., Niemyim, P., Sukchawalit, R., & Mongkolsuk, S. (2014). Cysteine desulfurase-encoding gene *sufS2* is required for the repressor function of RirA and oxidative resistance in *Agrobacterium tumefaciens*. *Microbiology*, *160*(Pt 1), 79–90.
- Blahut, M., Wise, C. E., Bruno, M. R., Dong, G., Makris, T. M., Frantom, P. A., et al. (2019). Direct observation of intermediates in the SufS cysteine desulfurase reaction reveals functional roles of conserved active-site residues. *The Journal of Biological Chemistry*, *294*(33), 12444–12458.
- Boniecki, M. T., Freibert, S. A., Mühlenhoff, U., Lill, R., & Cygler, M. (2017). Structure and functional dynamics of the mitochondrial Fe/S cluster synthesis complex. *Nature Communications*, *8*(1), 1287.
- Bonomi, F., Iametti, S., Morleo, A., Ta, D., & Vickery, L. E. (2011). Facilitated transfer of IscU-[2Fe₂S₂] clusters by chaperone-mediated ligand exchange. *Biochemistry*, *50*(44), 9641–9650.
- Bou-Abdallah, F., Adinolfi, S., Pastore, A., Laue, T. M., & Chasteen, D. N. (2004). Iron binding and oxidation kinetics in frataxin CyaY of *Escherichia coli*. *Journal of Molecular Biology*, *341*(2), 605–615.
- Boyd, E. S., Thomas, K. M., Dai, Y., Boyd, J. M., & Outten, F. W. (2014). Interplay between oxygen and Fe-S cluster biogenesis: Insights from the *suf* pathway. *Biochemistry*, *53*(37), 5834–5847.
- Braymer, J. J., & Lill, R. (2017). Iron-sulfur cluster biogenesis and trafficking in mitochondria. *The Journal of Biological Chemistry*, *292*(31), 12754–12763.
- Bühning, M., Friemel, M., & Leimkühler, S. (2017). Functional complementation studies reveal different interaction partners of *Escherichia coli* IscS and human NFS1. *Biochemistry*, *56*(34), 4592–4605.
- Burschel, S., Kreuzer Decovic, D., Nuber, F., Stiller, M., Hofmann, M., Zupok, A., et al. (2019). Iron-sulfur cluster carrier proteins involved in the assembly of *Escherichia coli* NADH:ubiquinone oxidoreductase (complex I). *Molecular Microbiology*, *111*(1), 31–45.
- Cai, K., Frederick, R. O., Dashti, H., & Markley, J. L. (2018a). Architectural features of human mitochondrial cysteine desulfurase complexes from crosslinking mass spectrometry and small-angle X-ray scattering. *Structure*, *26*(8), 1127–1136.e4.
- Cai, K., Frederick, R. O., Kim, J. H., Reinen, N. M., Tonelli, M., & Markley, J. L. (2013). Human mitochondrial chaperone (mtHSP70) and cysteine desulfurase (NFS1) bind preferentially to the disordered conformation, whereas co-chaperone (HSC20) binds to the

- structured conformation of the iron-sulfur cluster scaffold protein (ISCU). *The Journal of Biological Chemistry*, 288(40), 28755–28770.
- Cai, K., Frederick, R. O., Tonelli, M., & Markley, J. L. (2017). Mitochondrial cysteine desulfurase and ISD11 coexpressed in *Escherichia coli* yield complex containing acyl carrier protein. *ACS Chemical Biology*, 12(4), 918–921.
- Cai, K., Frederick, R. O., Tonelli, M., & Markley, J. L. (2018b). ISCU(M108I) and ISCU(D39V) differ from wild-type ISCU in their failure to form cysteine desulfurase complexes containing both frataxin and ferredoxin. *Biochemistry*, 57(9), 1491–1500.
- Campuzano, V., Montermini, L., Lutz, Y., Cova, L., Hindelang, C., Jiralerspong, S., et al. (1997). Frataxin is reduced in Friedreich ataxia patients and is associated with mitochondrial membranes. *Human Molecular Genetics*, 6(11), 1771–1780.
- Campuzano, V., Montermini, L., Moltò, M. D., Pianese, L., Cossée, M., Cavalcanti, F., et al. (1996). Friedreich's ataxia: Autosomal recessive disease caused by an intronic GAA triplet repeat expansion. *Science*, 271(5254), 1423–1427.
- Carey, J. N., Mettert, E. L., Roggiani, M., Myers, K. S., Kiley, P. J., & Goulian, M. (2018). Regulated stochasticity in a bacterial signaling network permits tolerance to a rapid environmental change. *Cell*, 173(1), 196–207.e14.
- Chandramouli, K., & Johnson, M. K. (2006). HscA and HscB stimulate [2Fe-2S] cluster transfer from IscU to apoferredoxin in an ATP-dependent reaction. *Biochemistry*, 45(37), 11087–11095.
- Chandramouli, K., Unciuleac, M.-C., Naik, S., Dean, D. R., Huynh, B. H., & Johnson, M. K. (2007). Formation and properties of [4Fe-4S] clusters on the IscU scaffold protein. *Biochemistry*, 46(23), 6804–6811.
- Choi, Y.-S., Shin, D.-H., Chung, I.-Y., Kim, S.-H., Heo, Y.-J., & Cho, Y.-H. (2007). Identification of *Pseudomonas aeruginosa* genes crucial for hydrogen peroxide resistance. *Journal of Microbiology and Biotechnology*, 17(8), 1344–1352.
- Cho, S. J., Lee, M. G., Yang, J. K., Lee, J. Y., Song, H. K., & Suh, S. W. (2000). Crystal structure of *Escherichia coli* CyaY protein reveals a previously unidentified fold for the evolutionarily conserved frataxin family. *Proceedings of the National Academy of Sciences of the United States of America*, 97(16), 8932–8937.
- Cory, S. A., Van Vranken, J. G., Brignole, E. J., Patra, S., Winge, D. R., Drennan, C. L., et al. (2017). Structure of human Fe-S assembly subcomplex reveals unexpected cysteine desulfurase architecture and acyl-ACP-ISD11 interactions. *Proceedings of the National Academy of Sciences of the United States of America*, 114(27), E5325–E5334.
- Cupp-Vickery, J. R., Peterson, J. C., Ta, D. T., & Vickery, L. E. (2004). Crystal structure of the molecular chaperone HscA substrate binding domain complexed with the IscU recognition peptide ELPPVKIHC. *Journal of Molecular Biology*, 342(4), 1265–1278.
- Cupp-Vickery, J. R., Urbina, H., & Vickery, L. E. (2003). Crystal structure of IscS, a cysteine desulfurase from *Escherichia coli*. *Journal of Molecular Biology*, 330(5), 1049–1059.
- Dahl, J.-U., Radon, C., Bühning, M., Nimtz, M., Leichert, L. I., Denis, Y., et al. (2013). The sulfur carrier protein TusA has a pleiotropic role in *Escherichia coli* that also affects molybdenum cofactor biosynthesis. *The Journal of Biological Chemistry*, 288(8), 5426–5442.
- Dahl, J. U., Urban, A., Bolte, A., Sriyabhaya, P., Donahue, J. L., Nimtz, M., et al. (2011). The identification of a novel protein involved in molybdenum cofactor biosynthesis in *Escherichia coli*. *The Journal of Biological Chemistry*, 286(41), 35801–35812.
- Das, D., Patra, S., Bridwell-Rabb, J., & Barondeau, D. P. (2019). Mechanism of frataxin “bypass” in human iron-sulfur cluster biosynthesis with implications for Friedreich's ataxia. *The Journal of Biological Chemistry*, 294(23), 9276–9284.
- David, L. A., & Alm, E. J. (2011). Rapid evolutionary innovation during an Archaeal genetic expansion. *Nature*, 469(7328), 93–96.

- Desnoyers, G., Morissette, A., Prévost, K., & Massé, E. (2009). Small RNA-induced differential degradation of the polycistronic mRNA *iscRSUA*. *The EMBO Journal*, *28*(11), 1551–1561.
- Dhe-Paganon, S., Shigeta, R., Chi, Y. I., Ristow, M., & Shoelson, S. E. (2000). Crystal structure of human frataxin. *The Journal of Biological Chemistry*, *275*(40), 30753–30756.
- Dong, Y., Zhang, D., Yu, Q., Zhao, Q., Xiao, C., Zhang, K., et al. (2017). Loss of Ssq1 leads to mitochondrial dysfunction, activation of autophagy and cell cycle arrest due to iron overload triggered by mitochondrial iron-sulfur cluster assembly defects in *Candida albicans*. *The International Journal of Biochemistry & Cell Biology*, *85*, 44–55.
- Dupont, C. L., Butcher, A., Valas, R. E., Bourne, P. E., & Caetano-Anollés, G. (2010). History of biological metal utilization inferred through phylogenomic analysis of protein structures. *Proceedings of the National Academy of Sciences of the United States of America*, *107*(23), 10567–10572.
- Dutkiewicz, R., Marszalek, J., Schilke, B., Craig, E. A., Lill, R., & Mühlhoff, U. (2006). The Hsp70 chaperone Ssq1p is dispensable for iron-sulfur cluster formation on the scaffold protein Isu1p. *The Journal of Biological Chemistry*, *281*(12), 7801–7808.
- Dutkiewicz, R., Nowak, M., Craig, E. A., & Marszalek, J. (2017). Fe-S cluster Hsp70 chaperones: The ATPase cycle and protein interactions. *Methods in Enzymology*, *595*, 161–184.
- Dutkiewicz, R., Schilke, B., Cheng, S., Knieszner, H., Craig, E. A., & Marszalek, J. (2004). Sequence-specific interaction between mitochondrial Fe-S scaffold protein Isu and Hsp70 Ssq1 is essential for their in vivo function. *The Journal of Biological Chemistry*, *279*(28), 29167–29174.
- Ellermeier, C. D., Ellermeier, J. R., & Schlauch, J. M. (2005). HilD, HilC and RtsA constitute a feed forward loop that controls expression of the SPI1 type three secretion system regulator *hilA* in *Salmonella enterica* serovar Typhimurium. *Molecular Microbiology*, *57*(3), 691–705.
- Ezraty, B., Vergnes, A., Banzhaf, M., Duverger, Y., Huguenot, A., Brochado, A. R., et al. (2013). Fe-S cluster biosynthesis controls uptake of aminoglycosides in a ROS-less death pathway. *Science*, *340*(6140), 1583–1587.
- Fernandes, A. P., Fladvad, M., Berndt, C., Andréßen, C., Lillig, C. H., Neubauer, P., et al. (2005). A novel monothiol glutaredoxin (Grx4) from *Escherichia coli* can serve as a substrate for thioredoxin reductase. *The Journal of Biological Chemistry*, *280*(26), 24544–24552.
- Fleischhacker, A. S., Stubna, A., Hsueh, K.-L., Guo, Y., Teter, S. J., Rose, J. C., et al. (2012). Characterization of the [2Fe-2S] cluster of *Escherichia coli* transcription factor IscR. *Biochemistry*, *51*(22), 4453–4462.
- Foster, M. W., Mansy, S. S., Hwang, J., Penner-Hahn, J. E., Surerus, K. K., & Cowan, J. A. (2000). A mutant human IscU protein contains a stable [2Fe-2S]₂⁺ center of possible functional significance. *Journal of the American Chemical Society*, *122*(28), 6805–6806.
- Fox, N. G., Yu, X., Feng, X., Bailey, H. J., Martelli, A., Nabhan, J. F., et al. (2019). Structure of the human frataxin-bound iron-sulfur cluster assembly complex provides insight into its activation mechanism. *Nature Communications*, *10*(1), 2210.
- Fuangthong, M., Jittawuttipoka, T., Wisitkamol, R., Romsang, A., Duang-nkern, J., Vattanaviboon, P., et al. (2015). IscR plays a role in oxidative stress resistance and pathogenicity of a plant pathogen, *Xanthomonas campestris*. *Microbiological Research*, *170*, 139–146.
- Garcia, P. S., Gribaldo, S., Py, B., & Barras, F. (2019). The SUF system: An ABC ATPase-dependent protein complex with a role in Fe-S cluster biogenesis. *Research in Microbiology*, *170*(8), 426–434.
- Gerber, J., Mühlhoff, U., & Lill, R. (2003). An interaction between frataxin and Isu1/Nfs1 that is crucial for Fe/S cluster synthesis on Isu1. *EMBO Reports*, *4*(9), 906–911.

- Gervason, S., Larkem, D., Mansour, A. B., Botzanowski, T., Müller, C. S., Pecqueur, L., et al. (2019). Physiologically relevant reconstitution of iron-sulfur cluster biosynthesis uncovers persulfide-processing functions of ferredoxin-2 and frataxin. *Nature Communications*, *10*(1), 3566.
- Giel, J. L., Nesbit, A. D., Mettert, E. L., Fleischhacker, A. S., Wanta, B. T., & Kiley, P. J. (2013). Regulation of iron-sulphur cluster homeostasis through transcriptional control of the Isc pathway by [2Fe-2S]-IscR in *Escherichia coli*. *Molecular Microbiology*, *87*(3), 478–492.
- Giel, J. L., Rodionov, D., Liu, M., Blattner, F. R., & Kiley, P. J. (2006). IscR-dependent gene expression links iron-sulphur cluster assembly to the control of O₂-regulated genes in *Escherichia coli*. *Molecular Microbiology*, *60*(4), 1058–1075.
- Gully, D., Moinier, D., Loiseau, L., & Bouveret, E. (2003). New partners of acyl carrier protein detected in *Escherichia coli* by tandem affinity purification. *FEBS Letters*, *548*(1–3), 90–96.
- Haines, S., Arnaud-Barbe, N., Poncet, D., Reverchon, S., Wawrzyniak, J., Nasser, W., et al. (2015). IscR regulates synthesis of colonization factor Antigen I fimbriae in response to iron starvation in enterotoxigenic *Escherichia coli*. *Journal of Bacteriology*, *197*(18), 2896–2907.
- Hoff, K. G., Silberg, J. J., & Vickery, L. E. (2000). Interaction of the iron-sulfur cluster assembly protein IscU with the Hsc66/Hsc20 molecular chaperone system of *Escherichia coli*. *Proceedings of the National Academy of Sciences of the United States of America*, *97*(14), 7790–7795.
- Hoff, K. G., Ta, D. T., Tapley, T. L., Silberg, J. J., & Vickery, L. E. (2002). Hsc66 substrate specificity is directed toward a discrete region of the iron-sulfur cluster template protein IscU. *The Journal of Biological Chemistry*, *277*(30), 27353–27359.
- Ikeuchi, Y., Shigi, N., Kato, J.-I., Nishimura, A., & Suzuki, T. (2006). Mechanistic insights into sulfur relay by multiple sulfur mediators involved in thiouridine biosynthesis at tRNA wobble positions. *Molecular Cell*, *21*(1), 97–108.
- Imlay, J. A. (2006). Iron-sulphur clusters and the problem with oxygen. *Molecular Microbiology*, *59*(4), 1073–1082.
- Jacobson, M. R., Cash, V. L., Weiss, M. C., Laird, N. F., Newton, W. E., & Dean, D. R. (1989). Biochemical and genetic analysis of the nifUSVWZM cluster from *Azotobacter vinelandii*. *Molecular & General Genetics*, *219*(1–2), 49–57.
- Jaroschinsky, M., Pinske, C., & Sawers, G. R. (2017). Differential effects of isc operon mutations on the biosynthesis and activity of key anaerobic metalloenzymes in *Escherichia coli*. *Microbiology*, *163*(6), 878–890.
- Johnson, D. C., Unciuleac, M.-C., & Dean, D. R. (2006). Controlled expression and functional analysis of iron-sulfur cluster biosynthetic components within *Azotobacter vinelandii*. *Journal of Bacteriology*, *188*(21), 7551–7561.
- Jones-Carson, J., Laughlin, J., Hamad, M. A., Stewart, A. L., Voskuil, M. I., & Vázquez-Torres, A. (2008). Inactivation of [Fe-S] metalloproteins mediates nitric oxide-dependent killing of *Burkholderia mallei*. *PLoS One*, *3*(4), e1976.
- Kalindamar, S., Lu, J., Abdelhamed, H., Tekedar, H. C., Lawrence, M. L., & Karsi, A. (2019). Transposon mutagenesis and identification of mutated genes in growth-delayed *Edwardsiella ictaluri*. *BMC Microbiology*, *19*(1), 55.
- Kambampati, R., & Lahun, C. T. (1999). IscS is a sulfurtransferase for the in vitro biosynthesis of 4-thiouridine in *Escherichia coli* tRNA. *Biochemistry*, *38*(50), 16561–16568.
- Kambampati, R., & Lahun, C. T. (2000). Evidence for the transfer of sulfane sulfur from IscS to ThiI during the in vitro biosynthesis of 4-thiouridine in *Escherichia coli* tRNA. *The Journal of Biological Chemistry*, *275*(15), 10727–10730.
- Kampinga, H. H., & Craig, E. A. (2010). The HSP70 chaperone machinery: J proteins as drivers of functional specificity. *Nature Reviews Molecular Cell Biology*, *11*(8), 579–592.

- Kim, J. H., Bothe, J. R., Frederick, R. O., Holder, J. C., & Markley, J. L. (2014). Role of IscX in iron-sulfur cluster biogenesis in *Escherichia coli*. *Journal of the American Chemical Society*, 136(22), 7933–7942.
- Kim, J. H., Frederick, R. O., Reinen, N. M., Troupis, A. T., & Markley, J. L. (2013). [2Fe-2S]-ferredoxin binds directly to cysteine desulfurase and supplies an electron for iron-sulfur cluster assembly but is displaced by the scaffold protein or bacterial frataxin. *Journal of the American Chemical Society*, 135(22), 8117–8120.
- Kim, J. H., Füzéry, A. K., Tonelli, M., Ta, D. T., Westler, W. M., Vickery, L. E., et al. (2009). Structure and dynamics of the iron-sulfur cluster assembly scaffold protein IscU and its interaction with the cochaperone HscB. *Biochemistry*, 48(26), 6062–6071.
- Kim, J. H., Tonelli, M., & Markley, J. L. (2012). Disordered form of the scaffold protein IscU is the substrate for iron-sulfur cluster assembly on cysteine desulfurase. *Proceedings of the National Academy of Sciences of the United States of America*, 109(2), 454–459.
- Koutnikova, H., Campuzano, V., Foury, F., Dollé, P., Cazzalini, O., & Koenig, M. (1997). Studies of human, mouse and yeast homologues indicate a mitochondrial function for frataxin. *Nature Genetics*, 16(4), 345–351.
- Kurihara, T., Mihara, H., Kato, S., Yoshimura, T., & Esaki, N. (2003). Assembly of iron-sulfur clusters mediated by cysteine desulfurases, IscS, CsdB and CSD, from *Escherichia coli*. *Biochimica et Biophysica Acta*, 1647(1–2), 303–309.
- Lange, H., Kaut, A., Kispal, G., & Lill, R. (2000). A mitochondrial ferredoxin is essential for biogenesis of cellular iron-sulfur proteins. *Proceedings of the National Academy of Sciences of the United States of America*, 97(3), 1050–1055.
- Lauhon, C. T. (2002). Requirement for IscS in biosynthesis of all thionucleosides in *Escherichia coli*. *Journal of Bacteriology*, 184(24), 6820–6829.
- Lauhon, C. T., Skovran, E., Urbina, H. D., Downs, D. M., & Vickery, L. E. (2004). Substitutions in an active site loop of *Escherichia coli* IscS result in specific defects in Fe-S cluster and thionucleoside biosynthesis in vivo. *The Journal of Biological Chemistry*, 279(19), 19551–19558.
- Lee, K.-C., Yeo, W.-S., & Roe, J.-H. (2008). Oxidant-responsive induction of the suf operon, encoding a Fe-S assembly system, through Fur and IscR in *Escherichia coli*. *Journal of Bacteriology*, 190(24), 8244–8247.
- Lim, J. G., & Choi, S. H. (2014). IscR is a global regulator essential for pathogenesis of *Vibrio vulnificus* and induced by host cells. *Infection and Immunity*, 82(2), 569–578.
- Li, D. S., Ohshima, K., Jiralerspong, S., Bojanowski, M. W., & Pandolfo, M. (1999). Knock-out of the *cyaY* gene in *Escherichia coli* does not affect cellular iron content and sensitivity to oxidants. *FEBS Letters*, 456(1), 13–16.
- Li, J., Ren, X., Fan, B., Huang, Z., Wang, W., Zhou, H., et al. (2019). Zinc toxicity and iron-sulfur cluster biogenesis in *Escherichia coli*. *Applied and Environmental Microbiology*, 85(9).
- Loiseau, L., Gerez, C., Bekker, M., Ollagnier-de Choudens, S., Py, B., Sanakis, Y., et al. (2007). ErpA, an iron sulfur (Fe S) protein of the A-type essential for respiratory metabolism in *Escherichia coli*. *Proceedings of the National Academy of Sciences of the United States of America*, 104(34), 13626–13631.
- Majewska, J., Ciesielski, S. J., Schilke, B., Kominek, J., Blenska, A., Delewski, W., et al. (2013). Binding of the chaperone Jac1 protein and cysteine desulfurase Nfs1 to the iron-sulfur cluster scaffold Isu protein is mutually exclusive. *The Journal of Biological Chemistry*, 288(40), 29134–29142.
- Mandin, P., Chareyre, S., & Barras, F. (2016). A regulatory circuit composed of a transcription factor, IscR, and a regulatory RNA, RyhB, controls Fe-S cluster delivery. *mBio*, 7(5).

- Marinoni, E. N., de Oliveira, J. S., Nicolet, Y., Raulfs, E. C., Amara, P., Dean, D. R., et al. (2012). (IscS-IscU)₂ complex structures provide insights into Fe₂S₂ biogenesis and transfer. *Angewandte Chemie*, 51(22), 5439–5442.
- Martin, J. E., & Imlay, J. A. (2011). The alternative aerobic ribonucleotide reductase of *Escherichia coli*, NrdEF, is a manganese-dependent enzyme that enables cell replication during periods of iron starvation. *Molecular Microbiology*, 80(2), 319–334.
- Masud, A. J., Kastaniotis, A. J., Rahman, M. T., Autio, K. J., & Hiltunen, J. K. (2019). Mitochondrial acyl carrier protein (ACP) at the interface of metabolic state sensing and mitochondrial function. *Biochimica et Biophysica Acta (BBA) - Molecular Cell Research*, 1866(12), 118540.
- Mayer, M. P., & Gierasch, L. M. (2019). Recent advances in the structural and mechanistic aspects of Hsp70 molecular chaperones. *The Journal of Biological Chemistry*, 294(6), 2085–2097.
- Mettert, E. L., & Kiley, P. J. (2014). Coordinate regulation of the Suf and Isc Fe-S cluster biogenesis pathways by IscR is essential for viability of *Escherichia coli*. *Journal of Bacteriology*, 196(24), 4315–4323.
- Mihara, H., Kurihara, T., Yoshimura, T., & Esaki, N. (2000). Kinetic and mutational studies of three NifS homologs from *Escherichia coli*: Mechanistic difference between L-cysteine desulfurase and L-selenocysteine lyase reactions. *Journal of Biochemistry*, 127(4), 559–567.
- Müller, H. K., Kwuan, L., Schwiesow, L., Bernick, D. L., Mettert, E., Ramirez, H. A., et al. (2014). IscR is essential for yersinia pseudotuberculosis type III secretion and virulence. *PLoS Pathogens*, 10(6), e1004194.
- Mühlenhoff, U., Gerber, J., Rüdhardt, N., & Lill, R. (2003). Components involved in assembly and dislocation of iron-sulfur clusters on the scaffold protein Isu1p. *The EMBO Journal*, 22(18), 4815–4825.
- Mühlenhoff, U., Richter, N., Pines, O., Pierik, A. J., & Lill, R. (2011). Specialized function of yeast Isa1 and Isa2 proteins in the maturation of mitochondrial [4Fe-4S] proteins. *The Journal of Biological Chemistry*, 286(48), 41205–41216.
- Musco, G., Stier, G., Kolmerer, B., Adinolfi, S., Martin, S., Frenkiel, T., et al. (2000). Towards a structural understanding of Friedreich's ataxia: The solution structure of frataxin. *Structure*, 8(7), 695–707.
- Nakamura, R., Hikita, M., Ogawa, S., Takahashi, Y., & Fujishiro, T. (2019). Snapshots of PLP-substrate and PLP-product external aldimines as intermediates in two types of cysteine desulfurase enzymes. *The FEBS Journal*. <https://doi.org/10.1111/febs.15081>.
- Nesbit, A. D., Giel, J. L., Rose, J. C., & Kiley, P. J. (2009). Sequence-specific binding to a subset of IscR-regulated promoters does not require IscR Fe-S cluster ligation. *Journal of Molecular Biology*, 387(1), 28–41.
- Nowinski, S. M., Van Vranken, J. G., Dove, K. K., & Rutter, J. (2018). Impact of mitochondrial fatty acid synthesis on mitochondrial biogenesis. *Current Biology*, 28(20), 1212–1219.
- Olson, J. W., Agar, J. N., Johnson, M. K., & Maier, R. J. (2000). Characterization of the NifU and NifS Fe-S cluster formation proteins essential for viability in *Helicobacter pylori*. *Biochemistry*, 39(51), 16213–16219.
- Otsuka, Y., Miki, K., Koga, M., Katayama, N., Morimoto, W., Takahashi, Y., et al. (2010). IscR regulates RNase LS activity by repressing mla transcription. *Genetics*, 185(3), 823–830.
- Pagnier, A., Nicolet, Y., & Fontecilla-Camps, J. C. (2015). IscS from *Archaeoglobus fulgidus* has no desulfurase activity but may provide a cysteine ligand for [Fe₂S₂] cluster assembly. *Biochimica et Biophysica Acta (BBA) - Molecular Cell Research*, 1853(6), 1457–1463.
- Pandey, A., Gordon, D. M., Pain, J., Stemmler, T. L., Dancis, A., & Pain, D. (2013). Frataxin directly stimulates mitochondrial cysteine desulfurase by exposing substrate-binding sites,

- and a mutant Fe-S cluster scaffold protein with frataxin-bypassing ability acts similarly. *The Journal of Biological Chemistry*, 288(52), 36773–36786.
- Parent, A., Elduque, X., Cornu, D., Belot, L., Le Caer, J.-P., Grandas, A., et al. (2015). Mammalian frataxin directly enhances sulfur transfer of NFS1 persulfide to both ISCU and free thiols. *Nature Communications*, 6, 5686.
- Pastore, C., Adinolfi, S., Huynen, M. A., Rybin, V., Martin, S., Mayer, M., et al. (2006). YfhJ, a molecular adaptor in iron-sulfur cluster formation or a frataxin-like protein? *Structure*, 14(5), 857–867.
- Patra, S., & Barondeau, D. P. (2019). Mechanism of activation of the human cysteine desulfurase complex by frataxin. *Proceedings of the National Academy of Sciences of the United States of America*, 116(39), 19421–19430.
- Pohl, T., Walter, J., Stolpe, S., Soufo, J. H. D., Grauman, P. L., & Friedrich, T. (2007). Effects of the deletion of the *Escherichia coli* frataxin homologue CyaY on the respiratory NADH:ubiquinone oxidoreductase. *BMC Biochemistry*, 8, 13.
- Prischi, F., Konarev, P. V., Iannuzzi, C., Pastore, C., Adinolfi, S., Martin, S. R., et al. (2010). Structural bases for the interaction of frataxin with the central components of iron-sulphur cluster assembly. *Nature Communications*, 1, 95.
- Przybyla-Toscano, J., Roland, M., Gaymard, F., Couturier, J., & Rouhier, N. (2018). Roles and maturation of iron-sulfur proteins in plastids. *Journal of Biological Inorganic Chemistry*, 23(4), 545–566.
- Puglisi, R., Yan, R., Adinolfi, S., & Pastore, A. (2016). A new Tessera into the interactome of the isc operon: A novel interaction between HscB and IscS. *Frontiers in Molecular Biosciences*, 3, 48.
- Py, B., Gerez, C., Angelini, S., Planel, R., Vinella, D., Loiseau, L., et al. (2012). Molecular organization, biochemical function, cellular role and evolution of NfuA, an atypical Fe-S carrier. *Molecular Microbiology*, 86(1), 155–171.
- Py, B., Gerez, C., Huguenot, A., Vidaud, C., Fontecave, M., Ollagnier de Choudens, S., et al. (2018). The ErpA/NfuA complex builds an oxidation-resistant Fe-S cluster delivery pathway. *The Journal of Biological Chemistry*, 293(20), 7689–7702.
- Rajagopalan, S., Teter, S. J., Zwart, P. H., Brennan, R. G., Phillips, K. J., & Kiley, P. J. (2013). Studies of IscR reveal a unique mechanism for metal-dependent regulation of DNA binding specificity. *Nature Structural & Molecular Biology*, 20(6), 740–747.
- Ramelot, T. A., Cort, J. R., Goldsmith-Fischman, S., Kornhaber, G. J., Xiao, R., Shastry, R., et al. (2004). Solution NMR structure of the iron-sulfur cluster assembly protein U (IscU) with zinc bound at the active site. *Journal of Molecular Biology*, 344(2), 567–583.
- Raulf, E. C., O'Carroll, I. P., Dos Santos, P. C., Unciuleac, M.-C., & Dean, D. R. (2008). In vivo iron-sulfur cluster formation. *Proceedings of the National Academy of Sciences of the United States of America*, 105(25), 8591–8596.
- Remes, B., Eisenhardt, B. D., Srinivasan, V., & Klug, G. (2015). IscR of *Rhodobacter sphaeroides* functions as repressor of genes for iron-sulfur metabolism and represents a new type of iron-sulfur-binding protein. *MicrobiologyOpen*, 4(5), 790–802.
- Richards, T. A., & van der Giezen, M. (2006). Evolution of the Isd11-IscS complex reveals a single alpha-proteobacterial endosymbiosis for all eukaryotes. *Molecular Biology and Evolution*, 23(7), 1341–1344.
- Rincon-Enriquez, G., Crété, P., Barras, F., & Py, B. (2008). Biogenesis of Fe/S proteins and pathogenicity: IscR plays a key role in allowing *Erwinia chrysanthemi* to adapt to hostile conditions. *Molecular Microbiology*, 67(6), 1257–1273.
- Roche, B., Agrebi, R., Huguenot, A., Ollagnier de Choudens, S., Barras, F., & Py, B. (2015a). Turning *Escherichia coli* into a frataxin-dependent organism. *PLoS Genetics*, 11(5), e1005134.

- Roche, B., Aussel, L., Ezraty, B., Mandin, P., Py, B., & Barras, F. (2013). Iron/sulfur proteins biogenesis in prokaryotes: Formation, regulation and diversity. *Biochimica et Biophysica Acta*, 1827(3), 455–469.
- Roche, B., Huguenot, A., Barras, F., & Py, B. (2015b). The iron-binding CyaY and IscX proteins assist the ISC-catalyzed Fe-S biogenesis in *Escherichia coli*. *Molecular Microbiology*, 95(4), 605–623.
- Rouault, T. A. (2012). Biogenesis of iron-sulfur clusters in mammalian cells: New insights and relevance to human disease. *Disease Models and Mechanisms Model*, 5(2), 155–164.
- Rouault, T. A., & Maio, N. (2017). Biogenesis and functions of mammalian iron-sulfur proteins in the regulation of iron homeostasis and pivotal metabolic pathways. *The Journal of Biological Chemistry*, 292(31), 12744–12753.
- Rüdiger, S., Buchberger, A., & Bukau, B. (1997). Interaction of Hsp70 chaperones with substrates. *Nature Structural Biology*, 4(5), 342–349.
- Saninjuk, K., Romsang, A., Duang-Nkern, J., Vattanaviboon, P., & Mongkolsuk, S. (2019). Transcriptional regulation of the *Pseudomonas aeruginosa* iron-sulfur cluster assembly pathway by binding of IscR to multiple sites. *PLoS One*, 14(6), e0218385.
- Schmucker, S., Martelli, A., Colin, F., Page, A., Wattenhofer-Donzé, M., Reutenauer, L., et al. (2011). Mammalian frataxin: An essential function for cellular viability through an interaction with a preformed ISCU/NFS1/ISD11 iron-sulfur assembly complex. *PLoS One*, 6(1), e16199.
- Schmucker, S., & Puccio, H. (2010). Understanding the molecular mechanisms of Friedreich's ataxia to develop therapeutic approaches. *Human Molecular Genetics*, 19(R1), R103–R110.
- Schwartz, C. J., Djaman, O., Imlay, J. A., & Kiley, P. J. (2000). The cysteine desulfurase, IscS, has a major role in in vivo Fe-S cluster formation in *Escherichia coli*. *Proceedings of the National Academy of Sciences of the United States of America*, 97(16), 9009–9014.
- Schwartz, C. J., Giel, J. L., Patschkowski, T., Luther, C., Ruzicka, F. J., Beinert, H., et al. (2001). IscR, an Fe-S cluster-containing transcription factor, represses expression of *Escherichia coli* genes encoding Fe-S cluster assembly proteins. *Proceedings of the National Academy of Sciences of the United States of America*, 98(26), 14895–14900.
- Seki, A., Nakano, T., Takahashi, H., Matsumoto, K., Ikeuchi, M., & Tanaka, K. (2006). Light-responsive transcriptional regulation of the *suf* promoters involved in cyanobacterium *Synechocystis* sp. PCC 6803 Fe-S cluster biogenesis. *FEBS Letters*, 580(21), 5044–5048.
- Seo, S. W., Kim, D., Latif, H., O'Brien, E. J., Szubin, R., & Palsson, B. O. (2014). Deciphering Fur transcriptional regulatory network highlights its complex role beyond iron metabolism in *Escherichia coli*. *Nature Communications*, 5, 4910.
- Shakamuri, P., Zhang, B., & Johnson, M. K. (2012). Monothiol glutaredoxins function in storing and transporting [Fe₂S₂] clusters assembled on IscU scaffold proteins. *Journal of the American Chemical Society*, 134(37), 15213–15216.
- Sheftel, A. D., Stehling, O., Pierik, A. J., Elsässer, H.-P., Mühlhoff, U., Webert, H., et al. (2010). Humans possess two mitochondrial ferredoxins, Fdx1 and Fdx2, with distinct roles in steroidogenesis, heme, and Fe/S cluster biosynthesis. *Proceedings of the National Academy of Sciences of the United States of America*, 107(26), 11775–11780.
- Sheftel, A. D., Wilbrecht, C., Stehling, O., Niggemeyer, B., Elsässer, H.-P., Mühlhoff, U., et al. (2012). The human mitochondrial ISCA1, ISCA2, and IBA57 proteins are required for [4Fe-4S] protein maturation. *Molecular Biology of the Cell*, 23(7), 1157–1166.
- Shen, G., Balasubramanian, R., Wang, T., Wu, Y., Hoffart, L. M., Krebs, C., et al. (2007). SufR coordinates two [4Fe-4S]₂₊, 1+ clusters and functions as a transcriptional repressor of the *sufBCDS* operon and an autoregulator of *sufR* in cyanobacteria. *The Journal of Biological Chemistry*, 282(44), 31909–31919.

- Shi, Y., Ghosh, M., Kovtunovych, G., Crooks, D. R., & Rouault, T. A. (2012). Both human ferredoxins 1 and 2 and ferredoxin reductase are important for iron-sulfur cluster biogenesis. *Biochimica et Biophysica Acta*, 1823(2), 484–492.
- Shi, Y., Ghosh, M. C., Tong, W.-H., & Rouault, T. A. (2009). Human ISD11 is essential for both iron-sulfur cluster assembly and maintenance of normal cellular iron homeostasis. *Human Molecular Genetics*, 18(16), 3014–3025.
- Shimomura, Y., Takahashi, Y., Kakuta, Y., & Fukuyama, K. (2005). Crystal structure of *Escherichia coli* YfhJ protein, a member of the ISC machinery involved in assembly of iron-sulfur clusters. *Proteins*, 60(3), 566–569.
- Shimomura, Y., Wada, K., Fukuyama, K., & Takahashi, Y. (2008). The asymmetric trimeric architecture of [2Fe-2S] IscU: Implications for its scaffolding during iron-sulfur cluster biosynthesis. *Journal of Molecular Biology*, 383(1), 133–143.
- Shi, R., Proteau, A., Villarrojo, M., Moukadiri, I., Zhang, L., Trempe, J.-F., et al. (2010). Structural basis for Fe-S cluster assembly and tRNA thiolation mediated by IscS protein-protein interactions. *PLoS Biology*, 8(4), e1000354.
- Silberg, J. J., Tapley, T. L., Hoff, K. G., & Vickery, L. E. (2004). Regulation of the HscA ATPase reaction cycle by the co-chaperone HscB and the iron-sulfur cluster assembly protein IscU. *The Journal of Biological Chemistry*, 279(52), 53924–53931.
- Smith, A. D., Agar, J. N., Johnson, K. A., Frazzon, J., Amster, I. J., Dean, D. R., et al. (2001). Sulfur transfer from IscS to IscU: The first step in iron-sulfur cluster biosynthesis. *Journal of the American Chemical Society*, 123(44), 11103–11104.
- Smith, A. D., Frazzon, J., Dean, D. R., & Johnson, M. K. (2005). Role of conserved cysteines in mediating sulfur transfer from IscS to IscU. *FEBS Letters*, 579(23), 5236–5240.
- Somprasong, N., Jittawuttipoka, T., Duang-Nkern, J., Romsang, A., Chaiyen, P., Schweizer, H. P., et al. (2012). *Pseudomonas aeruginosa* thiol peroxidase protects against hydrogen peroxide toxicity and displays atypical patterns of gene regulation. *Journal of Bacteriology*, 194(15), 3904–3912.
- Stehling, O., Wilbrecht, C., & Lill, R. (2014). Mitochondrial iron-sulfur protein biogenesis and human disease. *Biochimie*, 100, 61–77.
- Takahashi, Y., & Nakamura, M. (1999). Functional assignment of the ORF2-iscS-iscU-iscA-hscB-hscA-fdx-ORF3 gene cluster involved in the assembly of Fe-S clusters in *Escherichia coli*. *Journal of Biochemistry*, 126(5), 917–926.
- Takahashi, Y., & Tokumoto, U. (2002). A third bacterial system for the assembly of iron-sulfur clusters with homologs in archaea and plastids. *The Journal of Biological Chemistry*, 277(32), 28380–28383.
- Tanaka, N., Kanazawa, M., Tonosaki, K., Yokoyama, N., Kuzuyama, T., & Takahashi, Y. (2016). Novel features of the ISC machinery revealed by characterization of *Escherichia coli* mutants that survive without iron-sulfur clusters. *Molecular Microbiology*, 99(5), 835–848.
- Tanaka, N., Yuda, E., Fujishiro, T., Hirabayashi, K., Wada, K., & Takahashi, Y. (2019). Identification of IscU residues critical for de novo iron-sulfur cluster assembly. *Molecular Microbiology*, 112(6), 1769–1783.
- Tapley, T. L., & Vickery, L. E. (2004). Preferential substrate binding orientation by the molecular chaperone HscA. *The Journal of Biological Chemistry*, 279(27), 28435–28442.
- Tokumoto, U., Kitamura, S., Fukuyama, K., & Takahashi, Y. (2004). Interchangeability and distinct properties of bacterial Fe-S cluster assembly systems: Functional replacement of the isc and suf operons in *Escherichia coli* with the nifSU-like operon from *Helicobacter pylori*. *Journal of Biochemistry*, 136(2), 199–209.
- Tokumoto, U., Nomura, S., Minami, Y., Mihara, H., Kato, S.-I., Kurihara, T., et al. (2002). Network of protein-protein interactions among iron-sulfur cluster assembly proteins in *Escherichia coli*. *Journal of Biochemistry*, 131(5), 713–719.

- Tokumoto, U., & Takahashi, Y. (2001). Genetic analysis of the *isc* operon in *Escherichia coli* involved in the biogenesis of cellular iron-sulfur proteins. *Journal of Biochemistry*, *130*(1), 63–71.
- Touati, D. (2000). Iron and oxidative stress in bacteria. *Archives of Biochemistry and Biophysics*, *373*(1), 1–6.
- Tsai, C.-L., & Barondeau, D. P. (2010). Human frataxin is an allosteric switch that activates the Fe-S cluster biosynthetic complex. *Biochemistry*, *49*(43), 9132–9139.
- Uchida, T., Kobayashi, N., Muneta, S., & Ishimori, K. (2017). The iron chaperone protein CyaY from *Vibrio cholerae* is a heme-binding protein. *Biochemistry*, *56*(18), 2425–2434.
- Unciuleac, M.-C., Chandramouli, K., Naik, S., Mayer, S., Huynh, B. H., Johnson, M. K., et al. (2007). In vitro activation of apo-aconitase using a [4Fe-4S] cluster-loaded form of the IscU [Fe-S] cluster scaffolding protein. *Biochemistry*, *46*(23), 6812–6821.
- Urbina, H. D., Silberg, J. J., Hoff, K. G., & Vickery, L. E. (2001). Transfer of sulfur from IscS to IscU during Fe/S cluster assembly. *The Journal of Biological Chemistry*, *276*(48), 44521–44526.
- Van Vranken, J. G., Jeong, M.-Y., Wei, P., Chen, Y.-C., Gygi, S. P., Winge, D. R., et al. (2016). The mitochondrial acyl carrier protein (ACP) coordinates mitochondrial fatty acid synthesis with iron sulfur cluster biogenesis. *ELife*, *5*.
- Velayudhan, J., Karlinsey, J. E., Frawley, E. R., Becker, L. A., Nartea, M., & Fang, F. C. (2014). Distinct roles of the *Salmonella enterica* serovar Typhimurium CyaY and YggX proteins in the biosynthesis and repair of iron-sulfur clusters. *Infection and Immunity*, *82*(4), 1390–1401.
- Vergnes, A., Viala, J. P. M., Ouadah-Tsabet, R., Pocachard, B., Loiseau, L., Méresse, S., et al. (2017). The iron-sulfur cluster sensor IscR is a negative regulator of Spi1 type III secretion system in *Salmonella enterica*. *Cellular Microbiology*, *19*(4).
- Vickery, L. E., & Cupp-Vickery, J. R. (2007). Molecular chaperones HscA/Ssq1 and HscB/Jac1 and their roles in iron-sulfur protein maturation. *Critical Reviews in Biochemistry and Molecular Biology*, *42*(2), 95–111.
- Vinella, D., Brochier-Armanet, C., Loiseau, L., Talla, E., & Barras, F. (2009). Iron-sulfur (Fe/S) protein biogenesis: Phylogenomic and genetic studies of A-type carriers. *PLoS Genetics*, *5*(5), e1000497.
- Vinella, D., Loiseau, L., Ollagnier de Choudens, S., Fontecave, M., & Barras, F. (2013). In vivo [Fe-S] cluster acquisition by IscR and NsrR, two stress regulators in *Escherichia coli*. *Molecular Microbiology*, *87*(3), 493–508.
- Vuorijoki, L., Tiwari, A., Kallio, P., & Aro, E.-M. (2017). Inactivation of iron-sulfur cluster biogenesis regulator SufR in *Synechocystis* sp. PCC 6803 induces unique iron-dependent protein-level responses. *Biochimica et Biophysica Acta (BBA) - General Subjects*, *1861*(5 Pt A), 1085–1098.
- Wang, T., & Craig, E. A. (2008). Binding of yeast frataxin to the scaffold for Fe-S cluster biogenesis, Isu. *The Journal of Biological Chemistry*, *283*(18), 12674–12679.
- Wang, T., Shen, G., Balasubramanian, R., McIntosh, L., Bryant, D. A., & Golbeck, J. H. (2004). The *sufR* gene (*sll0088* in *Synechocystis* sp. strain PCC 6803) functions as a repressor of the *sufBCDS* operon in iron-sulfur cluster biogenesis in cyanobacteria. *Journal of Bacteriology*, *186*(4), 956–967.
- Webert, H., Freibert, S.-A., Gallo, A., Heidenreich, T., Linne, U., Amlacher, S., et al. (2014). Functional reconstitution of mitochondrial Fe/S cluster synthesis on Isu1 reveals the involvement of ferredoxin. *Nature Communications*, *5*, 5013.
- Weiss, M. C., Neukirchen, S., Roettger, M., Mrnjavac, N., Nelson-Sathi, S., Martin, W. F., et al. (2016). Reply to “Is LUCA a thermophilic progenote?”. *Nature Microbiology*, *1*, 16230.

- Wiedemann, N., Urzica, E., Guiard, B., Müller, H., Lohaus, C., Meyer, H. E., et al. (2006). Essential role of Isd11 in mitochondrial iron-sulfur cluster synthesis on Isu scaffold proteins. *The EMBO Journal*, 25(1), 184–195.
- Willemse, D., Weber, B., Masino, L., Warren, R. M., Adinolfi, S., Pastore, A., et al. (2018). Rv1460, a SufR homologue, is a repressor of the suf operon in *Mycobacterium tuberculosis*. *PloS One*, 13(7), e0200145.
- Wu, S.-P., Mansy, S. S., & Cowan, J. A. (2005). Iron-sulfur cluster biosynthesis. Molecular chaperone DnaK promotes IscU-bound [2Fe-2S] cluster stability and inhibits cluster transfer activity. *Biochemistry*, 44(11), 4284–4293.
- Wu, G., Mansy, S. S., Wu Sp, S., Surerus, K. K., Foster, M. W., & Cowan, J. A. (2002). Characterization of an iron-sulfur cluster assembly protein (ISU1) from *Schizosaccharomyces pombe*. *Biochemistry*, 41(15), 5024–5032.
- Wu, Y., & Outten, F. W. (2009). IscR controls iron-dependent biofilm formation in *Escherichia coli* by regulating type I fimbria expression. *Journal of Bacteriology*, 191(4), 1248–1257.
- Yan, R., Konarev, P. V., Iannuzzi, C., Adinolfi, S., Roche, B., Kelly, G., et al. (2013). Ferredoxin competes with bacterial frataxin in binding to the desulfurase IscS. *The Journal of Biological Chemistry*, 288(34), 24777–24787.
- Yeo, W.-S., Lee, J.-H., Lee, K.-C., & Roe, J.-H. (2006). IscR acts as an activator in response to oxidative stress for the suf operon encoding Fe-S assembly proteins. *Molecular Microbiology*, 61(1), 206–218.
- Yoon, H., Golla, R., Lesuisse, E., Pain, J., Donald, J. E., Lyver, E. R., et al. (2012). Mutation in the Fe-S scaffold protein Isu bypasses frataxin deletion. *The Biochemical Journal*, 441(1), 473–480.
- Yoon, H., Knight, S. A. B., Pandey, A., Pain, J., Turkarlan, S., Pain, D., et al. (2015). Turning *Saccharomyces cerevisiae* into a frataxin-independent organism. *PLoS Genetics*, 11(5), e1005135.
- Zbell, A. L., Benoit, S. L., & Maier, R. J. (2007). Differential expression of NiFe uptake-type hydrogenase genes in *Salmonella enterica* serovar Typhimurium. *Microbiology*, 153(Pt 10), 3508–3516.
- Zheng, L., White, R. H., Cash, V. L., & Dean, D. R. (1994). Mechanism for the desulfurization of L-cysteine catalyzed by the nifS gene product. *Biochemistry*, 33(15), 4714–4720.
- Zheng, L., White, R. H., Cash, V. L., Jack, R. F., & Dean, D. R. (1993). Cysteine desulfurase activity indicates a role for NIFS in metallocluster biosynthesis. *Proceedings of the National Academy of Sciences of the United States of America*, 90(7), 2754–2758.

I - 3 - The SUF machinery

I - 3 - 1 - Fe-S assembly

The SUF (Sulfur Utilization Factor) machinery is the most widespread Fe-S cluster biogenesis machinery in bacteria (Garcia *et al.* 2022). *E. coli* possess the ISC system as well as the SUF system. The SUF system follows the same steps as the ISC machinery to produce Fe-S clusters, *i.e.* acquisition of iron and sulfur, assembly of the cluster on a scaffold, and delivery of the cluster to the apoproteins target (Fig. 1). However, the SUF machinery displays key

differences with the ISC machinery that I will present briefly. The SUF machinery is genetically organized in an operon, *sufABCDSE*. SufS is a cysteine desulfurase that contains the pyridoxal 5'phosphate (PLP) cofactor required for its activity. SufS catalyzes the conversion of cysteine to alanine through the production of a persulfide, however it requires an additional protein to perform this task. SufE is a homodimeric protein that acts both as an enhancer of SufS activity and as a sulfur relay for the transfer of the sulfur on the scaffold. It is considered that SufSE forms a heterodimeric cysteine desulfurase (Loiseau *et al.* 2003, Outten *et al.* 2003). The SufBC₂D complex is the scaffold of the SUF system. It is constituted of a SufB and SufD interacting with two monomers of SufC (Fig. 1). After its formation on the scaffold, the cluster is loaded on the SufA homodimer for the delivery to the apoproteins target.

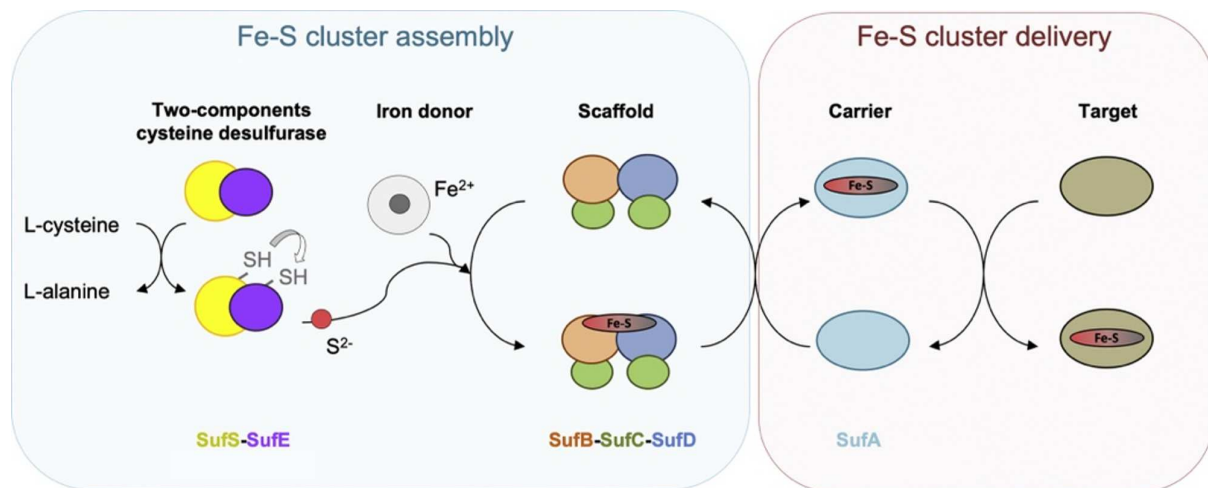


Figure 1. Fe-S cluster assembly and delivery by the SUF machinery in *E. coli*. Modified from (Garcia *et al.* 2019).

I - 3 - 2 - Physiological role of SUF in *E. coli*

ISC and SUF are thought to share the same substrates but the main difference between the two systems is their condition of expression. In *E. coli* SUF acts a backup system when the ISC system is unable to perform its function. This occurs when *E. coli* is exposed to stresses that affect Fe-S clusters. Those stresses include iron limitation as well as oxidative stress and nitrosative stress. It has been suggested that these stresses affect ISC capacity to produce Fe-S cluster which leads to the concomitant switch to the SUF system (Jang *et al.* 2010). Regulators controlling *suf locus* expression are IscR, Fur, OxyR and NsrR.

IscR is the regulator of Fe-S homeostasis and is the first gene encoded of *isc* operon. IscR exists under two forms, Holo- and Apo-form. When IscR is loaded with its [2Fe-2S] cluster, Holo-IscR represses the expression of the *isc* operon, whereas under its Apo-form it activates the *suf* operon expression.

Fur is the main regulator of iron homeostasis. When Fur is bound to Fe²⁺ it represses the expression of the *suf* operon as well as the expression of the non-coding RNA RyhB (Masse *et al.* 2002, Lee *et al.* 2008). When iron bioavailability decreases however, the Fe²⁺ cofactor is lost, and the repression is alleviated. Once RyhB is expressed, it targets the intergenic region between *iscR* and *iscS* and provokes the inhibition of translation of the downstream genes, *iscSUA*, while stabilizing *iscR* mRNA. Apo-IscR therefore accumulates and activates the expression of the *suf* operon (Desnoyers *et al.* 2009). Iron limitation leads to the expression of *suf* by both alleviating Fur repression and by permitting Apo-IscR accumulation (Fig. 2).

OxyR is a regulator of the LysR family, it is mainly known for its role in the activation of the oxidative stress response, in particular stress induced by hydrogen peroxide (H₂O₂). Under its reduced form, OxyR is inactive. However, oxidation of the solvent exposed Cys199 residue by sulfenylation (S-OH), sparks the formation of a disulfide bonds between the Cys199 and the Cys208 which leads to the activation of OxyR (Storz *et al.* 1992, Zheng *et al.* 1998, Kim *et al.* 2002, Lee *et al.* 2004). Oxidized OxyR (Ox-OxyR) controls the expression of around 30 genes, amongst which the *suf* operon, as well as the catalase gene *katG* and the sRNA gene *oxyS* that further extends OxyR regulon by 40 additional genes (Altuvia *et al.* 1997). It has been reported that OxyR binding to the *suf* promoter requires the Integration Host Factor (IHF) binding in a region located 139 nt upstream of *suf* transcription initiation site. IHF binding remodels the DNA structure of the region to bring the OxyR binding site in the vicinity of the -35 and -10 promoter elements (Fig. 2) (Outten *et al.* 2004). As oxidative stress is known to oxidize ferrous iron (Fe²⁺) into ferric iron (Fe³⁺) it is therefore reasonable to think that Fur repression could also be alleviated during oxidative stress. Moreover, IscR cluster has been described to be destabilized by H₂O₂, the consequence is the activation of the *suf* operon by Apo-IscR (Schwartz *et al.* 2001).

Expression of the *suf* operon is also repressed by the NsrR regulator. NsrR is a [4Fe-4S] protein that represses the expression of genes involved in the nitric oxide stress response,

(see II-2-4). Upon exposure to NO, NsrR cluster is damaged and NsrR-dependent repression of the *suf* operon is alleviated (Fig. 2) (Partridge *et al.* 2009).

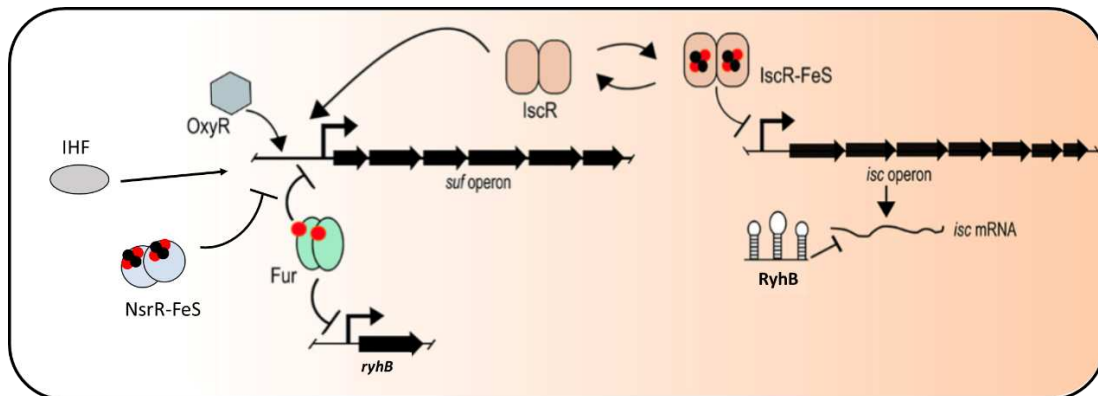


Figure 2. Regulation of Fe-S cluster synthesis in *Escherichia coli*. Red circles represent iron and black circles represent sulfur. Modified from (Esquilin-Lebron *et al.* 2021).

I - 3 - 3 - Two machineries, for what purpose?

While the molecular composition of ISC and SUF are different, the basic biochemistry of their mode of action is the same and they deliver Fe-S clusters to the same proteins. Under rich medium, in the presence of O₂, a strain lacking both ISC and SUF is not viable. This is because of the essentiality of two [4Fe-4S] enzymes, IspG and IspH (Loiseau *et al.* 2007). These enzymes catalyze the last step of the methylerythritol 4-phosphate (MEP) pathway. The ultimate products of this pathway are isopentenyl diphosphate (IPP) and dimethylallyl diphosphate (DMAPP) which are the two basic building blocks for isoprenoids. Isoprenoids are essential compounds required for the synthesis of peptidoglycan and lipopolysaccharides (Desai *et al.* 2016). The viability of a Δ *suf* mutant or of a Δ *isc* mutant demonstrates that IspG/H can obtain their cluster from either SUF or ISC machineries (Loiseau *et al.* 2007), illustrating how the presence of two Fe-S biogenesis machineries allow to maintain a constant Fe-S production under a wide range of growth conditions.

However, difference between ISC and SUF can be found in their efficiency in the maturation of the same targets. For example, the complex I and II of the electron transport chain (ETC) include Fe-S proteins, and their maturation by the SUF system is less efficient than

by the ISC machinery. Aminoglycosides enter the cell through the Proton Motive Force (PMF) which is generated by the activity of the proteins of the ETC. It has been reported that a $\Delta iscUA$ mutant, a strain producing Fe-S cluster through the SUF machinery only, displays an increased resistance to aminoglycosides. This phenotype can be explained by a low efficiency in the maturation of the Fe-S proteins of the ETC, a weaker activity of these proteins implies a weaker PMF and thus to less entry of aminoglycosides (Ezraty *et al.* 2013).

I - 4 - Fe-S carriers

E. coli makes use of dedicated proteins, called carriers, for the delivery of Fe-S clusters to the apoproteins target. The A-type carriers (ATCs) are IscA, SufA and ErpA (Fig. 3). They are small proteins that can bind clusters thanks to three cysteines. Interestingly, the SufA and IscA carriers are redundant and can both receive clusters from either ISC or SUF machineries and deliver them either to the Fe-S apoproteins or to ErpA (Loiseau *et al.* 2007). Under aerobiosis $\Delta erpA$ mutant and $\Delta sufA \Delta iscA$ mutant are not viable (Loiseau *et al.* 2007, Vinella *et al.* 2009). The choice of carriers can be influenced by the intrinsic features of the target protein but also by the environmental growth conditions as well. For instance, ErpA is required for IspG maturation under aerobiosis but can be replaced by IscA under anaerobiosis (Vinella *et al.* 2009).

NfuA has also been identified as an Fe-S carrier. While its N-terminal domain is similar to ATC's N-terminal domain, it lacks the cysteines residues involved in the binding of the cluster. It has been however reported that NfuA is able to reconstitute the clusters of the lipoate synthase LipA (McCarthy *et al.* 2017). Other non-ATC Fe-S carriers have been identified in *E. coli*, some of them thanks to their homology with eukaryotic Fe-S carriers, such is the case of Mrp. Mrp belongs to the Nbp35 ATPase family and has been shown to participate in the maturation of the complex I of the electron transport chain (Leipe *et al.* 2002, Burschel *et al.* 2019).

BolA cannot bind an Fe-S cluster on its own, however it has been suggested that it interacts with GrxD, a monothiol glutaredoxin, and forms a heterodimer capable of delivering a 2Fe-2S cluster to the Fdx protein in vitro (Li *et al.* 2012). GrxD can also bind another BolA-

like protein, IbaG. Dlouhy and collaborators demonstrate that GrxD-IbaG heterodimer is able to coordinate a [2Fe-2S] cluster *in vitro* (Dlouhy *et al.* 2016).

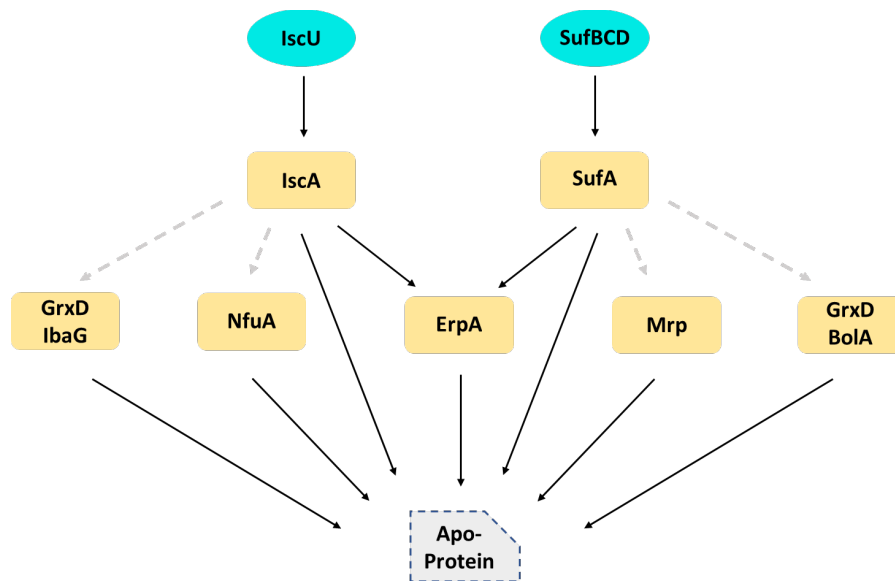


Figure 3. Schematic representation of the Fe-S carrier network in *E. coli*. Black arrows indicate the transfer of Fe-S cluster. Grey arrows represent presumed Fe-S cluster transfer.

I - 5 - The other Fe-S biogenesis machineries

I - 5 - 1 - The NIF machinery

The NIF (Nitrogen Fixation) system was the first described Fe-S biogenesis machinery. The NIF machinery is composed of a cysteine desulfurase NifS, a scaffold protein NifU, and an A-type carrier IscAnif. Some data suggest a role for the membrane associated Rnf complex for providing electrons to the NIF machinery (Curatti *et al.* 2005). NIF is often found in diazotroph and has been shown to provide Fe-S clusters for the nitrogenase of these bacteria. The most thoroughly studied diazotroph bacteria is *Azotobacter vinelandii*. This organism has three distinct systems for nitrogen fixation that uses Fe-S clusters as co-factors. However, the nature of the clusters is much more complex than the classical rhombic, cubane or cuboidal clusters. The FeMo-cofactor of the molybdenum dependent nitrogenase is an unusual Fe-S cluster composed of [7Fe-9S-Mo-C-Hemocitrate]. As for the vanadium dependent nitrogenase, it has an [7Fe-9S-V-C-Hemocitrate] cluster. Finally, the last nitrogenase contains a cluster that

contains neither Mo or V, [7Fe-9S-C-Hemocitrate] (Dos Santos *et al.* 2017). While the NIF system is able to form these unusual Fe-S clusters, it can also form classical [2Fe-2S], [4Fe-4S] and [3Fe-4S] clusters for other target proteins (Chatelet *et al.* 1999).

I - 5 - 2 - MIS and SMS

Amongst the other Fe-S cluster biogenesis machineries SMS and MIS minimal systems are the most recent addition. They stand for Minimal Iron-Sulfur (MIS) and SUF-like Minimal System (SMS). SMS and MIS have been identified by a phylogenetic and genomic context analysis combined approach that suggests that both MIS and SMS are ancestral systems dating back to the LUCA (Garcia *et al.* 2022). Moreover, since the discovery of the SMS and MIS machineries is still recent, there are still many bacteria whose Fe-S machineries are still miss-annotated. For instance, it was thought for a long time that *Helicobacter pylori* possess a NIF machinery, but the phylogenetic study of Garcia and collaborators has demonstrated that *H. pylori* machinery was in fact a MIS (Garcia *et al.* 2022). The MIS system is composed of a pair of IscS/IscU-like homologues called MisS/MisU. The MIS system can be found in archaea as well as in bacteria. As for the SMS system it is composed of two homologues of the SUF scaffold proteins SufBC called SmsCB. The SMS system can be found in both bacteria and archaea as well. The absence of carriers and in the case of SMS the absence of a desulfurase raises questions on the mode of action of these minimal systems.

II - Fe-S regulators of *E. coli*

II - 1 - Description of the Fe-S proteome of *E. coli*

Fe-S clusters are involved in most of the cellular processes, such as gene expression, RNA transcription and modification, translation, DNA replication and repair, vitamin, metabolite and amino acid biosynthesis, and bioenergetics (Fig. 4). Therefore, correctly identifying Fe-S protein has always been a major point of interest.

Characteristics of Fe-S proteins are various, an unwary mind might rely on imprecise criteria, such as the Fe-S binding motif, for the identification of Fe-S proteins. It is admitted that the ligation of Fe-S clusters involves cysteines. The thiol group of cysteines bind the iron atoms of the cluster. The presence of a four cysteine-containing motif is generally a good indication of an Fe-S cluster, however other parameters are also involved such as the proximity of the cysteines. Moreover, the cysteine motif is not exclusive to Fe-S clusters, other metals can be bound to these cysteines, such as Zinc (Jakob *et al.* 2000). The absence of multiple cysteines is not a proof of the absence of an Fe-S cluster as well, it has been reported that some Fe-S proteins coordinate their cluster using oxygen based (tyrosine, aspartate, glutamate) or nitrogen based (arginine or histidine) residues (Bak *et al.* 2014). Therefore, predicting an Fe-S protein based solely on the primary sequence can lead to false negatives and false positives. In 2022, Lenon and collaborators proposed a comprehensive approach for the identification and prediction of Fe-S proteins in *E. coli*, involving computational data such as Fe-S cluster binding motif and folding prediction by Alphafold as well as experimental based proof (Mössbauer spectroscopy, UV-visible, electron paramagnetic resonance EPR, resonance Raman, etc.). This resulted in the prediction of 181 proteins composing the Fe-S proteome of *E. coli* (Fig. 4). Fe-S proteins are present in all major cellular pathways, from biosynthetic pathways to gene regulation with respiration being the most represented process, roughly a third of the Fe-S proteome (Lenon *et al.* 2022). The participation of Fe-S proteins in all of these functions is favored by the physico-chemical properties of their clusters. Fe-S clusters can exhibit various redox states which makes them excellent catalysts for inter- and intramolecular electron transfer. Their redox values can range from -100 to -600mV SHE (Standard Hydrogen Electrode) depending on the electronic properties of the surrounding amino acids of the cluster (Beinert *et al.* 1997). One class of proteins that makes the best use of the properties of Fe-S clusters is the S-adenosylmethionine (SAM) family of enzymes. SAM enzymes use their clusters for the injection of one electron at low potential in order to generate free radicals used in a plethora of biosynthetic and metabolic process (Padovani *et al.* 2001, Ollagnier-de Choudens *et al.* 2002, Jarrett 2003). Fe-S clusters allow non-redox chemistry as well, with strong Lewis's acid properties thanks to the ferric ions, such is the case of hydratases like the aconitase (Beinert *et al.* 1996). Finally, Fe-S cluster can act as sensor in the regulatory function

of Fe-S transcriptional regulators, they can sense Reactive Oxygen Species (ROS), Reactive Nitrogen Species (RNS), superoxides (O_2^-) and nitric oxide (NO).

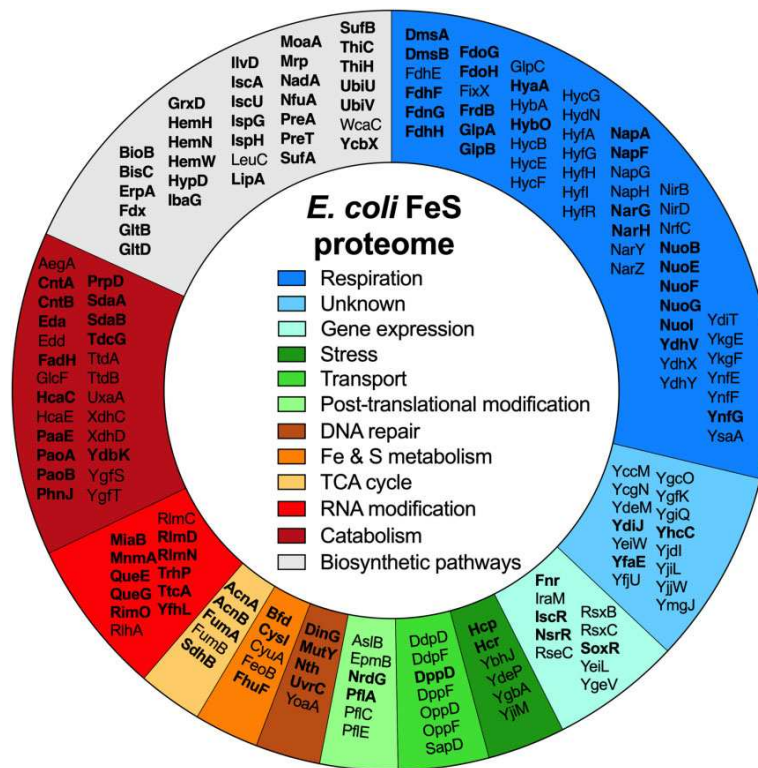


Figure 4. The Fe-S proteome of *E. coli*. Distribution of the *E. coli* Fe-S proteins according to their association with a specific biological process. Fe-S proteins characterized by biophysical approaches are in bold. Fe, iron; S, sulfur; TCA, tricarboxylic acid cycle. From (Lenon et al. 2022).

II - 2 - Diversity of Fe-S regulators in *E. coli*

E. coli possess 5 transcriptional regulators that bear an Fe-S cluster. The presence of an Fe-S cluster allows sensing of stresses such as ROS, RNS, O_2^- , and NO as well as low iron environment. However, some regulators are specialized in stress response such as SoxR for superoxide or NsrR for nitric oxide while others have a more global role like IscR the regulator of Fe-S homeostasis, or FNR the regulator of the transition between aerobic and anaerobic respiration. Finally, YeiL is a regulator of unknown function, and the Chapter II of my thesis is dedicated to its characterization.

II - 2 - 1 - FNR, the regulator of anaerobic adaptation

FNR (name originating from defective in Fumarate and Nitrate Reduction mutants) controls the adaptative response to the transition between aerobic and anaerobic environment (Salmon *et al.* 2003, Kang *et al.* 2005, Ireland *et al.* 2020). FNR belongs to the CRP/FNR family, this family of regulators is characterized by the presence of a C-terminal DNA binding domain, an extensive helical-coiled dimer interface and a sensory N-terminal domain (Fig. 5) (Korner *et al.* 2003). In the case of FNR the sensory component is the [4Fe-4S] cluster. FNR cluster is coordinated by the Cys20, Cys23, Cys29 and Cys122 residues (Lazazzera *et al.* 1996).

In anaerobic conditions FNR has a cubane [4Fe-4S] cluster. The presence of the cluster leads to the dimerization of the protein and FNR is then considered under its Holo active form. In presence of O₂ however, FNR cluster gets damaged by sulfur-based oxidation. Oxygen exposure leads to the transition of the [4Fe-4S] cluster to a rhombic [2Fe-2S] cluster which subsequently leads to the dissociation of the dimer thus provoking the loss of activity of FNR (Khoroshilova *et al.* 1997). Long exposure to oxygen can ultimately lead to the destruction of the cluster (Sutton *et al.* 2004, Reinhart *et al.* 2008). The structure of *Aliivibrio fischeri's* FNR provides great insight on the mechanism of this regulator (Fig. 5). In addition, *A. fischeri* FNR has the same length as *E. coli's* FNR and shares 84% of amino acid sequence identity with it. It can also complement a Δfnr *E. coli* strain (Septer *et al.* 2010, Volbeda *et al.* 2015). The dimerization of FNR is mediated by the α C helix. The interaction between the helices of each monomer involves a hydrophobic network as well as two critical residues, Arg140 and Asp130. The R140 is located at the beginning of the α C helix, and D130 is located on the α B helix of the second monomer (Fig. 5). These two residues seem to form a salt bridge that is crucial for dimerization (Volbeda *et al.* 2015). Moreover, Volbeda and collaborators suggest that a hydrophobic patch of interaction in the vicinity of the cluster might play the role of a relay between the cluster and the dimerization interface. When exposed to O₂, the rearrangement that takes place to accommodate the [2Fe-2S] cluster could propagate through the hydrophobic patch and break the salt bridges at the interface of the dimer. Interestingly, it has been demonstrated that two negatively charged residues at the interface of dimerization plays an important role in preventing apo-FNR dimerization via charge repulsion. Substituting

either D154 or E150 by an alanine leads to the dimerization of FNR even in absence of the cluster (Volbeda *et al.* 2015).

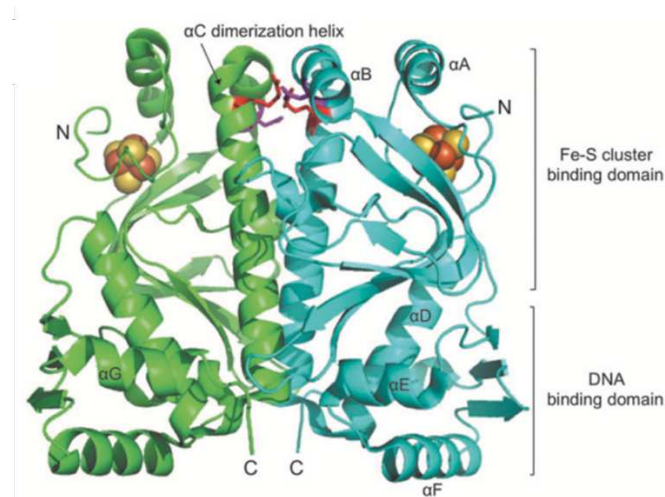


Figure 5. Crystallographic structure of [4Fe-4S]-FNR. The protein dimer is shown in cartoon representation, with individual protein subunits shown in *cyan* and *green*. Present in each subunit is a [4Fe-4S] cluster shown as *yellow* and *orange* spheres. Labeled are the N-terminal Fe-S cluster binding domain, the C-terminal DNA binding domain, and the seven α -helices present in FNR (designated with *letters A–G*), including the α C dimerization helix. Also shown are the side chains of residues R140 (*red*) and D130 (*magenta*), which form intersubunit salt bridges that contribute to dimerization. This figure originates from (Metttert *et al.* 2018) and was prepared with PyMOL using the structure available in the Research Collaboratory for Structural Bioinformatics PDB under the accession code 5E44 (Volbeda *et al.* 2015).

Altogether these results indicate that the FNR switch from apo to Holo form depends on conformational change mediated by the presence or absence of a [4Fe-4S] cluster. The state of the cluster is of course intimately linked to oxygen. FNR is therefore mainly active in absence of oxygen, it activates the expression of genes involved in the anaerobic oxidation of carbon sources and the reduction of terminal electron acceptors while repressing the expression of genes required during aerobic respiration. Amongst the most characterized functions activated by FNR we can find nitrate respiration, fumarate respiration, sugar fermentation, and acid resistance. FNR affects the expression of hundreds of genes in the cell, and it is admitted that FNR binds to at least 63 promoters (Kang *et al.* 2005, Metttert *et al.* 2018). A consensus for FNR binding has been defined (TTGATnnnnATCAA) but some degenerated sites have been shown to be also recognized by FNR. FNR binding sites are

located at variable positions within the promoter regions governing whether FNR acts as an activator or a repressor (Myers *et al.* 2013). At FNR activated promoters the binding site is usually found 41 nucleotides upstream of transcription start site (TSS) which places FNR in a position to interact with $\sigma 70$ and α subunits of the RNA polymerase. As for the repressed promoters, the binding site can be found just upstream of the -35 box up to overlapping the TSS thus interfering with the RNA polymerase binding (Lonetto *et al.* 1998, Barnard *et al.* 2004, Browning *et al.* 2004). One of the most strongly upregulated gene by FNR is a gene encoding a protein of unknown function, *ydfZ* (Kang *et al.* 2005). Interestingly it has been shown that this gene is still regulated by FNR under aerobiosis albeit with 60-fold less than in anaerobiosis. However, this residual activity suggests that under aerobic condition a small portion of FNR remains in Holo-form. This gene has since been used as a read-out for FNR activity under aerobiosis (Mettert *et al.* 2008).

II - 2 - 2 - IscR and Fe-S cluster homeostasis

IscR is a regulator belonging to the Rrf2 family of winged helix-turn-helix transcriptional factors. IscR has a [2Fe-2S] cluster that allows the sensing of the following signals: iron limitation, aerobiosis, oxidative stress and possibly nitrosative stress (Schwartz *et al.* 2001, Yeo *et al.* 2006, Rajagopalan *et al.* 2013). IscR cluster is coordinated by the Cys92, Cys98, Cys104 and His107 residues (Fleischhacker *et al.* 2012). IscR has two types of binding sites, Type 1 and Type 2. Type 1 is only bound by Holo-IscR whereas Type2 can be bound by both Apo- and Holo-IscR (Fig. 6) (Mettert *et al.* 2014).

iscR is the first gene of the *isc* operon and is separated from the rest of the operon by an intergenic region of a 111 bp. This region is the target of a small regulatory RNA (sRNA) RyhB. RyhB itself is repressed by the Fur regulator bound to ferrous iron (Fe^{2+}). When iron becomes limiting, the Fur mediated repression is alleviated and RyhB is expressed. The consequence is the down regulation of the genes downstream of *iscR* (*iscSUA*) resulting from a RyhB-dependent translation inhibition (Desnoyers *et al.* 2009). Holo-IscR represses the expression of the *isc* operon, which leads to a low expression of the genes of the ISC machinery to the point where Apo-IscR accumulates. At this point the repression is alleviated, the *isc* operon is expressed and the homeostatic negative feedback loop starts again (Giel *et al.* 2006).

As discussed earlier (see I-3-2) the expression of the *suf* operon, encoding the SUF machinery, is under the control of Apo-IscR. In fact, it has been shown that IscR is essential for *suf* expression. IscR is therefore a sensor of Fe-S clusters homeostasis and in turn it regulates their biogenesis.

Interestingly IscR role is not restricted to Fe-S clusters regulation, as a matter of fact, IscR regulates more than 40 genes in *E. coli* allowing to coordinate Fe-S homeostasis to non-related metabolic pathways (for more details about IscR see I-2) (Giel *et al.* 2006, Wu *et al.* 2009, Otsuka *et al.* 2010, Martin *et al.* 2011).

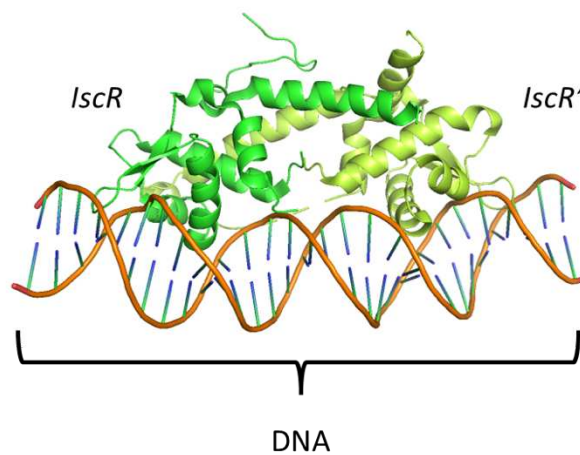


Figure 6. Crystallographic structure of Apo-IscR dimer bound to *hyA* promoter DNA. The protein dimer is shown in cartoon representation, with individual protein subunits shown in *lime* and *green*. This figure was prepared with PyMOL using the structure available in the Research Collaboratory for Structural Bioinformatics PDB under the accession code 4HF1 (Rajagopalan *et al.* 2013).

II - 2 - 3 - SoxR, a determinant regulator for oxidative stress response

SoxR (Superoxide response regulator) is a member of the MerR family. The signature of this family is found in the first 100 amino acids, they contain a helix-turn-helix motif followed by a coiled-coil region. Furthermore, many regulators of this family bind metal in their C-terminal region (Brown *et al.* 2003). In the case of SoxR it is a [2Fe-2S] cluster coordinated by the Cys119, Cys122, Cys124 and Cys130 residues (Watanabe *et al.* 2008). The most recent SoxR transcriptomic data suggests that this regulator directly controls the expression of only 11 genes (Seo *et al.* 2015). The most noteworthy target of SoxR is *soxS*.

SoxR activates the expression of *soxS* in response to various reactive oxygen species (ROS) like superoxide (O_2^-) and other redox-active molecules (Greenberg *et al.* 1990, Nunoshiba *et al.* 1992, Vasil'eva *et al.* 2001, Gu *et al.* 2011). SoxS controls the expression of 34 genes (Greenberg *et al.* 1990, Seo *et al.* 2015). Amongst them, *sodA* a gene encoding a superoxide dismutase (SOD), whose function plays a major role in the superoxide detoxification. By having two iron atoms and one sulfur atom solvent exposed SoxR cluster acts as a stress sensor (Fig. 7). Both Apo- and Holo-SoxR are able to bind to the promoter of *soxS*, but the activation of the promoter not only depends on the presence of the cluster but on its redox state as well (Hidalgo *et al.* 1994, Gaudu *et al.* 1996, Gaudu *et al.* 1997, Hidalgo *et al.* 1997). As a matter of fact, SoxR cluster exists in two redox states. The reduced $[2Fe-2S]^{1+}$ is actively maintained by the NADPH-dependent RSX system (Gaudu *et al.* 2000, Koo *et al.* 2003, Gu *et al.* 2011, Krapp *et al.* 2011, Siedler *et al.* 2014). When the cluster is oxidized to the $[2Fe-2S]^{2+}$ form it activates the expression of *soxS* by optimally positioning the -35 and -10 promoter elements for interaction with the RNA polymerase (Watanabe *et al.* 2008). The -35 and -10 elements of *soxS* promoter are separated by an unusual 19 bp spacer, compared to the more common 17 bp spacer, this feature is shared by other promoters regulated by the MerR-family of regulators (Ansari *et al.* 1995, Hidalgo *et al.* 1997, Outten *et al.* 1999). Distortion of the promoter region is therefore required for the expression of the target genes. However, the exact mechanism by which the oxidation of the cluster induces this DNA remodeling is still unknown. Watanabe and collaborators suggest that the electrostatic environment of the cluster could be modulated upon oxidation of the cluster, thus leading to a small but substantial conformational change required for SoxR activity (Watanabe *et al.* 2008).

It has been demonstrated that both ISC and SUF machineries are able to mature SoxR in absence of stress, but under oxidative stress conditions, the SUF system is the only system providing the cluster to SoxR (Gerstel *et al.* 2020).

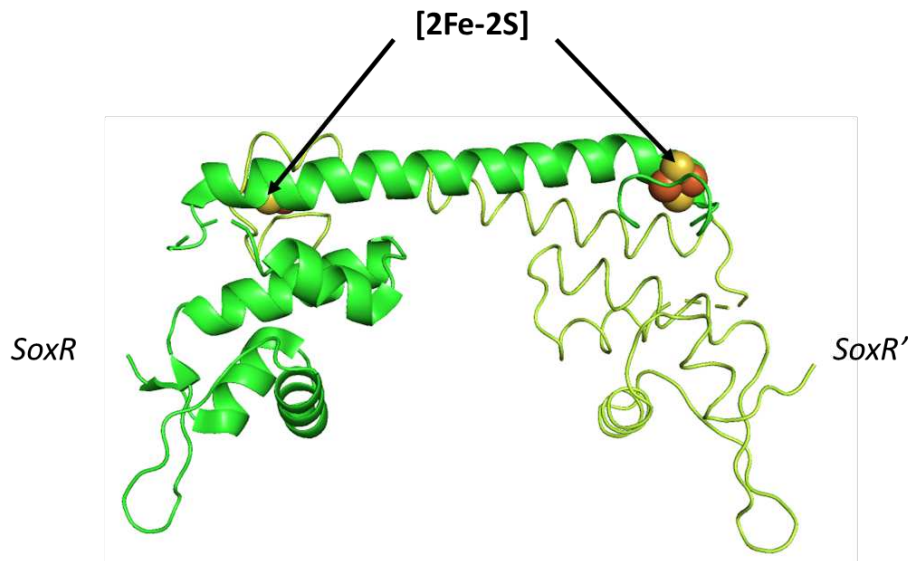


Figure 7. Crystallographic structure of Holo-SoxR. One monomer is shown in cartoon representation in *green*. The second monomer is shown in ribbon representation in *lime*. Present in each subunit is a [2Fe-2S] cluster shown as *yellow* and *orange* spheres. This figure was prepared with PyMOL using the structure available in the Research Collaboratory for Structural Bioinformatics PDB under the accession code 2ZHH (Watanabe *et al.* 2008).

II - 2 - 4 - NsrR, a nitrosative stress sensitive regulator

NsrR (Nitrite-Sensitive Repressor) is a transcriptional regulator from the Rrf2 family. In *E. coli*, NsrR represses the expression of at least 60 genes (Filenko *et al.* 2007). The NsrR regulon includes genes involved in the Nitric Oxide (NO) and Reactive Nitrogen Species (RNS) stress response. The most noteworthy genes are *hcp* and *hmpA* that I will discuss in the next chapter. As no *in vitro* characterization of *E. coli*'s NsrR has been reported, our understanding of NsrR comes mainly from reports on the *in vitro* properties of NsrR proteins from *Neisseria gonorrhoeae*, *Bacillus subtilis* and *Streptomyces coelicolor* (Tucker *et al.* 2008, Yukl *et al.* 2008, Isabella *et al.* 2009). NsrR binding motif corresponds to a 23 nucleotides stretch containing two half sites separated by 1 nt (11-1-11) where the second half site is an inverted repeat of the first (AAGATGCATTT) (Tucker *et al.* 2010). The *hcp* and *hmpA* promoters contain two NsrR binding sites with at least one of the binding sites overlapping the transcription initiation site (Tucker *et al.* 2010).

The nature of the cluster of the NsrR regulator is controversial. It has been reported that the cluster of *N. gonorrhoeae* NsrR is a [2Fe-2S] cluster whereas *B. subtilis* and *S. coelicolor* NsrR have a [4Fe-4S] cluster (Yukl *et al.* 2008, Isabella *et al.* 2009, Volbeda *et al.*

2017). It is however noteworthy that the only structure of a Holo-NsrR protein displays a [4Fe-4S] cluster (Fig. 8). The organism from which this structure was obtained is *S. coelicolor*, its NsrR primary sequence presents 39% of identity and 56% of similarity with *E. coli*'s NsrR. The *S. coelicolor* NsrR structure indicates that the cluster is coordinated by the Cys93, Cys99, Cys105 residues from one monomer and the Asp8 residue from the second monomer. As these four residues are conserved in *E. coli* the authors suggest that the same residues bind the cluster in *E. coli* (Volbeda *et al.* 2017).

Upon exposure to NO, NsrR cluster is nitrosylated on the iron atoms through the addition of a NO group, which leads to a conformational change mediated by the displacement of the DNA recognition helix that is thought to be sufficient to prevent DNA binding (Volbeda *et al.* 2017).

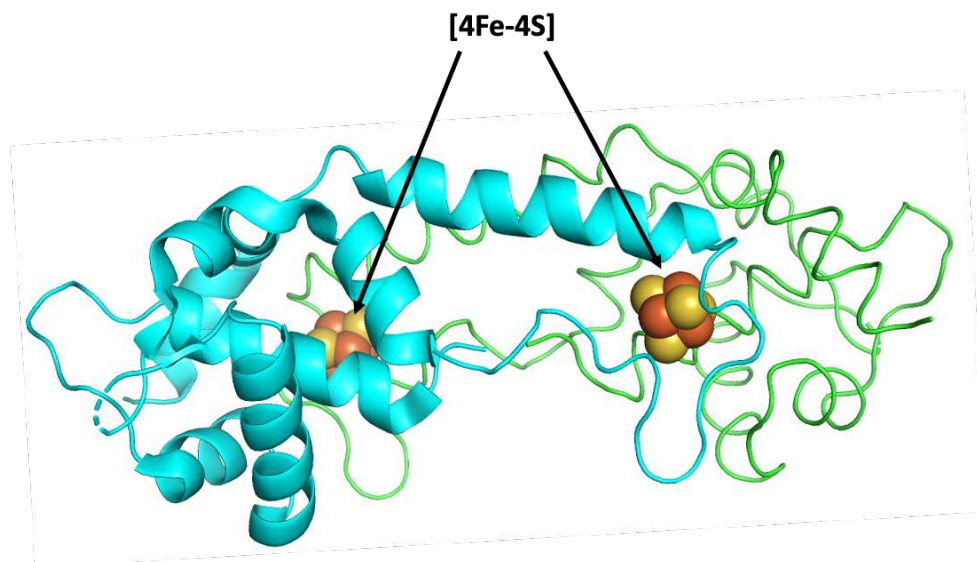


Figure 8. Crystallographic structure of Holo-NsrR. One monomer is shown in cartoon representation in *cyan*. The second monomer is shown in ribbon representation in *green*. Present in each subunit is a [4Fe-4S] cluster shown as *yellow* and *orange* spheres. This figure was prepared with PyMOL using the structure available in the Research Collaboratory for Structural Bioinformatics PDB under the accession code 5N07 (Volbeda *et al.* 2017).

III - Nitric oxide stress

III - 1 - Damage caused by NO to Fe-S clusters

Nitric Oxide is a short-lived, gaseous, membrane permeable, free radical that induces nitrosative stress in *E. coli*. NO can react with oxygen species such as superoxide or molecular oxygen to form Reactive Nitrogen Species (RNS) such as nitroxyl anions NO^- , nitrosium cation NO^+ , dinitrogen trioxide (N_2O_3), nitrogen dioxide radical (NO_2^\cdot) or peroxynitrite (ONOO^-) (Bartberger *et al.* 2002, Hughes 2008, Moller *et al.* 2019). The indiscriminate usage of both nitrosylation and nitrosation terms to refer to NO mediated damage has led to a state of confusion in this field regarding the correct nomenclature. For this reason, I will hereafter refer to all type of NO damage as S- or N- M-nitrosylation.

NO leads to the S-nitrosylation of thiol groups, N-nitrosylation of amino acids such as tryptophane, and nitrosative DNA damage. Metal cofactors like Fe-S are also a target of NO damage such as the M-nitrosylation of the iron atoms. Some Fe-S proteins like dehydratases (aconitase B and fumarase B) are particularly sensitive to NO damage, and the inactivation of these proteins can be responsible for the disruption of multiple functions in the cell (Gardner *et al.* 2002, Woodmansee *et al.* 2003, Gupta *et al.* 2012). It is reported that the M-nitrosylation of Fe-S cluster leads to the formation of the dinitrosyl iron complex (DNIC) $[\text{Fe}(\text{NO})_2(\text{RS})_2]^-$ and $[\text{Fe}_4(\text{NO})_8(\text{RS})_4]$ species but also dinuclear dinitrosyl species like Roussin's Red Ester (RRE) and another iron-nitrosyl species, Roussin's Black Salt (RBS) (Fig. 9). RRE species are composed of four iron ions bound by two NO ligands and bridged by cysteine residues, $[\text{Fe}_2(\text{NO})_4(\text{Cys})_2]$. RBS species are composed of a tetranuclear network of irons bridges by sulfides and bound to NO $[\text{Fe}_4(\text{NO})_7(\text{S})_3]^-$ (Fig. 9) (Harrop *et al.* 2008, Tonzetich *et al.* 2010). When Fe-S proteins are exposed to NO all of these four nitrosyl species can be found in various proportions and measured by EPR (For review Crack *et al.* 2014).

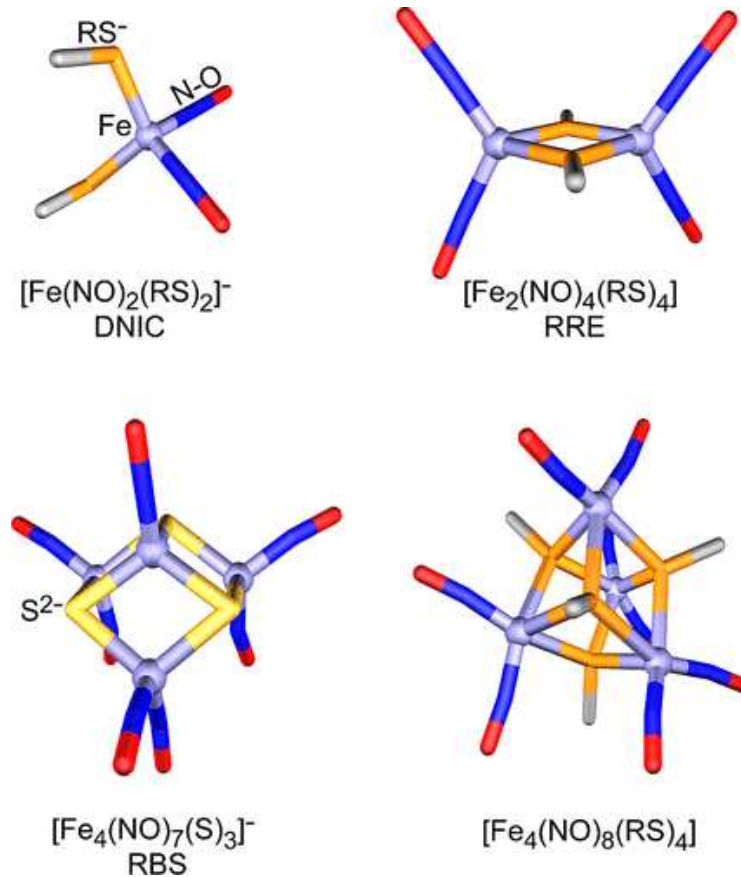


Figure 9. Structures of iron-nitrosyl species. Structures of (mono- nuclear iron) dinitrosyl iron complex (DNIC), Roussin's red ester (RRE), Roussin's black salt (RBS), and a tetranuclear iron octanitrosyl cluster species. Iron, sulfide, thiol, and NO are indicated. From (Crack *et al.* 2014).

III - 2 - NO sources

III - 2 - 1 - Host mediated NO production

In mammalian cells, NO is involved in various process including vasodilatation, muscle relaxation neurotransmission as well as defense against various pathogens including bacteria (Calabrese *et al.* 2007). NO is produced by Nitric Oxide Synthetase (NOS) enzymes. Three NOS enzymes are present in mammals. NOS1 and NOS3 or cNOSs are somewhat constitutively expressed and their activity is dependent on high intracellular Ca^{2+} level (Xie *et al.* 1992). cNOSs are considered to be the low-output pathway for NO production and are generally produced in a healthy host. NOS2 or iNOS, for inducible NOS, is engaged during inflammation

and infection (MacMicking *et al.* 1997). Induction of iNOS is generally promoted by cytokines such as TNF- α and interleukin-1 (IL-1). Although the type of cells might vary from a specie to another, iNOS is generally expressed in macrophages, T-cells, dendritic cells and neutrophils (Xue *et al.* 2018). All three NOS isoforms produce NO through the same biochemical pathway. NOS catalyzes the production of L-citrulline and NO from L-arginine. The reaction involves two sequential mono-oxygenase reactions, 1.5 molecules of NADH, two molecules of O₂, and the formation of the intermediate compound, N^ω-OH-arginine. NOS works as a dimer, it is associated with calmodulin protein, and uses 4 different co-factors to produce NO: heme, tetrahydrobiopterin, calmodulin, FMN and FAD flavins. The assembled complex is a 300 kDa complex (Cho *et al.* 1995, Ruan *et al.* 1996, Xie *et al.* 1996).

An Interesting side effect of NO production by the host immune system is the NO dependent production of diacid sugars. The NO released in the gut can lead to the conversion of simple sugars such as galactose or ribose to aldaric sugars, galactarate and ribaric acid respectively (Fig. 10). This reaction does not require any proteic catalyst to happen (Ouellette *et al.* 2014). The decreased bioavailability of fermentable sugars conjugated to the increased level of aldaric sugars provide, for the bacteria that are able to use these sugars (*E. coli*, *Salmonella typhimurium*), a considerable advantage over the bacteria that are unable to use it (Faber *et al.* 2016).

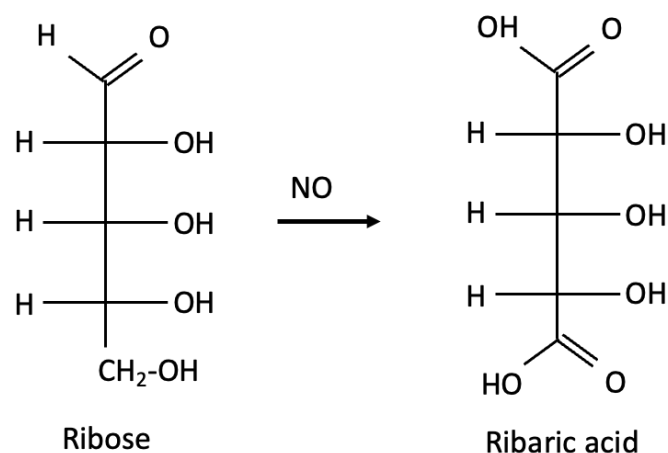


Figure 10. Fisher projection of ribose and ribaric acid. Exposure of Ribose to NO leads to the formation of a carboxylic group at each extremity of the sugar.

III - 2 - 2 - Endogenous NO production by *E. coli*

NO in bacteria can be produced from respiratory or non-respiratory routes. NO is enzymatically produced during ammonia oxidation, dissimilatory nitrate reduction and denitrification (Maia *et al.* 2014, Stern *et al.* 2014, Salas *et al.* 2021). The dissimilatory nitrate reduction to ammonium (DNRA) is considered to be the main source of NO in *E. coli*. The bacterium can use nitrate and nitrite as electron acceptors during anaerobic growth, the processes consist in the reduction of nitrate (NO_3^-) to nitrite (NO_2^-) and finally to ammonium (NH_4^+) (Simon *et al.* 2013). NO production can occur in the periplasm thanks to the enzymes encoded by the *nap* and *nrf* operons, or in the cytoplasm thanks to the *nar* and *nir* operon encoded enzymes (Fig. 11). The cytoplasmic membrane bound nitrate reductase complex (NarGHI) employs a redox loop to couple quinol oxidation with proton dislocation in order to generate proton motive force (PMF) (Unden *et al.* 1997). The periplasmic nitrate reductase complex (NapABC) can also help produce PMF by participating in the electron transport chain if coupled with a proton translocating enzyme, such as the NADH dehydrogenase I (NuoA-N enzyme) (Berks *et al.* 1995, Moreno-Vivian *et al.* 1998, Richardson 2000). NO production during anaerobic growth is the consequence of the reduction of nitrite by the cytoplasmic nitrate reductase, NarG as well as the nitrite reductase NrfA and NirB (Calmels *et al.* 1988, Ralt *et al.* 1988, Corker *et al.* 2003, Rowley *et al.* 2012).

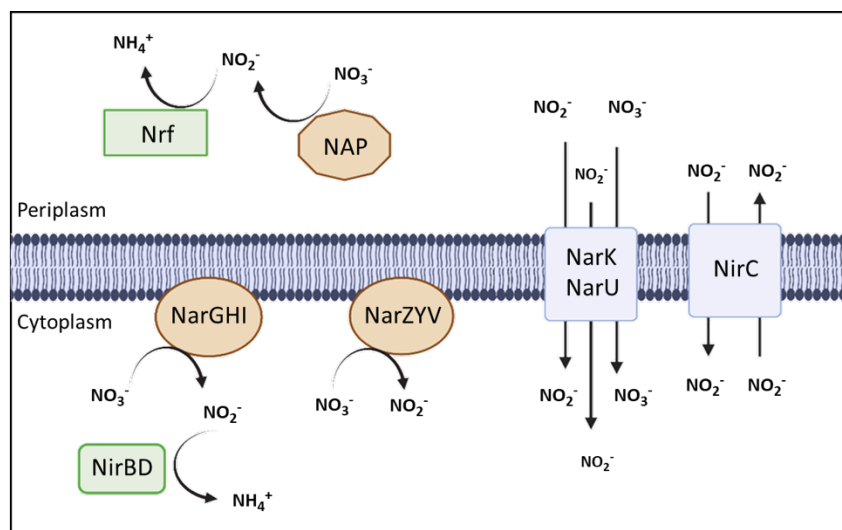


Figure 11. Representation of the nitrate respiratory chain in *E. coli*. The nitrate reductases are represented in brown, the nitrite reductases in green and the transporters in blue. Inspired by (Lundberg *et al.* 2004).

III - 3 - Defense systems against NO

Different studies aimed at the characterization of enzymes and protein responsive to NO have often been contradicting. This is often due to the use of NO-generating compounds such as GSNO or DEANO at concentrations that exceed by far the physiological concentration of NO encountered by the bacteria. While the use of such compounds can provide meaningful insight on the nitrosative stress response, they can also be misleading when the concentrations used lead to the inactivation of the activity of the proteins studied. Therefore, it is important that the results obtained with artificial NO generators are compared to physiological concentrations of NO in order prevent the mischaracterization of the proteins studied such as SoxR and FNR.

Bacteria have developed multiple ways to protect themselves from NO damages. *E. coli* relies on the activity of a handful of enzymes to detoxify the cell from NO. Upon NO exposure the transcriptional landscape varies greatly. Amongst the most up-regulated genes we can find *hcp-hcr*, *hmpA*, *norVW*, and *ytfE* (Constantinidou *et al.* 2006, Roos *et al.* 2006, Filenko *et al.* 2007)

III - 3 - 1 - Hcp, the first line of nitric oxide detoxification

Hcp (Hybrid-cluster protein) and Hcr (Hybrid-cluster reductase) are encoded in the same operon. Hcp is a protein that contains a [2Fe-2S] cluster and an unusual [4Fe-2S-2O] cluster (Pereira *et al.* 1999, van den Berg *et al.* 2000). The *hcp-hcr* operon is activated under nitrate respiration conditions. Hcp is a high affinity NO reductase that detoxifies low amount of NO accumulated during anaerobic nitrate respiration. The reaction involves two NO molecules for the production of N₂O (Wang *et al.* 2016). Latter, Seth and collaborators proposed that Hcp activity is rather to S-nitrosylate and M-nitrosylate proteins by transferring NO from Hcp's cluster (trans-nitrosylation) to proteins that have thiol groups (S-nitrosylation) and/or iron cofactors (Fe-nitrosylation) exposed (Seth *et al.* 2018). By comparing the total level of nitrosylation of proteins in a WT and a Δhcp strains, the authors observed a decrease of 90% of nitrosylated proteins in the mutant strain which led to the conclusion that Hcp was essential for the nitrosylation of proteins. The two apparent conflicting activities have

however been reconciled. Hagen and collaborators (2019) have shed additional light on the subject by demonstrating that the redox state of the hybrid-cluster is a key parameter for Hcp activity. They suggest that while both oxidized and reduced Hcp can be nitrosylated, only the reduced form is able to exhibit a NO reductase activity (Fig. 12) (Hagen 2019). This also explains the importance of Hcr activity in maintaining Hcp under its reduced form previously described (Wang *et al.* 2016). The biological importance of the trans-nitrosylative role of Hcp has yet to be understood.

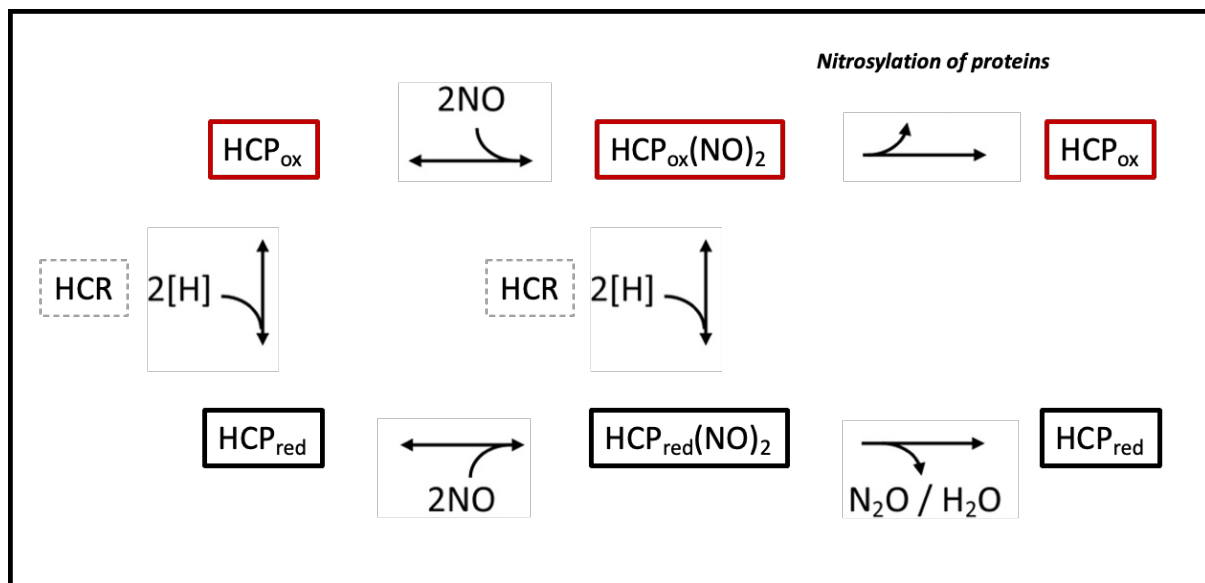


Figure 12. Representation of the proposed mode of action of HCP depending on its redox state. Red highlighted pathway represents the nitrosylation activity of Hcp whereas the black one represents the NO reductase pathway. Modified from (Hagen 2019).

III - 3 - 2 - HmpA and NO detoxification in aerobiosis

HmpA is a flavohemoglobin enzyme involved in the defense against nitrosative stress. An *E. coli* $\Delta hmpA$ strain is hyper-sensitive to NO (Stevanin *et al.* 2002). HmpA has been described as NO dioxygenase in presence of oxygen as well as a NO denitrosylase under anaerobiosis (Gardner *et al.* 1998, Hausladen *et al.* 2001). However, while the former activity has been confirmed by subsequent studies, the denitrosylase activity was refuted. The NO dioxygenase activity involves NADPH and FAD as cofactors. First NADPH reduces FAD which in turn reduces the heme iron of HmpA. The dioxygen then binds the reduced HmpA, which

dioxygenates the NO forming nitrate (NO_3^-). The requirement of O_2 for HmpA activity indicates that the enzyme is catalytically active in aerobic conditions. HmpA dependent NO removal activity was nonetheless measured in anoxic conditions. The rate of the reaction was found to be extremely slow in comparison to aerobic condition, which leaves the physiological relevance of the anaerobic activity up to debate (Kim *et al.* 1999, Gardner *et al.* 2002).

III - 3 - 3 - NorV a NO reductase

The *norVW* operon encodes a high-affinity flavorubredoxin NO reductase protein NorV and its associated protein the NADH-flavorubredoxin oxidoreductase NorW. NorV contains a non-heme di-iron catalytic center, a rubredoxin-like extension and a flavodoxin-like module (Wasserfallen *et al.* 1998, Gomes *et al.* 2000, Gomes *et al.* 2002). The NorVW system reduces NO thanks to an electron transfer chain. The electron is transferred from NADH to NorW to NorV that uses it to reduce NO into N_2O .

III - 3 - 4 - YtfE, an ambiguous role

The YtfE protein has been the subject of many studies, however up to today we are still unsure of its actual physiological role. YtfE has been proposed to be an iron donor for Fe-S cluster biogenesis, a repair protein for nitrosylated clusters a NO generating nitrite reductase or NO reductase (Justino *et al.* 2005, Justino *et al.* 2006, Lo *et al.* 2016, Silva *et al.* 2021, Crack *et al.* 2022). Whereas a role for YtfE regarding NO is fairly reasonable, as *ytfE* expression is both controlled by NsrR and NO-activated OxyR, further studies are still required to pinpoint its exact function in the cell.

III - 4 - Transcriptional regulations involved in NO defense

The three main NO detoxifying systems are under the control of transcriptional factors that sense different concentrations of NO.

III - 4 - 1 - *hcp-hcr* regulation

The *hcp-hcr* genes are organized in a single operon whose expression is under the control of 5 transcriptional regulators, FNR, NarL, NarP, NsrR and OxyR (Fig. 13).

III - 4 - 1 - 1 - FNR and anaerobic induction of *hcp*

FNR is the activator of *hcp-hcr* expression that is responsible for expression of the operon under anaerobiosis (Fig. 13) (Filenko *et al.* 2005, Chismon *et al.* 2010). However, FNR is not a transcriptional regulator specialized in NO sensing. In fact, previous reports indicating a role for FNR in NO stress response have since been disputed as the concentration of NO used in those experiments were way above the physiological conditions. FNR susceptibility to NO is a mere consequence of the presence of an Fe-S cluster which are known to be targets of NO damage.

III - 4 - 1 - 2 - The NarXL and NarPQ nitrate-responsive two-component systems

The *hcp-hcr* expression is activated by NarL and NarP transcriptional regulators. NarXL and NarPQ are two paralogous two-component systems in *E. coli* (Fig. 13) (Tyson *et al.* 1994, Pao *et al.* 1995). NarX is sensitive to nitrate and phosphorylate preferentially NarL, whereas NarQ is stimulated by both nitrate and nitrite and can phosphorylate both NarL and NarP. NarL and NarP share the same binding site albeit their affinities differ. NarXL and NarPQ regulate the expression of the genes involved in nitrate and nitrite reduction as well as the expression of the *hcp-hcr* operon (Filenko *et al.* 2005). The NarL and NarP are however not regulators induced by NO, their role is aimed at the regulation of the nitrate and nitrite reduction. However, since the reduction of these compounds involves NO generation, it is fitting that NarL and NarP activate the expression of the *hcp-hcr* NO defense system.

III - 4 - 1 - 3 - NsrR, the *ad hoc* NO responsive transcriptional repressor

The *hcp* operon is repressed by the transcriptional factor NsrR (Fig. 13). As mentioned earlier (see II-2-4), upon exposure to NO, NsrR cluster is damaged through the nitrosylation of the iron atoms. This modification induces a conformational change that affects NsrR affinity for DNA and therefore alleviates the repression exerted on *hcp* promoter. A mutational and deletion analysis of *hcp* promoter revealed that NsrR plays a major role in the expression of this operon (Chismon *et al.* 2010).

III - 4 - 1 - 4 - OxyR, a NO-stimulated activator

The most recent described regulator of *hcp-hcr* expression is OxyR. Although OxyR is mainly known for its role in the response to oxidative stress (see I-3-2) it was demonstrated that OxyR is responsive to NO as well and activates the expression of the *hcp-hcr* operon (Seth *et al.* 2012). The SNO-OxyR regulon was identified thanks to a transcriptomic approach comparing gene expression profile of a WT and a $\Delta oxyR$ strains grown anaerobically under nitrate or fumarate respiration. Reasoning that fumarate respiration does not lead to the S-nitrosylation of proteins, the authors identified over a 100 genes under the control of SNO-OxyR. Moreover, mass spectrometry identified the Cys199 residue as the target of SNO, the same cysteine crucial for the activity of OxyR under oxidative stress. However, it appears that Ox-OxyR regulon and SNO-OxyR show little to no overlap (Storz *et al.* 1992, Seth *et al.* 2012). OxyR is therefore a sensory protein that is able to activate two completely different set of genes in response to two different stresses. Exposure to SNO stress generators (GSNO) under anaerobic growth conditions revealed that OxyR is essential for the activation of *hcp* expression. In aerobiosis, however, the activity of OxyR seems important for a strong activation but not essential (Seth *et al.* 2012).

Interestingly, both stresses perceived by OxyR originate from bacterial respiration. Using oxygen as an electron acceptor leads to the unavoidable formation of ROS whereas using nitrate as an electron acceptor in anaerobiosis leads also to the unavoidable formation of NO and RNS. Since the same sensory cysteine is the target of the two modifications, one can only wonder on the consequence of encountering both type of stress concomitantly. Since oxygen and nitrate respiration are mutually exclusive, the only physiological conditions in

which the bacteria can face both oxygen and NO is during infection. When facing the immune response of host, the level of O₂ in the environment of the bacteria can range from microaerobia to complete anaerobia while facing the same time NO generated by macrophages and other immune cells. Moreover, the peroxisome of phagocytosing cells is an organelle in which both NO and H₂O₂ are present in high concentration (Di Cara *et al.* 2019), it would be interesting to study the activity of OxyR in presence of both ROS and RNS.

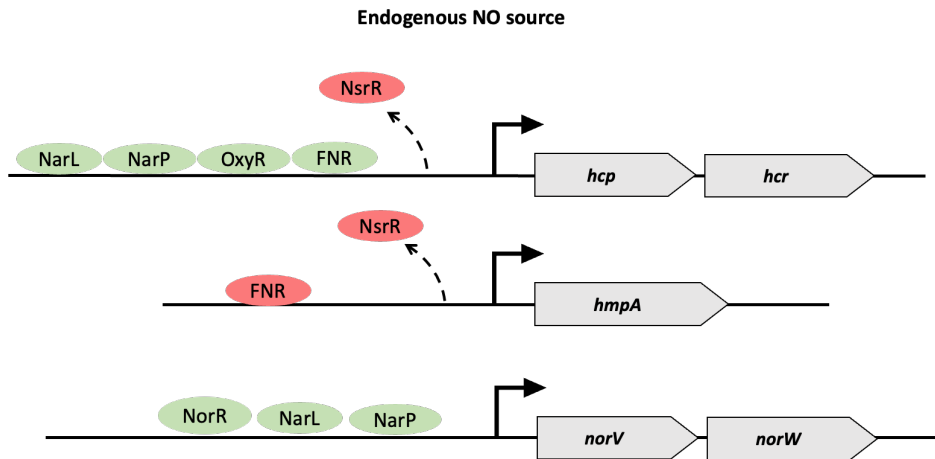
III - 4 - 2 - Regulation of *hmpA* and *norVW*

Expression of *hmpA* is under the control of three transcriptional factors, FNR, Fur and NsrR (Fig. 13). FNR represses the expression of *hmpA* under anaerobiosis and, upon transition to aerobiosis the repression is alleviated. Since HmpA acts as a NO dioxygenase, repressing its expression in anaerobiosis seems to be an efficient way to prevent the production of inactive proteins in the cell. The *hmpA* gene is also repressed by Fur-Fe²⁺ and Holo-NsrR. When the cell is exposed to NO, a nitrosylation of Fur's iron cofactor as well as the nitrosylation of NsrR cluster lead to the alleviation of the repression they exert on *hmpA* promoter activity, thus leading to the expression of the gene (Poole *et al.* 1996, D'Autreaux *et al.* 2002).

The *norVW* operon is activated by the NorR regulator and activated by NarL and NarP (Fig. 13). The *norR* gene is encoded upstream of the *norVW* operon in a divergent orientation. NorR activity is dependent of its N-terminal GAF domain that contains a mononuclear non-heme Iron. Nitrosylation of the iron is required for NorR activity. Binding of NO to the iron center activates the ATPase activity of the AAA+ domain enabling interaction with the RNA polymerase in order to activate the gene expression (D'Autreaux *et al.* 2005, D'Autreaux *et al.* 2008).

As for the NarL and NarP regulation of *norVW*, it is identical to their regulation of *hcp-hcr* operon (see III-4-1-2). They activate the expression of *norVW* in presence of nitrate and nitrite.

A)



B)

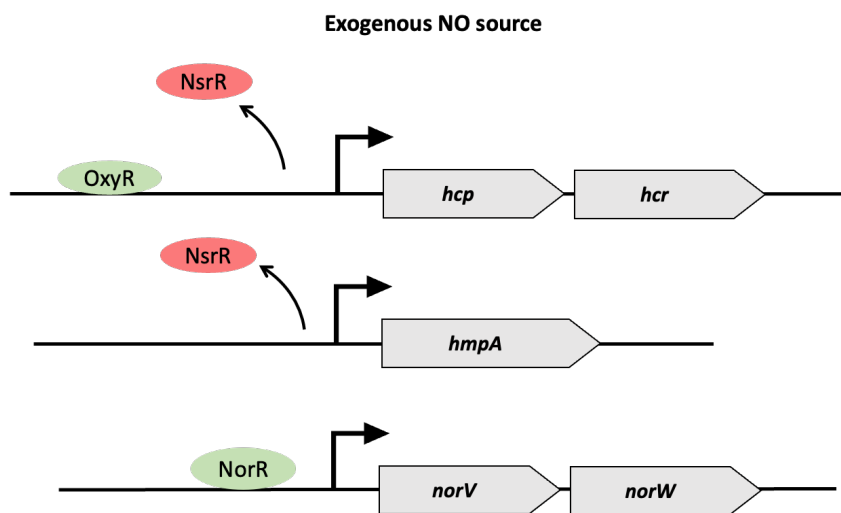


Figure 13. Genetic regulation of the NO defense systems in presence of endogenous or exogenous NO sources. In red repressors and in green activators. A) Regulation of the defense systems in during nitrate respiring conditions. B) Regulation of the defense systems in presence of exogenous NO source in aerobiosis.

IV - The Acyl Carrier Protein

IV - 1 - The role of ACP in the type II biogenesis of Fatty acids (FasII)

IV - 1 - 1 - The initiation step

The Acyl Carrier Protein, ACP, is an essential protein in most living organisms. ACP is a small cytoplasmic protein composed of 77 amino acids. *E. coli* produces around 6×10^4 molecules of ACP per cell which makes it the third most abundant protein in the cell (0,25% of the total soluble proteins) (Lu *et al.* 2007). The primary role of ACP is the biogenesis of fatty acids through the fatty acid synthesis (FasII) pathway. Fatty acids are essential components of the cell as they are required for the synthesis of the membrane, the formation of co-factors such as biotin and lipoic acid and participate in energy production. ACP is first produced under Apo-form, the conversion of Apo-ACP into Holo-ACP by the ACP synthase enzyme (AcpS) corresponds to the addition of a phosphopantetheine moiety (4'PP), originating from Co-enzyme A (CoA), on the serine 36 of ACP (Fig. 14). This Ser36 is located in the beginning of the second helix and is conserved in all the ACPs involved in fatty acid biogenesis (Thomas *et al.* 2005, Cronan 2014).

Malonyl-ACP is the major building block of fatty acids, it is obtained thanks to FabD activity which uses Malonyl-CoA and Holo-ACP as substrates (Fig. 14). The Holo-ACP carries the growing fatty acid chain through the thioester linkage of the fatty acyl intermediates to the thiol of the 4'PP group. The nascent-acyl chain is therefore bound to ACP and the fatty acid biogenesis cycle can proceed. ACP therefore exists under three forms, unmodified Apo-ACP, 4'PP attached Holo-ACP, and Acylated-ACP (Oefner *et al.* 2006).

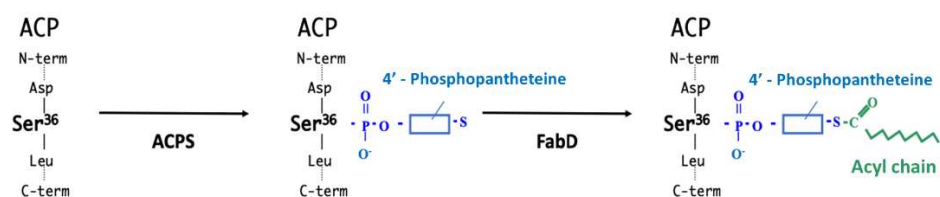


Figure 14. Maturation of ACP by ACPS and FabD.

IV - 1 - 2 - The fatty acid biogenesis cycle

During the biogenesis cycle ACP presents the acyl chain to the different enzymes responsible for the modification and elongation of the acyl chain. The first step, a condensation of the malonyl-ACP, is done by the β -Ketoacyl-ACP synthases FabB and FabF. The β -ketoacyl-ACP is then reduced into a 3-hydroxyacyl-ACP by the β -ketoacyl-ACP reductase FabG (Garwin *et al.* 1980, Heath *et al.* 1996, Edwards *et al.* 1997, Borgaro *et al.* 2011). Comes next a dehydration step of the β -hydroxyacyl-ACP into a *trans*-2-enoyl-ACP by either FabA or FabZ depending on the substrate (Heath *et al.* 1996, Leesong *et al.* 1996). Finally, an enoyl-ACP reductase converts the enoyl-ACP into acyl-ACP. At the end of the cycle FabH proceeds to add two additional carbons, originating from Acetyl-CoA, on the malonyl-ACP substrate in order to elongate the acyl chain (Fig. 15) (Magnuson *et al.* 1993, Heath *et al.* 1996, Beld *et al.* 2015).

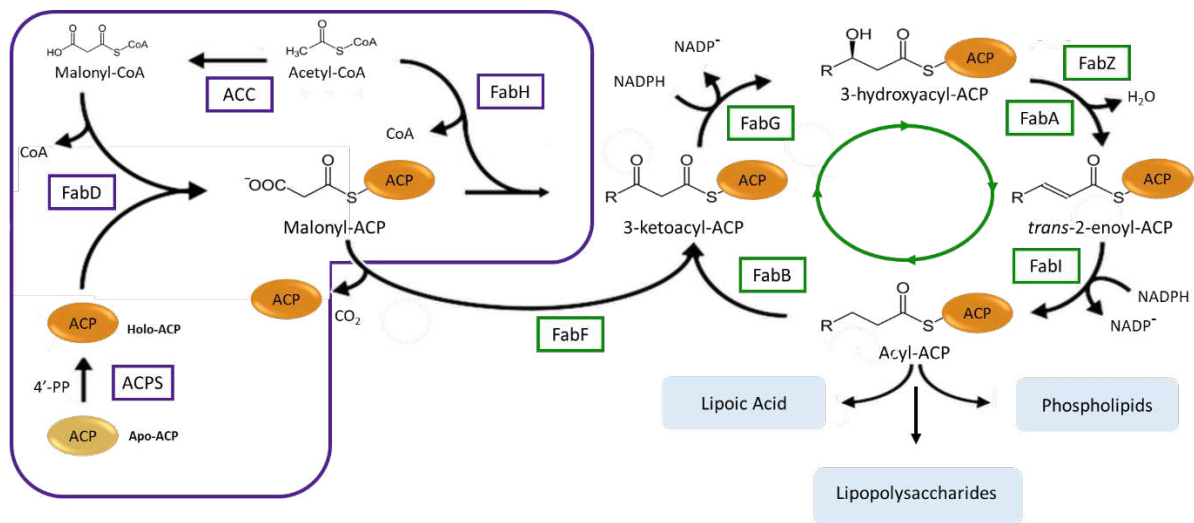


Figure 15. Fatty acid biogenesis (FasII) in *E. coli*.

IV - 2 - Acyl-ACP is important for the biosynthesis of fatty-acid derived compounds

IV - 2 - 1 - Phospholipid biosynthesis

Phospholipids are amphiphilic molecules that compose the membrane of the bacteria. Phospholipids are constituted of a glycerol backbone on which are attached two acyl chains and a polar head on a phosphate group.

De novo synthesis of phospholipids requires acyl chains. The acyl-chains originate from either the fatty acids biogenesis or degradation of exogenous fatty acids (β -oxidation pathway). When they originate from the fatty acid biogenesis, the acyl-ACP is used, whereas if they originate from the β -oxidation pathway, acyl-CoA is used. The first step involves the attachment of the acyl chain to the precursor of the phospholipid synthesis, the glycerol-3-Phosphate compound (G3P), thus forming the 1-acyl-G3P. This reaction is performed by the PlsB enzyme. The 1-acyl-G3P is then acylated furthermore by the PlsC enzyme using an additional acyl-ACP molecule as a substrate (Rock *et al.* 1981, Kessels *et al.* 1983, Gully *et al.* 2006).

IV - 2 - 2 - Lipopolysaccharide biosynthesis

ACP provides long chain fatty acids for the synthesis of the precursor of lipopolysaccharide (LPS) as well. The initiation of the LPS begins at the synthesis of the Lipid A. This process involves acyl-ACPs at multiple steps. First, there is the acylation of UDP-GlcNAc by LpxA using 3-hydroxytetradecanoyl-ACP as a substrate (Anderson *et al.* 1987, Galloway *et al.* 1990). The second step involving ACP is the acylation of the 3-myristoyl-UDP-GlcN by LpxD using myristoyl-ACP (Anderson *et al.* 1985, Helander *et al.* 1993, Kelly *et al.* 1993). Further down in the synthesis of LPS, the LpxL and LpxM enzymes use dodecanoyl-ACP and myristoyl-ACP respectively, for the acylation of two 3-Deoxy-d-manno-octulosonic Acid (Kdo) molecules on the lipid IVA intermediate thus finalizing the synthesis of the UDP-N-acetylglucosamine, the precursor for LPS synthesis (Emiola *et al.* 2014). Interestingly, exogenous fatty acids can bypass the need for the fatty acid biogenesis for all of the pathways diverging from the FasII but one, LPS synthesis (Yao *et al.* 2017).

IV - 2 - 3 - Lipoate Synthesis

Lipoic acid is an essential cofactor for the activity of the pyruvate dehydrogenase (PDH), the glycine cleavage system (GCV) and the α -ketoglutarate dehydrogenase (Reed *et al.* 1993). An octanoate group originating from octanoyl-ACP is first transferred to the LipB enzyme that subsequently insert it into the E2 subunits of the enzymes requiring lipoate for their activity. LipA catalyzes the insertion of two sulfur atoms into the octanoyl chain of the E2 subunits in order to form the lipoate cofactor. LipA belongs to the radical SAM family and contains two [4Fe-4S] clusters (Cicchillo *et al.* 2005) with one of the clusters, the auxiliary cluster, providing the sulfur atoms for the synthesis of lipoate (Fig. 16) (Ollagnier-De Choudens *et al.* 2000, Lanz *et al.* 2014).

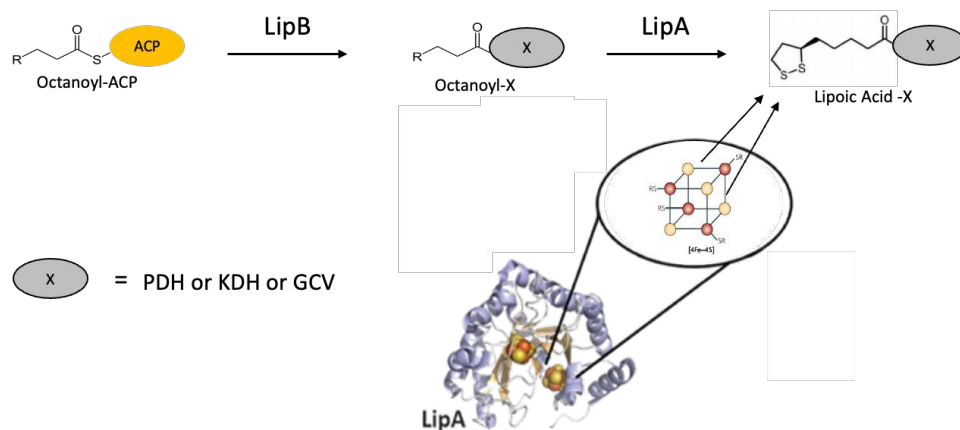


Figure 16. Lipoate biosynthesis pathway in *E. coli*. LipA auxiliary cluster provides the sulfurs necessary for the formation of lipoic acid.

IV - 2 - 4 - Biotin Synthesis

Biotin is an essential vitamin required for amino acids metabolism. The synthesis of biotin starts by the methylation by BioC of either a Malonyl-ACP or a Malonyl-CoA depending on the origin of the substrate. FabH combines a Malonyl-ACP with either a Malonyl-ACP methyl ester or a Malonyl-CoA methyl ester to form a 3-ketoglutaryl-ACP methyl ester. This intermediate product then enters the fatty acid biogenesis cycle and gets modified and elongated by the Fab enzymes until the production of a pimeloyl-ACP methyl ester. At which point the methylated fatty acid follows a subsequent set of reaction performed by the

BioHFADB enzymes (Lin *et al.* 2010). Much like lipoic acid the last step of the biotin synthesis involves a radical SAM enzyme BioB that uses its [4Fe-4S] and [2Fe-2S] clusters to insert the required sulfur atom to synthesize biotin (Fig. 17) (Tse Sum Bui *et al.* 2006).

In *E. coli*, only one enzyme uses biotin as a cofactor, the acetyl-CoA carboxylase (ACC) complex. The ACC complex catalyzes the formation of Malonyl-CoA from Acetyl-CoA by adding a carboxyl group. Biotin is used as a placeholder for the carboxyl in the two step-reaction (Broussard *et al.* 2013). As mentioned before (see IV-1-2) malonyl-CoA is the main source of carbon in the biogenesis of fatty acids and therefore its synthesis is crucial for the bacteria. It is interesting to note that the biotin is essential for the FasII pathway that is itself essential for the synthesis of biotin.

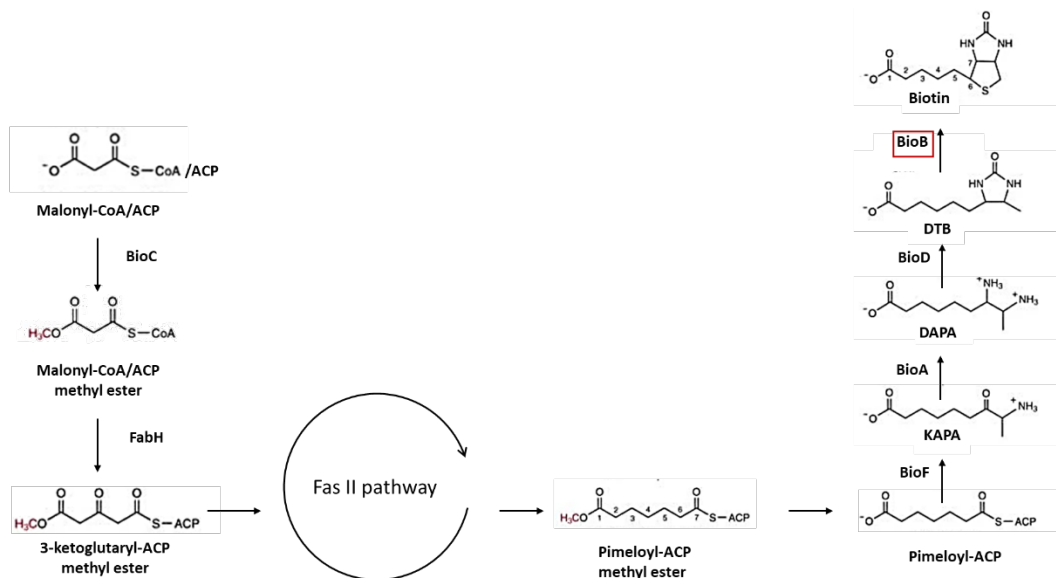


Figure 17. Biotin biosynthesis pathway. BioB is a radical SAM enzyme catalyzing the last step of the pathway.

IV - 3 - ACP's unexpected partners

IV - 3 - 1 - SpoT and the stringent response

ACP has been shown to participate in the regulation of guanosine 5'-(tri)diphosphate, 3'-diphosphate [(p)ppGpp] levels in the cell through its interaction with SpoT. The (p)ppGpp serves as an alarmone that can trigger the stringent response when it reaches a critical level. The outcome of the activation of this response is the growth arrest and the expression of resistance genes. SpoT possess both a (p)ppGpp hydrolase and a (p)ppGpp synthetase activity (Hernandez *et al.* 1991), which participate in the control of the level of (p)ppGpp in the cell depending on the cell needs. ACP interaction with SpoT involves an Holo-ACP although the presence of an acyl chain and its nature are uncertain. It has been proposed that ACP may play a regulatory role for SpoT activity, indeed ACP interaction with SpoT could tip the balance either in favor of the degradation or production of (p)ppGpp depending on the fatty acid metabolism status. (p)ppGpp also controls the expression of genes during the stringent response by modulating the activity of the RNA polymerase through direct interaction. Interestingly, amongst the genes affected by this interaction we can find the *fabH**BG* operon, essential for the FasII pathway. The connection between ACP and the stringent response is therefore bidirectional, ACP controls (p)ppGpp levels that in turn control FasII activity.

IV - 3 - 2 - The structural Maintenance of Chromosomes complex

MukB belongs to the Structural Maintenance of Chromosomes protein family. It plays a role in the partitioning condensation of the chromosome (Soppa 2001). MukB forms a complex with MukE and MukF that promotes the shrinkage of DNA. Cells lacking a functional MukBEF complex have disorganized chromosomes with misplaced genetic loci, their failure to properly segregate sister chromosomes leads to anucleated cell production. MukB was found to co-purify with ACP and a Cryo-EM study has confirmed the ACP-MukB interaction (Burmans *et al.* 2021). The interaction requires a functional ACP as the mutation of the serine 36, blocking ACP under its Apo-form, abolishes the interaction (Gully *et al.* 2003, Burmans *et al.* 2021). Moreover, it has been shown that ACP interaction is important for MukB ATPase activity

and disruption of the interaction *in vivo* leads to an altered localization of the MukBEF complex. ACP interaction with MukBEF is therefore important for MukBEF function *in vivo* (Prince *et al.* 2021). The role and biological significance of ACP in the structural maintenance of the chromosome has, however, yet to be identified.

IV - 4 - ACP and Fe-S biogenesis

IV - 4 - 1 - Mitochondrial ACP impacts Fe-S biogenesis

The mitochondrial ISC system is the dedicated system of production of Fe-S clusters in eukaryotes. The proteins involved are functional homologues of the *E. coli* ISC system and therefore works in an identical fashion. However slight differences exist, such as the presence of ISD11 (LYRM4), an essential member of the ISC machinery that belongs to LYRM proteins family (Wiedemann *et al.* 2006). The LYRM proteins family is characterized by a Leu-Tyr-Arg (LYR) motif. They are only found in mitochondria and are involved in a diversity of mitochondrial functions (Richards *et al.* 2006). ISD11 participates in the production of Fe-S clusters through its interaction with NFS1 the homologue of IscS in eukaryotes. ISD11 has been shown to help solubilize NFS1 and therefore is proposed to be a stabilizing cofactor for the cysteine desulfurase (Herrera *et al.* 2018). Interestingly a study aimed at the characterization of ACP1 (ACP homologue in *Saccharomyces cerevisiae*) interactome showed that Isd11 and NFS1 copurifies with ACP1. Furthermore, study of an ACP1 conditional KO showed an impairment of the activities of multiple Fe-S proteins, such as the aconitase and the respiratory complex I and II. Moreover, ectopic expression of the *acp1* gene rescued the Fe-S related phenotypes suggesting an important role of ACP1 in the biogenesis of Fe-S cluster (Van Vranken *et al.* 2016).

IV - 4 - 2 - Structure of the mitochondrial ACP-ISD11-NFS1 complex

In 2017 Boniecki and collaborators as well as Cory and collaborators sought to obtain the structure of the NFS1-ISD11 by crystallography (Boniecki *et al.* 2017, Cory *et al.* 2017). In order to purify the complex, the proteins were co-expressed and co-purified in *E. coli*. The most surprising outcome was the co-crystallization of *E. coli*'s ACP (ACPec) with the complex.

In both structures, Cory's and Boniecki's, an acylated-ACP is shown to interact with ISD11. The acyl-chain involved is of 16 carbon length in Cory's structure and 14 for Boniecki's. The two structures of the ACPEC-ISD11-NFS1 diverge, in Cory's case NFS1 dimer adopts an unusual conformation that has never been described in PLP-dependent desulfurase. Indeed, the structure displays two monomers of NFS1 making almost no contact with each other whereas Boniecki's structure is more coherent with previous desulfurase structures. I have decided to focus on their findings for this part (Fig. 18). The interaction between ACPEC and ISD11 involves the insertion of the acyl chain into a hydrophobic groove formed by the three helices of ISD11. The contacts between ACPEC and ISD11 are allowed by hydrophilic and charged sidechains, from ACPEC side the interaction involves the recognition helix α_2 , and from ISD11 it involves the helices α_1 and α_2 . A dimer of ISD11 interacts with a dimer of NFS1, it involves polar ionic interactions (Arg68^{ISD11}-Asp75^{NFS1} and Arg35^{ISD11}-Glu314^{NFS1}) and hydrogen bonds (Tyr31^{ISD11}-Arg72^{NFS1} and Asp38^{ISD11}-Tyr317^{NFS1}). Moreover, mutations of these residues have been described to cause human Fe-S deficiency diseases (Lim *et al.* 2013, Farhan *et al.* 2014). Although one might dismiss the crystallographic evidence for the interaction between ACPEC and ISD11 it is noteworthy to highlight that ACPEC shares 46% identity with the human ACP. Moreover, a crystallographic structure of the human mitochondrial ACP in complex with Isd11, NFS1, FXN (frataxin), and ISCU was obtained in 2019 and was consistent with Boniecki's structure (Fox *et al.* 2019). The exact role of the ACP-ISD11-NFS1 interaction is however unclear, some data suggest a role in the solubilization of NFS1 by ACP-Isd11 (Herrera *et al.* 2018).

It is interesting to note that in eukaryotes, multiple LYRM proteins have been described to interact with the mitochondrial ACP and involve the LYR motif in the interaction (Angerer 2013).

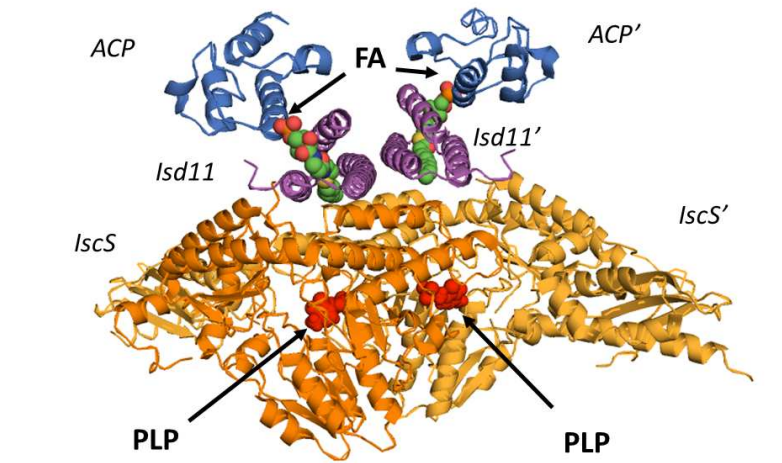


Figure 18. Crystallographic structure of the (ACP-ISD11-NFS1)². The complex is represented in cartoon. IscS dimer is represented in orange and light orange. Each IscS subunit contains a PLP co-factor. ISD11 monomers are represented in purple. ACP monomers are represented in blue. The fatty acid chain of 16 carbon is represented by green, blue, red, and yellow spheres. This figure was prepared with PyMOL using the structure available in the Research Collaboratory for Structural Bioinformatics PDB under the accession code 5WGB (Boniecki *et al.* 2017).

IV - 4 - 3 - ACP and IscS in *E. coli*

While the evidence for an interaction between ACP and ISD11 in mitochondria is relatively recent, an interaction between ACP and IscS in *E. coli* has been already described in the literature 27 years ago. Indeed, in the first characterization of IscS by D.H. Flint in 1996, ACP was found in the same purification fraction as IscS (Flint 1996). Since the addition of DTT seemed to disrupt the interaction, a disulfide linkage between the thiol of the 4'PP group of ACP and IscS was proposed.

This was not the only time an interaction between ACP and IscS was observed. A study on ACP interactome showed a co-purification of IscS with ACP. In this study the involvement of disulfide bridge was noticed as well (Gully *et al.* 2003). For a long time, this interaction was dismissed based the reactive cysteine of IscS and was regarded as artefactual but as recent studies link ACP to ISD11, a member of the Fe-S cluster biogenesis machinery, the interaction between ACP and IscS might need reevaluation.

RESULTS

Chapter I: Cross-talk between fatty acid biogenesis and Iron-Sulfur cluster biogenesis

Chapter I - Introduction

Fe-S clusters are metallic cofactors essential in most living organisms. They allow a diversity of reactions from electron transfer to redox and non-redox chemical catalysis. The biogenesis of Fe-S clusters is performed by multi-protein machineries. There have been 5 different machineries described, MIS and SMS in both bacteria and archaea, NIF in bacteria, ISC and SUF in bacteria and eukaryotes. *Escherichia coli* possess ISC and SUF. The biogenesis of Fe-S cluster involves 3 major steps, the acquisition of iron and sulfur, the assembly of the cluster and finally the delivery of the cluster to the apoprotein targets by dedicated carriers. In *E. coli*, the ISC machinery serves as a housekeeping machinery whereas SUF takes over in stress conditions. Different stresses can affect Fe-S cluster biogenesis such as oxidative stress, nitrosative stress or iron limitation. The ISC machinery contains 9 proteins, 8 of them encoded in a single operon. The ISC system contains a transcriptional regulator, IscR, a cysteine desulfurase, IscS, a scaffold protein, IscU, a carrier protein IscA, two dedicated chaperones, HscA and HscB, a ferredoxin Fdx, an accessory protein, IscX and the frataxin CyaY. In eucaryotes the ISC system is found in the mitochondria and contains the components functionally equivalents and structurally homologous to those of the *E. coli* ISC machinery. However, an additional protein ISD11, not present in prokaryotes, is also participating in the production of Fe-S clusters through its interaction with the cysteine desulfurase NFS1 (IscS homolog). ISD11 belongs to the LYRM family, a class of proteins characterized by a leucine-tyrosine-arginine motif (LYRM) only found in the mitochondria. In 2016 an interaction between the ISD11 protein and ACP has been documented. ACP is the acyl carrier protein, an essential protein involved in the biogenesis of fatty acid. Two crystallographic structures of ACP-ISD11-NFS1 complex have been presented although the exact conformation of the complex is unclear as the two structures seem to be conflicting. Nonetheless, studies on the tripartite interaction suggest a positive role of ACP in the biogenesis of Fe-S clusters in mitochondria (Van Vranken *et al.* 2016). It has been suggested that the role of ACP-ISD11 interaction is to stabilize NFS1 that is found to aggregate in absence of ACP-ISD11 complex (Herrera *et al.* 2018). In prokaryotes despite the absence of the ISD11 protein, an interaction between ACP and IscS in *E. coli* has been reported. In 1996 when D. H. Flint discovered a NifS-like protein that we now know under the name of IscS, ACP was found to co-purify with it

(Flint 1996). Moreover in 2003 Gully and collaborators reported that in *E. coli*, IscS co-purifies with ACP (Gully *et al.* 2003).

We undertook this study to decipher the role of ACP in the biogenesis of Fe-S clusters. In this chapter we present our findings on the relation between ACP and the ISC machinery. We show here, by a bacterial two hybrid assay, that ACP not only interacts with IscS but with the ferredoxin Fdx and the co-chaperon HscB of the ISC system as well. We studied the effect of ACP on the biogenesis of Fe-S by using the CRISPRi tool to decrease the expression of *acpP*. By monitoring the activity of Fe-S proteins such as transcriptional regulators or enzymes we demonstrated that ACP plays a positive role in the biogenesis of Fe-S clusters through the ISC machinery.

Chapter I - Materials and Methods

Media and growth conditions

Bacterial strains were grown in LB (Lysogeny Broth) rich medium. Antibiotics were added when necessary: ampicillin (Amp, 100 µg/ml); kanamycin (Kan, 50 µg/ml); chloramphenicol (Cm, 10 µg/ml) as well as anhydrotetracycline (aTc) for inducible expression from the Ptet promoter. For iron chelation, 2,2'-Dipyridyl (Dip) was added to the culture medium and for oxidative stress, we used paraquat 100 µM.

Bacterial strains and Plasmids

Escherichia coli K12 MG1655 strain, its derivatives and plasmids used in this study are listed in tables 1 and 2 respectively. *E. coli* K12 XL1B strain was used for cloning. Primers, with their sequences and descriptions are listed in table 3.

Standard procedures for preparation of DNA, amplification, digestion, ligation were used as previously described (Sambrook *et al.* 1989). Transformations were done by electroporation. Plasmids constructed for this study have been checked by sequencing (Eurofins).

MG1655 chromosome engineering

Deletion mutations were introduced by P1 transduction (Miller 1992). Transduced strains were verified by PCR using primers pair hybridizing upstream and downstream the deleted gene (see Table 3 for sequences).

Plasmids construction

Derived plasmids from psgRNA for CRISPRi, *i.e.* psgRNA-ACP1, 3, 4, 5, 6, were generated by inverse PCR as previously described (Larson *et al.* 2013). Primers used for the production of the DNA corresponding to each antisens RNA are indicated table 3 and psgRNA was used as template. Amplified fragments corresponding to whole plasmids (2580 bp) were then phosphorylated (T4 Polynucleotide Kinase, Biolabs) at their 5' extremities and circularized by ligation (T4 DNA ligase, Biolabs). *DpnI* was then used to remove the template DNA before transformation in XL1B.

For protein purification, IscS and ACP coding regions (PCR fragments generated from OSD56-57, 1248 bp, and OSD146-147, 263 bp respectively) were cloned between *EcoRI* and *XhoI* sites of pTet6his-TEV, generating pTet6his-TEV-iscS and pTet6his-TEV-ACP respectively.

RNA extraction

Strains were grown in LB-Amp-Cm added with 0.1 ng/ml aTc at 37°C with aeration until $OD_{600nm} = 1$. Cells were pelleted by centrifugation (10 ml) and immediately frozen at -20 °C. RNA extractions were then performed as previously described (Even *et al.* 2006). Briefly, bacterial pellets were resuspended in a buffer containing glucose 20%, Tris-HCl 25 mM, pH 7.6 and EDTA 50 mM. Cells were broken in presence of glass beads (0,1 mm diameter) and acid phenol (pH 4.5) in a cell disruptor. Successive purification steps with Trizol and chloroform were performed before isopropanol precipitation.

Purified RNAs were then treated with DNase I using the TURBO DNA-free reagent (Ambion) in order to eliminate residual contaminating genomic DNA.

Gene expression analysis by quantitative qRT-PCR

cDNA synthesis was carried out as previously described (Dubrac *et al.* 2007). Oligonucleotides were designed in order to synthesize 100-200 bp amplicons (see Table 3). Quantitative real-time PCRs (qRT-PCRs), critical threshold cycles (CT) and *n*-fold changes in transcript levels were performed and determined as previously described (Dubrac *et al.* 2007) using the SsoFast™ EvaGreen Supermix (Bio-Rad) and normalized with respect to 16s rRNA

whose levels did not vary under our experimental conditions. We analyzed the results using Bio-Rad CFX Maestro software. Assays were performed using quadruplicate technical replicates and repeated with three independent biological samples. Results are presented as the means of the technical replicates and error bars are the standard errors of the means. Biological replicates were treated independently and did not show any significant variations.

β-galactosidase assay

Cells were grown in LB medium at 37°C in biological triplicates. β-gal activity was determined as previously described (Miller 1992). Average values of β-gal unit/mg of bacteria are represented and error bars correspond to the standard deviation of the means.

Bacterial Adenylate Cyclase Two-Hybrid assay (BACTH)

We used BACTH to test protein-protein interactions as previously described (Karimova *et al.* 1998). DNA inserts encoding the proteins of interest were obtained by PCR with primers described table 3 using MG1655 genomic DNA as matrix. Mutated alleles of genes were obtained by PCR (with the PfuUltra II DNA polymerase) using primers containing the mutations (table 3), and the plasmids with the wild type alleles as template. After amplification, template DNA was removed using the *DpnI* restriction enzyme. DNA encoding proteins of interest were cloned into pT18 and pT25 plasmids between *EcoRI* and *XhoI* restriction sites. After co-electroporation of the BTH101 strain with the two plasmids expressing the hybrid proteins, cells were spread on LB-Amp-Kan plates with IPTG 0.5 mM and X-Gal 50 µg/mL plates and incubated at 30 °C for two days. Liquid cultures of clones in LB-Amp-Kan-IPTG were then spotted on LB-Amp-Kan plates with IPTG 0.5 mM and X-Gal 50 µg/mL plates and incubated at 30 °C for two days and scanned (SCAN 4000, Intersciences).

Aconitase enzymatic activity assay

Aconitase activity was measured by following transformation of isocitrate to cis-aconitate which can be monitored at 240 nm in a UV spectrophotometer as previously described (Varghese *et al.* 2003). Briefly, cells were grown in LB with Amp, Kan and aTc (0.1 ng/mL) when specified until OD_{600nm} around 2. Spheroplasts were immediately prepared by incubating cells (around 2X10⁹) in a Tris buffer 25 mM pH 7.8 with sucrose 0.5 M on ice for 10 min and a further lysozyme treatment (0,2 mg/mL). Spheroplasts were kept at -20°C and

treated individually to avoid any time laps before aconitase test. After sonication, extracts were immediately incubated in presence of isocitrate as substrate (Tris pH7.8 50 mM, MnCl₂ 0.5 mM, isocitrate 20 mM) at 30°C, and absorbance at 240 nm was followed during 2 min. For each extract, protein concentration was determined by a Bradford assay. Specific activities were calculated using an extinction coefficient of 3.6 mM⁻¹ cm⁻¹ for cis-aconitate.

Gentamycin killing assay

Strains were grown aerobically in LB at 37 °C to an OD_{600nm} of 2. Cultures were then diluted in LB for and equivalent OD_{600nm} = 1. At this point, gentamycin (5 µg/ml) was added to the cells. Aliquots were taken from the culture at indicated time points, diluted in phosphate buffered saline solution (PBS), and colony-forming units (CFUs) were determined. The CFUs at time-point 0 (used as the 100 %) was around 10⁹ CFU/mL in all experiments.

6His-Tagged proteins purification

Recombinant proteins 6His-IscS and 6His-ACP were purified as previously described with some modifications (Wahl *et al.* 2011). Briefly, MG1655/pet6HisTEV-*acpP* and MG1655/pet6HisTEV-*iscS* strains were grown in LB (500 ml) at 37°C until OD_{600nm} = 0.5, and then, 1 mM IPTG was added to induce fusion proteins genes expression. For MG1655/pet6HisTEV-*acpP* culture, 10 mM of panthotenate was added to the culture. Cultures were further incubated at 30°C for 4 hours. After pelleting, cells were broken using a cell disruptor in 50 mL of buffer 1 (50 mM Tris HCl pH 7.2 ; 200 mM NaCl ; 10% glycerol et 5 mM Imidazol) and the extract were then centrifuged for 30 min at maximum speed before incubation with 1 mL of Talon beads (Clontech) on a wheel for 2 h, at 4°C. The beads were washed twice with 10 mL buffer 1. Proteins were eluted in 1 mL buffer 1 added with 200 mM imidazole. The protein concentrations were determined by a Bradford assay.

Purified recombinant proteins quality were checked by SDS-PAGE analysis and further analysis by mass spectrometry, UV/Visible spectroscopy and dynamic light scattering to check purity, integrity, homogeneity and concentration of the purified proteins (in collaboration with the Molecular Biophysics Platform of the Institut Pasteur).

Cysteine desulfurase enzymatic activity assay

IscS cysteine desulfurase activity was determined using the methylene blue assay as previously described (Outten *et al.* 2003). The principal is as follows: sulfide produced by IscS desulfurase activity are incorporated in *N,N*-dimethyl-*p*-phenylenediamine (DMPD) in presence of ferrous chloride (FeCl₃) thus forming a compound called methylene blue. Briefly, reactions were carried out in presence of dithiothreitol (DTT) 2 mM. Cysteine (1 mM) was added to purified proteins and the mix was incubated for indicated times at 37°C. Reactions were quenched by the addition of DMPD 2.5 mM and FeCl₃ 3 mM. After 30 minutes of incubation at 37°C, reactions were centrifuged 5 min at 13000 rpm in order to eliminate protein aggregates. Methylene blue formation was monitored by spectrophotometry due to its absorbance at 670 nm. Sodium sulfide, Na₂S, was used as a standard for calibration in order to assess the quantity of sulfur produced by IscS activity.

Table 1: Strains used in this study

Lab reference	Name in the manuscript	Genotype	Reference
FBE051	MG1655	Wild type K12 <i>E. coli</i>	F. Barras, lab collection
FBE052	XL1B	<i>recA1 endA1 gyrA96 thi-1 hsdR17 supE44 relA1 lac</i> [F' <i>proAB lacIqΔM15 Tn10</i> (Tet ^r)]	Stratagene
FBE054	BTH101	F-, <i>cya-99, araD139, galE15, galK16, rpsL1</i> (Str ^R), <i>hsdR2, mcrA1, mcrB1, relA1</i>	(Karimova <i>et al.</i> 1998)
FBE001	<i>PsoxS-lacZ</i>	MG1655 Δ <i>lacZ PsoxS::lacZ</i>	B. Py
FBE005	<i>PiscR-lacZ</i>	MG1655 Δ <i>lacZ PiscR::lacZ</i>	B. Py
FBE009	<i>PhmpA-lacZ</i>	MG1655 Δ <i>lacZ PhmpA::lacZ</i>	B. Py
FBE204	<i>PydfZ-lacZ</i>	MG1655 Δ <i>lacZ PydfZ::lacZ</i>	B. Py
FBE227	Δ <i>iscS</i>	MG1655 Δ <i>iscS::kan</i>	This work
FBE321	Δ <i>iscUA</i>	MG1655 Δ <i>iscUA::Cm</i>	M. Lenon, lab collection
FBE374	Δ <i>sufBCD PhmpA-lacZ</i>	MG1655 Δ <i>lacZ ΔsufBCD PhmpA::lacZ</i>	This work
FBE404	Δ <i>iscR PiscR-lacZ</i>	MG1655 Δ <i>lacZ ΔiscR PiscR::lacZ</i>	F. D'Angelo, lab collection
FBE591	Δ <i>iscUA PydfZ-lacZ</i>	MG1655 Δ <i>lacZ ΔiscUA::Cm PydfZ::lacZ</i>	M. Lenon, lab collection

Table 2: Plasmids used in this study

Lab reference	Name	Description	Reference
pEB1976	pdCas9	Cm ^R , p15A ori, PTet-dCas9	(Larson <i>et al.</i> 2013)
pEB1977	psgRNA	Amp ^R , ColE1 ori, PJ23119 promoter	(Larson <i>et al.</i> 2013)
pSF1	psgRNA-ACP1	Generated by PCR with ebm1822-acp1	This study
pSF2	psgRNA-ACP3	Generated by PCR with ebm1822-acp3	This study
pSF3	psgRNA-ACP5	Generated by PCR with ebm1822-acp5	This study
pSF4	psgRNA-ACP6	Generated by PCR with ebm1822-acp6	This study
pSF5	psgRNA-ACP4	Generated by PCR with ebm1822-acp4	This study
pEB1188	pET-6His-TEV	Amp ^R , ColE1 ori, T7 promoter	(Wahl <i>et al.</i> 2011)
pSF19	pET-6His-TEV- <i>iscS</i>	Insertion of OSD56-57 in pET-6His-TEV (<i>EcoRI/XhoI</i>)	This study
pSF51	pET-6His-TEV- <i>acpP</i>	Insertion of OSD146-147 in pET-6His-TEV (<i>EcoRI/XhoI</i>)	This study

Table 3: Primers used in this study

Name	Sequence	Description
Construction of psgRNA derivatives		
ebm1822	ACTAGTATTATACCTAGGACTGAGCTAGC	Amplification of psgRNA with specific guide RNA primers
acp1	TTCCTATCAAAACTCGCTTTCGCGAGTTTTAGAGCTAGAAATAGCAAGTTAAATAAGGC	Construction of psgRNA-ACP1
acp3	ATCAAAACTCGCTTTCGCGAGTTTTAGAGCTAGAAATAGCAAGTTAAAATAAGGC	Construction of psgRNA-ACP3
acp4	AAAACACTCGCTTTCGCGAGTTTTAGAGCTAGAAATAGCAAGTTAAAATAAGGC	Construction of psgRNA-ACP4
acp5	ACTCGCTTTCGCGAGTTTTAGAGCTAGAAATAGCAAGTTAAAATAAGGC	Construction of psgRNA-ACP5
acp6	CGCTTTCGCGAGTTTTAGAGCTAGAAATAGCAAGTTAAAATAAGGC	Construction of psgRNA-ACP6
Construction of pET-6His-Tev derivatives		
OSD56	TATGAATTCATGAAATTACCGATTATCTCGA	<i>iscS</i> coding sequence (<i>EcoRI/XhoI</i>)
OSD57	AAACTCGAGTGATTCCGATACCGATTAATGAT	
OSD146	GGGCGGAATTCATGAGCACTATCGAA	<i>acpP</i> coding sequence (<i>EcoRI/XhoI</i>)
OSD147	GGAGCTCGAGTTCACTTACGCCTGGTGG	
qRT-PCR		
16sFor	AAGTTAATACCTTTGCTCATTGAC	16s
16sRev	GCTTTACGCCAGTAATTCC	
OSD10	CTGGGCGTTAAGCAGGAAGAAG	<i>acpP</i>
OSD11	CCAGAGCCATTACCAGCTCAAC	

Chapter I - Results

I - Study of the interactions between ACP and the ISC machinery

As mentioned before, in *E. coli*, an interaction between ACP and IscS was suggested by co-immunoprecipitation of the two proteins (Flint 1996, Gully *et al.* 2003). Furthermore, a link between ACP and NFS1 (IscS homologue in eukaryotes) has been shown by co-purification and co-crystallization (Boniecki *et al.* 2017, Cory *et al.* 2017). In eukaryotes, a third partner, ISD11, acts as a connector between ACP and NFS1, and there is no bacterial homologue of ISD11. This led us to wonder about interactions of ACP and the ISC system in *E. coli*. In order to study the potential interactions, we combined experimental approach to *in silico* modeling of the interactions done in collaboration with Guillaume Bouvier (Structural Bioinformatic Unit, Institut Pasteur).

I - 1 - ACP interacts with three members of the ISC system

We used the Bacterial Adenylate Cyclase Two-Hybrid system (BACTH) to test possible interactions between ACP and ISC system members (Karimova *et al.* 1998). The ACP protein has been fused to the T25 subunit of the *Bordetella pertussis* adenylate cyclase (pT25 vector) and ISC proteins to the T18 subunit (pT18 vector). The *E. coli* BTH101 strain was co-transformed with combinations of pT25 and pT18 derivatives, and to determine pair-wise interactions, strains were spotted on LB X-Gal plates. As we observe on the figure 1, ACP is able to interact with IscS, the cysteine desulfurase of the ISC system. This result is coherent with the previous reports on ACP and IscS interaction (Flint 1996, Gully *et al.* 2003). ACP also interacts with other members of the ISC machinery, HscB and Fdx (Fig. 1). HscB is the DnaJ-like co-chaperon of the ISC operon, functioning with the DnaK-like chaperon HscA. HscB has been described to interact with IscU to facilitate the release of the cluster (Bonomi *et al.* 2011). Moreover, it has also been reported that HscB interacts with IscS, although the role of this interaction is still unclear (Bonomi *et al.* 2011, Puglisi *et al.* 2016). Fdx is a ferredoxin, it interacts with IscS in order to provide the electrons required to produce sulfur ions (S^{2-}) for subsequent Fe-S cluster assembly.

We did not observe any interaction between ACP and IscU or CyaY, two other proteins of the ISC machinery that are known to interact with IscS, nor with IscR, IscA or HscA, the remaining components of the ISC machinery. Moreover, we tested the interaction with SufS the cysteine desulfurase of the SUF system and showed that ACP does not interact with this cysteine desulfurase (Fig. 1). Last, we also included a control to check that IscS, HscB and Fdx were not able to interact with TolB, a protein unrelated to Fe-S biogenesis, used as a control. None of these three proteins are able to interact with TolB, (Fig. 1 last row). The lack of interaction of ACP with the rest of the ISC machinery and the SufS protein, as well as the lack of interaction of IscS, HscB and Fdx with the TolB protein, suggest that the interactions observed between ACP and IscS, Fdx and HscB are all specific.

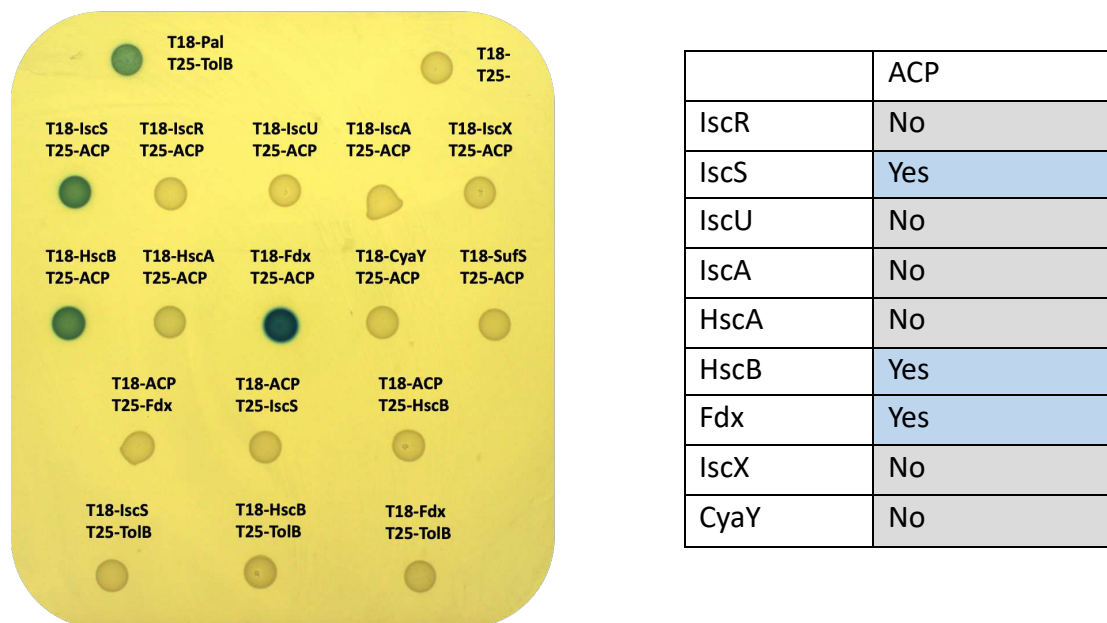


Figure 1. ACP interacts with three members of the ISC machinery. Bacterial two-hybrid system assay of ACP against the Fe-S cluster biogenesis components of the ISC system. Cells carrying the pT18 and pT25 derivative plasmids expressing the fusion proteins were grown overnight and spotted on LB X-Gal plates. The plasmids in each strain are indicated. A positive control of interaction (T18-Pal/T25-TolB) and a negative control (T18/T25) have been included in the test.

I - 2 - Modelization of the molecular interactions between ACP and IscS

In collaboration with Guillaume Bouvier from the Institut Pasteur, a model for the complex formed between ACP and IscS was generated using AlphaFold2 (Bryant *et al.* 2022). It suggested that a dimer of IscS could interact with two monomers of ACP (Fig. 2A). The predicted interaction involves a positive patch on IscS interacting with a negative patch on ACP (Fig. 2B), forming a network of polar interactions ($R67^{\text{IscS}}-E41^{\text{ACP}}$, $R220^{\text{IscS}}-D38^{\text{ACP}}$ and $R223^{\text{IscS}}-D35^{\text{ACP}}$). Interestingly, the arginine 220 and 223 of IscS have also been described as necessary residues for IscS interactions with other members of the ISC system, *i.e.* CyaY, IscX, Fdx and HscB (Shi *et al.* 2010, di Maio *et al.* 2017). On the other side, acidic residues of ACP (D35, D38 and E41), appears to be a major hub for proteins interactions. It has been shown by structural analysis their involvement in the interactions with FASII enzymes such as FabI or FabG, but also for AcpS, the enzyme responsible for the apo- to holo- maturation of ACP (addition of the phosphopantetheine group) (Parris *et al.* 2000, Zhang *et al.* 2003, Rafi *et al.* 2006)

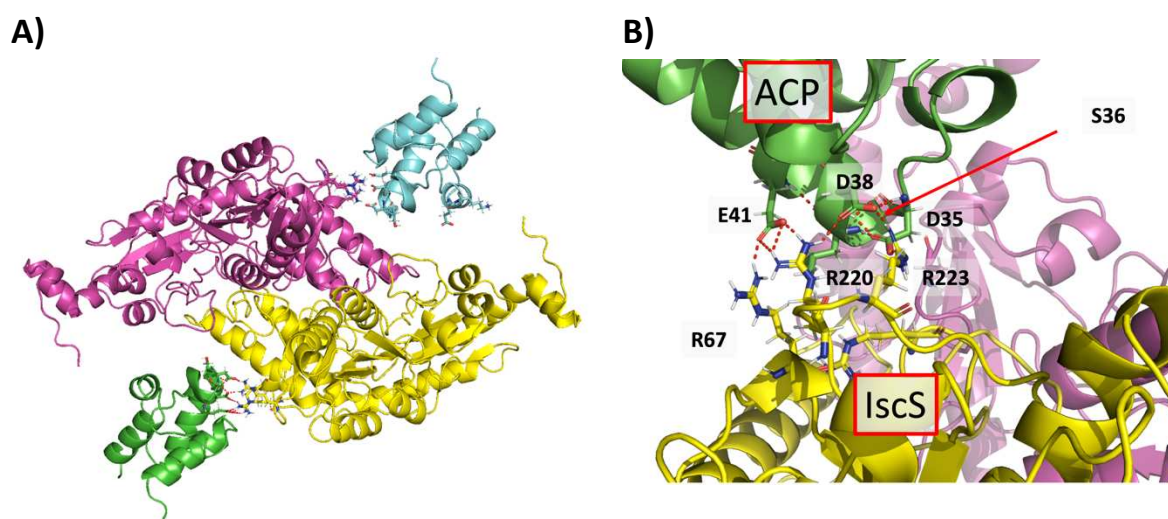


Figure2. AlphaFold2 predicts an interaction between ACP and IscS. A) AlphaFold2 prediction of the interaction between a dimer of IscS (purple and yellow) and two monomers of ACP (blue and green). **B)** The amino acids involved in the interaction are represented in sticks (green for ACP and yellow for IscS).

We tested the role of the charged amino acids in the interactions between ACP and IscS. By site directed mutagenesis, we replaced each of the aforementioned negatively charged amino acids of ACP by neutral residues: D₃₅N; D₃₈N and E₄₁Q. This allowed us to determine that the two aspartate residues at position 35 and 38 of ACP are crucial for the interaction with IscS, whereas the glutamate at position 41 is not (Fig. 3). As for the interactions between ACP and either Fdx or HscB, the three negatively charged residues, D₃₅, D₃₈ and E₄₁, are required (Fig. 3).

Through the interaction study of ACP variants, we showed that a patch of negatively charged residues on ACP is responsible for interactions with IscS, HscB and Fdx.

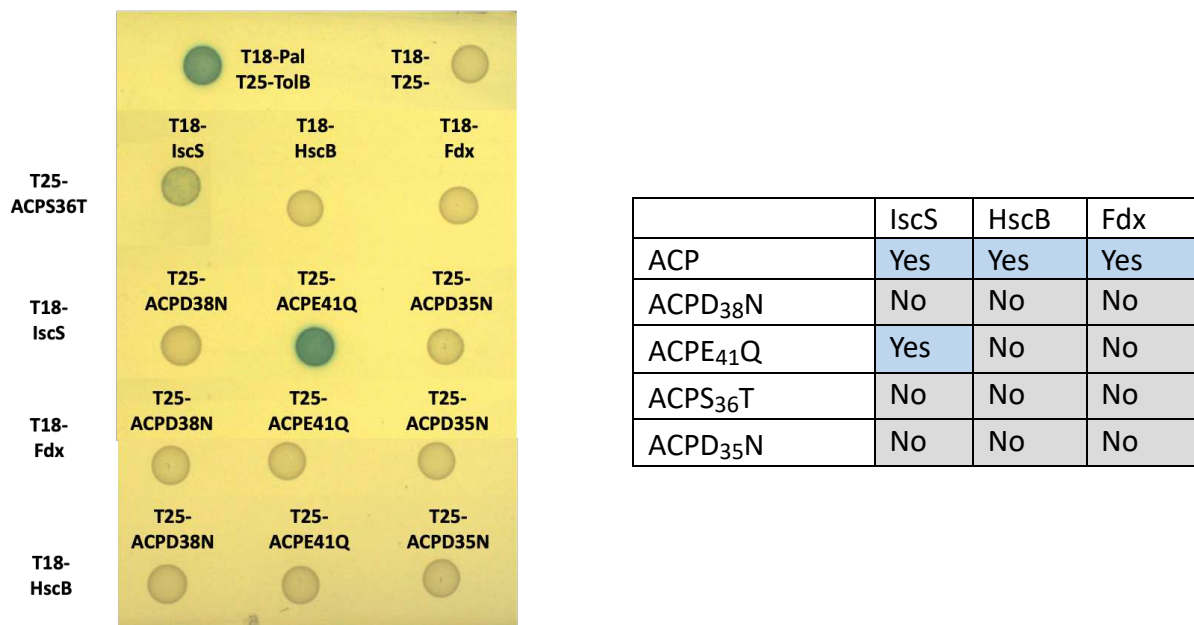


Figure 3. The negative patch of ACP contains critical residues for its interaction with IscS, Fdx and HscB. Interactions between variants of ACP and IscS, Fdx and HscB are presented. Overnight cultures were spotted on LB X-Gal plates. The plasmids in each strain are indicated. A positive control of interaction (T18-Pal/T25-TolB) and a negative control (T18/T25) have been included in the test.

I - 3 - Impact of ACP maturation in the interactions with the ISC system

Interestingly, we noticed that the surface of interaction on ACP includes the serine 36 on which the phosphopantheteine moiety of the coenzyme A and therefore the acyl chain is bound (Fig. 2). Previously published data suggested that the serine residue at position 36 of ACP, which is the binding site of the phosphopantheteine group, was necessary for interaction with IscS (Gully *et al.* 2003). We then wondered whether an active form of ACP (bound to the phosphopantheteine group) was required for the BATCH observed interactions. We have generated a variant of ACP, ACP S₃₆T, unable to be post-translationally matured by the addition of the phosphopantheteine group. We first confirmed that ACP S₃₆T is not able to bind IscS and we also showed that it is impaired in its capacity to interact with HscB and Fdx (Fig. 3).

The lack of interaction with the ACP S₃₆T variant highlights the importance of the binding of the phosphopantheteine prosthetic group on ACP for the interactions with the ISC Fe-S biogenesis system.

II - ACP involvement in Fe-S phenotypes

II - 1 - Setting up the CRISPRi tool to repress *acpP* expression

Using bacterial two-hybrid assays, we revealed specific interactions between ACP and components of the ISC machinery. We therefore wondered whether such interactions could influence, positively or negatively, the efficiency of ISC-dependent Fe-S biogenesis.

In *E. coli*, *acpP* is an essential gene, it was thus not possible to inactivate this gene to measure the effect on Fe-S biogenesis. Therefore, in order to tackle this question, we used the CRISPR-based RNA interference (CRISPRi) to decrease *acpP* expression.

CRISPRi is a tool that is based on the CRISPR system for genome manipulation. The Cas9 used is a variant of *Streptococcus pyogenes* Cas9 nuclease that has been inactivated by two point mutations, D₁₀A and H₈₄₀A, producing the catalytically inactive dead Cas9 (dCas9). The guide RNA of the system contains a base-pairing region that is complementary to a portion of the target gene and dCas9-handle region that is required for the formation of the dCas9-

guide RNA complex. The complex then binds to the target locus provided that a Protospacer Adjacent Motif (PAM) is present. Binding of the dCas9-guide RNA complex interferes, by steric hindrance, with transcript elongation by the RNA polymerase. This results in a reduced expression of the target gene (Qi *et al.* 2013). The system we used in this study involves two plasmids: 1) the psgRNA plasmid on which the guide RNA of the system is under the control of a constitutive promoter and 2) the pdCas9 plasmid in which the dCas9 gene is under the control of the TetR-regulated promoter, pTet, inducible by anhydrotetracycline (aTc) (Larson *et al.* 2013). We have designed 5 guide RNAs of different lengths that target the non-template strand of the 5'UTR region of *acpP* in order to lower its expression (Fig. 4). The first step was to test the efficiency of each guide to turn off *acpP* expression. As *acpP* is an essential gene, our read out for guide RNA efficiency was based on its ability to inhibit bacterial growth.



Figure 4: The guide RNAs target the 5'UTR region of *acpP*. Transcriptional start site of the *acpP* gene is indicated by an arrow. The length and complementarity of each guide RNA designed is indicated and the PAM motif allowing binding of the sgRNA-dCAS9 complex is indicated in red.

First, we checked that the production of the dCas9, without any specific guide RNA, was not toxic for *E. coli*. The MG1655 strain was co-transformed by the psgRNA-control/pdCas9 and the growth of the strain was assessed with increasing concentrations of aTc. As we can observe in figure 5 A, the growth curve is unaffected by aTc addition. This result shows that induction of dCas9 expression by aTc does not exhibit any toxicity up to 125 ng/mL of aTc.

The second step was to test the efficiency of the guide RNAs to repress *acpP* gene by monitoring the growth of the strains carrying the corresponding psgRNA-ACP/pdCas9 couple.

The strains fell into three categories, those that exhibited no growth inhibition regardless of the concentration of aTc used (guide RNAs *acp1* and *acp3*), those who exhibited a strong growth inhibition at the lowest amounts of aTc used (guide RNAs *acp4* and *acp5*) and finally those who showed intermediate levels of inhibition (guide RNA *acp6*) (see Fig. 5. B, C and D respectively).

Overall, 3 out of the 5 designed guide RNAs seemed efficient to lockdown *acpP* expression. To study the effect of ACP on Fe-S biogenesis, we needed to decrease the *acpP* expression without strong growth inhibition in order to avoid any side effect caused by a general bacterial stress. It is the reason why we further focused on the *acp6* guide RNA. Indeed, we have observed that the growth of the strain producing this guide RNA was unaffected at very low concentration of aTc (0,1 ng/mL), whereas a dose-dependent growth inhibition was observed at higher concentrations, suggesting that the expression of *acpP* was too low to support an optimal bacterial growth (Fig. 5D).

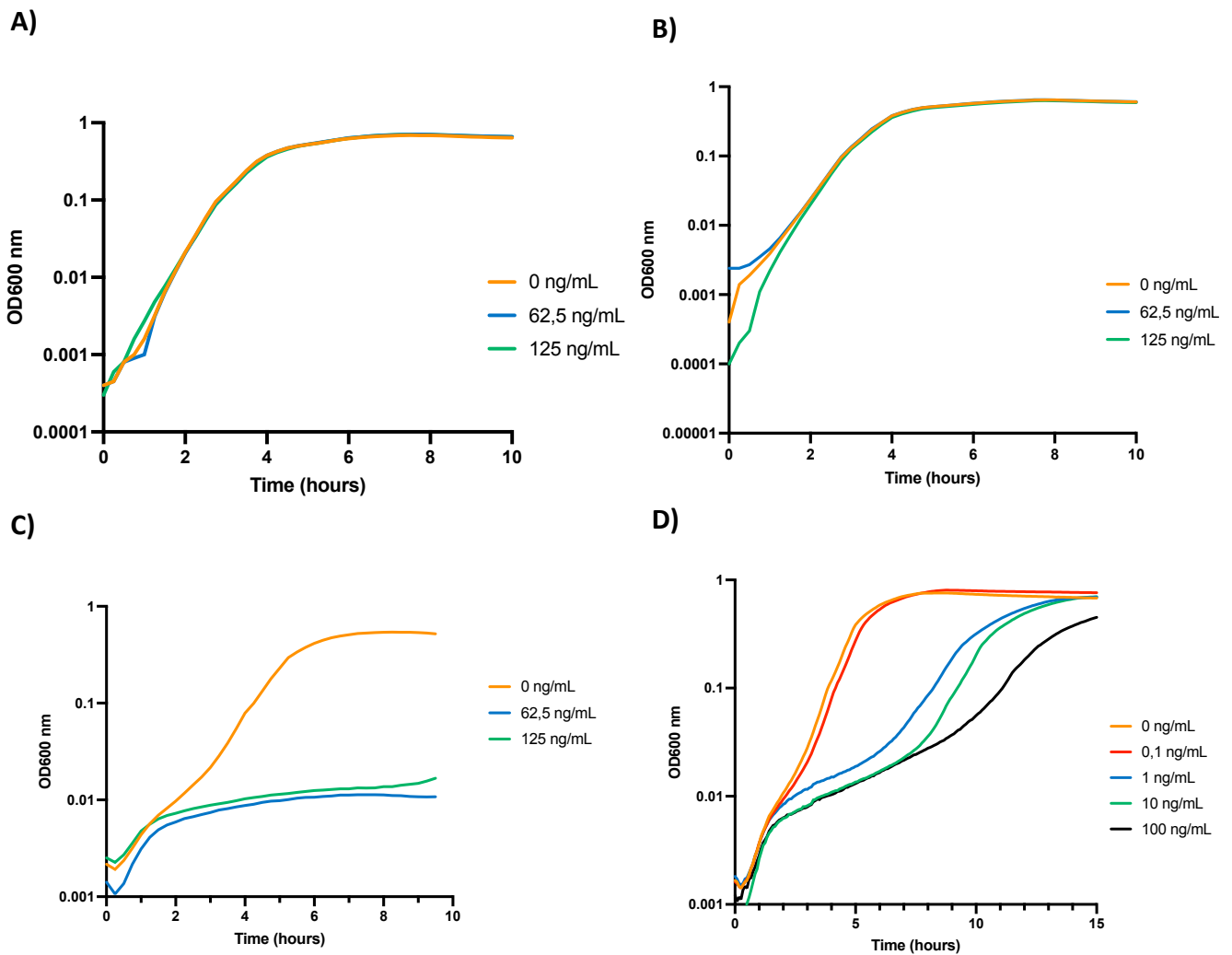


Figure 5. Different gRNA length leads to differential growth defect. Growth curve of a WT with different CRISPRi plasmids. Cells were cultivated in a 96-wells in LB at 37°C under agitation with various concentration of anhydrotetracycline. Growth and OD_{600nm} recording were done in a Tecan microplate reader. **A)** Growth curve of a WT/pdCas9/psgRNA-e.v. **B)** Growth curve of a pdCas9/psgRNA-*acp3* **C)** Growth curve of a pdCas9/psgRNA-*acp5* **D)** Growth curve of a pdCas9/psgRNA-*acp6*

Finally, we checked whether the chosen guide RNA (*acp6*), induced with aTc at 0,1 ng/mL was sufficient to repress *acpP* expression. We measured the relative expression of *acpP* in the pdCas9/psgRNA-e.v. and pdCas9/psgRNA-*acp6* strains (hereafter named psgRNA-e.v. and psgRNA-*acp* respectively) grown at 0,1 ng/mL of aTc. As we can observe on figure 6, the level of expression of *acpP* in the pdCas9/psgRNA-*acp6* is 4 times lower than in the pdCas9/psgRNA-e.v. strain.

Although the strain producing the *acp6* guide RNA did not exhibit growth defect in presence of 0,1 ng/mL of aTc, it proved to be sufficient to repress the expression of the *acpP* gene. The plasmid psgRNA-*acp6* will be hereafter named psgRNA-*acp*.

Thanks to the CRISPRi genetic tool we were able to decrease the expression of *acpP* without affecting impacting cell viability.

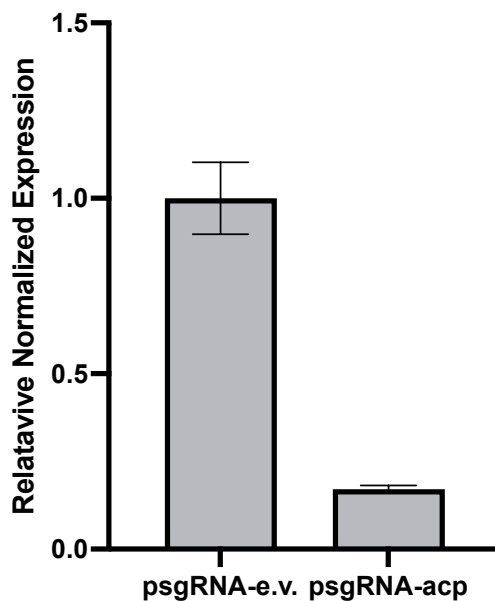


Figure 6. CRISPRi system is efficient in repressing *acpP* expression. *acpP* expression was measured by qRT-PCR. psgRNA and a psgRNA-*acp6* strains were cultivated in LB at 37°C until OD 2 in presence of 0,1 ng/mL of aTc. RNA was extracted and treated as described in the Materials and Methods section. Quantitative Real-Time PCR was used to quantify *acpP* cDNA derived from RNA. Results are presented as the mean of 4 technical replicates and standard errors to the means are indicated.

II - 2 - ACP decrease leads to Fe-S dependent growth defect

Fe-S biogenesis is essential for bacterial growth and survival. In *E. coli*, there are two biogenesis systems, ISC and SUF. In the absence of one of them, the other is able to compensate and there is no major effect on growth rate (Fig. 7). We therefore wondered whether ACP depletion could alter the ISC efficiency, and thus its capacity to provide the cell with Fe-S clusters, in the absence of SUF.

For that purpose, we monitored the effect of a decrease in ACP production in a WT strain and in a Δ *sufBCD* strain. Strains carrying the CRISPRi plasmids, either pdCAS9/psgRNA-e.v. pair, or the pdCAS9/psgRNA-*acp* pair, were grown in LB with aTc 0,1 ng/ml. As we can observe in figure 7, the exponential growth rate of the MG1655/psgRNA-*acp* strain is slightly slower than that of the MG1655/psgRNA-e.v. strain (doubling time of $67,4 \pm 4,13$ min and 61,4

$\pm 1,09$ min respectively). As for the Δ *sufBCD*, we first noticed that inactivating the SUF system slightly affects growth too, the doubling time of a Δ *sufBCD*/psgRNA-e.v. being of $66,55 \pm 1,58$ min. Interestingly, when ACP was decreased in a Δ *sufBCD* background, the growth was strongly impaired and the doubling time of a Δ *sufBCD*/psgRNA-acp was of $85 \pm 4,51$ min. Thus, ACP depletion in a Δ *sufBCD* background provokes a growth delay that is almost three times higher than in a WT. Moreover, this delay cannot be imputed to an additional effect of the deletion of *sufBCD* and the decrease of ACP. This synergistic effect could be explained by the role of ACP on Fe-S cluster biogenesis. As mentioned previously, in a Δ *sufBCD* strain Fe-S clusters originate solely from the ISC system, as they are essential, any negative impact on their production leads to severe growth impairment.

This result suggests that ACP could impact the ISC-dependent pathway of Fe-S biogenesis.

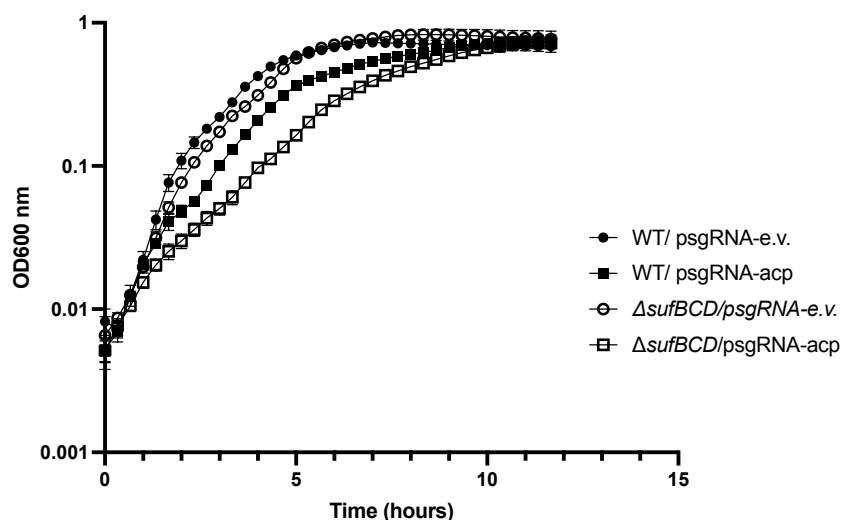


Figure 7. Decreasing ACP level in a Δ *sufBCD* strain leads to growth defects. Growth curves of a WT/psgRNA-e.v., a WT/psgRNA-acp, a Δ *sufBCD*/psgRNA-e.v. and a Δ *sufBCD*/psgRNA-acp. Cells were cultivated in a 96-wells in LB with 0,1 ng/mL of aTc. Growth and OD_{600nm} recording were done in a Tecan microplate reader. Represented values are the mean of three independent biological replicates and the error bars represent the standard deviations. The doubling time was calculated for each strain: WT/psgRNA-e.v. ($61,37\text{min} \pm 1,09$); WT/psgRNA-acp ($67,36\text{min} \pm 4,13$); Δ *sufBCD*/psgRNA-e.v. ($66,55\text{min} \pm 1,58$); Δ *sufBCD*/psgRNA-acp ($85,56\text{min} \pm 4,51$).

II - 3 - ACP plays a role in gentamycin sensitivity

Aminoglycosides are antibiotics that inhibit protein synthesis. They use the proton motive force (PMF) to enter the cell and their bactericidal activity is dependent on bacterial respiration efficiency (Taber *et al.* 1987). It has been shown that Fe-S cluster biogenesis plays an important role in the sensitivity of *E. coli* to aminoglycosides. In particular, maturation of respiration complex I and II has been mainly imputed to the ISC machinery. Therefore, a defective ISC machinery leads to a decrease sensitivity to aminoglycosides (Ezraty *et al.* 2013).

We therefore tested the ability of ACP to impact Fe-S cluster biogenesis by the ISC and, as a consequence, to decrease sensitivity to gentamycin, an aminoglycoside. A WT/pdCas9 /psgRNA-e.v. and a WT/pdCas9 /psgRNA-acp strains have been cultivated in LB until $OD_{600nm} = 2$. Cells were then exposed to 5 $\mu\text{g}/\text{mL}$ of gentamycin for three hours and the CFUs were subsequently quantified. A WT and $\Delta iscS$ strain were also included as controls since the *iscS* inactivation has been shown to highly decrease the sensitivity to gentamycin (Ezraty *et al.* 2013). As we can observe after three hours of incubation in presence of gentamycin, only 2% of the WT cells are still alive whereas a $\Delta iscS$ strain is not affected by gentamycin and continues growing (Fig. 8 left panel). The strain carrying the CRISPRi empty vector, psgRNA-e.v., is as sensitive as the WT strain, with only 2% of survival cells after 3 hours of incubation with gentamycin. The psgRNA-acp is however less sensitive than the psgRNA-e.v. strain, with seven percent of the cells remaining after three hours (Fig. 8 right panel). The effect of ACP here is moderate yet statistically significant. Although the molecular determinants of this effect have not been investigated, these data provide further support for the notion that ACP might be a positive effector for ISC-mediated Fe-S biogenesis and, in particular, maturation of the respiratory complexes I and II.

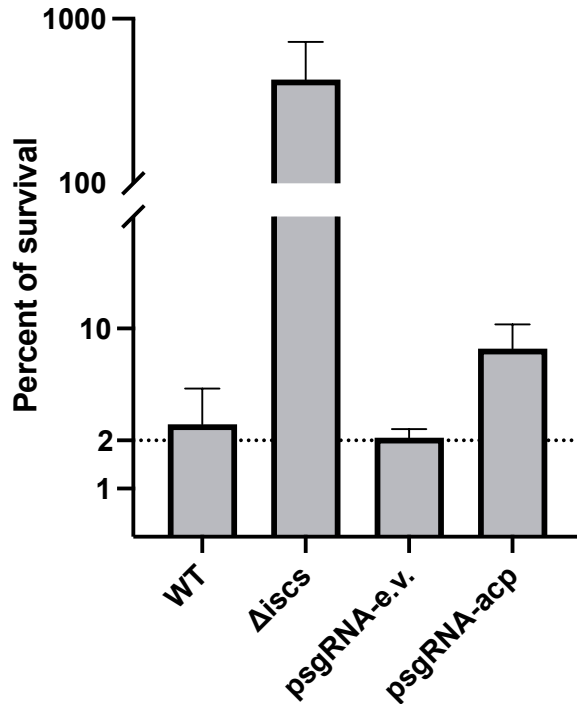


Figure 8. Decreasing ACP leads to a better survival to gentamycin treatment. A WT and a Δ iscS strains (left panel), and a psgRNA-e.v. and a psgRNA-acp strains (right panel) were cultivated in LB until $OD_{600nm} = 2$. Gentamycin was then added to the cultures at a concentration of 5 μ g/mL for three hours. The CFU of the strains was then measured and the survival of the strains is expressed in percent of survival (CFUs after 3 hours of treatment/CFUs at initial time of treatment). Results are presented as means of three independent biological replicates and error bars represent standard deviations to the means.

III - The role of ACP in the activity of Fe-S proteins

Indeed, Fe-S clusters are metallic co-factors necessary for activity of a wide range of proteins including transcriptional regulators and central metabolism enzymes. The impact of decreasing ACP on the biogenesis of Fe-S clusters was analyzed using a set of diverse Fe-S proteins as read-outs reasoning that any change in their maturation level should result in a recordable change in their activity.

III - 1 - Study of Fe-S regulators

The IscR regulator

IscR is the Fe-S homeostasis dedicated sensor. Under its Holo-form, it represses the *isc* operon expression, whereas under its Apo-form, *i.e.* when Fe-S availability decreases, the repression is alleviated. For instance, in condition of iron depletion, it has been shown that IscR is mainly under its Apo-form and the IscR-dependent repression of the *isc* operon is

alleviated (Outten *et al.* 2004). In order to monitor the activity of IscR we used a strain in which the *lacZ* gene is under the control of the *iscR* promoter (*PiscR-lacZ* chromosomal fusion). Therefore, the activity of the promoter can be measured by assessing the activity of the β -galactosidase enzyme. The *PiscR-lacZ* strain was co-transformed by pdCas9 and either psgRNA-e.v. or psgRNA-acp plasmids.

We first measured the effect of a decrease of ACP on the *PiscR-lacZ* expression in LB and we did not observe any effect of ACP level on β -galactosidase activity (Fig. 9A, left panel). We also noticed that the *PiscR-lacZ* fusion was very lowly expressed, indicating that IscR was mainly under its holo-form and represses its own expression, as well as the expression of all the entire *isc* operon. We therefore wondered what would be the effect of ACP on the expression of *iscR* if we lowered the amount of holo-IscR in the cell. In order to address this question, we cultivated the strains in presence 2,2'-Dipyridyl (DIP) an iron chelator. It was described that a drastic chelation of intracellular iron leads to the switch from the ISC system to the SUF system for Fe-S biogenesis (Outten *et al.* 2004). To avoid this switch, we tested various concentrations of DIP from 62.5 to 250 μ M, and measured the activity of *iscR* promoter when we decrease the level of ACP. DIP concentrations higher than 62.5 μ M led to a growth defect (data not shown), probably because iron chelation was too strong, therefore we choose to perform the following analysis in presence of 62.5 μ M of DIP. As we can see on the figure 9, the level of expression of *iscR* increased by almost two folds in presence of DIP in a control strain compared to the condition without DIP, meaning that, in these conditions, the level of holo-IscR was lowered. In the psgRNA-acp strain *iscR* is 7 times more expressed than in the control strain (psgRNA-e.v.) (Fig. 9A right panel). This result showed that ACP affects *iscR* expression. In order to test whether the effect of ACP on *iscR* expression was dependent on the activity of the IscR regulator, we tested the effect of ACP on *iscR* expression in a Δ *iscR* background. In absence of the IscR repressor, the level of *iscR* expression is 1000-fold higher than in a WT background (Fig. 9B). Nonetheless, ACP depletion did not impact *iscR* expression in this context.

These results showed that ACP has a negative impact on *iscR* expression and that it is dependent on the activity of IscR itself. As IscR control of its expression depends on the bulk of Holo-IscR in the cell, our results suggest that ACP has a positive impact on IscR maturation.

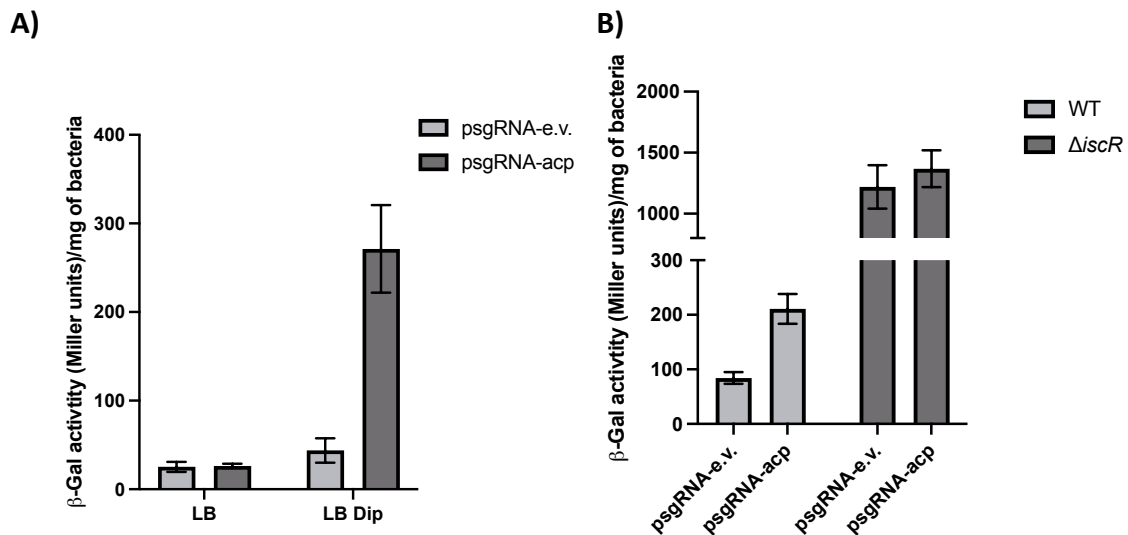


Figure 9. ACP positively affects IscR activity. IscR promoter activity was assessed by measuring the β -gal activity (Miller units) of the *PiscR-lacZ* strains carrying the indicated plasmids. **A)** *PiscR-lacZ*/psgRNA-e.v. and *PiscR-lacZ*/psgRNA-acp strain have been grown in LB with 0.1ng/mL of aTc with or without DIP 62.5 μ M until $OD_{600nm} = 2$. **B)** *PiscR-lacZ*/psgRNA-e.v., *PiscR-lacZ*/psgRNA-acp, $\Delta iscR$ *PiscR-lacZ*/psgRNA-e.v. and $\Delta iscR$ *PiscR-lacZ*/psgRNA-acp have been grown in LB with 0.1ng/mL of aTc and DIP 62.5 μ M until $OD_{600nm} = 2$. Represented values are the mean of three independent biological replicates and the error bars represent the standard deviations.

The FNR regulator

Fnr is the main Fe-S regulator of the adaptation to anaerobiosis, and it regulates the expression of hundreds of genes. FNR is active when it is loaded with its [4Fe-4S] cluster, however FNR loses most of its activity in aerobiosis because its cluster is very sensitive to oxygen (Kang *et al.* 2005). Nonetheless, due to the high affinity of their promoters to FNR, some genes retain FNR regulation, albeit with a lower factor, even in presence of oxygen (Mettert *et al.* 2008, Shan *et al.* 2012) One of these genes is *ydfZ*, a gene encoding a putative seleno-protein with no identified function nor any similarity with characterized protein. The expression of *ydfZ* is activated by FNR even in presence of oxygen, while it is also activated in anaerobiosis by FNR to a greater extent (Mettert *et al.* 2008). A strain carrying a fusion between the *ydfz* promoter and the *lacZ* gene was used to monitor the activity FNR (*Pydfz-lacZ* chromosomal fusion) under aerobiosis.

As we can see on the figure 10, lowering the amount of ACP through the CRISPRi system leads to a decrease of expression of *ydfZ* of 4-fold compared to the control strain with the psgRNA-e.v. In order to test if the effect of ACP on the activity of FNR was related to the

ISC-dependent Fe-S cluster biogenesis, we performed the same experiment in an *iscUA* knocked out strain. In such a strain, production of Fe-S cluster is catalyzed by the SUF system. As observed on the figure 10, the level of expression of *ydfZ* in the Δ *iscUA* psgRNA-e.v. is lower than in the WT background, showing that the ISC system is important for the activity of FNR. However, there is no effect of ACP on the activity of *ydfZ* promoter in this Δ *iscUA* context.

These results show that ACP affects the activity of the Fe-S regulator FNR in an ISC-dependent fashion, suggesting that ACP has a positive effect on the ISC Fe-S biogenesis machinery.

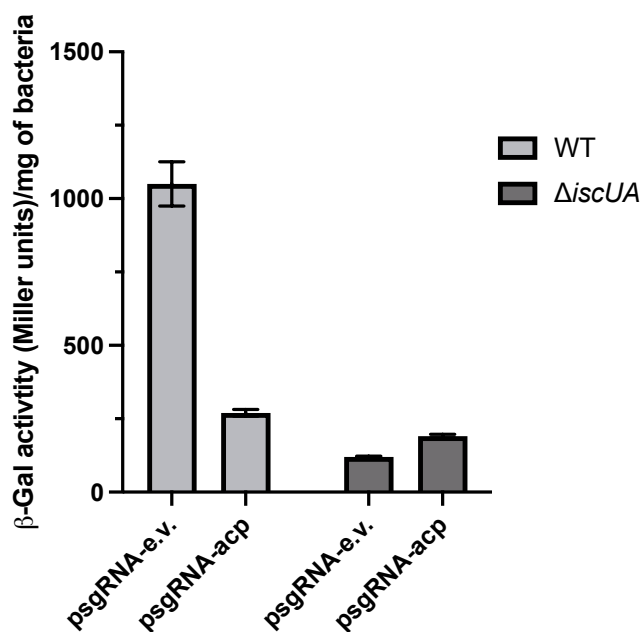


Figure 10. ACP positively affects FNR activity. *ydfZ* promoter activity was assessed by measuring the β -gal activity (Miller units) of the *PydfZ-lacZ* strains carrying the indicated plasmids. *PydfZ-lacZ*/psgRNA-e.v. and *PydfZ-lacZ*/psgRNA-acp strain have been grown in LB with 0.1ng/mL of aTc until $OD_{600nm} = 2$. Light gray bars show the results in a WT background and dark grey bars in a Δ *iscUA* background. Represented values are the mean of three independent biological replicates and the error bars represent the standard deviations.

The NsrR regulator

NsrR is an Fe-S regulator that represses the expression of genes, such as *hmpA* or *hcp-hcr* operon, involved in the response to nitrosative stress. These genes are tightly repressed by the holo-form of NsrR in absence of NO. However, when the cell is exposed to NO or RNS (Reactive Nitrogen Species), the NsrR cluster is inactivated through nitrosylation and NsrR shifts to its apo form and loses its repressing activity (Crack *et al.* 2018). We tested the effect of ACP on NsrR activity by monitoring the activity of the NsrR-repressed *hmpA* promoter. We used a strain in which the *lacZ* gene is under the control of the *hmpA* promoter, *PhmpA-lacZ* that we co-transformed with pdCas9 and psgRNA-e.v. or psgRNA-acp.

In our experimental conditions, *i.e.* growth in LB medium, without any NO source, NsrR is mainly under its holo-form and shuts off *hmpA* expression (Fig. 11, left panel). ACP has no effect on the expression of *hmpA* in these conditions. Surprisingly, in a strain lacking *sufBCD*, the expression of *hmpA* is a 100 times higher than in a WT (Fig. 11). This result shows that the SUF system plays a major role in the maturation of NsrR whereas previously published data suggested that ISC was the main NsrR maturation system (Vinella *et al.* 2013). Moreover, when the level of ACP is decreased in *sufBCD* strain, the expression of *hmpA* is higher by a 1.5-fold compared to the strain carrying the empty vector (Fig. 11, right panel). Although the effect of ACP seems to be mild this result has been observed consistently with three independent biological replicates and suggests that ACP has a positive impact on the NsrR maturation through the ISC system.

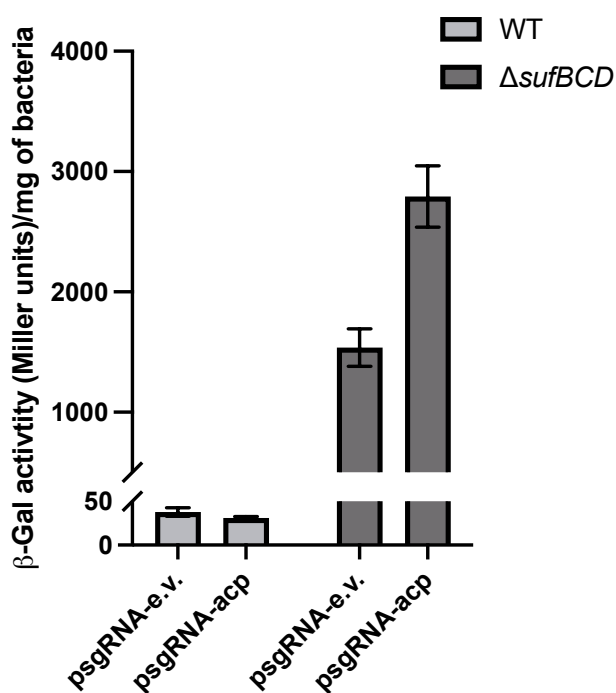


Figure 11. ACP positively affects NsrR activity in a ISC-dependent fashion. *hmpA* promoter activity was assessed by measuring the β -gal activity (Miller units) of the *PhmpA-lacZ* strains carrying the indicated plasmids. *PhmpA-lacZ/psgRNA-e.v.* and *PhmpA-lacZ/psgRNA-acp* strain have been grown in LB with 0.1ng/mL of aTc until $OD_{600nm} = 2$. Light gray bars show the results in a WT background and dark grey bars in a Δ *sufBCD* background. Represented values are the mean of three independent biological replicates and the error bars represent the standard deviations.

The SoxR regulator

Our results show that ACP can impact the activity of regulators that obtain their cluster from the ISC machinery. We therefore questioned what would be the effect of ACP on Fe-S regulators that do not obtain their cluster from the ISC system. The regulator SoxR is the

regulator of oxidative stress response, it is activated through redox state change of its Fe-S cluster (from +1 to +2) by redox-cycling drugs (Gu *et al.* 2011). Previous analysis showed that under oxidative stress, SoxR acquires its cluster from the SUF system only (Gerstel *et al.* 2020). The only target of SoxR is the *soxS* gene. Therefore, we used a *soxS-lacZ* transcriptional fusion as reporter of SoxR activity. A *PsoxS-lacZ*/pdCas9/psgRNA-e.v. strain and a *PsoxS-lacZ*/pdCas9/psgRNA-acp strain were grown in LB, and paraquat, an oxidative stress generator, was added at a concentration of 100 μ M at OD_{600nm} = 0.8 for 2 hours in order to induce SoxR activity. As we can observe in figure 12, ACP decrease does not affect the expression of *soxS*.

This result indicates that ACP does not play a role in the maturation of SoxR and therefore does not affect the activity of the SUF system.

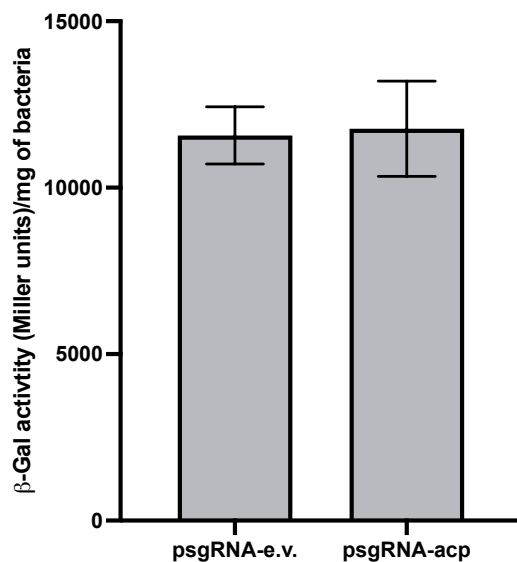


Figure 12. ACP does not affect SoxR activity. *soxS* promoter activity was assessed by measuring the β -gal activity (Miller units) of the *PsoxS-lacZ* strains carrying the indicated plasmids. *PsoxS-lacZ*/psgRNA-e.v. and *PsoxS-lacZ*/psgRNA-acp strains have been grown in LB with 0,1ng/mL of aTc until OD_{600nm} = 2. Represented values are the mean of three independent biological replicates and the error bars represent the standard deviations.

A non-Fe-S reporter, the β -galactosidase activity from the endogenous *lacZ* gene

Additionally, we tested the effect of ACP decrease on the activity of a promoter not regulated by an Fe-S regulator. We have chosen to record the activity of *lacZ* expressed from its own endogenous promoter, *Plac* (endogenous *E. coli lac locus*). This promoter activity is inducible by lactose or IPTG, a non-metabolizable analog of lactose.

As we can observe, in absence of induction (LB medium), the level of β -galactosidase is very low and the decrease of ACP does not affect this level (Fig. 13A). Upon exposure to

IPTG, the *Plac* promoter is induced and the level of β -galactosidase activity is much higher than without induction. In this context neither, ACP does not impact *lacZ* expression (Fig. 13B).

Altogether these results show that the effect of ACP on the previous regulators are specific to the biogenesis of Fe-S.

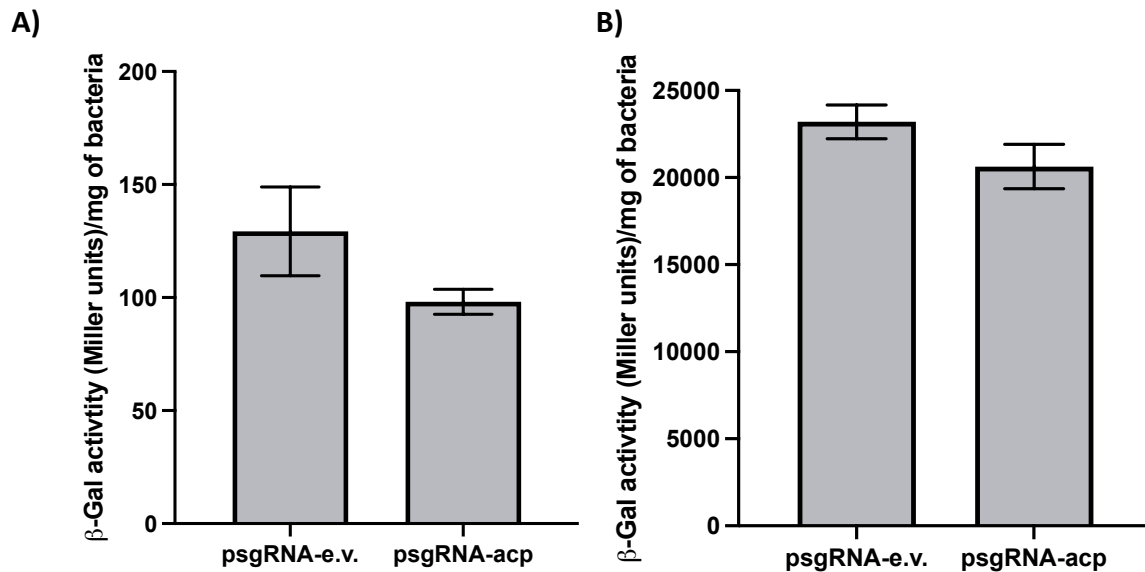


Figure 13. ACP does not affect the activity of the Beta-galactosidase. Activity of *Plac-lacZ* from the *E. coli* endogenous locus was assessed by measuring the β -gal activity (Miller units) of a wild type MG1655 strain carrying the indicated plasmids. **A) psgRNA-e.v. and psgRNA-acp strain have been grown in LB with 0.1ng/mL of aTc until $OD_{600nm} = 2$. **B)** psgRNA-e.v. and psgRNA-acp strain have been grown in LB with 0.1ng/mL of aTc and 0,5mM of IPTG until $OD_{600nm} = 2$. Represented values are the mean of three independent biological replicates and the error bars represent the standard deviations.**

III - 2 - Study of Fe-S enzymes: the aconitases

Aconitases are Fe-S enzymes of the central metabolism, they catalyze the reversible isomerization of citrate and isocitrate via cis-aconitate. *E. coli* possess two aconitases, Aconitase A (AcnA) and Aconitase B (AcnB). Both have a [4Fe-4S] cluster although AcnA cluster is well protected and therefore is very resistant to O_2 (Varghese *et al.* 2003). AcnB has been described as the main catabolic enzyme whereas AcnA is the maintenance or survival one in case of oxidative stress (Varghese *et al.* 2003).

We first assessed the participation of the ISC machinery in the maturation of AcnA and AcnB by measuring aconitase activity in WT, $\Delta iscS$ and $\Delta iscUA$ strains. The strains were grown in LB until $OD_{600nm} = 2$, the aconitase activity was subsequently determined in crude extracts. The substrate of the aconitase, isocitrate, was added in excess to the crude extracts and the apparition of cis-aconitate was monitored at 240 nm. As we can observe, deleting *iscS* leads to a decrease of fifty percent of the activity compared to a WT strain, the same result is observed in a $\Delta iscUA$ background (Fig. 14A). This result showed that the ISC system is important for the activity of the aconitase.

The same experiment was performed with a MG1655/pdCAS9/psgRNA-e.v. and a MG1655/pdCAS9/psgRNA-acp. The aconitase activity is lower when ACP is decreased, corresponding to a 30% drop (Fig. 14B). This result showed that ACP has a positive effect on the activity of an Fe-S enzyme.

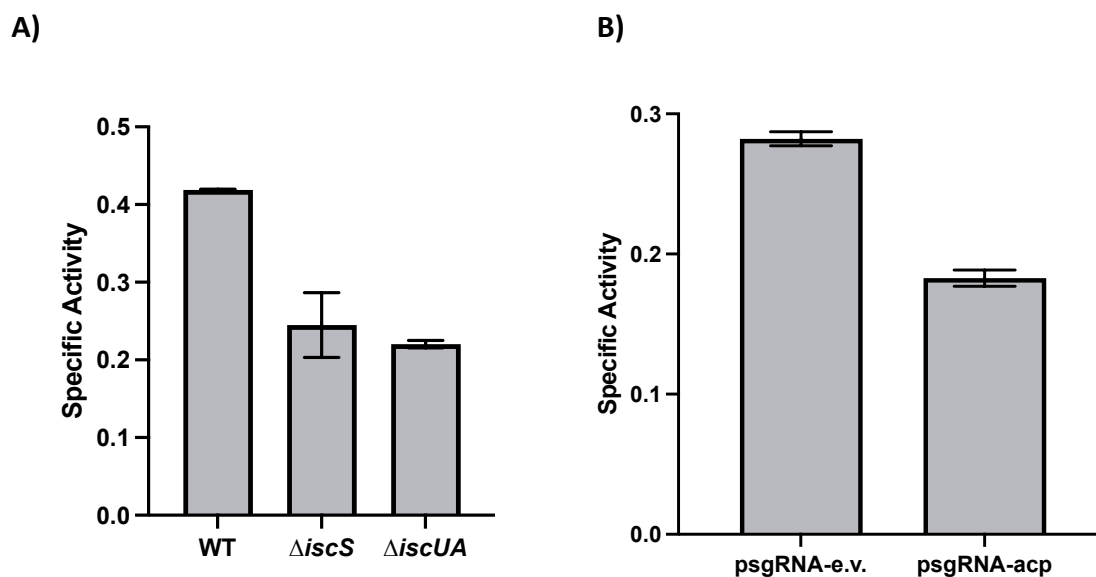


Figure 14. ACP affects positively the activity of the aconitase enzymes. Aconitase activity was measured on crude extracts. **A)** WT, $\Delta iscS$ and $\Delta iscUA$ strains have been grown in LB until $OD_{600nm} = 2$. **B)** psgRNA-e.v. and psgRNA-acp strains have been grown in LB with 0.1 ng/mL of aTc until $OD_{600nm} = 2$. Represented values are the mean of three independent replicates and the error bars represent the standard deviation.

IV - Interaction between ACP and IscS *in vitro*

We collected evidences supporting the notion that ACP positively impacts ISC-dependent Fe-S biogenesis in the cell. However the mechanism underlying this effect is still unknown. In this chapter IV we describe our investigations about the mechanisms underlying the positive effect of ACP on the ISC Fe-S biogenesis system.

IV - 1 - Does ACP impact IscS cysteine desulfurase activity?

IscS is the cysteine desulfurase providing the sulfur for Fe-S assembly by the ISC system. Its efficiency is therefore crucial for the ISC machinery. As we have shown a positive effect of ACP on the efficiency of the ISC system and a specific interaction between ACP and IscS, we have measured IscS activity *in vitro* and tested if ACP could enhance its activity.

In order to test the impact of ACP on cysteine desulfurase activity of IscS, 6His-IscS and 6His-ACP were purified on a nickel resin (see Materials and Methods section). We checked the solubility and the quality of the purified proteins by mass spectrometry, UV/Visible spectroscopy and dynamic light scattering (in collaboration with the Molecular Biophysics Platform of the Institut Pasteur). Proteins were also quantified by a Bradford assay giving concentrations of 1.55 mg/mL for 6His-ACP and 14.5 mg/mL for 6His-IscS.

IscS activity was then measured using the methylen blue assay as previously described (Outten *et al.* 2003). IscS was pre-incubated for 20 minutes with or without ACP in presence of DTT before adding the substrate (cysteine), and sulfur release was monitored 5, 10 and 20 min after de addition of substrate. As we can observe on figure 16, sulfur production increases overtime in a linear fashion. The curve corresponding to the reaction containing ACP and IscS is however very similar to the one corresponding to IscS alone thus demonstrating that in our condition ACP does not enhance IscS activity. Specific cysteine desulfurase activity of IscS alone and IscS pre-incubated by ACP were similar with 6.2 and 5.7 nmol [S]/nmol [IscS]/min respectively. We tested various ratio of ACP and IscS (as well as longer incubation of the two proteins together). No effect of ACP on *in vitro* IscS activity was observed. This indicates that either ACP does not affect Fe-S biogenesis by enhancing IscS activity or that our experimental conditions are not fitted to observe such effect.

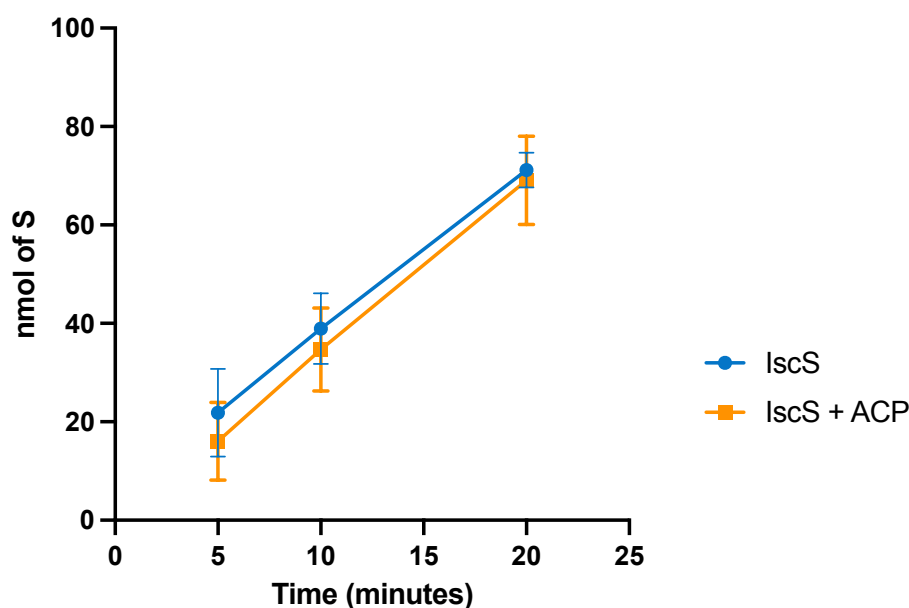


Figure 15. ACP does not enhance IscS desulfurase activity *in vitro*. IscS activity was measured by a methylene blue assay. 0.6 nmol of 6His-IscS and 0.34 nmol of 6His-ACP were used. The absorbance at 670 nm was measured after 5, 10 and 20 minutes of incubation with the substrate (cysteine). The quantity of sulfur released was then determined using a Na_2S standard-curve.

IV - 2 - Characterization of the interaction by analytical ultracentrifugation

As the *in vitro* cysteine desulfurase assay did not show any effect of ACP on IscS activity we attempted to test if purified 6His-ACP and 6His-IscS were able to bind *in vitro*. For this purpose, we have performed a sedimental velocity analytical ultracentrifugation assay (SV-AUC) in collaboration with the Molecular Biophysics Platform of the Institut Pasteur. The SV-AUC is a technique that uses the sedimentation coefficient of a sample exposed to ultracentrifugation in order to provide various information on the sample including but not restricted to, gross shape of macromolecule, conformational change of macromolecules, number subunits and their stoichiometry in complexes.

Using this technique, we tested the ability of 6His-IscS and 6His-ACP to form complexes *in vitro*. The purified proteins were mixed together at equimolar concentrations in the same buffer used for their purifications, the corresponding spectrum of the SV-AUC is exhibited in the figure 17 below. The different peaks correspond to different macromolecules, and their sizes are indicated above each peak. A peak corresponding to a monomer of 5His-ACP is

noticeable and its measured molecular weight is of 12 kDa (theoretical mass: 11.34 kDa). A second peak, corresponding to a weight of 43.6 kDa, is visible and corresponds to a monomer of 6His-IscS (theoretical mass: 47.79 kDa). The following peak corresponds to a weight of 83.9 kDa and has been identified as a dimer of 6His-IscS. The last peak is of 157 kDa, it does not contain 6His-ACP and is predicted to be a trimer of 6His-IscS. We have tested different ratios of ACP/IscS, from 1/3 to 3/1, but no complex of ACP with IscS has been observed. The SV-AUC indicates that the interaction between 6His-ACP and 6His-IscS is not observable *in vitro* in our conditions.

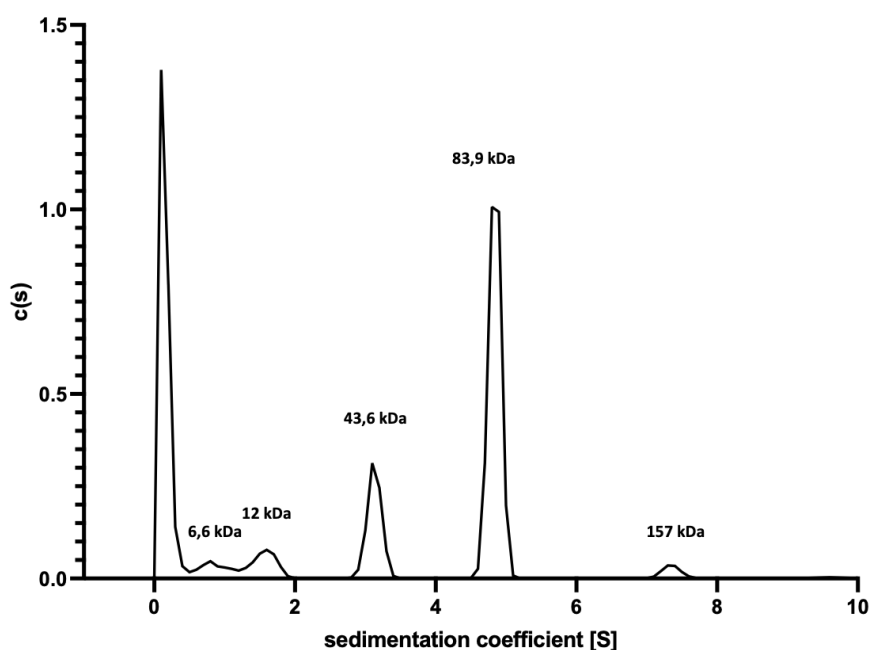


Figure 16. 6His-ACP and 6His-IscS do not form a complex *in vitro*. SV-AUC spectrum of 6His-IscS and 6His-ACP mixed at equimolar concentration of 15 mM. Peaks are annotated with the molecular weight corresponding.

Altogether, these *in vitro* experiments do not allow to conclude on a direct binding of ACP on IscS nor on any effect of ACP on cysteine desulfurase activity of IscS. Whether other partners are needed to allow ACP to favor cysteine desulfurase activity, or ACP could favor another step of ISC-dependent Fe-S assembly needs to be further explored. Furthermore, our BACTH assays showed that the residue on which the phosphopantethein group and the acyl chain are bound on ACP(Ser36) was required for the interaction with IscS. As the purified 6His-ACP should be mainly under a non-acylated form (Emmanuelle Bouveret, personal communication), we now plan to acylate purified 6His-ACP and to test matured ACP for its capacity to bind IscS and/or to favor its cysteine desulfurase activity.

Chapter I – Discussion

A functional and structural link between fatty acid metabolism and Fe-S cluster biosynthesis was suggested by studies performed in two eukaryotic models, yeast and human (Van Vranken *et al.* 2016, Boniecki *et al.* 2017, Cory *et al.* 2017, Fox *et al.* 2019). Furthermore, in *E. coli*, an interaction between ACP and IscS was suggested by a Tap-tag coimmunoprecipitation using ACP as bait (Gully *et al.* 2003).

Our work demonstrates that the functional link between fatty acid metabolism and Fe-S cluster biogenesis is conserved between eukaryotes and prokaryotes. Thanks to a CRISPRi strategy to decrease *acpP* expression, we showed that ACP has a positive impact of ISC-dependent Fe-S cluster biogenesis by showing that decreased ACP leads to i) impaired capacity of the ISC system to compensate the absence of the SUF system, ii) decreased sensitivity to aminoglycosides, iii) a lower activity of Fe-S transcriptional regulators matured by the ISC system, and iv) a lower intracellular Fe-S dependent aconitase activity.

However, the major difference between eukaryotes and bacteria regarding ACP's role in Fe-S biogenesis is ACP interacting partners. In eukaryotes, ACP forms a multi-protein complex (ACP-ISD11-NFS1) that involves ISD11, a protein only found in mitochondria (LYRM family), and NFS1, the mitochondrial structural and functional homologue of IscS. Our results, however, suggest that ACP binds multiple members of the ISC machinery in *E. coli*: IscS the cysteine desulfurase, Fdx, the ferredoxin, and HscB, one of the two co-chaperones of the system. Based on AlphaFold prediction, we propose that a positive patch on IscS (R₆₇, R₂₂₀, and R₂₂₃) and a negative patch on ACP (D₃₅, D₃₈, and E₄₁) could support electrostatic interactions between the two proteins. By replacing these negatively-charged residues of ACP by neutral residues, we have shown that they are indeed necessary for the binding to IscS and for the binding to Fdx and HscB as well (except for E₄₁ which seems to be dispensable for ACP binding to IscS).

In human, ISD11 binds at the surface of NFS1 dimer. The dimer surface forms a large hydrophobic patch that is thought to contribute to the observed aggregation of NFS1 when expressed alone. In the ISD11-NFS1 complex, the hydrophobic patch is covered by ISD11, thus preventing aggregation (Boniecki *et al.* 2017). Moreover, it has been proposed that ACP interaction with ISD11 stabilizes the LYRM protein thus forming a stable ACP-ISD11-NFS1

complex that prevent NFS1 aggregation (Herrera *et al.* 2018). Interestingly, in *E. coli* the dimer surface of IscS presents a hydrophobic patch that is disrupted by at least one charged residue, the D₃₀. The presence of this aspartate is thought to be sufficient to explain the absence of observed aggregation of IscS (Boniecki *et al.* 2017). This suggests that ACP's role in prokaryotes is different from the one suggested in eukaryotes, *i.e.* NFS1 stabilization.

Additionally, Alphafold prediction as well as our experimental data suggest that the binding site of ACP on IscS is completely different from the site of interaction of ACP-ISD11 on NFS1. Indeed, our model shows an interaction that is closer to IscS's active site, which is located at the flip side of the hydrophobic patch. What is striking is that the residues involved, meaning the negative patch of ACP and the positive patch on IscS, are extremely well conserved on their respective eukaryotic homologues. It is therefore intriguing that ACP do not bind directly to NFS1 on this surface. The binding of ACP in the vicinity of IscS catalytic site could indicate a role for ACP in IscS activity. Whether ACP impacts IscS cysteine desulfurase activity and/or IscS sulfur transfer to IscU has to be determined. Moreover, while electrostatic interactions are involved in the formation of the ACP-IscS complex, we noticed that the catalytic relevant residue of ACP, the S₃₆, is important as well. ACP's Ser₃₆ is involved in binding of the 4'-phosphopantethein (4'-PP) prosthetic group, and therefore is crucial for the acylation of ACP. It has been described that ACP's acyl chain is important for the stabilization of the interaction between ACP and various partners, namely ISD11 in eukaryotes (Boniecki *et al.* 2017, Cory *et al.* 2017, Herrera *et al.* 2018). We were unable to demonstrate an *in vitro* interaction between purified ACP and IscS. Considering the importance of the acyl chain of ACP in eukaryotes for its interactions with other proteins, we plan to maturate ACP post-purification (Angelini *et al.* 2012), and re-examine interactions of this matured form with IscS.

We showed that ACP interacts with Fdx and HscB as well. However, our lack of knowledge about ACP's interacting surface on Fdx and HscB is for now a hinderance to our understanding of the mechanism and role of theses interactions. We are now working, in collaboration with Guillaume Bouvier from the Institut Pasteur, on a model of the interaction between ACP and Fdx and between ACP and HscB. The prediction that would be obtained by Alphafold could help us understand more on the role of these interactions.

It is interesting to note that two of the IscS arginine residues (R₂₂₀ and R₂₂₃) involved in the interaction with ACP have been shown to be crucial for interactions between IscS and proteins involved in sulfur-relays originating from IscS (Thil and TusA involved in thiamine biosynthesis and tRNA thiolation respectively) (Shi *et al.* 2010). Thus, ACP's binding to IscS might decrease IscS availability for sulfur-relays, and, as a consequence, might lead to the orientation of IscS activity towards Fe-S biogenesis.

Another aspect never addressed is the impact of the ISC system, or more generally Fe-S homeostasis, on the fatty acid biosynthesis. Indeed, the residues involved in the interaction of ACP with the ISC members are localized in the helix II domain of ACP and this domain is important for the interaction of ACP with many other partners (AcpS, FabI, FabA, BioH for instance (Nguyen *et al.* 2014, Beld *et al.* 2015). Thus, occupancy of this ACP helix by ISC members could interfere with ACP availability for fatty acid biogenesis. We plan to answer this question by measuring membrane stress induction upon perturbation of Fe-S homeostasis. One way of doing that is to study the activity of DolP (division and outer membrane stress-associated lipid-binding protein), a membrane bound protein involved in the membrane damage stress response whose expression is dependent on RpoE (Bryant *et al.* 2020).

Another way to address the question of the biological meaning of interplay between fatty acids and Fe-S biogenesis is to identify metabolic pathways linked to both fatty acids and Fe-S clusters. To our knowledge, there are only two pathways combining fatty acids and Fe-S enzymes, the biosynthesis of lipoate and the biosynthesis of biotin. Lipoate is an essential cofactor for the activity of crucial enzymes such the pyruvate dehydrogenase, the glycine cleavage system, and the α -ketoglutarate dehydrogenase (Reed *et al.* 1993). The last step of lipoate biosynthesis involves LipA, an Fe-S enzyme, that catalyzes sulfur transfer from one of its two clusters to the octanoyl cofactor that originates from ACP. Biotin is an essential vitamin for fatty acid biosynthesis. Biotin production requires a pimeloyl-ACP precursor that undergoes a series of reactions, the last step being catalyzed by an Fe-S enzyme, BioB. Whether disruption of interactions between ACP and the ISC system could impact the efficiency of lipoate and/or biotin biosynthesis is under testing.

While the mode of action differs, the cross-talk between fatty acid metabolism and Fe-S cluster biogenesis is found in both prokaryotes and eukaryotes. Finding the biological meaning of this cross-talk is therefore crucial as it can provide a better understanding of how living organisms coordinate essential processes.

**Chapter II: Study of YeiL, the last uncharacterized Fe-S
regulator in *E. coli***

Chapter II - Introduction

Iron-Sulfur (Fe-S) clusters are metallic co-factors present in all living organisms. They are essential to life and their absence or impairment has drastic consequences on cell viability. Properties of Fe-S clusters provide the cell with a variety of reactions (electron transfer and storage, redox and non-redox chemical catalysis) which explains that Fe-S proteins can be found in most of cellular processes, *i.e.* DNA replication, respiration, central metabolism, transcriptional regulation. In *Escherichia coli*, it has been predicted that Fe-S proteins constitute 4% of the proteome (181 proteins) and for about half of them, it has been validated by experimental data (Lenon *et al.* 2022). Fe-S clusters exist mainly in three different forms, they can be rhombic [2Fe-2S], cubane [4Fe-4S] or cuboidal [3Fe-4S], although some unusual forms exist too, with a higher number of iron and sulfur atoms (for review, see Johnson *et al.* 2005, Fontecave *et al.* 2008). Fe-S clusters are synthesized through dedicated machineries in the cell, and five machineries have been described so far: SMS, MIS, NIF, ISC and SUF systems. *E. coli* only possess the two latter, ISC is the house-keeping system, being active under Fe-S favorable conditions, whereas SUF is the stress system that is active under oxidative or nitrosative stress and low iron environment. The biogenesis of Fe-S clusters goes through 2 major steps: 1) the assembly of the cluster on scaffold proteins and 2) the delivery of the clusters to the target apo-proteins. First a cysteine desulfurase (IscS for the ISC system and SufS for the SUF system) acquires the sulfur from cysteines and provide it to the scaffold protein (IscU and SufBCD complex), the iron is concomitantly provided but its origin and particularly whether it is mobilized by a specific protein has yet to be determined. The cluster is then transported and inserted into the target proteins thanks to carrier proteins (for review, see Py *et al.* 2010, Esquilin-Lebron *et al.* 2021).

Binding of the Fe-S cluster requires at least four amino acids that bind the iron atoms of the cluster, in most cases the binding residues are cysteines. While a CxxC motif in the primary structure is usually a good indicator of an Fe-S protein it can also be misleading as some other metals are coordinated by cysteines as well. However, cysteines can sometimes

be substituted by other amino acids to bind the cluster, such as aspartate or histidine (Bak *et al.* 2014).

Fe-S clusters are very sensitive to oxidation, not only does the O₂ can directly damage clusters, but free Fe²⁺ can react with hydrogen peroxide through Fenton reaction to produce reactive oxygen species (ROS) that will damage Fe-S clusters. The clusters are also sensitive to reactive nitrogen species that can induce nitrosylation of the exposed iron atoms of the cluster and lead to the formation of a blend of products primarily composed of di-nitrosyl iron complex DNIC [Fe(NO)₂](RS)₂, Roussin's Red Easter species (RRE, [Fe₂(NO)₄](RS)₂) and Roussin's Black Salt (RBS, [Fe₃S₄(NO)₇](RS)₂) (Crack *et al.* 2018). These modifications can not only damage the cluster but also lead to the inactivation of the proteins containing them. Finally, low iron availability may reduce Fe-S cluster assembly.

E. coli has 5 transcriptional Fe-S regulators, 4 of them FNR, IscR, SoxR and NsrR are well characterized. The cluster of these regulators plays a key role in the regulation they perform (for review (Crack *et al.* 2012)). FNR possess a [4Fe-4S] cluster that is very sensitive to oxygen. This sensitivity allows FNR to be the regulator of the adaptation from aerobic to anaerobic growth through the regulation of hundreds of genes. FNR mainly activates the expression of genes involved in anaerobic respiration and metabolism and represses the ones of aerobic metabolism. In anaerobic conditions the cluster is present, FNR dimerizes and is considered to be in its holo active form. In presence of O₂ the cluster is damaged which leads to the dissociation of the dimer and the loss of activity of FNR (Sutton *et al.* 2004, Reinhart *et al.* 2008). IscR, the regulator of the Fe-S biogenesis, has a [2Fe-2S] cluster. When IscR is loaded with the cluster it inhibits the expression of the *isc* operon leading to a negative retro control. However, when IscR is in its Apo form, it activates the expression of the secondary Fe-S biogenesis operon: *SUF*, which is less sensitive to stress and thus allowing a continuous Fe-S biogenesis whatever the environmental conditions (Fleischhacker *et al.* 2012). Hence, IscR shows a dual activity that depends on the presence or absence of the cluster, the two forms bind distinct DNA sequences (Rajagopalan *et al.* 2013). NsrR is the regulator of genes involved in the response to nitrosative stress caused by reactive nitrogen species (RNS), mainly nitric oxide (NO), that can be endogenously produced during nitrate respiration (Lundberg *et al.* 2004). When NsrR is in its Holo form it represses the expression of genes encoding detoxifying enzymes such as *hmpA* or *hcp*. When NsrR is exposed to NO, the cluster is nitrosylated which

leads to a conformational change and the repression performed by NsrR is alleviated (Volbeda *et al.* 2017). SoxR possess a [2Fe-2S] cluster, when exposed to redox cycling compounds, the cluster is oxidized which allows SoxR to activate the expression of another transcriptional regulator, SoxS, that activates the expression of oxidative stress response (Gu *et al.* 2011). In the case of SoxR the presence of the cluster is required for its activity however a simple single-electron oxidation of the cluster is enough to unlock the activity of SoxR.

As seen with these examples the metallic cluster is an important feature of Fe-S regulators, and its presence is usually required for their activity. However, modification of the cluster through oxidation or nitrosylation can alter the activity of Fe-S regulators.

In this manuscript we present the work we performed on the characterization of YeiL, the fifth Fe-S regulator, and the last one still uncharacterized. There is only one published study on this regulator (Anjum *et al.* 2000), and the scarce information available is presented below. YeiL belongs to the CRP-FNR family, it displays 22 % sequence identity and 42 % similarity to FNR and a 17 % identical 45 % similar sequence to the CRP of *E. coli*. The main characteristic of this family is the presence of a helix-turn-helix (HTH) DNA binding motif in their C-terminal part and a putative nucleotide binding domain in their N-terminal part. The high similarity to CRP/FNR dimerizing domain suggests that YeiL is also prone to dimerize. YeiL possess five cysteine residues and presence of a [4Fe-4S] cluster inside the YeiL structure have been shown (Anjum *et al.* 2000). It is interesting to note that the Holo-form has been reconstituted under anaerobiosis, but upon exposure to oxygen the cluster seemed quite stable. It is noteworthy to mention that all of the published *in vitro* experiments were performed with a YeiL tagged to the MBP protein, and this was the only construct allowing a purification of the protein without major aggregation. Growth of a *yeiL* deleted strain and its parental strain were assessed in different media, and it appears that the $\Delta yeiL$ strain does not exhibit any growth defect, except a very slight lower bacterial density in stationary phase during aerobic growth. The *yeiL* gene appears to be mainly expressed during stationary phase. Furthermore, it has been shown that the *yeiL* promoter activity was repressed by FNR but activated by RpoS, Lrp and YeiL itself, while the effect of these regulators on *yeiL* expression were modest (Anjum *et al.* 2000). A role for YeiL in survival under nitrogen limiting conditions was also proposed. These conclusions drawn from a paper published by Anjum and coll. in

2000 are the only information available up to date and the absence of follow-up on this study prompted us to characterize YeiL.

The goal of this project was to characterize the role of YeiL by deciphering its regulon, testing the role of its cluster in the regulation, and finally identifying the physiological/environmental conditions for its expression. In this study we therefore demonstrated how YeiL production affects the expression of hundreds of genes amongst which key functions such as anaerobic respiration, sugar metabolism and nitric oxide stress response. We investigated the mechanism by which YeiL is able to repress the expression of the genes of the aldaric acid metabolism and showed that it is an indirect effect that goes through the control of the expression of the regulator of this pathway, CdaR. We demonstrated an interference between YeiL and OxyR for the control of the expression of *hcp*, a reductase involved in the NO stress response. As *yeiL* gene is very lowly expressed, we also studied the *yeiL* expression determinants. Using several fusions between the *yeiL* locus and the *lacZ* gene, we collected evidence that the 3' region of the *yeiL* gene itself is responsible for its low expression.

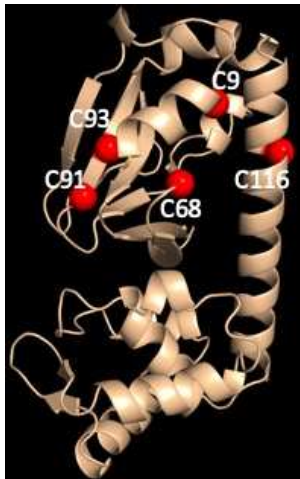


Figure 1. AlphaFold prediction of the structure of YeiL. The five cysteines of the protein are represented by red spheres. Three of them are close enough (less than 9 Å of each other) to bind an [Fe-S] cluster, C₆₈, C₉₁ and C₉₃. The last amino acid to bind the cluster could be either one of the two last cysteines or another amino acid that has yet to be identified.

Chapter II - Materials and Methods

Media and growth conditions

Bacterial strains were grown in LB (Lysogeny Broth) rich medium or M9 minimal medium supplemented with glycerol (0.2%), MgSO₄ (1 mM), thiamine (250 ng/mL), CaCl₂ (0.1 mM), casamino acids (0.05%) and nitrate or fumarate (25 mM). Antibiotics were added when necessary: ampicillin (Amp, 100 µg/mL); kanamycin (Kan, 50 µg/mL); chloramphenicol (Cm, 10 µg/mL); zeocine (Zeo, 50 µg/mL). When specified, galactarate 0,1% was added to the LB medium. Expression from the *Ptet* promoter was induced using 50 to 500 ng/mL of anhydrotetracycline (aTc). For nitric oxide (NO) stress, Spermine NONOate (50 µM) was added to bacterial culture for 30 min before collecting bacteria for further analysis. Anaerobic conditions were met using a Glove box set up to maintain less than 1 ppm of oxygen (Jacomex).

Bacterial strains and Plasmids

All the strains and plasmids used in this study are listed in tables 1 and 2 respectively. Primers, with their sequences and descriptions are listed in table 3.

Standard procedures for preparation of DNA, amplification, digestion, ligation were used as previously described (Sambrook *et al.* 1989). Transformations were done by electroporation. Plasmids constructed for this study have been checked by sequencing (Eurofins). Chromosomal gene deletions have been checked by PCR and *lacZ* chromosomal fusions have been checked by PCR and sequencing of the PCR fragments (Eurofins).

Escherichia coli K12 XL1B strain was used for cloning and experiments were performed in *E. coli* K12 MG1655 or UPEC UTI89 derivatives.

Chromosome engineering

Deletion strains $\Delta yeiL::kan$, $\Delta nsrR::kan$ and $\Delta cdaR::kan$ were obtained by P1 transduction (Miller 1992) with phages prepared from the corresponding strains of the *E. coli* KEIO knockout collection in the MG1655 strain as receiver (Baba *et al.* 2006). The MG1655 $\Delta oxyR::cm$ strain was obtained from the JM. Ghigo's lab. The MG1655 $\Delta hfq::kan$ strain

was obtained using the homologous recombination via the λ red system (Datsenko *et al.* 2000). Briefly, primers ebp353-354 were used to amplify the kanamycin cassette from pKD13 and the amplicon was transformed into MG1655/pKD46 strain to allow recombination and replacement of the *hfq* gene by the kanamycin cassette. In order to combine deletions in the same strain, the *kan* resistance cassette of the $\Delta yeiL::kan$ strain was flipped using pCP20 as previously described (Datsenko *et al.* 2000), and the deletion strain without antibiotic cassette is indicated as $\Delta yeiL^\circ$. Combination of deletions were obtained by P1 transductions. To fuse the SPA tag encoding sequence at the 3' end of *yeiL*, we used homologous recombination via the λ red system using a DNA fragment containing the SPA tag coding sequence, the kanamycin cassette and *yeiL* region fragments for homologous recombination. This DNA was obtained by PCR performed with OSD196-167 as primers and pJL148 as matrix. Chromosomal fusions between *yeiL* and *lacZ* were obtained using the NM580 strain as previously described (Parker *et al.* 2017). Briefly, amplicons corresponding to the *yeiL* promoter (*yeiL* Prom, OSD16-17, 248 bp), the *yeiL* promoter and half of the *yeiL* coding sequence (*yeiL* Mid, OSD16-204, 550 bp) and the *yeiL* promoter and the complete *yeiL* coding sequence (*yeiL* Full, OSD16-205, 866 bp) and 40 bp each side for the insertion in NM580, namely the Zeo^R marker at the 5' end and the *lacZ* ORF at the 3'end, were synthesized. Amplicons were introduced by electroporation into λ red-proficient NM580 cells. Recombinants cloned were screened for sensitivity to kanamycin. The fusions were then transduced using P1 into MG1655 recipient strain or derivatives and transductants were selected for zeocin resistance.

Deletion of the *yeiL* gene and replacement of its coding sequence by the chloramphenicol marker in UTI89 was obtained using the homologous recombination with a PCR fragment generated with the OSD79-80 primers (1015 bp) and pKD3 as matrix via the λ red system (Datsenko *et al.* 2000).

Plasmids construction

For *yeiL* inducible expression, the complete *yeiL* gene has been amplified using MG1655 genomic DNA as template and primers OSD18-19 (717 bp) and cloned in the pTet (notag) vector between the *EcoRI* and *XhoI* restriction sites. The *yeiL** allele is derived from the *yeiL* gene except the following mutations: TG bases in positions 202-203, 271-272, 277-278 and 346-347 have been replaced by GC bases in order to encode alanine residues instead of cysteines in position 68, 91, 93 and 116 of the protein. The *yeiL** allele has been cloned in

pTet(notag) using the same primers and restrictions sites as described for the *yeiL* wild type gene, except that the template DNA used for PCR amplification was a synthetic DNA fragment designed with the mutations (Twist Bioscience).

Plasmids carrying the transcriptional fusions between *PcdaR*, *Phcp* and *gfpmut2* (pUA66 vector) were obtained from the Zaslaver collection (Zaslaver *et al.* 2006). Transcriptional reporter fusions between *PyeiL*, *PgarD*, *PgudP* and *gfpmut2* were obtained by cloning the upstream regions of *yeiL*, *garD* and *gudP* generated by PCR using MG1655 genomic DNA as template (OSD32-33, 186 bp; OSD126-127, 387 bp and OSD128-129, 452 bp respectively) between the *XhoI* and *BamHI* sites of pUA66.

The pAcyC-*yeiL* plasmid has been obtained by insertion of the *yeiL* gene with its own promoter (PCR fragment using OSD104-105 primers, 884 bp) at the *BamHI/SalI* sites of the pAcyC184 vector.

For purification of the YeiL-MBP and YeiL*-MBP fusion proteins, we cloned the *yeiL* and *yeiL** alleles (OSD151-152) downstream the *malE* gene (*A/wNI/EcoRI* sites) of the pMAL-c6T vector (New England BioLabs).

Site-directed mutagenesis on plasmids pUA66-*PcdaR* and pAcyC-*yeiL* have been done by PCR (with the PfuUltra II DNA polymerase) using primers containing the mutations (OSD274-275 for *PcdaR*^{Mut1}, OSD276-277 for *PcdaR*^{Mut2}, OSD210-211 for *yeiL*^{Mut1} and OSD212-213 for *yeiL*^{Mut2}, table 3 for primers sequences), and the plasmids with the wild type alleles as template. After amplification, template DNA was removed using the *DpnI* restriction enzyme.

RNA extraction

Strains were grown in LB added with 500 ng/mL aTc at 37°C for the strains containing the Ptet derivatives, and LB added with NONOate 50 µM when specified, with aeration until OD_{600nm} = 1. Cells were pelleted by centrifugation (10 mL) and immediately frozen at -20 °C. RNA extractions were then performed as previously described (Even *et al.* 2006). Briefly, bacterial pellets were resuspended in a buffer containing glucose 20%, Tris-HCl 25 mM, pH 7.6 and EDTA 50 mM. Cells were broken in presence of glass beads (0.1 mm diameter) and acid phenol (pH 4.5) in a cell disruptor. Successive purification steps with Trizol and chloroforme were performed before isopropanol precipitation. Purified RNAs were then treated with DNase I using the TURBO DNA-free reagent (Ambion) in order to eliminate residual contaminating genomic DNA.

Gene expression analysis by quantitative qRT-PCR

cDNA synthesis was carried out as previously described (Dubrac *et al.* 2007). Oligonucleotides were designed in order to synthesize 100-200 bp amplicons (see Table 3). Quantitative real-time PCRs (qRT-PCRs), critical threshold cycles (CT) and *n*-fold changes in transcript levels were performed and determined as previously described (Livak *et al.* 2001) using the SsoFast™ EvaGreen Supermix (Bio-Rad) and normalized with respect to 16s rRNA whose levels did not vary under our experimental conditions. A CFX Opus Real-Time PCR System (Bio-Rad) was used for amplification reactions and detection. We analyzed the results using Bio-Rad CFX Maestro software (Bio-Rad). All assays were performed using quadruplicate technical replicates and repeated with three independent biological samples. Results are presented as the means of the technical replicates and error bars are the standard errors of the means. Biological replicates were treated independently and did not show any significant variations.

Transcriptome analysis by RNAseq

RNAseq experiments have been performed by the Biomix Platform of the Institut Pasteur. Three independent biological replicates of the MG1655/pTet, MG1655/pTet-yeiL, and MG1655/pTet-yeiL* strains were used for RNA-Seq analysis. Strains were grown in LB-Amp-aTc (500 ng/mL) until OD_{600nm} = 1. Total RNA was isolated as described above, and 1 µg were treated using the MicroExpress kit (Ambion) in order to remove rRNA. The rRNA depleted fraction was used for construction of strand specific single end cDNA libraries using the Truseq Stranded Total RNA sample prep kit according to the manufacturer's instructions (Illumina). Libraries were sequenced using an Illumina HiSeq2000 sequencer according to the manufacturer's instructions (Illumina).

The RNA-seq analysis was performed with Sequana using an RNA-seq pipeline (https://github.com/sequana/sequana_rnaseq) (Desvillechabrol *et al.* 2018). Reads were trimmed from adapters and low-quality bases then mapped to *E. coli* MG1655 genome using bowtie2. Statistical analysis was performed to identify differentially regulated genes using DeSeq2. Parameters of the statistical analysis included the significance (Benjamini-Hochberg adjusted p-values, false discovery rate FDR < 0.05) and the effect size (fold change) for each comparison.

Measurement of gene expression using *gfp* fusions

Strains containing pUA66 derivatives with the studied promoters upstream the *gfpmut2* gene were grown in deep well plates at 37°C, in LB or specified medium added with kanamycin and in conditions mentioned in the figure's legends. After 7 hours of growth, bacterial cultures (150 µL) were transferred in 96 well Black Greiner plates to read the absorbance at 600 nm and the fluorescence (excitation: 485 nm; emission: 530 nm). The measurements of absorbance and fluorescence were read with the TECAN Infini M200Pro reader. For cultures grown in anaerobiosis an additional step of incubation in PBS with Cm (100 µg/mL) during 1 hour at 4°C to recover fluorescence was done (Pinilla-Redondo *et al.* 2018) The level of expression was calculated dividing the intensity of the fluorescence by the absorbance at 600 nm, and the intrinsic fluorescence of the wild type MG1655 strain grown in the same conditions was subtracted. At least, four independent biological replicates were analyzed for each strain and/or condition. Results are presented as the means of the replicates and error bars are the standard errors of the means.

β-galactosidase assay

Cells were grown in LB medium at 37°C in biological triplicate. β-gal activity was determined as previously described (Miller 1992). Average values of β-gal unit/mg of bacteria are represented and error bars correspond to the standard errors of the means.

SDS-PAGE and Western-Blot analysis of proteins

Crude extracts from the *yeiL*-SPA strain and derivatives were prepared in LB medium added with galactarate (0.1 or 1%, in the culture medium at the time of inoculation), paraquat (100 µM, one hour stress), dipyriddy (250 µM, in the culture medium at the time of inoculation) or NONOate (50 µM, one hour stress) when specified. When the cultures have reached an OD_{600nm} around 1-1.5, cells were pelleted, resuspended in Laemmli buffer (around 10⁸ cells in 30 µL buffer), and incubated 10 min at 100°C. Crude extracts were then stocked at -20°C until further analysis.

SDS-PAGE, semi-dry electrotransfer on nitrocellulose membranes, and Western blot analysis were performed as previously described (Gully *et al.* 2003). SPA tag was detected with monoclonal anti-Flag and a secondary antibody 680 iR Dye goat anti-mouse (Sigma). YbgF was

detected with home-made anti-YbgF antibodies (E. Bouveret) and an 800 goat anti-mouse (Sigma). A fluorescent imager (Li-Cor) was used to read the membranes.

MBP-Tagged proteins purification

MG1655/pMAL-*yeiL* and MG1655/pMAL-*yeiL** strains were grown in LB (500 mL) at 37°C until $OD_{600nm}=0.5$, and then, 1 mM IPTG was added to induce fusion proteins expression. Cultures were further incubated at 30°C for 4 hours. Proteins were then purified as recommended (New England BioLabs, Large Scale Affinity Chromatography). Briefly, after pelleting, cells were resuspended in MBP-column binding buffer (Tris-HCl pH 7.5 20 mM, NaCl 200 mM, EDTA 1 mM, DTT 1 mM) and broken using a cell disruptor. After centrifugation to remove the cells debris, supernatants were applied on a MBPTrap HP column (Merck). After a wash step using the MBP-column binding buffer, the MBP fusion proteins were eluted in the same buffer containing maltose (10 mM). All the steps from binding to elution of the proteins were done using an ÄKTA liquid chromatography system. After purification, MBP-proteins fusions were cleaved using the TEV protease (20 TEV units for 100 µg of protein to be cleaved). Proteins were subjected to an additional dialysis step against a buffer containing Tris-HCl 20 mM pH 7.5, NaCl 200 mM, glycerol 10% and kept at -80°C.

Electromobility shift assay (EMSA)

Fluorescent DNA fragments corresponding to *ydhY* and *ynfE* promoter regions were generated by PCR using Cy55-labelled primers: CY-OSD155/OSD156 for *ydhY* (240 bp) and CY-OSD157/OSD158 for *ynfE* (338 bp). Protein/DNA binding reactions were done by mixing approximately 1 pmol of DNA with 10-100 pmol of proteins in a buffer containing potassium buffer pH 7 25 mM, NaCl 150 mM, EDTA 0.1 mM, MgSO₄ 2 mM, DTT 1 mM, glycerol 10%, and PolydIdC 0.5 µg. After 20 min of incubation at 25°C, reactions were loaded on a 6% polyacrylamide gel in TBE buffer and run for 1 hour at 100V. Gels were visualized using a fluorescent imager (Li-Cor).

Mice colonization experiments

Groups of female C57BL/6 mice aged 7–8 weeks (Charles River) were pretreated with a single dose of streptomycin (1 g/kg in 200 µL water) *per os* 1 day prior to gavage and infected

with the strains derived from UTI89. Mice were infected *per os* with 2×10^8 CFU of each strain either alone or in 1:1 mix (WT: mutant strains) for the competitive index (CI) in 200 μ L PBS. Fecal pellets were collected from every individual mouse at indicated times, weighted, and homogenized in 500 μ L phosphate-buffered saline (PBS, pH 7.2). CFUs were determined by plating serial dilutions on selective LB agar plates. For infection, bacterial cultures were prepared in LB and incubated at 37°C under static conditions for 18–24 h. Bacteria were then washed twice in cold PBS and concentrated in PBS at approximately 2×10^8 CFU per 200 μ L. Inocula titers were verified in parallel for each infection. The value of CI was calculated as: CFU WT output strain/CFU mutant output strain, with the verification in each experiment that CFU WT input strain/CFU mutant input strain was very close to 1.

Table 1: Strains used in this study

Lab reference	Name in the manuscript	Genotype	Reference
FBE051	MG1655	Wild type K12 <i>E. coli</i>	F. Barras, lab collection
FBE052	XL1B	<i>recA1 endA1 gyrA96 thi-1 hsdR17 supE44 relA1 lac</i> [F' <i>proAB lacIqZΔM15 Tn10</i> (Tet ^R)]	Stratagene
FBE211	NM580	MG1655 <i>lacI- zeo^R-pBRPlacO-kan-pBAD-ccdB</i> Mini- λ -Red::tet ^R	(Battesti <i>et al.</i> 2015)
FBE637	UTI89	Wild type UPEC	E. Lemichez
FBE711	UTI Δ <i>yeiL</i>	UTI89 Δ <i>yeiL::cm</i>	This work
FBE721	Δ <i>oxyR</i>	MG1655 Δ <i>oxyR::cm</i>	J-M. Ghigo
FBE767	Δ <i>yeiL</i>	MG1655 Δ <i>yeiL::kan</i>	This work
FBE771	Δ <i>yeiL</i> [°]	MG1655 Δ <i>yeiL</i>	This work
FBE1169	Δ <i>yeiL</i> Δ <i>oxyR</i>	MG1655 Δ <i>yeiL</i> [°] Δ <i>oxyR::cm</i>	This work
FBE1174	Δ <i>yeiL</i> Δ <i>nsrR</i>	MG1655 Δ <i>yeiL</i> [°] Δ <i>nsrR::kan</i>	This work
FBE1175	Δ <i>nsrR</i>	MG1655 Δ <i>nsrR::kan</i>	This work
FBE1232	Δ <i>cdaR</i>	MG1655 Δ <i>cdaR</i>	This work

Table 2: Plasmids used in this study

Lab reference	Name	Description	Reference
pEB266	pCP20	ori Rep101 ^{ts} , Cm ^R , Amp ^R , FLP recombinase gene	(Cherepanov <i>et al.</i> 1995)
pEB267	pKD46	ts, Amp ^R , λ Red gene	(Datsenko <i>et al.</i> 2000)

pEB268	pKD3	Amp ^R , FRT-flanked Cm ^R cassette	(Datsenko <i>et al.</i> 2000)
pEB270	pKD13	Amp ^R , FRT-flanked Kan ^R cassette	(Datsenko <i>et al.</i> 2000)
pEB0794	pJL148	Amp ^R , FRT-flanked SPA-kan ^R cassette	(Zeghouf <i>et al.</i> 2004)
pEB898	pUA66	Kan ^R , sc101 ori, <i>gfpmut2</i> transcriptional fusion	(Zaslaver <i>et al.</i> 2006)
pZ1	pUA66- <i>PcdaR</i>	Zaslaver collection	(Zaslaver <i>et al.</i> 2006)
pZ4	pUA66- <i>Phcp</i>	Zaslaver collection	(Zaslaver <i>et al.</i> 2006)
pSD18	pUA66- <i>PyeiL</i>	Insertion of OSD32-33 fragment in pEB898 (<i>XhoI/BamHI</i>)	This study
pSD25	pUA66- <i>PgarD</i>	Insertion of OSD126-127 fragment in pEB898 (<i>XhoI/BamHI</i>)	This study
pSD26	pUA66- <i>PgudP</i>	Insertion of OSD128-129 fragment in pEB898 (<i>XhoI/BamHI</i>)	This study
pSD48	pUA66- <i>PcdaR</i> ^{Mut1}	Site directed mutagenesis on pZ1 with OSD274/275	This study
pSD49	pUA66- <i>PcdaR</i> ^{Mut2}	Site directed mutagenesis on pZ1 with OSD276/277	This study
pEB1823	pTet(noTag)	Amp ^R , ColE1 ori, Tet ^R promoter	BioTAGnology
pSD5	pTet- <i>yeiL</i>	Insertion of OSD17-18 fragment in pEB1823 (<i>EcoRI/XhoI</i>)	This study
pSD6	pTet- <i>yeiL</i> *	Insertion of <i>yeiL</i> mutated allele (TG-->GC in positions 202-203, 271-272, 277-278, 346-347) in pEB1823 (<i>EcoRI/XhoI</i>)	This study
pEB37	pAcyC184	Cm ^R , Tet ^R , p15A ori	(Chang <i>et al.</i> 1978)
pSF45	pAcyC- <i>yeiL</i>	Insertion of OSD104-105 fragment in pEB37 (<i>BamHI/SalI</i>)	This study
pSF46	pAcyC- <i>yeiL</i> ^{Mut1}	Site directed mutagenesis on pSF45 with OSD210/211	This study
pSF47	pAcyC- <i>yeiL</i> ^{Mut2}	Site directed mutagenesis on pSF45 with OSD212/213	This study
pVP224	pMAL-c6T	Amp ^R , ColE1 ori, <i>Plac</i> promoter, TEV cleavable MBP tag	New England Biolabs
pSD22	pMAL- <i>yeiL</i>	Insertion of OSD151-152 fragment in pVP224 (<i>AnwNI/EcoRI</i>)	This study
pSD23	pMAL- <i>yeiL</i> *	Insertion of OSD151-152 fragment amplified from pSD6 (<i>yeiL</i> *) in pVP224 (<i>AnwNI/EcoRI</i>)	This study

Table 3: Primers used in this study

Name	Sequence	Description
Chromosome engineering		
ebp353	GAAAGGTTCAAAGTACAAATAAGCATATAAGGAAAAGAGAGAatgATTCCGG GGATCCGTCGACC	PCR fragment on pKD13 for replacement of <i>hfq</i> by the Kan cassette
ebp354	GCAGGATCGCTGGCTCCCCGTGTAACAAAAACAGCCCGAAACCTtaTG TAGGC TGGAGCTGCTTCG	

OSD79	CATCGTCAAAGAAATCCACAATAATGATCTTAAGCAGCAATTGATGCATATGA ATATCCTCCTTAG	PCR fragment on pKD3 for replacement of <i>yeiL</i> by the Cm cassette in UT189
OSD80	ATTAAGCGTTGCATCCGGCAATCGCACTATTGCCAATAATTTTATGTGTAGGC TGGAGCTGCTTC	
OSD196	GCGCTGGAGATGGACCCGGAGAATAAATTCTCCGGGATGATGCACTCCATG GAAAAGAGAAG	PCR fragment on pJL1778 for insertion of the SPA tag and kan at the 3' end of <i>yeiL</i>
OSD197	CGTATTAAGCGTTGCATCCGGCAATCGCGCTATTGAAAATAATTTTCATATGAAT ATCCTCCTTAG	
OSD16	TACTATGCCGATATACTATGCCGATGATTAATTGTCAACTGTTTATTTCCCTCTGT TTCCAGTT	Insertion of <i>yeiL</i> Prom (16-17), <i>yeiL</i> Mid (16- 204), and <i>yeiL</i> Full (16- 205) fragments in front of <i>lacZ</i> in NM580 strain
OSD17	GTTGTAACGACGCGCCAGTGAATCCGTAATCATGGTCATCAATTGCTGCTTA AGATCAT	
OSD204	GTTGTAACGACGCGCCAGTGAATCCGTAATCATGGTcatAGCTGTTTCCTATA GCGTGTCTGTTAATAACAG	
OSD205	GTTGTAACGACGCGCCAGTGAATCCGTAATCATGGTcatAGCTGTTTCCTATC ATCCCGGAGAATTTATTCTCC	
Construction of pTet-<i>yeiL</i>/<i>yeiL</i>*		
OSD18	CAGGAATTCATGAGTGAATCCGCGTTTAAGGAT	<i>yeiL</i> coding sequence (<i>EcoRI</i> / <i>XhoI</i>)
OSD19	AAACTCGAGAAGCGTTGCATCCGGCAATCGCGCT	
Construction of <i>gfp</i> transcriptional fusions in pUA66		
OSD32	CTTCTCGAGTGTATTTCCTCTGTTTCCAGTT	<i>yeiL</i> promoter region (<i>XhoI</i> / <i>Bam</i> HI)
OSD33	TTCGGATCCAATTGCTGCTTAAGATCATTATTG	
OSD126	TCACTCGAGTTACCTCGGGTACTTATGCT	<i>garD</i> promoter region (<i>XhoI</i> / <i>Bam</i> HI)
OSD127	CAAGGATCCTGTGCAATATTCTCCAGCCA	
OSD128	TTGCTCGAGTATGTTTCAGCGAGCGGTAA	<i>gudP</i> promoter region (<i>XhoI</i> / <i>Bam</i> HI)
OSD129	AGAGGATCCTGTGCACTCCTGAAAATTCG	
Construction of pAcyC-<i>yeiL</i>		
OSD104	CTTGGATCCTGTTTATTTCCCTCTGTTTCCAGTT	<i>yeiL</i> promoter and coding sequence (<i>Bam</i> HI/ <i>Sall</i>)
OSD105	AAAGTCGACAAGCGTTGCATCCGGCAATCGCGCT	
Construction of pMAL-<i>yeiL</i>/<i>yeiL</i>*		
OSD151	AAGCAGATGCTGATGAGTGAATCCGCGTTTAAGGAT	<i>yeiL</i> coding sequence (<i>Alw</i> NI/ <i>Eco</i> RI)
OSD152	AAAGAATTCAAGCGTTGCATCCGGCAATCGCGCT	
Site directed mutagenesis on plasmids		
OSD210	AAAGAATTCAAGCGTTGCATCCGGCAATCGCGCT	pAcyC- <i>yeiL</i> ^{Mut1} from pAcyC- <i>yeiL</i>
OSD211	GCTATTGAAAATAATTTTACTGCATCATGGCCGTATATTTATTCTCCGGGTCC A	
OSD212	GGCGCTGGAGATGGATCCAGAAAACAAATTTCCGGGATGATG	pAcyC- <i>yeiL</i> ^{Mut2} from pAcyC- <i>yeiL</i>
OSD213	CATCATCCCGGAGAATTTGTTTTCTGGATCCATCTCCAGCGCC	
OSD274	CCACAACCTCATACTCCCCCATCCTTTAGGCATTTGCA	pUA66-PcdaR ^{Mut1} from pUA66-PcdaR
OSD275	TGCAAATGCCTAAAGGATGGGGGGGATGTATGGAGTTGTGG	
OSD276	CTTACCACAACCTCCCCCCTTCATCATCCTTTAGGCAT	pUA66-PcdaR ^{Mut2} from pUA66-PcdaR
OSD277	ATGCCTAAAGGATGATGAAGGGGGGGGAGTTGTGGTGAAG	
qRT-PCR		
16sFor	AAGTTAATACCTTTGCTCATTGAC	16s
16sRev	GCTTTACGCCAGTAATTCC	
OSD5	AGCCGTCCTGGCTGTTTTACC	<i>yeiL</i>
OSD6	ATCAGCGACACGCGACCAT	
OSD90	ACTTCGATTCTCCGCGTATTGT	<i>hcp</i>
OSD91	TCTTTGTTAGGGGTAAATCTGCT	
OSD92	CTACCCTCCGTATAACGTTGAA	<i>ibpA</i>
OSD93	GCGATGCCCTGGTACAGATA	
OSD94	TCCGGCAATGTCGATGGTTTC	<i>narG</i>
OSD95	CAGATTCGGTACGTCAGTT	

OSD96	CGAACGCGCTATCACCATCAA	<i>nirB</i>
OSD97	GTTGAGGTCTTCAATAGTGCGAT	
CY55-labelled primers for EMSA		
OSD155	CACATTATCGACTGAACGCCGGATATGA	<i>ynfE</i>
OSD156	TGTTCTGCGGCTGATGCCACCAT	
OSD157	CTGCAATGAAAGTCACAAATAATTGTC	<i>ydhY</i>
OSD158	ATAGTGGACGATCAACCGGGTTCAT	

Chapter II - Results

I - Identification of the YeiL-regulated genes

I - 1 - Global analysis of the YeiL regulon

We first analyzed *yeiL* expression in different growth conditions. We measured *yeiL* expression by quantitative Real Time-PCR (qRT-PCR) in a MG1655 WT strain and included a $\Delta yeiL$ strain as a negative control. We tested *yeiL* expression in exponential and stationary growth phases, in presence and absence of oxygen, in rich and minimal (M9) growth media. Unfortunately, none of these conditions allowed the detection of a specific signal for *yeiL* expression. The signal detected in all these conditions was the same in the WT and $\Delta yeiL$ background, meaning that if *yeiL* was expressed its level was beneath the threshold of detection.

Because we were unable to identify conditions favorable for *yeiL* expression, we used an overexpression strategy to decipher the YeiL regulon. The *yeiL* gene was cloned under the control of the Ptet inducible promoter (pTet vector) to induce its expression with anhydrotetracycline (aTc), (see Materials and Methods). We also cloned a mutated allele of *yeiL*, called *yeiL**, in which 4 out of the 5 cysteines were substituted by alanine residues (C₆₁A, C₆₃A, C₉₁A, C₁₁₆A). By substituting these cysteines, we made the assumption that YeiL* is locked in an Apo form that cannot bind the Fe-S cluster. We then compared gene expression in strains overexpressing *yeiL* (e.g. MG1655/pTet-*yeiL*) or *yeiL** (e.g. MG1655/pTet-*yeiL**) to a reference strain containing the empty vector (MG1655/pTet). Strains were grown until mid-exponential phase in LB rich medium at 37°C under agitation, and aTc (0,5 µg/mL) was added to induce the expression of *yeiL* or *yeiL**. Total mRNAs were extracted from three independent biological replicates of each condition. A transcriptome sequencing analysis (RNA-seq, Biomics Platform, Institut Pasteur) was then performed in which we compared the level of expression in the three conditions.

A global analysis of RNAseq data was performed using a volcano plot representation of regulated genes. First, we noticed the higher number of genes regulated with YeiL* (Fig. 1B) compared to YeiL (Fig. 1A). Indeed, after applying a cut-off of p-value > 0.05, we found 218 genes differentially expressed upon expression of *yeiL*, whereas expression of 1324 genes

varied upon expression of *yeiL**. Moreover, the expression fold changes were far higher upon *yeiL** overexpression than with the *yeiL* wild type allele (see Fig. 1). Notably, the expression of *yeiL** led to more than 10-fold differential expression of 154 genes whereas under *yeiL* expression the most activated and the most repressed genes showed a 5-fold change of expression.

This result showed that *YeiL** is more active than the native *YeiL* regulator, this may indicate that the Apo form of *YeiL* is the active form of the regulator.

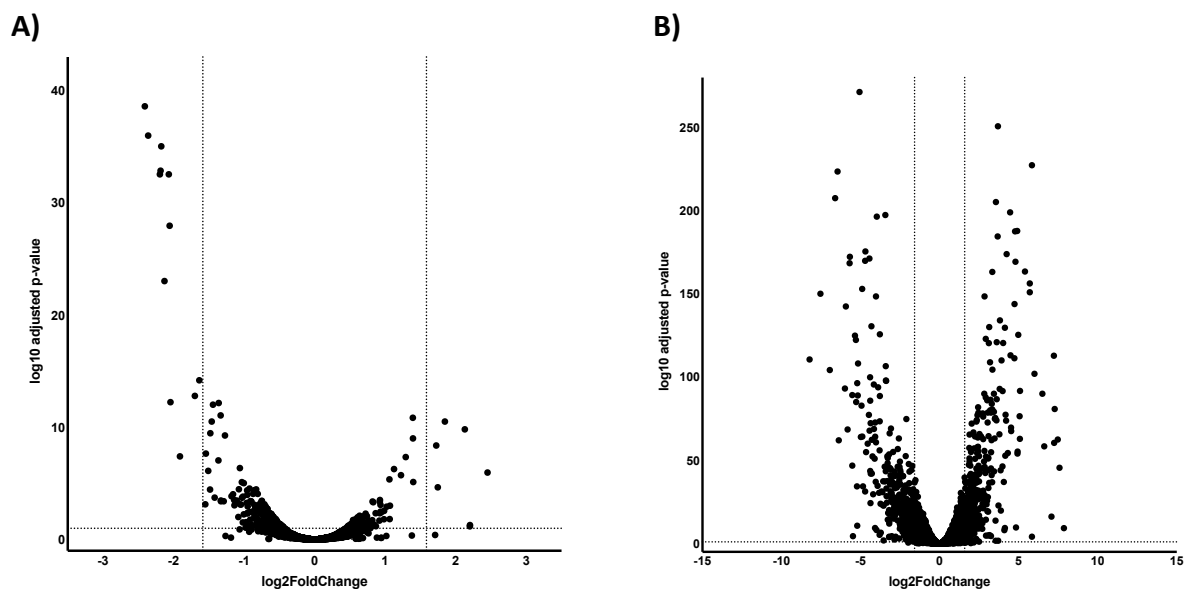


Figure 1. Overview of the *YeiL*- and *YeiL-regulated genes.** Volcano plots of datasets from *YeiL* (A) and *YeiL** (B) RNA-seq. Horizontal dotted line corresponds to a p-value cut-off of 0.05 and vertical dotted lines correspond to a FC cut-off of 3.

To analyze the results of the transcriptome, in addition to the cut-off of $p\text{-value} > 0.05$ we subjected the results of *YeiL** to a fold-change cut-off ($FC > 3$) to focus on the most regulated genes. Using these parameters, we found 218 genes differentially expressed when overexpressing *yeiL* (55 up- and 163 down-regulated, $p\text{-value} > 0.05$) and 699 when overexpressing *yeiL** (355 up- and 344 down-regulated, $p\text{-value} > 0.05$ and $FC > 3$) (Table 4 and Supplementary Table 1).

Genes down-regulated by <i>yeiL</i> overexpression	163
Genes up-regulated by <i>yeiL</i> overexpression	55
Genes down-regulated by <i>yeiL</i> * overexpression	344
Genes up-regulated by <i>yeiL</i> * overexpression	355

Table 4. YeiL- and YeiL*-regulated genes. Number of genes up-regulated and down-regulated due to either *yeiL* (p-value>0.05) or *yeiL** (p-value>0.05 and FC>3) overexpression.

We performed a comparison between the YeiL and YeiL* regulons. Surprisingly the overlap of the set of genes affected by both alleles of the regulator was overall limited with 13 genes up-regulated and 82 genes repressed by both YeiL and YeiL* (Fig. 2 A and B).

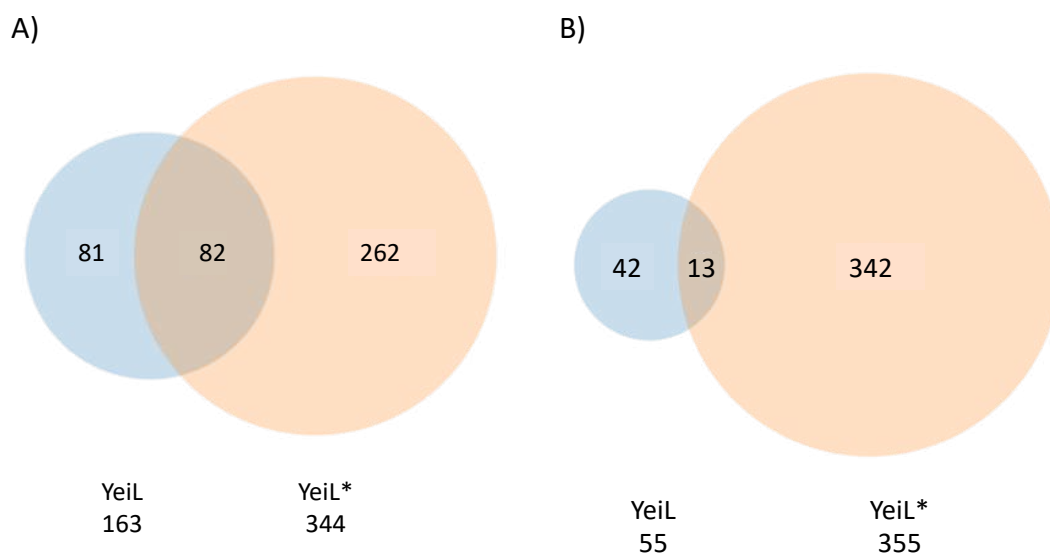


Figure 2. Overlap of YeiL and YeiL* regulon. Venn diagram representation of YeiL- and YeiL*- regulated genes **A.** Repressed genes by YeiL (blue) and YeiL*(salmon). **B.** Activated genes by YeiL (blue) and YeiL*(salmon).

An ontologic analysis of regulated genes was performed. Genes were classified into Clusters of Orthologous Groups (COGs) (Fig. 3). In agreement with the volcano plot, we observed that YeiL* (Fig. 3A) affects more pathways than YeiL (Fig. 3B). Carbohydrate transport and metabolism, and energy production and conversion are the two most regulated pathways in both YeiL and YeiL* transcriptomes.

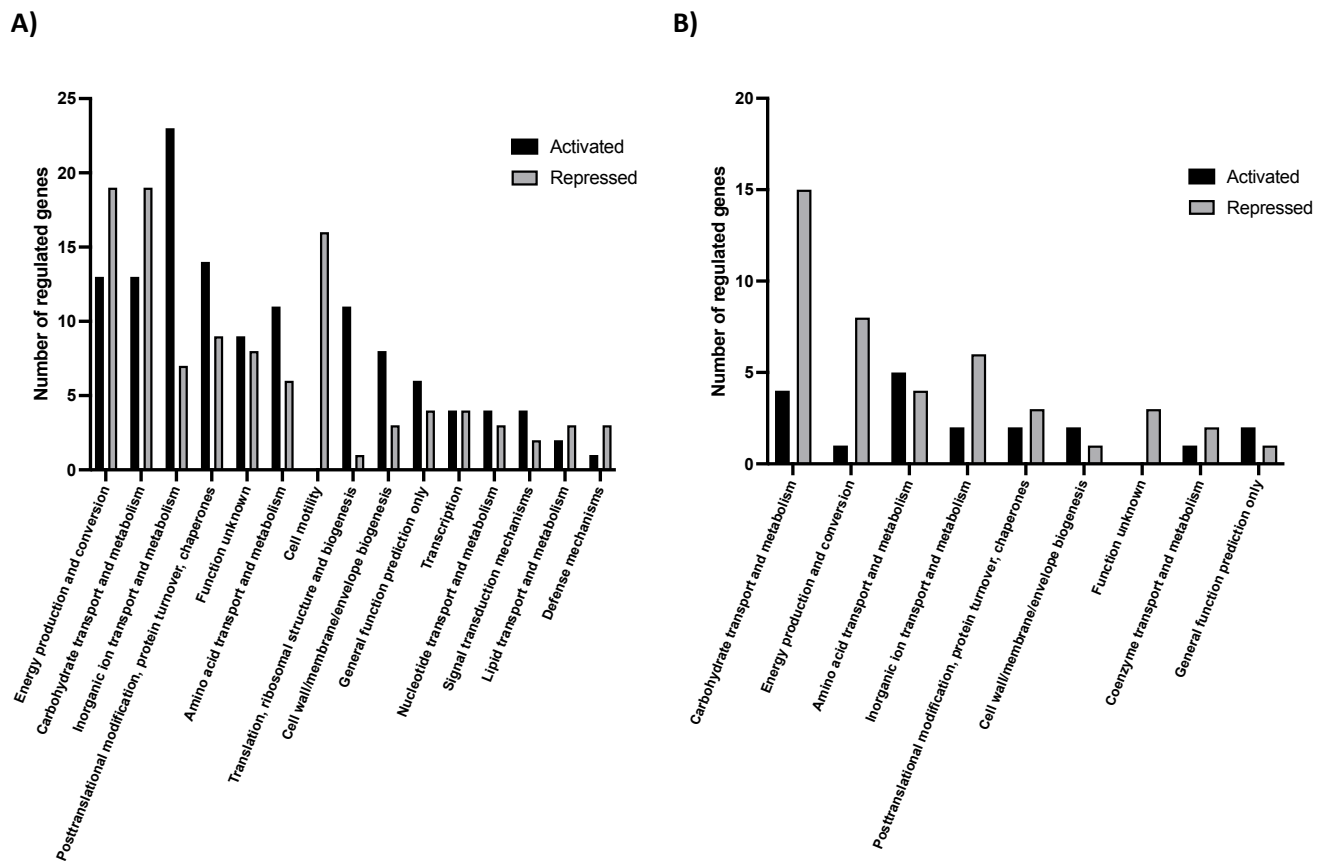


Figure 3. Analysis of the most regulated functions. The Clusters of Orthologous Genes (COGs) was retrieved from the NCBI COG webservice (<https://www.ncbi.nlm.nih.gov/research/cog/webervices/>) via BioServices. **A)** Pathways affected by Yeil*. **B)** Pathways affected by Yeil.

I - 2 - Overproduction of Yeil leads to a general stress response

We noticed that strains producing Yeil or Yeil* exhibited a considerable delay in growth with a doubling time during exponential phase of 29 minutes for the strains carrying the empty vector and 84 minutes for the strains producing Yeil and Yeil* (Fig. 4A). Comparison of the Yeil/Yeil* transcriptomic data with the RpoH regulon (Ecocyc database) showed that about 10% of Yeil -and Yeil*-activated genes (4 on 55 Yeil-activated and 38 on 355 Yeil*-activated) are part of the RpoH regulon, with a strong activation of genes encoding IbpA, IbpB and GroEL chaperones. We confirmed *ibpA* induction upon Yeil/Yeil* production by qRT-PCR (Fig. 4B). Induction of the RpoH regulon suggested general proteostasis stress and possibly

missfolding of the produced YeiL and YeiL* regulators. A well-known way to enhance solubility of proteins is to fuse them with the maltose-binding protein (MBP) (Raran-Kurussi *et al.* 2015). We cloned the *yeiL* and *yeiL** genes in-frame behind the *malE* gene (pMAL-c6T vector) to produce MBP-YeiL and MBP-YeiL* fusion proteins. We then tested the effect of the production of these fusion proteins on gene expression. As mentioned before a stress-induced gene, *ibpA* expression was largely induced upon YeiL/YeiL* production (Fig. 4B), whereas its expression was unchanged upon production of the MBP-YeiL and MPB-YeiL* fusion proteins (Fig. 4C). This result indicated that induction of RpoH stress-activated genes is the result of missfolded YeiL and YeiL* proteins. We then wondered whether other genes identified by the transcriptomic approach could be affected by the missfolded protein stress. We picked-up two genes of interest, *garP*, whose expression was down regulated by overexpressing YeiL or YeiL* and *hcp* whose expression was down regulated by overexpressing YeiL*. As shown on figure 4C, both *garP* and *hcp* were down regulated by the fusion proteins as observed from the RNA-seq analysis. Therefore, we concluded that down regulation of these genes did not result from YeiL or YeiL* misfolding-mediated stress but rather was a true consequence of overexpressing either one.

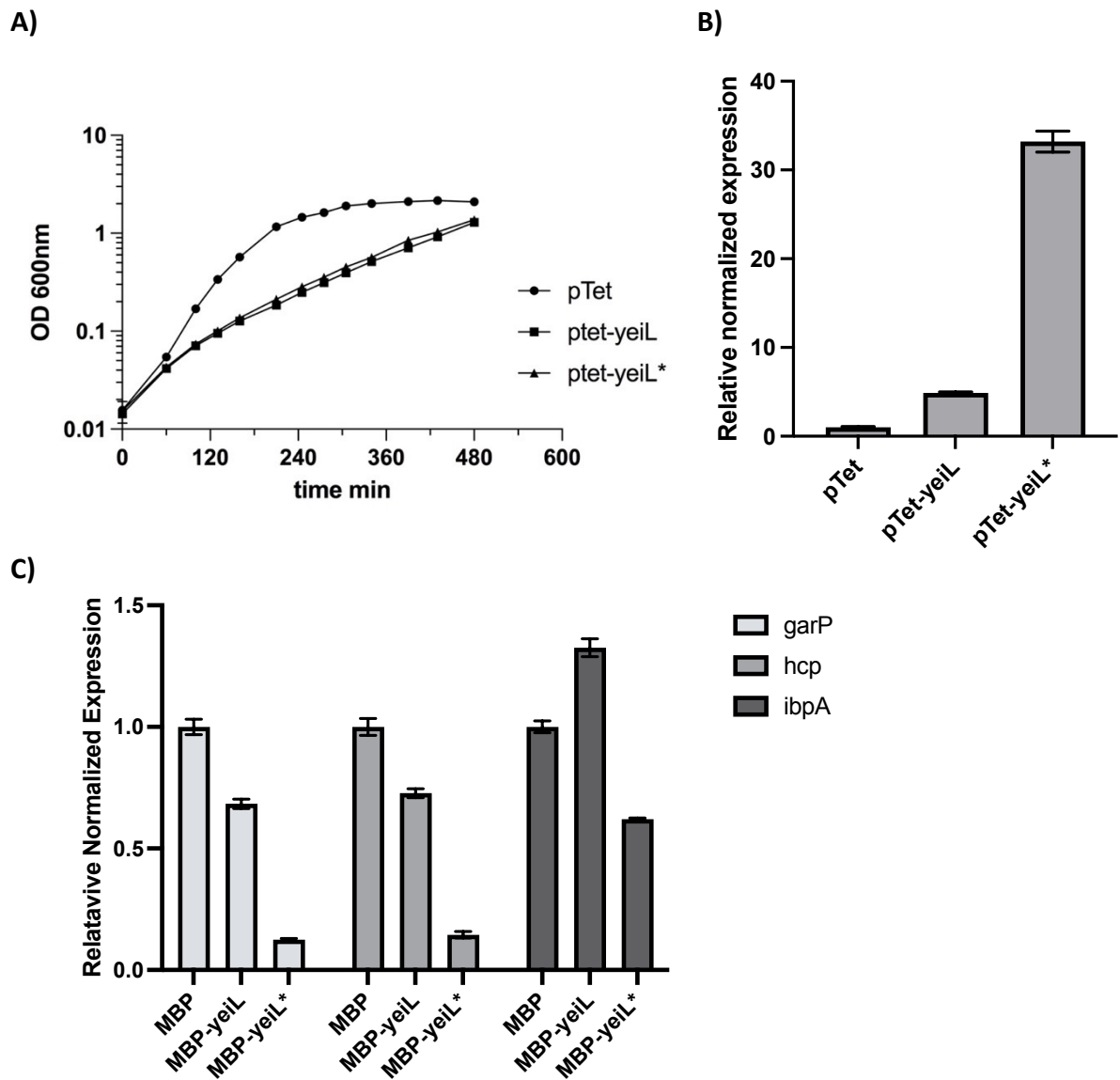


Figure 4. Yeil and Yeil* production induce a stress response. A) Growth curves of MG1655/pTet, MG1655/pTet-yeiL and MG1655/pTet-yeiL* strains grown in LB-Amp with 0.5 $\mu\text{g/mL}$ aTc, at 37°C under agitation. B) *ibpA* expression measured by qRT-PCR performed on cDNA prepared from culture of MG1655/pTet, MG1655/pTet-yeiL and MG1655/pTet-yeiL* strains grown in LB-Amp with 0.5 $\mu\text{g/mL}$ aTc, at 37°C under agitation until OD_{600nm} = 1. C) Expression *garP*, *hcp* and *ibpA* measured by qRT-PCR performed on cDNA prepared from culture of MG1655/pMAL-c6T (MBP), MG1655/ pMAL-c6T-yeiL (MBP-yeiL) and MG1655/ pMAL-c6T-yeiL* (MBP-yeiL*) strains grown in LB with IPTG 1mM, at 37°C under agitation until OD_{600nm} = 1.

I - 3 - YeilL regulates anaerobic nitrate respiration

Analysis of RNA-Seq data showed that YeilL as well as YeilL* regulates several genes involved in nitrate respiration (see below) and other anaerobic respiration (fumarate respiration with *frdABCD*, DMSO respiration with *dmsABC*). We focused on the effect of YeilL* on nitrate respiration. Indeed, YeilL* activates the expression of genes encoding cytoplasmic nitrate reductases (*narG* and *narZ*), whereas it represses the expression of genes encoding periplasmic nitrate and nitrite reductases (*napFDAGHBC* and *nrfABCDEFG* respectively) (Fig. 5).

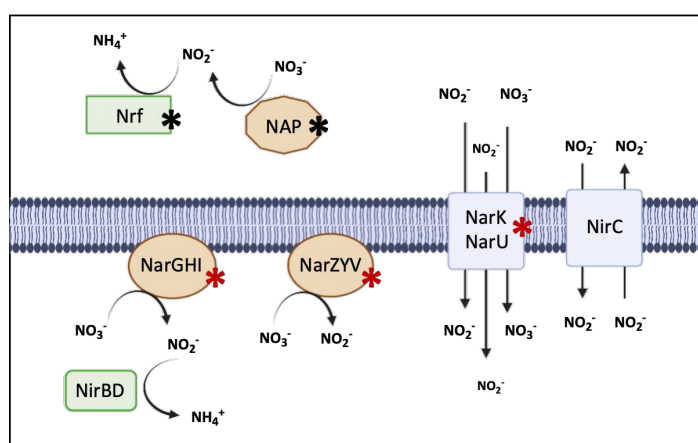


Figure 5. YeilL* regulates expression of genes involved in nitrate respiration. Cytoplasmic nitrate reductases (red stars) are activated by YeilL* and periplasmic nitrate and nitrite reductases are repressed (black stars). YeilL*-regulated nitrate respiration genes are listed in the table. Fold change expression (YeilL*/control) and p-values are indicated.

Gene	Fold change	P-value
<i>narG</i>	17,154	8,66E-09
<i>narH</i>	7,63	4,16E-15
<i>narI</i>	4,248	3,40E-07
<i>narJ</i>	4,858	6,23E-11
<i>narK</i>	17,565	4,44E-10
<i>narU</i>	5,067	1,95E-37
<i>narW</i>	3,9	6,39E-14
<i>narY</i>	3,727	4,17E-28
<i>narZ</i>	3,227	1,13E-20
<i>napA</i>	0,122	1,23E-40
<i>napB</i>	0,126	1,86E-25
<i>napC</i>	0,2	2,70E-22
<i>napD</i>	0,099	2,68E-25
<i>napF</i>	0,097	8,06E-34
<i>napG</i>	0,117	3,00E-45
<i>napH</i>	0,141	1,16E-36
<i>nrfA</i>	0,11	7,58E-05
<i>nrfB</i>	0,083	7,69E-24
<i>nrfC</i>	0,082	1,17E-31
<i>nrfD</i>	0,103	4,71E-15
<i>nrfE</i>	0,186	1,43E-13
<i>nrfF</i>	0,303	4,22E-05
<i>nrfG</i>	0,269	2,94E-09

We confirmed RNA-Seq data by studying *narG* and *nirB* expression upon YeilL* production by qRT-PCR (Fig. 6). We found that the expression of *narG* in MG1655/pTet-*yeilL** is 5 times higher than in the MG1655/pTet control strain whereas the expression of *nirB* is unaltered in the MG1655/pTet-*yeilL** strain.

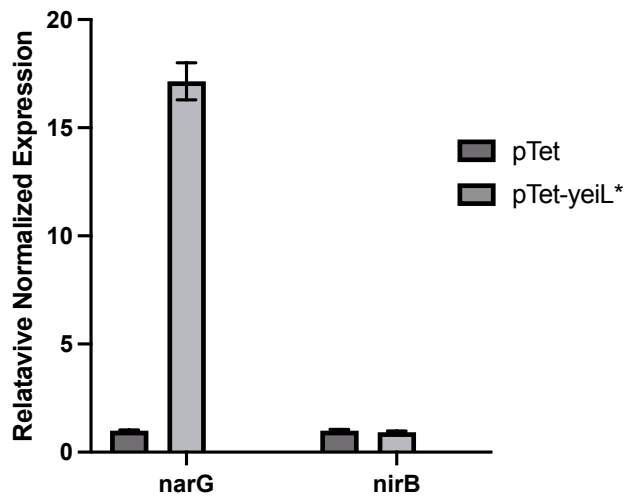


Figure 6. Yeil* activates expression of cytoplasmic nitrate reductase gene. Expression of *narG* and *nirB* genes in strains MG1655/pTet and MG1655/pTet-*yeiL** was measured by qRT-PCR. cDNA were prepared from cultures grown in LB with aTc 0.5 µg/mL at 37°C under agitation until OD_{600nm} = 1. Results are presented as the mean of 4 technical replicates and standard errors to the means are indicated.

I - 4 - Connection between Yeil and OxyR in regulation of nitric oxide stress response

We noticed that Yeil* down-regulates several genes involved in NO detoxification: *hcp*, *hcr* and *hmpA* (0.076, 0.11 and 0.229 Fold Change respectively, see Annex 1). This prompted further interest as the Yeil-activated gene, *narG*, described above, has also been proposed to favor formation of toxic nitric oxide (NO) as a by-product of nitrate respiration NirB (Calmels *et al.* 1988, Ralt *et al.* 1988, Corker *et al.* 2003, Rowley *et al.* 2012). The bi-cistronic operon *hcp-hcr* encodes the Hybrid cluster protein, Hcp, and its reductase (Hcr) that are involved in NO detoxification (van den Berg *et al.* 2000, Wang *et al.* 2016). The *hmpA* gene encodes a NO detoxifying enzyme with two activities: NO dioxygenase (in presence of oxygen, major activity) and NO reductase (under anaerobiosis, low activity) (Gardner *et al.* 1998). While *hmpA* appears to be mainly expressed under aerobiosis, *hcp* is activated by the FNR anaerobic activator. The *hcp* gene is also activated by the NarX/NarL and NarQ/NarP two-components systems in presence of nitrate. Furthermore, *hcp* expression is increased upon NO exposure. Indeed, *hcp* is activated by a nitrosylated form of OxyR, and its repression by NsrR is alleviated in the presence of NO (Filenko *et al.* 2007, Seth *et al.* 2012).

We studied the effect of Yeil* on *hcp* expression under anaerobiosis respiring conditions (M9 minimal medium supplemented with glycerol as a non-fermentable carbon

source) and in presence of fumarate or nitrate as final electron acceptor. A plasmid carried transcriptional fusion between the *hcp* promoter and *gfp* (pUA66 vector) was co-transformed in MG1655 strain with either the pTet empty vector or the pTet-*yeiL** plasmid.

Expression of *hcp* was induced 7-fold in presence of nitrate as compared to the fumarate condition (Fig. 7A). In presence of nitrate, *yeiL** expression led to a 3-fold decrease in the expression of *hcp* compared to the control strain, whereas there was no significant effect of *YeiL** in presence of fumarate (Fig. 7A). *hcp* expression was unchanged by *yeiL* deletion whatever the terminal electron acceptor present (Fig. 7B). As expected, *oxyR* deletion led to a decrease of *hcp* expression in presence of nitrate (Fig. 7B). Interestingly, in presence of nitrate, deletion of *yeiL* in a $\Delta oxyR$ background allowed the *hcp* expression to increase and to reach the level of expression measured in the wild type background (Fig. 7B, light grey bars). Moreover, under fumarate respiration, neither *OxyR* nor *YeiL* influenced *hcp* expression (Fig. 7B, dark grey bars).

Altogether, our results showed a repression of *hcp* by *YeiL* under nitrate respiration. Moreover, the $\Delta yeiL$ mutation acted as a suppressor of the $\Delta oxyR$ mutation, suggesting a genetic interaction between both regulators within the control of the *hcp* operon.

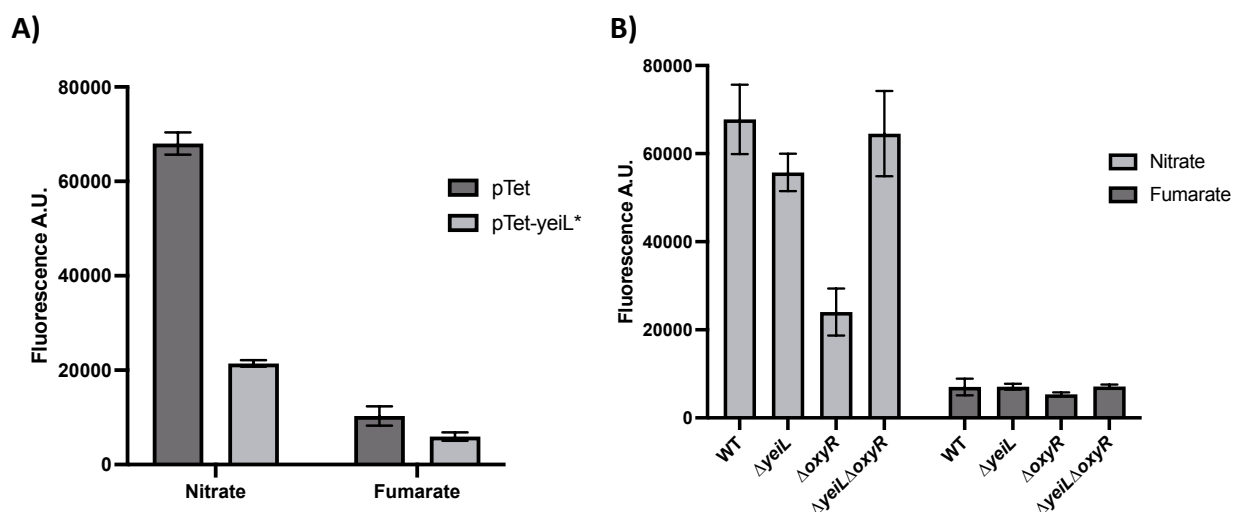


Figure 7. *YeiL* and *OxyR* cross-regulations of *hcp* under nitrate respiration. Activity of the *hcp* promoter was determined using a *Phcp-gfp* fusion. **A.** *Phcp-gfp* expression in cells carrying either the pTet empty vector or the pTet-*yeiL** plasmid **B.** *Phcp-gfp* expression in WT, $\Delta yeiL$, $\Delta oxyR$, and $\Delta yeiL\Delta oxyR$ strains. Cells were grown anaerobically in M9 minimal medium with glycerol and casaminoacids, containing either nitrate or fumarate as final electron acceptor. For the strains carrying pTet derivatives, aTc 0.5 $\mu\text{g}/\text{mL}$ was added to the growth medium. Values are the mean of at least 4 biological replicates and standard errors to the means are indicated.

We then tested the expression of *hcp* in presence of NO (NONOate exposure). Based upon the literature, *hcp* expression should be highly induced in presence of NONOate because of both alleviation of NsrR repression (inactive nitrosylated form of NsrR) and activation by SNO-OxyR (active nitrosylated form of OxyR) (Seth *et al.* 2012).

Bacteria were grown in LB and, at OD_{600nm} around 0.8, NONOate, an NO generator, was added (50 μM) or not (control condition) in the growth medium. After 30 minutes of treatment, cells were harvested, total RNA was extracted, and *hcp* expression was measured by qRT-PCR. In the MG1655 WT strain, *hcp* expression increased upon NO exposure (150-fold induction) (Fig. 8A). In the $\Delta yeiL$ background, the same *hcp* expression profile was observed, with a high induction in presence of NONOate compared to the control condition without stress. In the $\Delta oxyR$ strain, NO-dependent induction of *hcp* expression was much more modest than in the wild type strain (75-fold induction vs 150-fold in the wild type background) (Fig. 8A). Last, the $\Delta oxyR\Delta yeiL$ backgrounds showed a higher expression in all conditions tested. This result indicates that YeiL is repressing *hcp* expression in absence of OxyR and confirms a genetic interaction between YeiL and OxyR regulatory activities.

We also studied NsrR-dependent regulation of *hcp* expression. *hcp* expression was studied by qRT PCR in WT, $\Delta yeiL$, $\Delta nsrR$ and $\Delta yeiL\Delta nsrR$ strains, in presence and absence of NO generated by NONOate. As observed in figure 8B, induction of *hcp* expression was enhanced under NO exposure in both WT and $\Delta yeiL$ strains. In a $\Delta nsrR$ strain, the *hcp* expression was constitutively activated with around 400-fold more expression than in a wild type strain grown in LB. *hcp* expression was similar in a $\Delta nsrR\Delta yeiL$ and $\Delta nsrR$ mutants, indicating that there is no link between the regulatory activities of YeiL and NsrR on the *hcp* promoter.

Collectively these results showed that i) OxyR is a NO-dependent activator of *hcp* expression, ii) NsrR represses *hcp* expression and is sensitive to NO, and iii) YeiL is a repressor of *hcp* expression in the absence of OxyR.

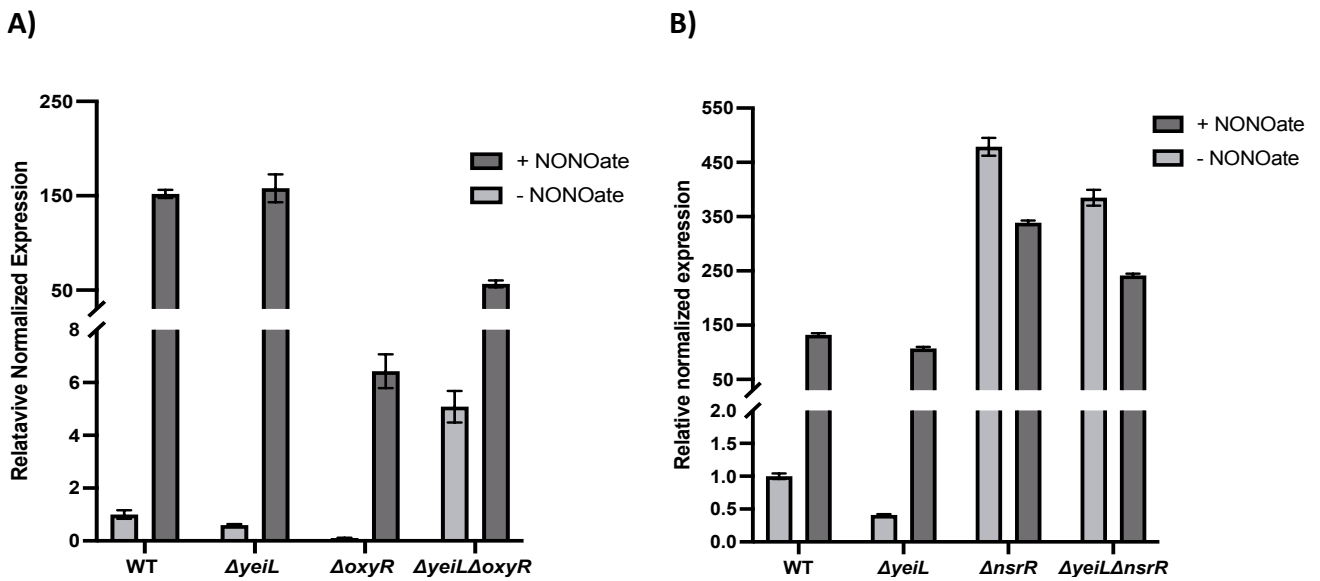
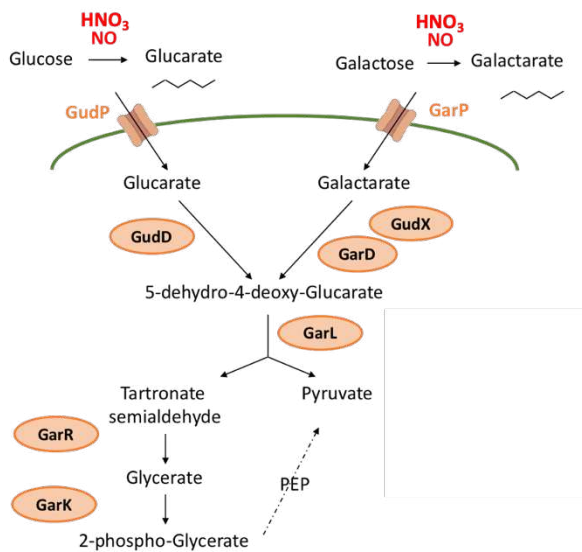


Figure 8. Study of *hcp* expression under NO exposure. Expression of *hcp* was measured by qRT-PCR with cDNA from indicated strains grown in LB at 37°C under agitation until $OD_{600nm} = 0.8$. Then NONOate was added. Cells were harvested after 30 min treatment. **(A)** *hcp* relative expression in MG1655 strain and $\Delta yeiL$, $\Delta oxyR$ and $\Delta yei\Delta oxyR$ derivatives. **(B)** *hcp* relative expression in MG1655 strain and $\Delta yeiL$, $\Delta nsrR$ and $\Delta yei\Delta nsrR$ derivatives.

I - 5 - Aldaric acid metabolism is repressed by Yeil

Aldaric acids are di-acid linear sugars. Conversion of aldoses to aldaric acids results from oxidation of aldoses by either nitric oxide (NO) or nitric acid (HNO_3) (Mehltretter *et al.* 1947, Faber *et al.* 2016). In our transcriptomic study we noticed that all the genes involved in the metabolism of aldaric acids (*gar* and *gud* genes) are downregulated (Fig.9 A and B). These genes are divided in 4 units of transcription, the *garPLRK* operon, the *gudPXD* operon, the *garD* gene and *cdaR* (Fig. 9C). CdaR is the only known activator of this pathway (Monterrubio *et al.* 2000).

A)



B)

Genes	YeiL	YeiL*
<i>cdaR</i>	0,415	0,202
<i>garD</i>	0,239	0,028
<i>garK</i>	0,219	0,046
<i>garL</i>	0,22	0,01
<i>garP</i>	0,222	0,003
<i>garR</i>	0,241	0,024
<i>gudD</i>	0,229	0,095
<i>gudP</i>	0,189	0,019
<i>gudX</i>	0,195	0,05

C)

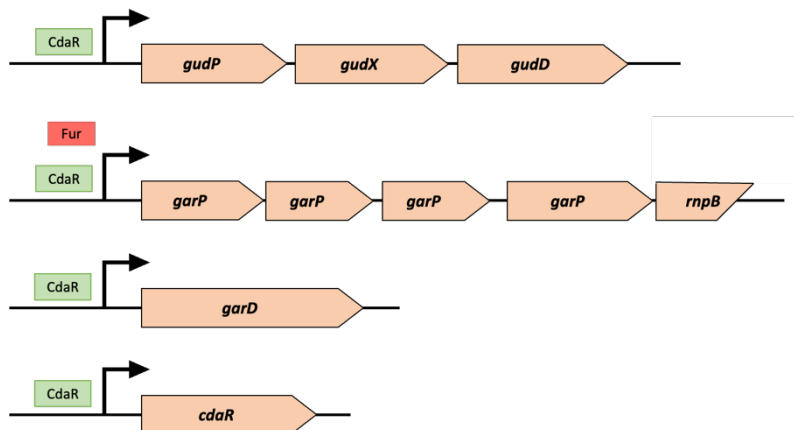


Figure 9. Aldaric acid metabolism is repressed by both YeiL and YeiL*. **A)** Aldaric acid catabolic pathway, all the genes highlighted are repressed by YeiL and YeiL*. **B)** Gene expression fold change from YeiL and YeiL* RNA-seq data sets. **C)** Aldaric acids metabolism genes genetic organization, known transcriptional regulators for these loci are indicated in green boxes for activators and red boxes for repressors.

Expression of *cdaR* was assessed by using a derivative of pUA66 with a transcriptional fusion between the *cdaR* promoter and the *gfp* gene. We showed that the *PcdaR-gfp* fusion is 2-3 times less expressed when overexpressing *yeiL* and *yeiL** compared to the control strain (Fig. 10, light grey bars). Since the transcription of all the *gar* and *gud* genes, as well as *cdaR* itself is activated by CdaR (Monterrubbio *et al.* 2000), we tested whether *cdaR* repression by YeiL was dependent on CdaR. In the $\Delta cdaR$ strain the production of YeiL or YeiL* did not affect

the expression of *cdaR* (Fig. 10, dark grey bars). Epistatic effect of the *cdaR* deletion shows that CdaR is required for YeiL to repress the expression of *cdaR* and probably the other genes of the pathway.

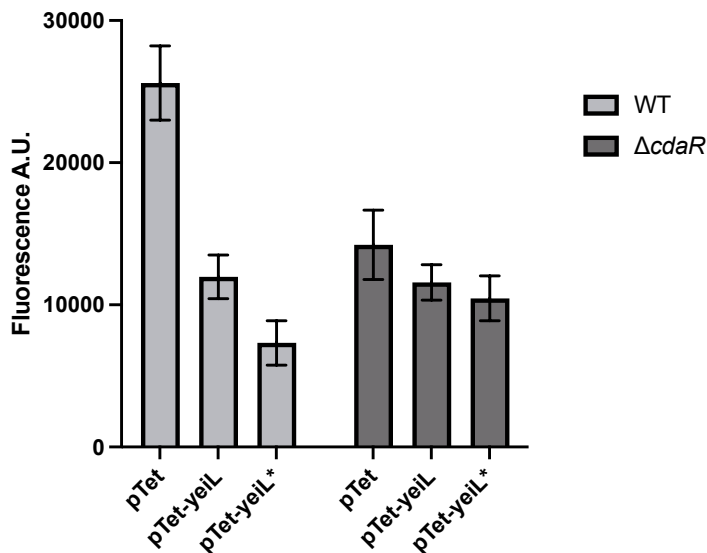


Figure 10. YeiL and YeiL* down-regulate *cdaR* expression. MG1655 and $\Delta cdaR$ strains carrying pUA66-*PcdaR-gfp* and either pTet, pTet-*yeiL* or pTet-*yeiL**. Strains were grown in LB-Kan-Amp with aTc 0.5 $\mu\text{g}/\text{mL}$ at 37°C under agitation. After 7 H of growth, activity of the promoter was determined by measuring fluorescence. Values are the mean of at least 4 biological replicates and standard errors to the means are indicated.

CdaR is the cognate activator of all the genes specifically involved in aldaric acids metabolism, and its activity is triggered in presence of the substrate, aldaric acids. It has been proposed that the CdaR is weakly produced under a regulatory inactive form and, upon aldaric acid exposure, there is a conformational activation of CdaR leading to activation of its own expression and in turn activation of aldaric acids metabolism genes (Monterrubbio *et al.* 2000). We tested the induction of genes of the pathway in presence of a non-limiting amount of aldaric acids (LB- galactarate 0.1%) in strains producing YeiL and YeiL*. Three transcriptional fusions were studied, *PgarD-gfp*, *PgudP-gfp* and *PcdaR-gfp* (pUA66 derivatives).

The expression of *cdaR* displays a 10-fold increase in the strain carrying the empty vector (pTet) when grown in LB supplemented with galactarate 0,1% compared to the LB medium (Fig. 11A). A similar effect is observed with the *gudP* and *garD* genes (Fig. 11 B and C). Production YeiL or YeiL* in presence of galactarate yields a 20-fold reduction in the levels of expression of *cdaR*, *garD* and *gudP* genes, almost abolishing induction of their expression by galactarate.

Therefore, the most likely mechanism for YeilL-dependent repression of aldaric acids metabolism genes is through the transcriptional repression of *cdaR* expression preventing responsiveness to aldaric acids.

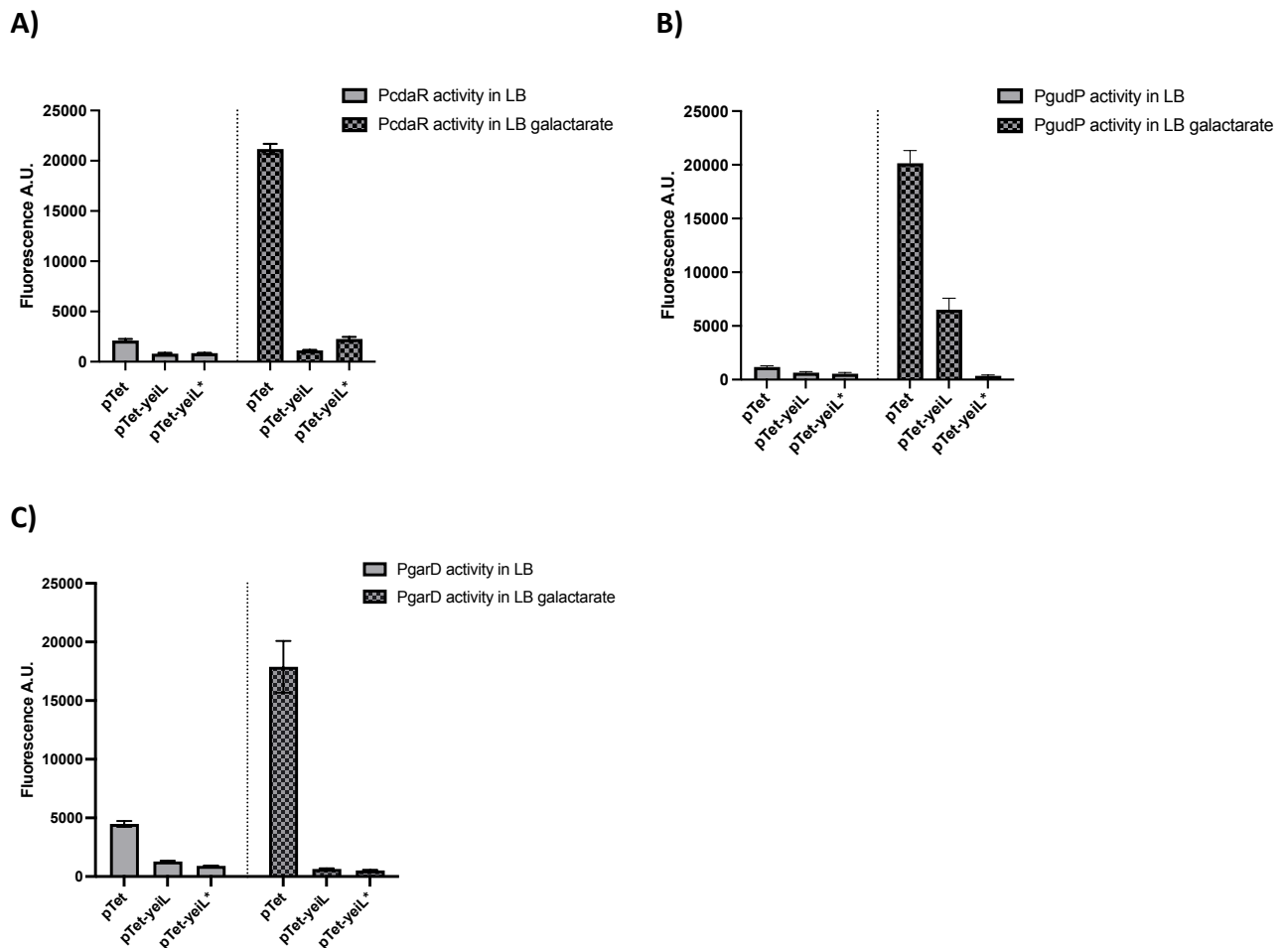


Figure 11. YeilL and YeilL* prevent aldaric acid induction. Strains carrying fusion between the promoter regions of *cdaR* (A) *gudP* (B) or *garD* (C) and *gfp* (pUA66 derivatives), and either pTet, pTet-*yeilL* or pTet-*yeilL** were grown in LB-Kan-Amp with aTc 0.5 $\mu\text{g}/\text{mL}$ supplemented or not with 0.1% of galactarate at 37°C under agitation. After 7H of growth, activity of the promoter was determined by measuring fluorescence. Values are the mean of at least 4 biological replicates and standard errors to the means are indicated.

I - 6 - Study of the YeiL direct regulon

We performed Electrophoretic Mobility Shift Assays (EMSA) to identify direct targets of YeiL. YeiL and YeiL* were purified with an MBP tag in order to help solubilize the protein (Fig. 12 A for MBP-YeiL* purification). We tested YeiL and YeiL* binding on two promoter regions localized in front of the *ynfE* and *ydhY* genes because they appeared amongst the more repressed genes in the RNA-seq data. Moreover, these genes were described to be regulated by FNR. As FNR and YeiL belong to the same family of regulators, binding control using purified FNR thus provided a positive control for the binding in the conditions used.

The promoter regions of *ynfE* and *ydhY* were amplified by PCR using primers marked with fluorescent dye (Cy55). Purified FNR D_{154A} (hereafter named FNR*, from E. Bouveret) was used as a DNA binding positive control because it contains a mutation that makes it more resistant to oxygen (Lazazzera *et al.* 1996).

Incubation of *ynfE* and *ydhY* promoter regions with MBP-YeiL or MBP-YeiL* did not lead to any band shift (Fig. 12B). On the contrary, incubation with FNR* led to a band shift indicating a binding of FNR* to both promoters (Fig. 12 B). Multiple attempts to optimize the conditions for visualizing a binding of YeiL or YeiL* were unsuccessful. We tested different conditions such as the use of YeiL and YeiL* untagged proteins (TEV site between MBP and YeiL), different protein/DNA ratio (10:1, 50:1, 100:1) or different buffers (NaH₂PO₄/Na₂HPO₄; KH₂PO₄/K₂HPO₄).

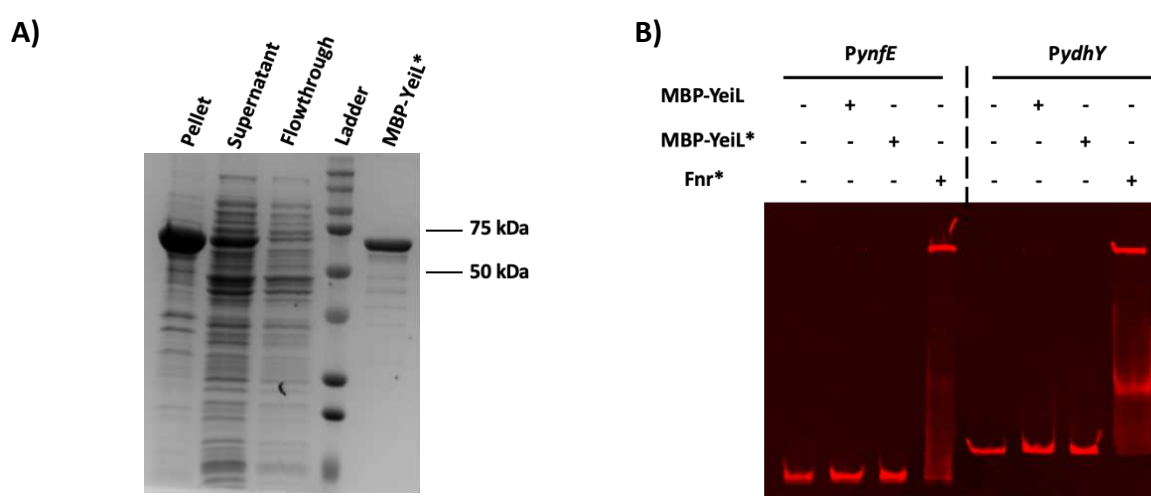


Figure 12. MBP-YeiL/YeiL* purification and EMSA experiments. A) SDS-PAGE analysis of MBP-YeiL* purification. **B)** EMSA using MBP-tagged purified YeiL and YeiL* and fluorescent (Cy55) labelled-probes corresponding to the *ynfE* and *ydhY* promoter regions. Binding reactions were performed as described in the Materials and Methods section using 1 pmol of DNA and 10 pmol of purified proteins.

I - 7 - Looking for the YeiL binding motif

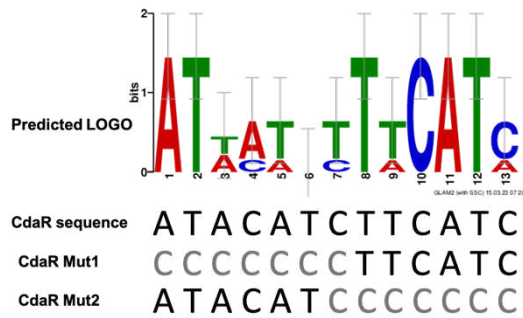
We set up an *in silico* approach based on alignment of promoter regions of YeiL-regulated genes to identify a potential YeiL binding site. We used the MEME suite website (GLAM2, <http://meme-suite.org>) to identify a potential binding motif shared by promoter of genes ranking amongst the most highly regulated in the YeiL and YeiL* RNA-seq data sets. Exclusion of FNR regulation was also taken as a criterion since YeiL belongs to the FNR/CRP family of regulators and FNR regulates around 20% of the genes regulated by YeiL and we wanted to avoid picking up the FNR binding site by such approach. The logo provided by the software was an imperfect inverted repeat ATACATCTTCATC (Fig. 13 A).

Two derivatives of the pUA66-*PcdaR-gfp* plasmid were constructed with replacement of the 6 first bases of the motif (CCCCCCTTCATC), called *PcdaR_Mut1*, and another with the 7 last (ATACATCCCCC), called *PcdaR_Mut2* (Fig. 13 A). pUA66 derivatives (with WT *cdaR* promoter, *PcdaR_Mut1* and *PcdaR_Mut2*) were co-transformed in *E. coli* with the empty pTet vector or carrying the *yeiL* and *yeiL** alleles.

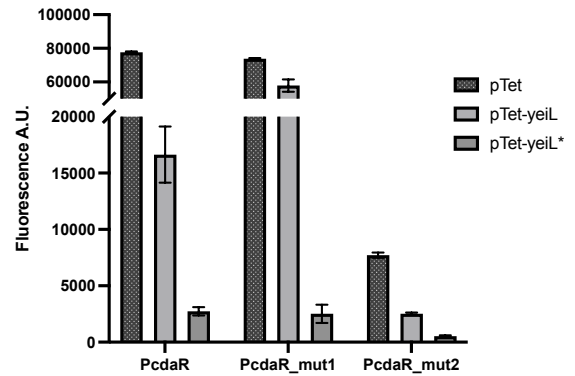
We compared the effect of YeiL and YeiL* production plasmids versus the empty vector on the *PcdaR* promoter and its mutated variants in presence of galactarate. YeiL, and to a higher extent YeiL*, repressed the activity of WT *PcdaR*. In contrast, YeiL failed to repress *PcdaR_Mut1* promoter while repression by YeiL* remained. Moreover, repression by both YeiL and YeiL* of *PcdaR_Mut2* was attenuated (Fig. 13 B). However, the activity of *PcdaR_Mut2* promoter was highly reduced compared to the wild type promoter. Therefore, we tested the effect of the CdaR activator on this modified promoter. Plasmids carrying *PcdaR-gfp* and *PcdaR_Mut2-gfp* were introduced in the wild type and the $\Delta cdaR$ strains. Inactivation of *cdaR* led to a huge decrease of the wild type promoter activity, whereas the expression from the *PcdaR_Mut2* mutated promoter was much lower and notably totally unresponsive to the presence of CdaR (Fig. 13 C).

Collectively these results suggested that YeiL binds directly *cdaR* promoter on the inverted repeat ATACATCTTCATC. Interestingly, YeiL was much more sensitive to sequence modification in this site than YeiL*, which is consistent with the notion that YeiL* is more active. We also identified a nucleotide stretch crucial for the CdaR auto-activation. The proximity between the YeiL and CdaR binding sites leads us to hypothesize that YeiL might affect the expression of *cdaR* by displacing the CdaR activator.

A)



B)



C)

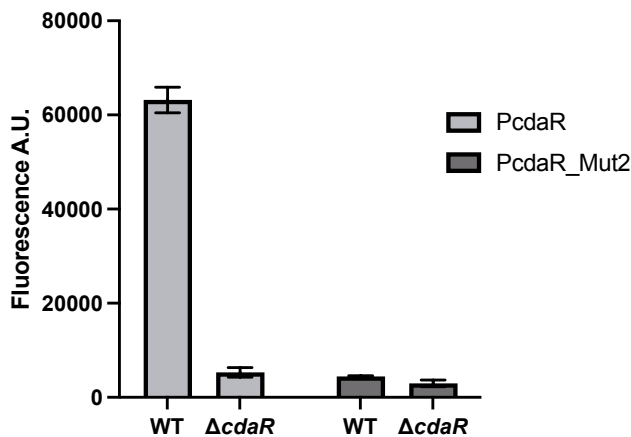


Figure 13. Identification of the Yeil and CdaR binding sites in the *cdar* promoter region. A) Selection of 4 Yeil and Yeil* highly repressed genes allowed to define a sequence motif logo using GLAM2 (MEME suite). Under the logo, sequence from the *cdar* promoter region (starting 85 bp upstream of the coding sequence) matching with the defined logo and sequences of the derived *Pcdar_Mut1* and 2. **B)** Fluorescence of MG1655 strain carrying pUA66-*Pcdar-gfp* and Mut1 and 2 derivatives and either pTet, pTet-*yeiL* or pTet-*yeiL**. **C)** Fluorescence of MG1655 and Δ *cdar* strains carrying pUA66-*Pcdar-gfp* and Mut2 derivative. Strains were grown in LB supplemented with galactarate 0.1%. Amp and aTc were added for strains carrying the pTet-derived plasmids. Values are the mean of at least 4 biological replicates and standard errors to the means are indicated.

I - 8 - YeiL has a positive impact on mice gut colonization

Work described above revealed that YeiL is involved in regulation of anaerobic respiration, NO defense and aldaric acids metabolism. NO production by inducible NO synthase (iNOS) is part of the innate immune response (for review see Ramachandran *et al.* 2018). Furthermore, in the inflamed gut, anaerobic respiration using nitrate, TMAO and DMSO as respiratory electrons acceptors is the main source of energy (for review see Winter *et al.* 2013). Last, aldaric acids are present in the gut, and it has been shown that the deletion of *gud* operon genes in *E. coli* UTI89 leads to a reduced gut colonization efficiency (Faber *et al.* 2016).

These prompted us to test whether YeiL could impact gut colonization efficiency of *E. coli*. For these experiments, we studied an uropathogenic *E. coli* (UPEC), UTI89, because prevalence of UTIs depends on the production of specific virulence factors that allow intestinal colonization and further migration into the urinary tract. Then intestinal colonization is an essential step for the virulence of this strain.

Colonization efficiency of a UTI89 $\Delta yeiL$ was tested in mice. First, growth of UTI89 and its $\Delta yeiL$ derivative were assessed in LB under aerobiosis. As shown in figure 14A, deleting *yeiL* in a UTI89 did not affect in vitro growth. In a first experiment, streptomycin-pretreated C57Bl/6 mice were orally infected with the WT UTI89 or its $\Delta yeiL$ derived strain. Bacterial load in feces was assessed at different days post infection. While bacterial loads were identical until 10 days post-infection (p.i.), at day 13th, the number of CFU from the $\Delta yeiL$ strain was 2 logs less than the WT, indicating a less efficient long-term colonization of the $\Delta yeiL$ strain (Fig. 14 B). Additionally, a competition index was determined during co-infection of the WT and the $\Delta yeiL$ strains. Comparably to the mono-infection experiment the two bacterial population evolved similarly at the beginning of the infection, but from 20 days p.i. the WT/ $\Delta yeiL$ ratio increased significantly, thus reinforcing the hypothesis that YeiL is beneficial for long term gut colonization (Fig. 14 C). These results are encouraging in providing an important role for YeiL. Evidently, it is difficult to pinpoint what genetic regulation exerted by YeiL entices this observation as multiple genes, whose expression is influenced by YeiL, could impact gut colonization. However, as a framework for future studies, aldaric acids metabolism, nitrate respiration, and NO stress response are good candidates to further explore. Next studies will aim at deciphering the genetic regulations involved in this phenotype.

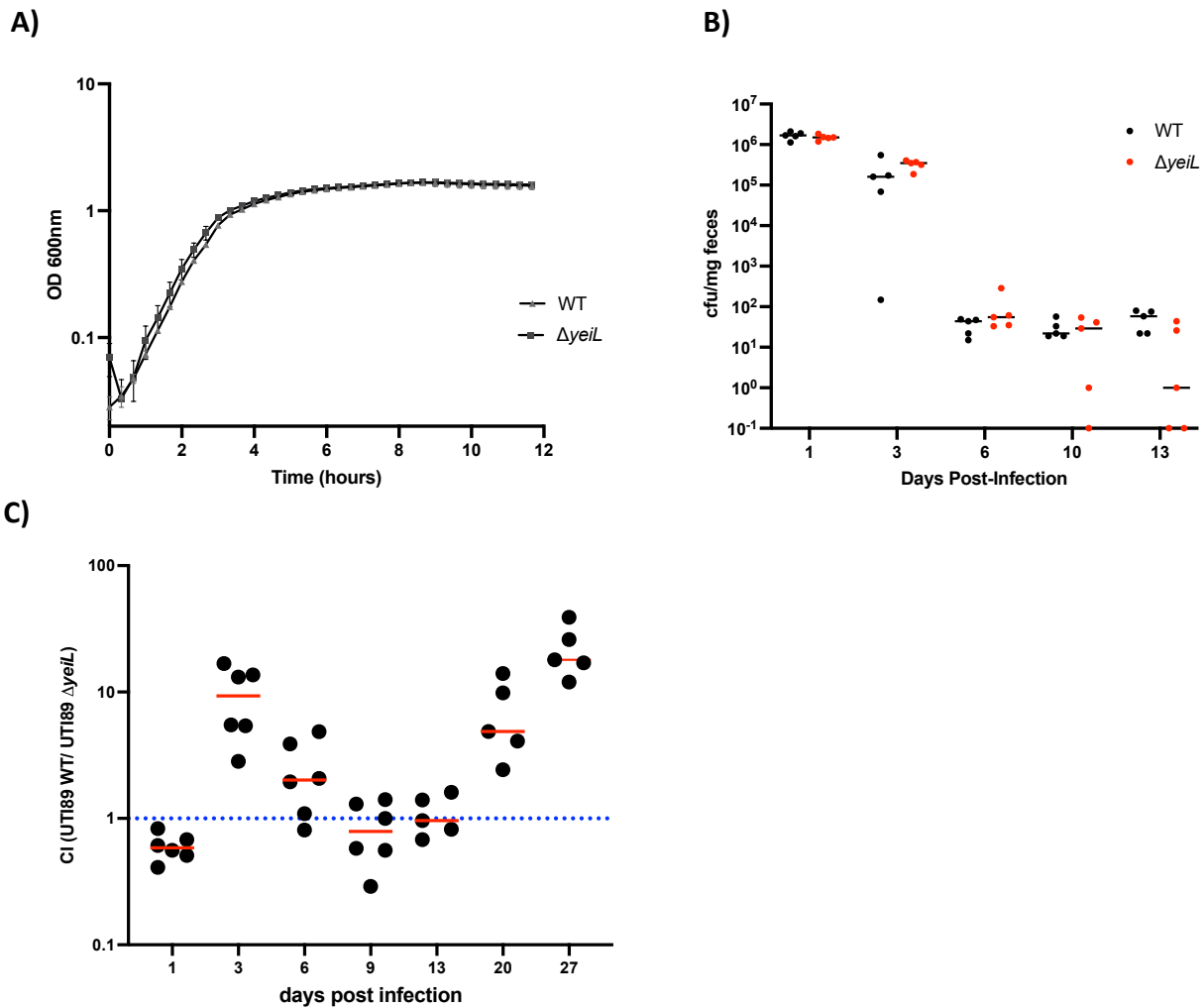


Figure 14. Yeil plays a role in gut colonization. **A.** Growth curves of the UT189 WT and UT189 Δ yeil in LB at 37°C under agitation. **B.** Streptomycin pre-treated C57BL/6 mice (5 for each group) were infected *per os* with 2×10^8 CFU of either UT189 WT strain (black dots) or its Δ yeil derivative (red dots). CFUs in fecal pellets were counted at indicated days post-infection. **C.** Streptomycin pre-treated C57BL/6 mice (6 mice) were infected *per os* with 2×10^8 CFU of a mix of UT189 WT strain and the Δ yeil::Cm derivative. CFUs in fecal pellets were counted at indicated days post-infection on LB plates (WT and Δ yeil::Cm strains) and LB-Cm plates (Δ yeil::Cm strain). The value of CI was calculated as: CFU WT output strain/CFU mutant output strain.

II - Study of the *yeiL* gene expression

II - 1 - *yeiL* is poorly expressed despite its active promoter

It has been previously published that YeiL is positively autoregulated, *i.e.* it activates its own expression (Anjum *et al.* 2000). MG1655 was co-transformed with pTet, pTet-*yeiL*, or pTet-*yeiL** and pUA66 in which *yeiL* promoter was cloned upstream the *gfp* gene. The cells were grown in LB until exponential phase (OD_{600nm} around 1) and the fluorescence was measured. Both YeiL and YeiL* down regulated 2-fold expression of the *yeiL* promoter (Fig. 15).

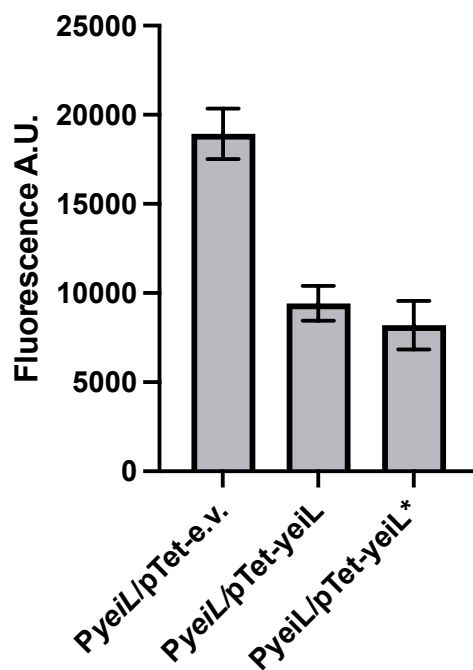


Figure 15. YeiL down-regulates its own expression. MG1655 strain bearing pUA66-PyeiL and either pTet, pTet-*yeiL* or pTet-*yeiL**. Cells were grown in LB-Kan-Amp in presence of aTc 0.5 µg/mL at 37°C under agitation until OD_{600nm} = 1. Fluorescence was measured to assess the activity of the *yeiL* promoter. Values are the mean of at least 4 biological replicates and standard errors to the means are indicated.

We were surprised by the high level of fluorescence emitted by the strains carrying the pUA66-PyeiL-*gfp*, which suggested that the *yeiL* gene was highly expressed. This was at odds with both the RNA-seq and qRT-PCR data, which showed *yeiL* was a poorly expressed if at all (see above). Furthermore, a global analysis of the *E. coli* transcription starts sites pinpointed *yeiL* amongst the least expressed genes in the *E. coli* genome (Thomason *et al.* 2015). In order to further study the *yeiL* expression, we constructed a chromosomal fusion between the *yeiL* promoter and *lacZ* (latter referred as Prom-fusion) (Fig. 16 A). A high level of β-galactosidase

activity, 4000 Miller units/mg of bacteria, was produced by this strain, indicating a very efficient promoter (Fig. 16 B). Two new gene fusions were constructed, referred to as Mid-fusion and Full-fusion. Mid-fusion was obtained by fusing a DNA fragment containing the promoter up to half of the *yeiL* coding sequence region in front of the *lacZ* gene. Full fusion was obtained by fusing a DNA fragment containing the full gene in front of the *lacZ* gene (Fig. 16 A). β -galactosidase activities of strains encoding either one of the fusions grown in LB were measured. Mid-fusion exhibited an activity similar to the Prom-fusion, however the Full-fusion showed a very low expression level (3 800 units for the Prom-fusion vs 93 units for the Full-fusion, see Fig. 16B). This indicated that a component located in the 3' region of the *yeiL* gene, in the last 330 bases of its coding sequence, was causing the loss of expression.

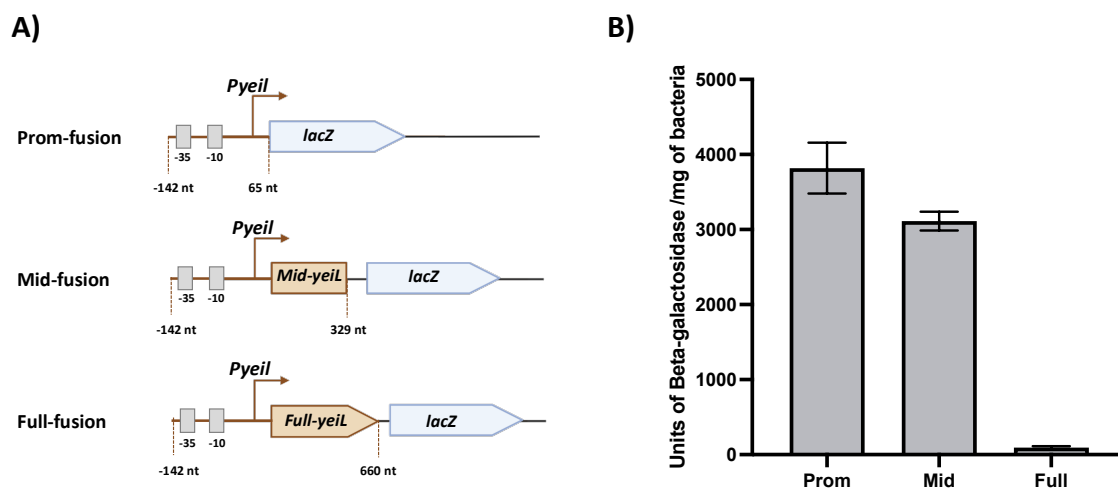


Figure 16. The determinant for *yeiL* low expression is present in its distal coding region. A) Scheme of the three constructed strains bearing chromosomal transcriptional fusions between: the promoter of *yeiL* (Prom-fusion), the promoter up to 329 nucleotides of the *yeiL* coding sequence (Mid-fusion), or the promoter and the full *yeiL* coding sequence (Full-fusion) fused to the *lacZ* gene. Coordinates are indicated in respect to the transcriptional start site. **B)** Activity of each fusion was determined by measuring the β -gal activity (Miller units) from cultures grown in LB at 37°C under agitation until $OD_{600nm} = 1$. Values are the mean of 3 biological replicates and standard errors to the means are indicated.

Detailed analysis of this region allowed the identification of a palindromic sequence located within the coding sequence, at the 3'end of the *yeiL* gene (nucleotides 626 to 648, Fig. 17 A). A plasmid containing the *yeiL* gene and its promoter (pAcyC-*yeiL*) and two derivatives carrying mutations disrupting the palindromic sequence by loss of pairing, were generated.

PalMut1 mutation alters amino acid sequence of YeiL but not PalMut2 (Fig. 17 A). A $\Delta yeiL$ strain was transformed with either pAcyC-*yeiL*, pAcyC-*yeiL*PalMut1 or pAcyC-*yeiL*PalMut2 and a qRT-PCR was performed to assess the relative level of *yeiL* expression.

Expression of mutated *yeiL* alleles was lower than from the wild type. This suggested that disrupting the palindromic sequence had opposite effects to those one could expect if it were to slow down transcription. Alternatively, the palindrome might be a binding site for a positive regulator acting in trans. In any case however, this region appears to be involved in *yeiL* expression (Fig. 17 B).

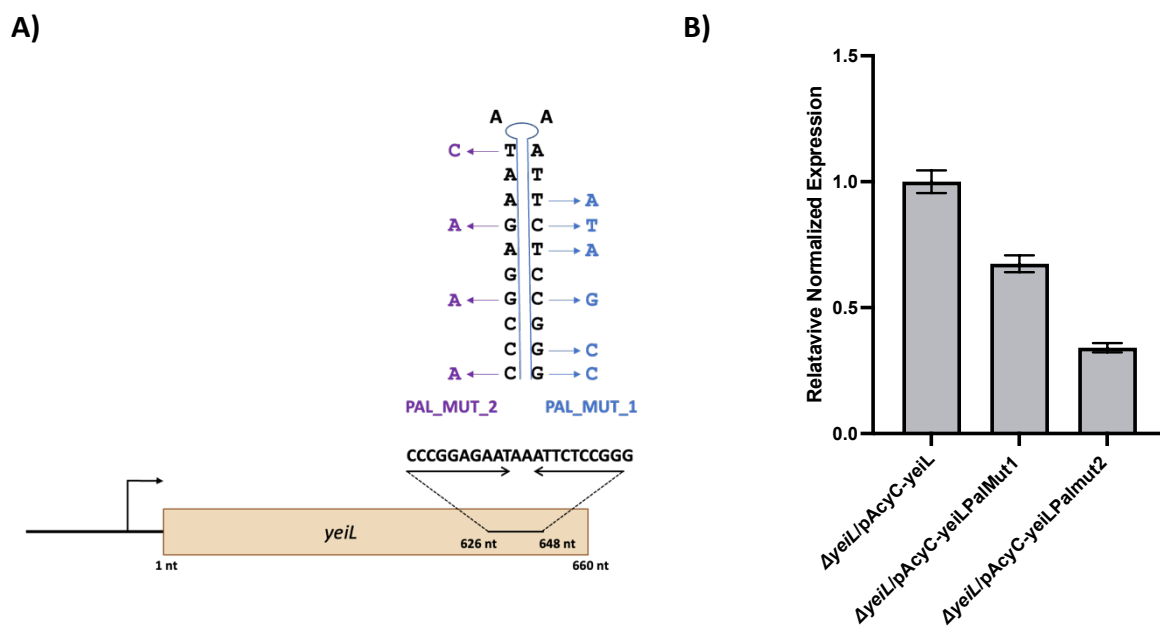


Figure 17. A palindromic sequence inside the *yeiL* coding sequence is involved in *yeiL* expression. A) A perfect palindromic sequence (N10xN10) is localized the end of the *yeiL* coding sequence; We substituted nucleotides of this palindromic sequence to generate *yeiL*PalMut1 (blue) and *yeiL*PalMut2 (purple), modifications are shown on the scheme. **B)** MG166 $\Delta yeiL$ strain carrying either pAcyC-*yeiL*, pAcyC-*yeiL*PalMut1 or pAcyC-*yeiL*PalMut2 were grown in LB-Cm at 37°C under agitation until OD_{600nm} = 1. Expression of *yeiL* and the mutated alleles was measured by qRT-PCR. Values are the mean of 4 technical replicates and standard errors to the means are indicated.

II - 2 - Set up of a suppressor approach to identify factors involved in *yeiL* expression control

We reasoned that if a protein (repressor, RNase...) is responsible for the low *yeiL* expression, any mutation abolishing its function could lead to a higher expression of *yeiL*. This led us to set up a suppressor approach. We used a growth screen of the Full *yeiL-lacZ* fusion strain on M9 medium supplemented with lactose. We checked that the strain carrying the Full *yeiL-lacZ* fusion produced insufficient levels of β -galactosidase to allow the use of lactose as the sole carbon source (Fig. 18 A). Any mutation allowing *yeiL* expression should lead to Full *yeiL-lacZ* fusion expression, production of β -galactosidase, and thus the ability to metabolize lactose and to grow on minimal medium supplemented with lactose.

The strain with the Full *yeiL-lacZ* fusion was grown until stationary growth phase in rich LB medium and after several washes, was plated on M9-lactose medium and let at 37°C until apparition of Lac⁺ colonies (frequency around 10⁻⁷). Twelve Lac⁺ colonies were kept for further analysis (Sup 1 to Sup 12, Fig. 18 B). We also checked that they showed blue color when grown on LB-Xgal plate (Fig. 18 C). Then we transduced a chromosomal SPA-tagged *yeiL* allele in each of the twelve suppressor strains and we performed a Western-blot to detect the YeiL-SPA fusion protein. Surprisingly no difference in YeiL-SPA production was observed between the wild type and any of the suppressors (Fig. 18 D). A whole genome sequencing analysis was performed (Eurofins Genomics Europe Sequencing GmbH) to compare the genomes of two independent suppressors to the parental strain. For both suppressors, we observed an amplification of the chromosomal region carrying the Full-fusion. Since no other significant modification between the parental strain and the suppressors was identified, we concluded that this genetic amplification was responsible, by its own, for the increase of the β -galactosidase activity.

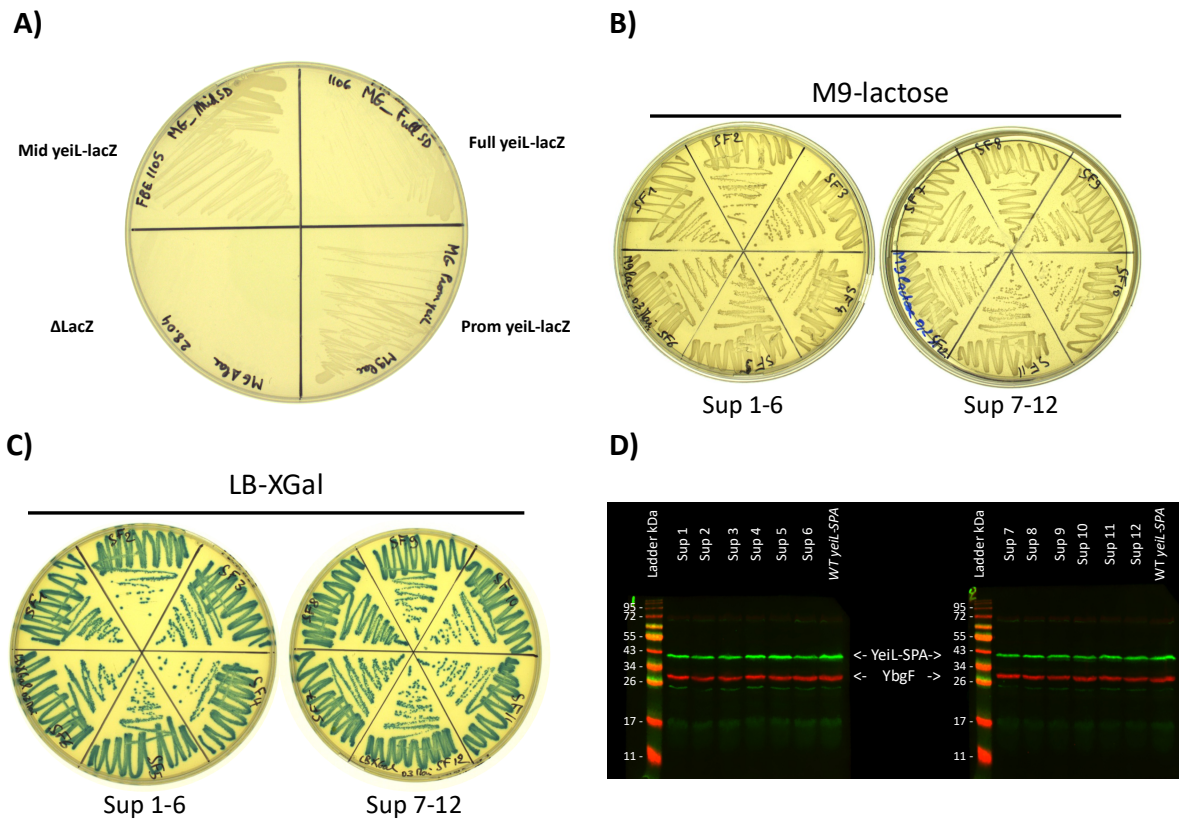


Figure 18. Screen of suppressors for *yeiL* expression determinants. **A)** Growth of strains carrying the chromosomal transcriptional fusions Prom *yeiL*-, Mid *yeiL*-, and Full *yeiL*-lacZ on M9-lactose plates. a Δ *lacZ* strain was plated as control. **B)** Selection of 12 suppressors of the Full *yeiL*-lacZ for their ability to grow on M9-lactose plates. **C)** Test of the 12 suppressors of the Full *yeiL*-lacZ for their ability metabolize X-Gal. **D)** YeiL-SPA was transduced in each of the suppressor strain by P1 transduction. Strains were grown in LB until $OD_{600nm} = 1$ before preparation of crude extracts. The MG1655 WT strain carrying the *yeiL-spa* fusion was included as a control. The level of *yeiL*-SPA in the cell was measured by Western-Blot using monoclonal anti-Flag antibody. YbgF was used as internal control and detected with polyclonal anti-YbgF antibody.

We have shown that our genetic approach allows to pick up potential suppressors for *yeiL* expression. New run of suppressors selection is needed to identify potential genetic determinants involved in *yeiL* expression.

II - 3 - Screening of conditions for YeiL production

In parallel to the suppressor approach above, different environmental conditions were tested for their effect on *yeiL* expression and/or YeiL production. We used YeiL-SPA protein fusion to detect any effect on protein production by Western-blot experiments and qRT-PCR to test effect on *yeiL* expression.

Surprisingly, production of the YeiL-SPA protein fusion could be detected by Western-blot (see Fig. 18). This contrasted with the fact that the *yeiL* gene expression was nearly undetectable (see above). Expression of the *yeiL* native gene and *yeiL-SPA* fusion gene were compared by qRT-PCR. The fusion gene is around 4-fold more expressed than the native *yeiL* gene (Fig. 19). This expression amplification is probably responsible for the YeiL-SPA detection by Western-blot.

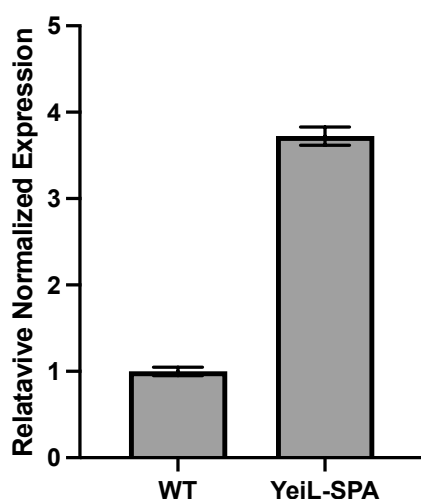


Figure 19. The SPA tag leads to increased *yeiL* mRNA steady state. MG1655 WT strain and its derivative bearing a *yeiL-spa* chromosomal fusion were grown in LB until $OD_{600nm} = 1$. Expression of wild type *yeiL* and *yeiL-spa* fusion was measured by qRT-PCR. Values are the mean of 4 technical replicates and standard errors to the means are indicated.

We showed that YeiL negatively regulates its own expression. As YeiL is predicted to be an Fe-S regulator, we wondered whether conditions that are known to perturb Fe-S homeostasis could affect *yeiL* expression. YeiL-SPA protein was equally produced in presence and absence of oxygen as well as after addition of paraquat (Fig. 20 A and B). Low iron availability is a limiting factor for Fe-S biogenesis and therefore is a limiting factor for Fe-S proteins maturation. Nonetheless, addition of dipyrldil (an iron chelator) to the growth medium did not impact the production of the YeiL-SPA protein (Fig. 20 B). Last, no induction of YeiL-SPA production under was observed NO exposure (Fig. 20 B). Absence of OxyR did not

modify *yeiL* expression (Fig. 21). Last, the quantity of YeiL-SPA seems identical without or with 0,1 and 1 % galactarate (Fig. 20).

To conclude, it then appears that none of these conditions, known to perturb Fe-S homeostasis, and none of the two pathways regulated by YeiL, have any effect on YeiL production.

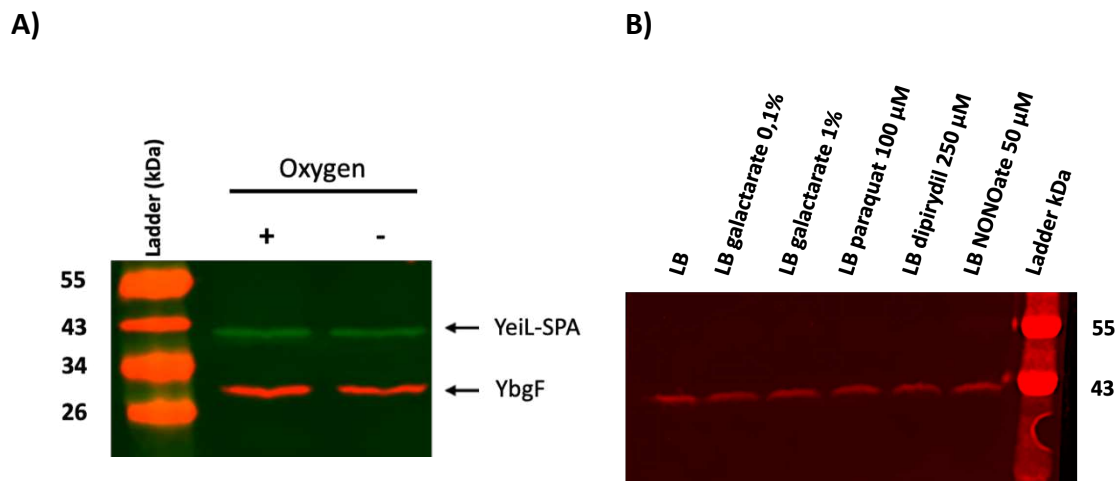


Figure 20. YeiL production is not changed upon exposure to Fe-S related stress or galactarate. Western-Blot detection of YeiL-SPA protein fusion using monoclonal anti-Flag antibody. YbgF was used as internal control and detected with polyclonal anti-YbgF antibody. **A)** MG1655 strain with the chromosomal *yeiL-spa* fusion was grown LB in presence or absence of oxygen at 37°C during 7 H before preparation of crude extracts. **B)** MG1655 strain with the chromosomal *yeiL-spa* fusion was grown LB supplemented by the indicated compounds at 37°C under agitation until $OD_{600nm} = 1.5$ before preparation of crude extracts.

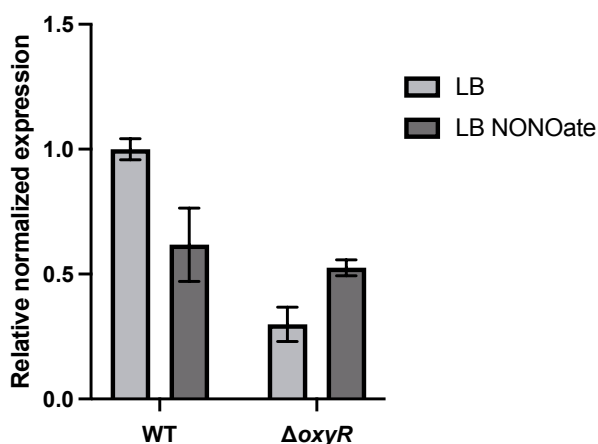


Figure 21. Expression of *yeiL* is not regulated by OxyR and nitric oxide. MG1655 WT strain and the $\Delta oxyR$ derivative were grown in LB at 37°C under agitation. Around $OD_{600nm} = 0.8$, NONOate was added (50 µM) or not (control condition) in the growth medium. After 30 minutes in presence of NONOate, cells were harvested, total RNA was extracted, and *yeiL* expression was measured by qRT-PCR. Values are the mean of 4 technical replicates and standard errors to the means are indicated.

Chapter II - Discussion

Iron-sulfur regulators have been largely studied and most of them are well characterized in *E. coli*. Surprisingly, while the YeiL regulator has been identified as an Fe-S regulator in 2000 yet its function has never been thoroughly studied or characterized (Anjum *et al.* 2000).

The *yeiL* gene is located inside a genomic locus dedicated to nucleotides/nucleosides metabolism. The region contains the *psuK*, *psuG* and *psuT* genes that encode proteins involved in pseudouridine catabolism, *rihB* that encodes a putative ribonucleoside hydrolase and *nupX* that encodes a putative nucleoside transporter. The first difficulty encountered in the study of YeiL function was its very low expression. We have tested expression of the genes surrounding *yeiL* (*psuK*, *nupX*, *rihB*) and none of them appeared to be expressed. We also noted that the *rihB* gene is essentially silent (Petersen *et al.* 2001). It thus appears that *yeiL* and surrounding genes are located in a silent locus. Both our experimental attempts and available transcriptomic data in the literature failed to provide environmental conditions that allow an enhanced *yeiL* expression. A new line of investigations aiming at testing the impact of specific nucleosides to turn on the expression of this locus is considered. We will also pursue our suppressor approach to identify the genetic determinants behind *yeiL* expression.

To circumvent the absence of *yeiL* expression, we adopted a strategy consisting of using an inducible promoter to drive *yeiL* expression. Since the cluster of Fe-S regulators play a major role in their activity, we compared the transcriptome of a strain expressing the wild type YeiL regulator and a strain expressing a YeiL variant, called YeiL*, lacking the Cys residues predicted to bind the Fe-S cluster. Overall, the expression of 699 genes was affected by YeiL* (355 up-regulated and 344 down-regulated) and 218 by YeiL (55 up-regulated and 163 down-regulated). The higher number of genes regulated by YeiL* as well as the stronger fold changes observed suggest that Apo-YeiL could display a regulatory activity. However, this observation does not disqualify Holo-YeiL from being active.

Amongst the major functions identified as YeiL and/or YeiL*-regulated, we noticed that anaerobic respiration was greatly represented. More specifically, 23 genes involved in nitrate respiration are either up- or down-regulated by YeiL*. Indeed, production of YeiL* leads to an increased expression of genes encoding cytoplasmic nitrate reductases (*narGHI* and *narVZY*)

and a decreased expression of genes encoding periplasmic nitrate and nitrite reductases (*nap* and *nrf* operons). We tested the effect of YeiL (using either Δ *yeiL* strain, or *yeiL/yeiL** expressing strains) under anaerobic nitrate respiring growth condition and we observed growth defect in none of these strains.

The nitrate reductase NarG has been shown to be responsible for nitric oxide (NO) release by non-specific reduction of nitrite (Vine *et al.* 2011, Vine *et al.* 2011, Rowley *et al.* 2012). YeiL induces the *narG* expression but has no effect on the expression of cytoplasmic nitrite reductase gene. We plan to measure the impact of the YeiL-dependent activation of cytoplasmic nitrate reductase genes on intracellular accumulation of nitrite. If YeiL favors intracellular nitrite accumulation, we hypothesize that it could lead to reduction of nitrite by NarG and then production of NO. We attempted to quantify NO production in condition of nitrate respiration using a NO fluorescent indicator compound (DAF-FM DA, 4-Amino-5-Methylamino-2',7'-Difluorofluorescein Diacetate) but it seemed that it was not enough sensitive to detect the low level of NO produced by bacterial cells.

NO is a protein-damaging compound that can react with accessible cysteine residues, leading to protein nitrosylation (SNO), or with metallic cofactors such as iron, leading to metal nitrosylation (MNO) (Toledo *et al.* 2012). These modifications are deleterious for proteins activities, and defense mechanisms are induced upon NO exposure. Unexpectedly, our data showed that YeiL has a negative effect on the expression of at least three genes involved in NO detoxification, *i.e.* the *hcp-hcr* operon and the *hmpA* gene. The *hcp-hcr* operon encodes the Hybrid-cluster protein (Hcp), a NO reductase, and its associated protein the Hybrid-cluster reductase (Hcr), whereas *hmpA* codes for a NO dioxygenase. We focused our analysis on *hcp-hcr* regulation network and showed that YeiL is a repressor of this operon and that YeiL negative regulation is abolished by the action of OxyR, an activator of *hcp-hcr* expression. Since YeiL negative regulation is only observable in the absence of OxyR we predict that OxyR and YeiL compete one with the other for binding to the *hcp* operator region. We plan to address this question by testing *in vitro* binding of YeiL, OxyR and eventual competition between both regulators to *hcp* promoter.

Finally, we noticed that a specific pathway, the aldaric acids metabolic pathway, was entirely down-regulated by YeiL and YeiL*. Aldaric acids are oxidized linear sugars and their metabolism depends on the activity of the Gar and Gud proteins. The genes encoding them are divided in three distinct transcriptional units that are all repressed by YeiL. The only

characterized regulator of this pathway is CdaR, a transcriptional activator responding to aldaric acids availability and activating the expression of all the genes of the aldaric acids pathway as well as its own expression. We showed that regulation of aldaric acids metabolism genes by YeiL goes through the down-regulation of *cdaR* expression. Moreover, we localized the CdaR and YeiL binding site in the *cdaR* promoter region. These two regulators bind on very closed sequences, suggesting that the binding of YeiL could prevent CdaR binding and/or remove the CdaR activator from the *cdaR* promoter region. This proposed mechanism is further supported by our experimental observations, *i.e.* a prevention of CdaR-dependent activation in presence of aldaric acids by overexpression of *yeiL*. We now plan to confirm the proposed sequences for YeiL and CdaR binding using EMSA. The competition between YeiL and CdaR will also be tested *in vitro*. If we obtain clear results with EMSA experiments, we will refine the YeiL binding site in order to characterize the YeiL direct regulon by looking for the binding site in the pool of YeiL-regulated genes.

The three functions we studied, nitrate respiration, NO stress response and aldarate metabolism are all involved in host colonization. Indeed, inside the inflamed gut, the low availability of oxygen as well as the presence of alternative terminal electron acceptors (mainly nitrate, DMSO and TMAO) favor anaerobic respiration. Moreover, host inflammatory response leads to NO formation which can lead to bacterial proteins damages, and oxidation of available sugars into aldaric acids (Faber *et al.* 2016). Aldaric acid utilization has been shown to favor gut colonization of mice by both *Salmonella enterica* and UPEC *E. coli* (Faber *et al.* 2016). We have shown that YeiL up-regulates cytoplasmic nitrate respiration but down-regulated NO stress response and aldaric acids metabolism genes. Hence, it was interesting to test whether YeiL could influence gut colonization. Our results support that UTI89 strain lacking YeiL is less efficient in long term colonization of the gut. Since NO stress response and aldaric acid metabolism favor gut colonization, it is unlikely that YeiL positive impact on gut colonization is due to YeiL regulation of these two pathways. While it is tempting to ascribe YeiL role in colonization to the positive impact on nitrate respiration, we must keep in mind that the sum of both YeiL and YeiL* regulated genes (provided by the transcriptomic approach) is of roughly 800 genes. It is therefore too early to identify the YeiL-regulated pathway(s) responsible for YeiL beneficial role in gut colonization.

While there is still much more to learn on YeiL regulation, we have provided in this study multiple leads for the full characterization of this Fe-S regulator.

Chapter II - Supplementary data

Supplementary Table 1: Lists of genes significantly regulated by YeiL (up- and down-regulated with P-values<0.05) and YeiL* (up- and down-regulated with Fc>3 and P-values<0.05). Genes are ordered by decreasing FC.

YeiL up-regulated genes

Name	Fc	P-value	Function
ibpB	5,47	1,07E-06	small_heat_shock_protein_IbpB
ibpA	4,376	1,50E-10	small_heat_shock_protein_IbpA
flu	3,596	3,00E-11	self_recognizing_antigen_43_(Ag43)_autotransporter
puuA	3,354	2,18E-05	glutamate-putrescine_ligase
yeeR	3,304	4,17E-09	CP4-44_prophage;_inner_membrane_protein_YeeR
mgIC	2,636	7,35E-06	D-galactose/methyl-galactoside_ABC_transporter_membrane_subunit
mgIA	2,629	9,52E-10	D-galactose/methyl-galactoside_ABC_transporter_ATP_binding_subunit
hdeA	2,624	1,40E-11	HdeA_monomer_chaperone_active_form
gadW	2,448	4,41E-08	DNA-binding_transcriptional_dual_regulator_GadW
nanA	2,337	1,82E-06	N-acetylneuraminate_lyase
gadX	2,184	5,16E-07	DNA-binding_transcriptional_dual_regulator_GadX
hdeD	2,096	0,00096412	acid-resistance_membrane_protein
hdeB	2,092	0,01488193	periplasmic_acid_stress_chaperone
metE	2,085	4,27E-06	cobalamin-independent_homocysteine_transmethylase
yeeD	2,031	0,00118006	putative_sulfurtransferase_YeeD
mgIB	1,981	0,00273744	D-galactose ABC transporter periplasmic binding protein
ybeD	1,978	0,01550506	DUF493_domain-containing_protein_YbeD
cysJ	1,926	0,00367149	sulfite_reductase,_flavoprotein_subunit
slp	1,911	0,00081738	starvation_lipoprotein
gadB	1,91	0,00328508	glutamate_decarboxylase_B
glsA	1,901	0,00029457	glutaminase_1
nanT	1,897	0,00041978	N-acetylneuraminate:H(+)_symporter
ybaT	1,897	0,00449216	putative_transporter_YbaT
gadA	1,891	0,02045019	glutamate_decarboxylase_A
yeiR	1,822	0,00447511	zinc-binding_GTPase_YeiR
yhcO	1,801	0,04817896	putative_barnase_inhibitor
ndk	1,78	0,00046811	nucleoside_diphosphate_kinase
thrA	1,766	0,00040689	fused_aspartate_kinase/homoserine_dehydrogenase_1
cysD	1,763	0,01858145	sulfate_adenyltransferase_subunit_2
cysI	1,71	0,04383357	sulfite_reductase,_hemoprotein_subunit
yhjY	1,695	0,02098205	conserved_protein_YhjY
csiD	1,672	0,00810481	PF08943_family_protein_CsiD
mlrA	1,67	0,03868682	DNA-binding_transcriptional_activator_MlrA
yeeE	1,668	0,03053344	inner_membrane_protein_YeeE
yidD	1,659	0,04938727	membrane_protein_insertion_efficiency_factor
ybjX	1,651	0,0049422	DUF535_domain-containing_protein_YbjX
sdiA	1,622	0,04938727	DNA-binding_transcriptional_dual_regulator_SdiA
queE	1,616	0,00844873	putative_7-carboxy-7-deazaguanine_synthase_QueE
galP	1,61	0,02523588	galactose:H(+)_symporter
mgo	1,592	0,01296226	malate:quinone_oxidoreductase
rstB	1,589	0,02952446	sensory_histidine_kinase_RstB

ygiV	1,575	0,03721551	DNA-binding_transcriptional_repressor_YgiV
rlmE	1,559	0,01033793	23S_rRNA_2'-O-ribose_U2552_methyltransferase
degP	1,556	0,00745212	periplasmic_serine_endoprotease_DegP
gcd	1,55	0,03883935	quinoprotein_glucose_dehydrogenase
yqjC	1,549	0,01057158	DUF1090_domain-containing_protein_YqjC
can	1,545	0,00982744	carbonic_anhydrase_2
ampH	1,536	0,03484436	peptidoglycan_DD-carboxypeptidase/peptidoglycan_DD-endopeptidase
clcA	1,532	0,03610266	chloride:H(+)_antiporter_ClcA
atpH	1,529	0,01666144	ATP_synthase_F1_complex_subunit_delta
bcp	1,525	0,01057158	thiol_peroxidase
guaC	1,504	0,01548615	GMP_reductase
ytfK	1,481	0,0174362	stringent_response_modulator_YtfK
malk	1,459	0,01811753	maltose_ABC_transporter_ATP_binding_subunit
proW	1,434	0,03868682	glycine_betaine_ABC_transporter_membrane_subunit_ProW

YeiL down-regulated genes

Name	Fc	P-value	Function
gudP	0,189	2,43E-39	galactarate/glucarate/glycerate_transporter_GudP
gudX	0,195	9,86E-37	glucarate_dehydratase-related_protein
garK	0,219	2,80E-33	glycerate_2-kinase_1
garL	0,22	1,35E-33	alpha-dehydro-beta-deoxy-D-glucarate_aldolase
garP	0,222	8,99E-36	galactarate/glucarate/glycerate_transporter_GarP
gudD	0,229	9,25E-24	D-glucarate_dehydratase
garD	0,239	2,80E-33	galactarate_dehydratase
garR	0,241	1,08E-28	tartronate_semialdehyde_reductase
glcD	0,243	5,64E-13	glycolate_dehydrogenase,_putative_FAD-linked_subunit
glcE	0,266	3,90E-08	glycolate_dehydrogenase,_putative_FAD-binding_subunit
dhaR	0,308	1,56E-13	DNA-binding_transcriptional_dual_regulator_DhaR
tdcE	0,322	6,33E-15	2-ketobutyrate_formate-lyase/pyruvate_formate-lyase_4
glcA	0,342	0,00071735	glycolate/lactate:H(+)_symporter_GlcA
glcB	0,344	2,20E-08	malate_synthase_G
ydeN	0,352	7,58E-07	putative_sulfatase
yjiY	0,358	3,46E-05	pyruvate:H+ symporter
yqfA	0,359	3,39E-10	hemolysin-III_family_protein
tdcD	0,364	3,00E-11	propionate_kinase
tdcC	0,368	9,44E-13	threonine/serine:H(+)_symporter
glcG	0,375	0,00018163	putative_heme-binding_protein_GlcG
tdcB	0,389	8,92E-08	catabolic_threonine_dehydratase
srlA	0,39	6,73E-13	sorbitol-specific_PTS_enzyme_IIC2_component
srlE	0,397	8,60E-12	sorbitol-specific_PTS_enzyme_IIBC1_component
tdcG	0,398	0,00038489	L-serine_deaminase_III
ygfK	0,399	0,00033503	putative_oxidoreductase,_Fe-S_subunit
adiY	0,41	0,00038489	DNA-binding_transcriptional_activator_AdiY
cdaR	0,415	5,24E-10	DNA-binding_transcriptional_activator_CdaR
serW	0,442	0,00013777	tRNA-Ser(GGA)
glyV	0,449	9,11E-05	tRNA-Gly(GCC)
srlM	0,454	0,00029457	DNA-binding transcriptional activator GutM
yjhQ	0,455	0,00089072	putative_acetyltransferase_TopAI_antitoxin_YjhQ
serX	0,46	0,00038489	tRNA-Ser(GGA)
glyY	0,465	0,00033121	tRNA-Gly(GCC)
tdcF	0,473	0,00976271	putative_enamine/imine_deaminase
srlB	0,475	3,33E-05	sorbitol-specific_PTS_enzyme_IIA_component
nirD	0,48	4,32E-07	nitrite_reductase_subunit_NirD
glyX	0,481	0,00071735	tRNA-Gly(GCC)
glcF	0,485	0,00075451	glycolate_dehydrogenase,_putative_iron-sulfur_subunit
nirC	0,489	7,58E-06	nitrite_transporter_NirC
prIF	0,49	0,00018566	antitoxin_PrIF
wbbJ	0,494	0,02989975	putative_acyl_transferase
glpT	0,495	0,0001507	sn-glycerol_3-phosphate:phosphate_antiporter
uxaC	0,499	9,22E-06	D-gluconate/D-galacturonate_isomerase
ydhV	0,499	0,00563993	putative_oxidoreductase

ykgR	0,51	0,02842868	putative_membrane_protein_YkgR
exuT	0,513	0,00054239	hexuronate_transporter
fnrS	0,515	4,17E-05	small_regulatory_RNA
hokB	0,516	0,00010198	toxin_HokB
yjhP	0,516	0,00468683	KpLE2_phage-like_element;_putative_methyltransferase_YjhP
ynfE	0,517	0,00431275	putative_selenate_reductase_YnfE
napG	0,518	0,00110844	ferredoxin-type_protein_NapG
dmsC	0,526	0,00367149	dimethyl_sulfoxide_reductase_subunit_C
raiA	0,528	2,88E-05	stationary_phase_translation_inhibitor_and_ribosome_stability_factor
dmlA	0,531	0,01666144	D-malate/3-isopropylmalate_dehydrogenase
yjiT	0,532	0,00037741	putative_uncharacterized_protein_YjiT
entF	0,536	0,00040689	apo-serine_activating_enzyme
uxaB	0,537	0,00040375	tagaturonate_reductase
wbbL	0,539	0,04959872	interrupted_rhamnosyltransferase
nrfB	0,542	0,00315235	periplasmic_nitrite_reductase_penta-heme_c-type_cytochrome
ryfD	0,547	8,57E-05	small_regulatory_RNA
ryeA	0,552	0,00078039	small_antisense_RNA
narI	0,553	0,00276442	nitrate_reductase_A_subunit_gamma
putA	0,553	0,00879618	fused_DNA-binding/_proline_dehydrogenase/1-pyrroline-5
yehH	0,553	0,00451512	stress-induced_protein
ykgE	0,553	3,99E-05	putative_lactate_utilization_oxidoreductase_YkgE
napH	0,559	0,01057158	ferredoxin-type_protein_NapH
yqeB	0,559	0,0013839	XdhC-CoxI_family_protein_YqeB
gatZ	0,56	0,01490751	tagatose-1,6-bisphosphate_aldolase_2_subunit_GatZ
tnaA	0,563	3,37E-05	tryptophanase
feoC	0,564	0,00093965	ferrous_iron_transport_protein_FeoC
yeiQ	0,567	0,01296226	putative_dehydrogenase,_NAD-dependent
ynfF	0,568	0,02989975	putative_selenate_reductase_YnfF
ykgG	0,569	0,00154776	DUF162_domain-containing_lactate_utilization_protein_YkgG
mntS	0,571	0,00154776	small_protein_MntS
ompF	0,572	8,34E-05	outer_membrane_porin_F
dmsB	0,574	0,002956	dimethyl_sulfoxide_reductase_subunit_B
yjhX	0,577	0,03175247	toxin_of_the_TopAI-YjhQ_toxin-antitoxin_system_TopA
wzxB	0,578	0,04817896	polyisoprenol-linked_O16-antigen_repeat_unit_flippase
ftnA	0,581	0,02006237	ferritin_iron_storage_protein
fucP	0,585	0,03205673	L-fucose:H(+)_symporter
ydchH	0,585	0,00445551	protein_YdchH
zntA	0,586	0,00062708	Zn(2+)/Cd(2+)/Pb(2+)_exporting_P-type_ATPase
entB	0,589	0,03452887	enterobactin_synthase_component_B
narJ	0,589	0,00273744	nitrate_reductase_1_molybdenum_cofactor_assembly_chaperone
uxaA	0,59	0,00448483	D-altronate_dehydratase
ykgF	0,593	0,00062708	putative_amino_acid_dehydrogenase
narH	0,594	0,00037741	nitrate_reductase_A_subunit_beta
gcvB	0,595	0,00542957	small_regulatory_RNA_GcvB
glpF	0,595	0,00356122	glycerol_facilitator
ansB	0,596	0,0003511	L-asparaginase_2
metY	0,601	0,01666144	tRNA-initiator_Met(CAU)
napA	0,601	0,00071639	periplasmic_nitrate_reductase_subunit_NapA
ompW	0,601	0,00105823	outer_membrane_protein_W
nrfA	0,603	0,00081738	cytochrome_c552_nitrite_reductase
putP	0,609	0,03259556	proline:Na(+)_symporter
nirB	0,611	0,00071735	nitrite_reductase_catalytic_subunit_NirB
nmpC	0,613	0,00879197	putative_outer_membrane_porin_NmpC
srlD	0,613	0,00157231	sorbitol-6-phosphate_2-dehydrogenase
bssR	0,615	0,00977004	regulator_of_biofilm_formation
pgaA	0,617	0,01809858	poly-beta-1,6-N-acetyl-D-glucosamine_outer_membrane_porine
adhE	0,618	0,00110844	aldehyde-alcohol_dehydrogenase
ffs	0,62	0,00875043	signal_recognition_particle_4.5S_RNA
cysG	0,621	0,00448483	siroheme_synthase
feoA	0,621	0,00195345	ferrous_iron_transport_protein_A
sibA	0,624	0,03259556	small_RNA_SibA
ydhR	0,624	0,00972516	putative_monooxygenase_YdhR
cstA	0,625	0,01666144	carbon_starvation_protein_A

gatY	0,625	0,01491536	tagatose-1,6-bisphosphate_aldolase_2_subunit_GatY
yfcZ	0,626	0,00170535	DUF406_domain-containing_protein_YfcZ
glnX	0,628	0,01134633	tRNA-Gln(CUG)
atoC	0,629	0,02590909	ornithine_decarboxylase_inhibitor
sibD	0,629	0,01165068	small RNA SibD
feoB	0,63	0,00187707	Fe(2(+))_transporter_FeoB
serV	0,632	0,0136604	tRNA-Ser(GCU)
ssrS	0,634	0,00671255	6S RNA
uspF	0,635	0,00374638	nucleotide_binding_filament_protein
oppA	0,638	0,01293048	oligopeptide_ABC_transporter_periplasmic_binding_protein
ycbJ	0,638	0,00448483	putative_phosphotransferase_YcbJ
fdhF	0,643	0,00848726	formate_dehydrogenase_H
agp	0,644	0,00451512	glucose-1-phosphatase
atoS	0,648	0,0302479	sensory_histidine_kinase_AtoS
fhuA	0,648	0,00634004	ferrichrome_outer_membrane_transporter/phage_receptor
glgS	0,65	0,03205673	surface_composition_regulator
manX	0,651	0,00529039	mannose-specific_PTS_enzyme_IIB_component
csrB	0,652	0,00508759	small regulatory RNA CsrB
uspE	0,654	0,00556541	universal_stress_protein_with_a_role_cellular_motility
yqeC	0,654	0,03868682	uncharacterized_protein_YqeC
frdB	0,656	0,00607851	fumarate_reductase_iron-sulfur_protein
ndh	0,657	0,01561152	NADH:quinone_oxidoreductase_II
dmsA	0,66	0,00812204	dimethyl_sulfoxide_reductase_subunit_A
nagE	0,662	0,00791843	N-acetylglucosamine_specific_PTS_enzyme_IIBC_component
hyaA	0,663	0,02002229	hydrogenase_2_iron-sulfur_protein
ydjA	0,663	0,01947406	putative_oxidoreductase
frdC	0,664	0,02002229	fumarate_reductase_membrane_protein_FrdC
cydB	0,667	0,00982744	cytochrome_bd-I_ubiquinol_oxidase_subunit_II
manY	0,667	0,00913902	mannose-specific_PTS_enzyme_IIC_component
yqhD	0,669	0,01852877	NADPH-dependent_aldehyde_reductase_YqhD
ftnB	0,673	0,02774375	putative_ferritin-like_protein
ygjR	0,673	0,02006237	putative_oxidoreductase_YgjR
glnV	0,675	0,04636823	tRNA-Gln(CUG)
hisR	0,678	0,03452887	tRNA-His(GUG)
hypB	0,682	0,02114546	hydrogenase_isoenzymes_nickel_incorporation_protein_HypB
narG	0,682	0,01463916	nitrate_reductase_A_subunit_alpha
glk	0,683	0,02064021	glucokinase
ypfM	0,686	0,01947406	uncharacterized_protein_YpfM
hypD	0,687	0,03247189	Fe-(CN)2CO_cofactor_assembly_scaffold_protein_HypD
hyaO	0,689	0,03053344	hydrogenase_2_small_subunit
moaB	0,689	0,04817896	MoaB_protein
ygdH	0,69	0,02045023	nucleotide 5'-monophosphate_nucleosidase_PpnN
sseA	0,692	0,02500378	3-mercaptopyruvate_sulfurtransferase
tdcA	0,693	0,03013306	DNA-binding_transcriptional_activator_TdcA
nagB	0,695	0,04962024	glucosamine-6-phosphate_deaminase
rihC	0,695	0,03247189	ribonucleoside_hydrolase_RihC
mgsA	0,697	0,0416446	methylglyoxal_synthase
lrhA	0,699	0,04374146	DNA-binding_transcriptional_dual_regulator_LrhA
aphA	0,702	0,04208313	acid_phosphatase/phosphotransferase
sodB	0,705	0,03736997	superoxide_dismutase_(Fe)
dcuA	0,71	0,0414845	C4-dicarboxylate_transporter_DcuA
dtpB	0,71	0,04739456	dipeptide/tripeptide:H(+)_symporter_DtpB
pck	0,71	0,0435277	phosphoenolpyruvate_carboxykinase_(ATP)
rnpB	0,711	0,04856034	RNase P catalytic RNA componen
clpA	0,715	0,04560869	ATP-dependent_Clp_protease_ATP-binding_subunit_ClpA
fdoG	0,717	0,04938727	formate_dehydrogenase_O_subunit_alpha

YeIL* up-regulated genes

Name	Fc	P-value	Function
ythA	232,962	5,74E-10	KpLE2_phage-like_element;_uncharacterized_protein_YthA
ariR	192,195	3,01E-46	regulator_of_acid_resistance,_influenced_by_indole
ymgC	178,34	2,90E-63	protein_YmgC
nrdH	155,978	1,36E-81	glutaredoxin-like_protein
ymgA	151,836	2,77E-61	putative_two-component_system_connector_protein_YmgA
yjhB	150,595	1,26E-113	putative_sialic_acid_transporter
ycgZ	135,163	6,38E-17	putative_two-component_system_connector_protein_YcgZ
yjhC	98,458	4,01E-59	KpLE2_phage-like_element;_putative_oxidoreductase_YjhC
entC	90,64	9,57E-91	isochorismate_synthase_EntC
nrdI	64,29	9,25E-103	dimanganese-tyrosyl_radical_cofactor_maintenance_flavodoxin_NrdI
kdpF	57,529	7,97E-05	K(+)_transporting_P-type_ATPase_subunit_KdpF
ibpB	57,334	4,68E-228	small_heat_shock_protein_ibpB
fhuF	52,274	9,13E-152	hydroxamate_siderophore_iron_reductase
uidC	52,259	5,02E-157	outer_membrane_porin_family_protein
uidB	42,158	3,31E-164	glucuronide:H(+)_symporter
ibpA	38,842	8,67E-296	small_heat_shock_protein_ibpA
betT	34,062	1,85E-92	choline:H(+)_symporter
lldP	33,871	1,12E-63	lactate/glycolate:H(+)_symporter_LldP
bfd	33,525	2,92E-77	bacterioferritin-associated_ferredoxin
uidA	31,515	3,72E-126	beta-glucuronidase
efeU	30,659	5,32E-56	inactive ferrous iron permease
fes	30,367	8,63E-55	enterochelin_esterase
nanA	30,176	1,38E-188	N-acetylneuraminatase_lyase
ybdZ	28,499	1,95E-10	enterobactin_biosynthesis_protein_YbdZ
nrdE	27,907	4,25E-170	ribonucleoside-diphosphate_reductase_2_subunit_alpha
betI	27,389	2,27E-188	DNA-binding_transcriptional_repressor_BetI
betA	26,788	1,11E-144	choline_dehydrogenase
betB	26,566	4,39E-112	betaine_aldehyde_dehydrogenase
astC	23,071	2,50E-68	succinylornithine_transaminase
mgo	23,031	2,17E-70	malate:quinone_oxidoreductase
efeO	22,432	8,04E-114	ferrous_iron_transport_system_protein_EfeO
ybeD	22,022	9,96E-200	DUF493_domain-containing_protein_YbeD
fepD	19,909	3,81E-55	ferric_enterobactin_ABC_transporter_membrane_subunit_FebD
gcd	18,941	1,07E-174	quinoprotein_glucose_dehydrogenase
astA	18,517	1,42E-74	arginine_N-succinyltransferase
yojI	18,072	3,93E-78	ABC_transporter_family_protein/microcin_J25_efflux_protein
kdpA	17,813	1,55E-53	K(+)_transporting_P-type_ATPase_subunit_KdpA
narK	17,565	4,44E-10	nitrate:nitrite_antipporter_NarK
nrdF	17,562	2,08E-130	ribonucleoside-diphosphate_reductase_2_subunit_beta
narG	17,154	8,66E-09	nitrate_reductase_A_subunit_alpha
fepC	16,715	8,61E-38	ferric_enterobactin_ABC_transporter_ATP_binding_subunit
yncE	16,232	2,84E-121	PQQ-like_domain-containing_protein_YncE
rspB	15,876	2,05E-92	putative_zinc-binding_dehydrogenase_RspB
nanC	15,735	4,75E-47	N-acetylneuraminic_acid_outer_membrane_channel
lldR	15,162	8,02E-111	DNA-binding_transcriptional_dual_regulator_LldR
ydfK	14,711	1,60E-20	Qin_prophage;_cold_shock_protein_YdfK
entS	14,549	9,21E-45	enterobactin_exporter_EntS
nanT	14,077	7,87E-135	N-acetylneuraminatase:H(+)_symporter
entE	13,93	1,23E-93	2,3-dihydroxybenzoate-AMP_ligase
sodA	13,747	2,16E-66	superoxide_dismutase_(Mn)
ynaE	13,262	1,28E-23	Rac_prophage;_uncharacterized_protein_YnaE
oweS	13,079	0,01814851	putative defective phage replication protein O
dnaK	12,896	1,71E-251	chaperone_protein_DnaK
hslV	12,809	2,92E-185	peptidase_component_of_the_HslVU_protease
ycjF	12,279	1,81E-87	conserved_inner_membrane_protein_YcjF
fecl	12,233	9,37E-122	RNA_polymerase_sigma_factor_Fecl
csiD	12,087	8,82E-75	PF08943_family_protein_CsiD
hslU	11,853	6,40E-206	ATPase_component_of_the_HslVU_protease
micC	11,662	0,0201943	small regulatory RNA MicC

ugpA	11,638	1,54E-14	sn-glycerol_3-phosphate_ABC_transporter_membrane_subunit_UgpA
rspA	11,49	3,40E-76	mandelate_racemase/muconate_lactonizing_enzyme_family_protein
ycjX	11,267	1,01E-75	DUF463_domain-containing_protein_YcjX
fxsA	11,189	7,36E-64	protein_FxsA
fepB	10,913	4,37E-44	ferric_enterobactin_ABC_transporter_periplasmic_binding_protein
gabT	10,839	9,91E-91	4-aminobutyrate_aminotransferase_GabT
astD	10,833	6,26E-80	aldehyde_dehydrogenase
gabD	10,131	3,26E-105	NADP(+)-dependent_succinate-semialdehyde_dehydrogenase
efeB	10,102	2,60E-81	heme-containing_peroxidase/deferrochelatase
dnaJ	10,093	5,54E-164	chaperone_protein_DnaJ
yeaR	10,054	1,40E-37	DUF1971_domain-containing_protein_YeaR
gabP	9,866	1,05E-84	4-aminobutyrate:H(+)_symporter
yjhD	9,791	7,28E-42	KpLE2 phage-like element; surface adhesin E-like protein
exbB	9,768	7,40E-63	Ton_complex_subunit_ExbB
acs	9,602	1,20E-55	acetyl-CoA_synthetase_(AMP-forming)
yncH	9,54	3,03E-05	DUF5445_domain-containing_protein_YncH
lhgO	9,506	1,83E-79	L-2-hydroxyglutarate_oxidase
dadA	9,498	6,72E-46	D-amino_acid_dehydrogenase
alsE	9,332	3,63E-87	D-allulose-6-phosphate_3-epimerase
exbD	9,173	9,33E-81	Ton_complex_subunit_ExbD
hslR	9,161	1,13E-109	heat_shock_protein_Hsp15
feoA	8,914	8,05E-06	ferrous_iron_transport_protein_A
fhuA	8,828	3,55E-37	ferrichrome_outer_membrane_transporter/phage_receptor
htpG	8,817	7,50E-131	chaperone_protein_HtpG
katE	8,675	3,66E-121	catalase_II
lldD	8,588	2,96E-65	L-lactate_dehydrogenase
yjcH	8,501	3,64E-34	conserved_inner_membrane_protein_YjcH
alsK	8,466	2,82E-52	D-allose_kinase
nanE	8,434	8,01E-45	putative_N-acetylmannosamine-6-phosphate_epimerase
yohP	8,429	7,85E-52	putative_membrane_protein_YohP
yceA	8,425	1,49E-05	UPF0176_protein_YceA
gtrS	8,424	6,54E-20	CPS-53 (KpLE1) prophage; serotype-specific glucosyl transferase YfdI
dosC	8,331	1,13E-28	diguanylate_cyclase_DosC
tonB	8,251	2,13E-79	Ton_complex_subunit_TonB
clpB	8,249	1,66E-73	ClpB_chaperone
yoaG	8,122	3,04E-20	DUF1869_domain-containing_protein_YoaG
hslO	8,096	8,48E-87	molecular_chaperone_Hsp33
astE	8,024	1,56E-26	succinylglutamate_desuccinylase
puuA	7,828	2,54E-24	glutamate-putrescine_ligase
lipB	7,715	3,28E-28	lipoyl(octanoyl)_transferase
alsC	7,668	4,95E-53	D-allose_ABC_transporter_membrane_subunit
yjdQ	7,648	1,65E-05	pseudogene
narH	7,63	4,16E-15	nitrate_reductase_A_subunit_beta
nanK	7,592	1,59E-88	N-acetylmannosamine_kinase
yebV	7,562	1,01E-123	protein_YebV
osmY	7,426	3,71E-43	periplasmic_chaperone_OsmY
ugpE	7,406	5,48E-25	sn-glycerol_3-phosphate_ABC_transporter_membrane_subunit_UgpE
ytjA	7,234	7,33E-30	DUF1328_domain-containing_protein_YtjA
dadX	7,218	8,35E-47	alanine_racemase_2
lon	7,202	3,18E-149	Lon_protease
alsA	7,149	2,02E-56	D-allose_ABC_transporter_ATP_binding_subunit
yhch	7,113	8,62E-91	DUF386_domain-containing_protein_YhcH
puuC	7,102	4,29E-26	gamma-glutamyl-gamma-aminobutyraldehyde_dehydrogenase
astB	7,03	4,57E-50	N-succinylarginine_dihydrolase
mutM	6,791	1,62E-63	DNA-formamidopyrimidine_glycosylase
puuB	6,791	3,93E-30	gamma-glutamylputrescine_oxidase
sdiA	6,788	5,46E-77	DNA-binding_transcriptional_dual_regulator_SdiA
yeeE	6,781	1,02E-23	inner_membrane_protein_YeeE
entB	6,778	1,53E-32	enterobactin_synthase_component_B
yncD	6,767	5,63E-22	putative_TonB-dependent_outer_membrane_receptor
fadE	6,623	5,61E-79	acyl-CoA_dehydrogenase
dgoT	6,595	6,56E-46	putative_D-galactonate_transporter
ydel	6,591	1,09E-24	BOF_family_protein_Ydel

fadB	6,576	3,62E-29	dodecenoyl-CoA_delta-isomerase
ydcl	6,527	5,61E-13	putative_DNA-binding_transcriptional_repressor_Ydcl
trpT	6,516	6,48E-32	tRNA-Trp(CCA)
yoel	6,496	1,28E-09	uncharacterized_protein_Yoel
cyoA	6,183	6,63E-15	cytochrome_bo3_ubiquinol_oxidase_subunit_2
nanM	6,178	4,47E-65	N-acetylneuraminate_mutarotase
fecR	6,169	1,92E-28	regulator_for_fec_operon_periplasmic
actP	6,148	1,21E-28	acetate/glycolate:cation_symporter
bgIJ	6,055	2,81E-22	DNA-binding_transcriptional_regulator_BgIJ
fiu	5,894	4,59E-28	putative_iron_siderophore_outer_membrane_transporter
ydjO	5,846	3,66E-12	protein_YdjO
groS	5,829	2,45E-43	cochaperonin_GroES
yeiQ	5,817	3,27E-45	putative_dehydrogenase,_NAD-dependent
ybjJ	5,739	1,48E-66	inner_membrane_protein_YbjJ
feoB	5,701	1,56E-10	Fe(2(+))_transporter_FeoB
ddpX	5,669	8,13E-28	D-alanyl-D-alanine_dipeptidase
ydiE	5,665	1,37E-17	PF10636_family_protein_YdiE
kdpB	5,661	4,10E-38	K(+)_transporting_P-type_ATPase_subunit_KdpB
dgoD	5,64	2,80E-53	D-galactonate_dehydratase
plaP	5,631	8,07E-13	putrescine:H(+)_symporter_PlaP
entF	5,596	2,01E-42	apo-serine_activating_enzyme
ycgG	5,571	9,49E-10	putative_c-di-GMP_phosphodiesterase_PdeG
yiaG	5,535	8,34E-46	putative_DNA-binding_transcriptional_regulator_YiaG
tusB	5,531	1,51E-32	sulfurtransferase_complex_subunit_TusB
sufC	5,51	1,77E-47	Fe-S_cluster_scaffold_complex_subunit_SufC
prpR	5,49	5,33E-21	DNA-binding_transcriptional_dual_regulator_PrprR
yahK	5,485	2,36E-79	aldehyde_reductase,_NADPH-dependent
groL	5,418	1,16E-82	chaperonin_GroEL
yhdN	5,401	6,13E-59	conserved_protein_YhdN
sufD	5,377	2,75E-56	Fe-S_cluster_scaffold_complex_subunit_SufD
zntR	5,363	7,77E-43	DNA-binding_transcriptional_activator_ZntR
adhP	5,362	2,00E-64	ethanol_dehydrogenase/alcohol_dehydrogenase
aroM	5,352	2,06E-27	protein_AroM
poxB	5,345	3,02E-56	pyruvate_oxidase
glcA	5,304	5,27E-31	glycolate/lactate:H(+)_symporter_GlcA
rapA	5,273	1,34E-58	RNA_polymerase-binding_ATPase_and_RNAP_recycling_factor
tktB	5,256	6,75E-78	transketolase_2
cirA	5,201	4,83E-55	ferric_dihydroxybenzoylserine_outer_membrane_transporter
insL1	5,113	6,95E-75	IS186/IS421_transposase
ynfN	5,078	0,00569696	Qin_prophage;_protein_YnfN
narU	5,067	1,95E-37	nitrate/nitrite_transporter_NarU
yjiR	5,059	7,81E-33	putative_aminotransferase
ddpA	5,05	1,31E-37	putative_D,D-dipeptide_ABC_transporter
cyoB	5,04	4,89E-12	cytochrome_bo3_ubiquinol_oxidase_subunit_1
otsA	5,026	5,12E-74	trehalose-6-phosphate_synthase
hspQ	5,02	4,20E-29	heat_shock_protein,_hemimethylated_DNA-binding_protein
ybgS	5,014	8,88E-46	PF13985_family_protein_YbgS
waaS	5,013	1,19E-09	lipopolysaccharide_core_biosynthesis_protein
otsB	4,991	7,64E-40	trehalose-6-phosphate_phosphatase
norR	4,96	7,21E-27	DNA-binding_transcriptional_dual_regulator_NorR
ndk	4,955	0,00132278	nucleoside_diphosphate_kinase
yrfG	4,945	2,26E-41	purine_nucleotidase
fepG	4,928	9,54E-17	ferric_enterobactin_ABC_transporter_membrane_subunit_FepG
proV	4,918	2,27E-30	glycine_betaine_ABC_transporter_ATP_binding_subunit_ProV
potF	4,889	5,03E-19	putrescine_ABC_transporter_periplasmic_binding_protein
ggt	4,885	2,50E-42	glutathione_hydrolase_proenzyme
yjjZ	4,873	4,28E-16	protein_YjjZ
narJ	4,858	6,23E-11	nitrate_reductase_1_molybdenum_cofactor_assembly_chaperone
ynfL	4,804	3,47E-42	putative_DNA-binding_transcriptional_regulator
yfdR	4,784	0,02965022	CPS-53_(KpLE1)_prophage;_5'-deoxynucleotidase
uxuB	4,775	3,49E-29	D-mannonate_oxidoreductase
putA	4,772	7,21E-11	proline_dehydrogenase/1-pyrroline-5
sdhC	4,767	1,29E-14	succinate:quinone_oxidoreductase,_membrane_protein_SdhC

dppF	4,743	1,16E-51	dipeptide_ABC_transporter_ATP_binding_subunit_DppF
prlC	4,741	3,85E-65	oligopeptidase_A
aceA	4,697	6,63E-38	isocitrate_lyase
yahA	4,691	4,72E-18	c-di-GMP phosphodiesterase PdeL
cysP	4,675	2,81E-22	thiosulfate/sulfate_ABC_transporter_periplasmic_binding_protein
arfA	4,668	5,29E-25	alternative_ribosome-rescue_factor_A
putP	4,667	2,14E-13	proline:Na(+)_symporter
uxuA	4,605	1,81E-33	D-mannonate_dehydratase
iraM	4,599	7,55E-07	anti-adaptor_protein_IraM,_inhibitor_of_sigma(S)_proteolysis
sufB	4,584	6,51E-30	Fe-S_cluster_scaffold_complex_subunit_SufB
sufS	4,581	6,44E-58	L-cysteine_desulfurase
mgtA	4,579	1,10E-18	Mg(2+)_importing_P-type_ATPase
mokA	4,574	0,01988293	pseudogene
sdhD	4,568	5,48E-16	succinate:quinone_oxidoreductase,_membrane_protein_SdhD
aldA	4,556	3,81E-19	aldehyde_dehydrogenase_A
sufA	4,55	2,70E-30	iron-sulfur_cluster_insertion_protein_SufA
ahr	4,545	1,18E-37	aldehyde_reductase,_NADPH-dependent
sufE	4,542	4,22E-24	sulfur_acceptor_for_SufS_cysteine_desulfurase
yqjH	4,532	5,04E-29	NADPH-dependent ferric-chelate reductase NfeF
mcbR	4,52	2,34E-19	DNA-binding_transcriptional_dual_regulator_McbR
cynR	4,47	2,13E-36	DNA-binding_transcriptional_dual_regulator_CynR
yciG	4,467	5,07E-08	protein_YciG
ugpB	4,454	1,84E-11	sn-glycerol_3-phosphate_ABC_transporter
grpE	4,409	1,55E-67	nucleotide_exchange_factor_GrpE
rpiB	4,402	2,23E-18	allose-6-phosphate_isomerase/ribose-5-phosphate_isomerase_B
fepE	4,391	5,58E-07	polysaccharide_co-polymerase_family_protein_FepE
yibA	4,377	1,01E-27	putative_lyase_containing_HEAT-repeat
wcaF	4,349	0,04460871	putative_acyl_transferase
alsB	4,248	7,45E-33	D-allose_ABC_transporter_periplasmic_binding_protein
narI	4,248	3,40E-07	nitrate_reductase_A_subunit_gamma
aroH	4,238	7,63E-18	3-deoxy-7-phosphoheptulonate_synthase,_Trp-sensitive
ecnB	4,224	8,91E-38	bacteriolytic_entericidin_B_lipoprotein
rimO	4,222	6,13E-11	ribosomal_protein_S12_methylthiotransferase_RimO
mhpR	4,208	9,56E-15	DNA-binding_transcriptional_activator_MhpR
arpA	4,207	5,08E-31	regulator_of_acetyl_CoA_synthetase
nanS	4,191	8,33E-31	N-acetyl-9-O-acetylneuraminate_esterase
potG	4,172	8,81E-11	putrescine_ABC_transporter_ATP_binding_subunit
ybaY	4,169	5,13E-35	PF09619_family_lipoprotein_YbaY
proW	4,159	6,31E-41	glycine_betaine_ABC_transporter_membrane_subunit_ProW
dppD	4,152	5,24E-31	dipeptide_ABC_transporter_ATP_binding_subunit_DppD
sdhA	4,141	7,32E-22	succinate:quinone_oxidoreductase,_FAD_binding_protein
fepA	4,124	9,17E-38	ferric_enterobactin_outer_membrane_transporter
ugpC	4,104	1,04E-34	sn-glycerol_3-phosphate_ABC_transporter_ATP_binding_subunit
rpoD	4,089	7,70E-73	RNA_polymerase,_sigma_70_(sigma_D)_factor
yncl	4,083	3,53E-06	putative transposase Yncl
rsxD	4,081	2,02E-29	SoxR [2Fe-2S] reducing system protein RsxD
ydeJ	4,081	3,54E-22	conserved_protein_YdeJ
uhpT	4,08	7,01E-17	hexose-6-phosphate:phosphate_antiporter
yghD	3,999	8,17E-13	putative_type_II_secretion_system_M-type_protein
rsxC	3,993	1,98E-25	SoxR [2Fe-2S] reducing system protein RsxC
sucD	3,976	1,35E-26	succinyl-CoA_synthetase_subunit_alpha
patA	3,968	2,47E-29	putrescine_aminotransferase
yigl	3,968	5,35E-06	putative_thioesterase_Yigl
aceK	3,967	9,28E-56	isocitrate_dehydrogenase_kinase/phosphatase
yjdP	3,955	6,37E-20	protein_YjdP
yegS	3,952	2,43E-24	lipid_kinase
pgrR	3,937	1,40E-42	DNA-binding_transcriptional_repressor_PgrR
ynbB	3,937	0,00174968	putative_CDP-diglyceride_synthase
phoH	3,936	1,27E-12	ATP-binding_protein_PhoH
nfuA	3,928	3,15E-35	iron-sulfur_cluster_carrier_protein_NfuA
ybbN	3,919	1,56E-38	chaperedoxin
narW	3,9	6,39E-14	putative_private_chaperone_for_NarZ_nitrate_reductase_subunit
yibU	3,88	0,01826254	pseudogene

glf	3,875	6,70E-07	UDP-galactopyranose_mutase
yehW	3,865	7,34E-25	glycine_betaine_ABC_transporter_membrane_subunit_YehW
talA	3,848	1,34E-47	transaldolase_A
fhuC	3,817	1,50E-18	iron(III)_hydroxamate_ABC_transporter_ATP_binding_subunit
rhuA	3,791	1,23E-29	23S_rRNA_pseudouridine_and_tRNA_pseudouridine_synthase
sdaB	3,763	2,04E-41	L-serine_deaminase_II
wza	3,763	0,00344107	outer_membrane_polysaccharide_export_protein_Wza
ldhA	3,727	4,49E-50	D-lactate_dehydrogenase
narY	3,727	4,17E-28	nitrate_reductase_Z_subunit_beta
topA	3,717	3,05E-66	DNA_topoisomerase_1
bhsA	3,71	1,15E-22	putative_stress_resistance_outer_membrane_protein
yhhQ	3,707	1,28E-20	putative_queuesine_precursor_transporter
ybeZ	3,704	6,57E-52	PhoH-like_protein
puuD	3,694	4,49E-10	gamma-glutamyl-gamma-aminobutyrate_hydrolase
ryhB	3,686	2,84E-07	small regulatory RNA RyhB
hicB	3,685	1,17E-31	antitoxin_of_the_HicA-HicB_toxin-antitoxin_system
rlmE	3,679	3,47E-58	23S_rRNA_2'-O-ribose_U2552_methyltransferase
gntP	3,672	8,49E-29	fructuronate_transporter
ybiU	3,63	1,03E-15	DUF1479_domain-containing_protein_YbiU
ydaM	3,62	5,03E-48	diguanylate_cyclase_DgCM
yhhZ	3,604	0,02223514	putative_endonuclease_YhhZ
yedN	3,603	6,93E-07	SoxR [2Fe-2S] reducing system protein RxB
cyoC	3,598	5,19E-07	cytochrome_bo3_ubiquinol_oxidase_subunit_3
gntX	3,598	2,75E-31	protein involved in utilization of DNA as a carbon source
rsxA	3,578	8,47E-10	S SoxR [2Fe-2S] reducing system protein RxA
yedR	3,578	8,52E-07	putative_inner_membrane_protein
hcaA	3,562	1,51E-29	protein/nucleic_acid_deglycase_1
wcaE	3,551	0,02247226	putative_colanic_acid_biosynthesis_glycosyl_transferase
yoeB	3,55	7,11E-16	ribosome-dependent_mRNA_interferase_toxin_YoeB
iscS	3,548	5,74E-24	cysteine_desulfurase
puuE	3,531	1,10E-23	4-aminobutyrate_aminotransferase_PuuE
elaB	3,517	4,55E-23	tail_anchored_inner_membrane_protein
hcaR	3,517	1,53E-07	DNA-binding_transcriptional_dual_regulator_HcaR
dosP	3,515	4,87E-27	oxygen-sensing_c-di-GMP_phosphodiesterase_DosP
ydfJ	3,514	8,56E-06	putative_transporter_YdfJ
ylaC	3,504	6,57E-12	putative_inner_membrane_protein
argT	3,493	1,68E-10	lysine/arginine/ornithine_ABC_transporter
rzpQ	3,489	0,03740232	Qin_prophage; DUF2514_domain-containing_protein_RzpQ
dppB	3,486	3,04E-16	dipeptide_ABC_transporter_membrane_subunit_DppB
sucC	3,486	1,66E-23	succinyl-CoA_synthetase_subunit_beta
rsxG	3,484	2,62E-31	SoxR [2Fe-2S] reducing system protein RxB
yfdE	3,469	2,51E-08	acetyl-CoA:oxalate_CoA-transferase
kgtP	3,461	1,25E-16	alpha-ketoglutarate:H(+)_symporter
ygiQ	3,46	3,13E-18	radical_SAM_superfamily_protein_YgiQ
sdhB	3,454	8,03E-17	succinate:quinone_oxidoreductase
yegQ	3,453	9,42E-12	putative_peptidase_YegQ
ygaM	3,453	8,18E-26	DUF883_domain-containing_protein_YgaM
insK	3,451	1,59E-09	IS150_conserved_protein_InsB
mntH	3,448	6,04E-16	Mn(2+)/Fe(2+):_H(+)_symporter_MntH
ydiU	3,445	1,54E-32	UPF0061_family_protein_YdiU
waaR	3,425	1,81E-06	UDP-D-glucose:lipopolysaccharide_glycosyltransferase
yehX	3,411	5,77E-18	glycine_betaine_ABC_transporter_ATP_binding_subunit_YehX
umuD	3,404	4,13E-15	DNA_polymerase_V_protein_UmuD
kdpC	3,395	2,30E-13	K(+)_transporting_P-type_ATPase_subunit_KdpC
proP	3,395	1,35E-37	osmolyte:H(+)_symporter_ProP
yeaJ	3,393	8,86E-24	diguanylate_cyclase_DgCJ
wbbK	3,388	3,04E-06	putative_lipopolysaccharide_biosynthesis_protein
fadD	3,386	7,91E-15	fatty_acyl-CoA_synthetase
iscR	3,377	1,43E-13	DNA-binding_transcriptional_dual_regulator_IscR
yncG	3,36	3,76E-10	putative_glutathione_S-transferase_YncG
hscB	3,343	1,03E-13	co-chaperone_for
cyoD	3,329	3,53E-06	cytochrome_bo3_ubiquinol_oxidase_subunit_4
ybhN	3,328	7,25E-07	conserved_inner_membrane_protein_YbhN

gnsB	3,309	4,31E-05	Qin_prophage;_protein_GnsB
rnb	3,281	2,73E-15	RNase_II
rsxB	3,258	3,03E-11	SoxR [2Fe-2S] reducing system protein RsxB
ybcK	3,252	4,44E-07	DLP12_prophage;_putative_recombinase
ybgA	3,252	4,54E-22	DUF1722_domain-containing_protein_YbgA
yeaQ	3,252	3,49E-26	PF04226_family_protein_YeaQ
ybhP	3,248	1,90E-16	endonuclease/exonuclease/phosphatase_domain-containing_protein
ddpB	3,24	2,66E-11	putative_D,D-dipeptide_ABC_transporter_membrane_subunit
narZ	3,227	1,13E-20	nitrate_reductase_Z_subunit_alpha
dppC	3,226	5,82E-21	dipeptide_ABC_transporter_membrane_subunit_DppC
apt	3,224	9,41E-07	adenine_phosphoribosyltransferase
yfcG	3,217	2,47E-19	disulfide_reductase
ydcD	3,212	9,90E-08	uncharacterized_protein_YdcD
higB	3,201	1,09E-18	ribosome-dependent_mRNA_interferase_toxin_HigB
cysU	3,182	1,68E-16	sulfate/thiosulfate_ABC_transporter_inner_membrane_subunit
yjdN	3,176	2,33E-09	conserved_protein_YjdN
Int	3,175	9,57E-23	apolipoprotein_N-acyltransferase
hicA	3,172	6,37E-24	toxin_of_the_HicA-HicB_toxin-antitoxin_system
ybeY	3,17	4,89E-37	endoribonuclease_YbeY
ycaO	3,169	6,55E-16	ribosomal_protein_S12_methylthiotransferase_accessory_factor
csgF	3,162	0,00029381	curli_assembly_component
yibG	3,147	0,00106251	tetratricopeptide-like_domain-containing_protein_YibG
cspl	3,135	0,000751	Qin_prophage;_cold_shock_protein_Cspl
yehY	3,124	4,14E-26	glycine_betaine_ABC_transporter_membrane_subunit_YehY
yefM	3,118	1,18E-15	antitoxin_of_the_YoeB-YefM_toxin-antitoxin_pair
yegP	3,118	5,20E-19	DUF1508_domain-containing_protein_YegP
ydcX	3,107	1,74E-10	orphan_toxin_OrtT
yebF	3,093	7,34E-34	secreted_protein_YebF
aceB	3,072	8,14E-38	malate_synthase_A
ybjI	3,066	2,68E-22	5-amino-6-(5-phospho-D-ribitylamino)uracil_phosphatase
yqeG	3,059	6,41E-18	putative_transporter_YqeG
amyA	3,057	3,71E-28	alpha-amylase
yfdS	3,05	0,0160385	CPS-53_(KpLE1)_prophage;_protein_YfdS
miaB	3,049	2,08E-16	isopentenyl-adenosine_A37_tRNA_methylthiolase
yccT	3,043	2,37E-07	DUF2057_domain-containing_protein_YccT
ycgl	3,031	0,03420527	protein_Ycgl
yhcG	3,03	2,51E-15	DUF1016_domain-containing_protein_YhcG
yfeR	3,029	2,68E-20	putative_LysR-type_DNA-binding_transcriptional_regulator
pmrR	3,021	2,95E-15	putative_bitopic_inner_membrane_protein
ycgB	3,014	4,12E-06	PF04293_family_protein_YcgB
rlmN	3,013	1,20E-12	tRNA_m(2)A37_methyltransferase
yfiM	3,005	1,42E-16	protein_YfiM
iscU	3,001	3,38E-26	scaffold_protein_for_iron-sulfur_cluster_assembly
rbsA	3	2,24E-40	ribose_ABC_transporter_ATP_binding_subunit

YeiL* down-regulated genes

Name	Fc	P-value	Function
garP	0,003	2,30E-111	galactarate/glucarate/glycerate_transporter_GarP
ydhY	0,005	6,90E-151	putative_4Fe-4S_ferredoxin-type_protein
ompW	0,008	5,46E-105	outer_membrane_protein_W
garL	0,01	2,57E-208	alpha-dehydro-beta-deoxy-D-glucarate_aldolase
ydhV	0,011	2,81E-224	putative_oxidoreductase
tdcB	0,012	9,44E-63	catabolic_threonine_dehydratase
dcuB	0,016	6,20E-94	anaerobic_C4-dicarboxylate_transporter_DcuB
ynfE	0,016	3,54E-143	putative_selenate_reductase_YnfE
tdcC	0,018	2,53E-69	threonine/serine:H(+)_symporter
gudP	0,019	3,60E-169	galactarate/glucarate/glycerate_transporter_GudP
iraP	0,02	4,83E-173	anti-adaptor_protein_for_sigma(S)_stabilization
ansB	0,022	3,40E-05	L-asparaginase_2
fumB	0,022	5,66E-90	fumarase_B
tdcD	0,022	1,32E-47	propionate_kinase

garR	0,024	1,21E-125	tartronate_semialdehyde_reductase
flgB	0,026	8,09E-86	flagellar_basal-body_rod_protein_FlgB
ynfF	0,026	3,88E-123	putative_selenate_reductase_YnfF
preT	0,027	4,03E-97	NAD-dependent_dihydropyrimidine_dehydrogenase_subunit_PreT
tdcA	0,027	1,83E-11	DNA-binding_transcriptional_activator_TdcA
tdcE	0,027	3,89E-35	2-ketobutyrate_formate-lyase/pyruvate_formate-lyase_4
garD	0,028	9,52E-90	galactarate_dehydratase
ynfG	0,028	5,84E-109	putative_oxidoreductase_YnfG
frdD	0,03	4,72E-272	fumarate_reductase_membrane_protein_FrdD
frdA	0,032	8,25E-65	fumarate_reductase_flavoprotein_subunit
frdB	0,033	1,40E-83	fumarate_reductase_iron-sulfur_protein
dmsB	0,034	4,97E-65	dimethyl_sulfoxide_reductase_subunit_B
frdC	0,034	9,09E-154	fumarate_reductase_membrane_protein_FrdC
tdcF	0,035	4,20E-35	putative_enamine/imine_deaminase
flgC	0,038	4,66E-32	flagellar_basal-body_rod_protein_FlgC
pgaA	0,038	1,12E-170	poly-beta-1,6-N-acetyl-D-glucosamine_outer_membrane_porin
yciE	0,039	2,65E-176	DUF892_domain-containing_protein_YciE
glpA	0,04	1,02E-55	anaerobic_glycerol-3-phosphate_dehydrogenase_subunit_A
borD	0,043	9,18E-61	DLP12_prophage;_prophage_lipoprotein_BorD
malE	0,045	5,04E-78	maltose_ABC_transporter_periplasmic_binding_protein
flgD	0,046	1,41E-68	flagellar_biosynthesis,_initiation_of_hook_assembly
garK	0,046	5,69E-172	glycerate_2-kinase_1
dmsA	0,048	4,82E-25	dimethyl_sulfoxide_reductase_subunit_A
dmsC	0,048	1,18E-100	dimethyl_sulfoxide_reductase_subunit_C
hybA	0,048	2,25E-44	hydrogenase_2_iron-sulfur_protein
lamB	0,048	1,35E-86	maltose_outer_membrane_channel/phage_lambda_receptor_protein
ydhW	0,049	4,64E-73	protein_YdhW
yqeC	0,049	9,53E-43	uncharacterized_protein_YqeC
gudX	0,05	2,54E-131	glucarate_dehydratase-related_protein
caiF	0,051	7,34E-43	DNA-binding_transcriptional_activator_CaiF
malK	0,051	4,17E-63	maltose_ABC_transporter_ATP_binding_subunit
hybB	0,053	3,92E-53	hydrogenase_2_membrane_subunit
tdcG	0,055	2,38E-30	L-serine_deaminase_III
malF	0,056	1,27E-69	maltose_ABC_transporter_membrane_subunit_MalF
malM	0,056	2,75E-96	maltose_regulon_periplasmic_protein
yqeB	0,058	9,47E-52	XdhC-CoxI_family_protein_YqeB
hybO	0,059	4,46E-10	hydrogenase_2_small_subunit
ydhX	0,059	6,04E-65	putative_4Fe-4S_ferredoxin-type_protein
malG	0,06	1,70E-73	maltose_ABC_transporter_membrane_subunit_MalG
slp	0,061	8,41E-38	starvation_lipoprotein
tnaB	0,061	3,18E-149	tryptophan:H(+)_symporter_TnaB
preA	0,062	1,56E-61	NAD-dependent_dihydropyrimidine_dehydrogenase_subunit_PreA
tdcR	0,063	7,64E-09	DNA-binding_transcriptional_activator_TdcR
nmpC	0,064	3,24E-197	DLP12_prophage;_putative_outer_membrane_porin_N
yjiL	0,066	1,96E-35	putative_ATPase,_activator_of_(R)-hydroxyglutaryl-CoA_dehydratase
flgE	0,068	1,20E-94	flagellar_hook_protein_FlgE
ftnB	0,071	2,79E-31	putative_ferritin-like_protein
fnrS	0,072	5,47E-06	small_regulatory_RNA_FnrS
hybC	0,072	1,05E-56	hydrogenase_2_large_subunit
glpT	0,073	3,36E-74	sn-glycerol_3-phosphate:phosphate_antipporter
yjiT	0,073	1,82E-126	putative_uncharacterized_protein_YjiT
ynfH	0,073	2,20E-89	putative_menaquinol_dehydrogenase
adiY	0,075	1,28E-24	DNA-binding_transcriptional_activator_AdiY
hcp	0,076	2,90E-07	protein_S-nitrosylase
yjiM	0,079	5,11E-32	putative_dehydratase_subunit
nrfC	0,082	1,17E-31	putative_menaquinol-cytochrome_c_reductase_4Fe-4S_subunit
nrfB	0,083	7,69E-24	periplasmic_nitrite_reductase_penta-heme_c-type_cytochrome
manY	0,084	3,89E-38	mannose-specific_PTS_enzyme_IIC_component
fixX	0,086	0,01375143	putative_ferredoxin_FixX
manX	0,086	1,75E-23	mannose-specific_PTS_enzyme_IIB_component
glpB	0,09	6,84E-47	anaerobic_glycerol-3-phosphate_dehydrogenase_subunit_B
nudI	0,091	4,77E-38	pyrimidine_deoxynucleotide_diphosphatase_NudI
ftnA	0,093	3,54E-198	ferritin_iron_storage_protein

flgF	0,095	3,26E-44	flagellar_basal-body_rod_protein_FlgF
gudD	0,095	9,86E-99	D-glucarate_dehydratase
phoA	0,095	2,62E-107	alkaline_phosphatase
malS	0,096	1,61E-98	alpha-amylase
napF	0,097	8,06E-34	ferredoxin-type_protein
caiE	0,098	3,33E-29	putative_transferase_CaiE
napD	0,099	2,68E-25	NapA_signal_peptide-binding_chaperone_NapD
glpF	0,101	3,34E-53	glycerol_facilitator
malP	0,102	2,75E-38	maltodextrin_phosphorylase
hybE	0,103	5,47E-49	hydrogenase_2-specific_chaperone
manZ	0,103	3,39E-52	mannose-specific_PTS_enzyme_IID_component
nrfD	0,103	4,71E-15	putative_menaquinol-cytochrome_c_reductase_subunit_NrfD
yehD	0,105	4,23E-19	putative_fimbrial_protein_YehD
gldA	0,107	2,92E-19	L-1,2-propanediol_dehydrogenase/glycerol_dehydrogenase
pgaB	0,109	2,61E-54	poly-beta-1,6-N-acetyl-D-glucosamine_N-deacetylase
ygfK	0,109	2,05E-46	putative_oxidoreductase_Fe-S_subunit
yhjA	0,109	2,12E-15	cytochrome_c_peroxidase_CCP
hcr	0,11	9,62E-13	NADH_oxidoreductase
nrfA	0,11	7,58E-05	cytochrome_c552_nitrite_reductase
tnaC	0,11	6,74E-21	tnaAB_operon_leader_peptide
ycbJ	0,11	0,00013239	putative_phosphotransferase_YcbJ
arrS	0,111	4,30E-14	small regulatory RNA
tnaA	0,112	5,39E-67	tryptophanase
ygeW	0,115	3,32E-36	putative_carbamoyltransferase_YgeW
fliL	0,116	9,24E-42	flagellar_protein_FliL
hybD	0,116	6,90E-46	putative_hydrogenase_2_maturation_protease
napG	0,117	3,00E-45	ferredoxin-type_protein_NapG
ulaB	0,117	3,91E-32	L-ascorbate_specific_PTS_enzyme_IIB_component
ghoS	0,118	1,97E-19	antitoxin_of_the_GhoTS_toxin-antitoxin_system
fliF	0,119	4,70E-31	flagellar_basal-body_MS-ring_and_collar_protein
glpK	0,119	8,05E-70	glycerol_kinase
fdhF	0,121	9,04E-28	formate_dehydrogenase_H
hybF	0,122	1,11E-26	hydrogenase_maturation_protein_HybF
napA	0,122	1,23E-40	periplasmic_nitrate_reductase_subunit_NapA
yjjW	0,122	4,70E-31	putative_glycyl-radical_enzyme_activating_enzyme_YjjW
yjji	0,123	3,45E-05	DUF3029_domain-containing_protein_Yjji
ybcW	0,125	2,31E-37	DLP12_prophage;_protein_YbcW
napB	0,126	1,86E-25	periplasmic_nitrate_reductase_cytochrome_c550_protein
pyrB	0,126	7,62E-27	aspartate_carbamoyltransferase_catalytic_subunit
yahD	0,126	1,13E-37	ankyrin_repeat-containing_protein_YahD
yfbM	0,127	4,92E-18	DUF1877_domain-containing_protein_YfbM
pspE	0,13	8,90E-56	thiosulfate_sulfurtransferase_PspE
fliA	0,133	1,13E-28	RNA_polymerase_sigma_28_(sigma_F)_factor
fliH	0,134	1,91E-21	flagellar_biosynthesis_protein_FliH
uspC	0,135	5,13E-27	universal_stress_protein_C
hypC	0,136	9,87E-16	hydrogenase_3_maturation_protein_HypC
pepE	0,136	1,61E-35	peptidase_E
dcuA	0,137	3,21E-41	C4-dicarboxylate_transporter_DcuA
hypD	0,137	4,21E-23	Fe-(CN)2CO_cofactor_assembly_scaffold_protein_HypD
dcuC	0,138	0,00381404	anaerobic_C4-dicarboxylate_transporter_DcuC
malQ	0,139	4,57E-44	4-alpha-glucanotransferase
uspF	0,139	3,43E-22	nucleotide_binding_filament_protein
ygeV	0,139	5,13E-21	putative_sigma(54)-dependent_transcriptional_regulator_YgeV
cydB	0,141	8,13E-28	cytochrome_bd-I_ubiquinol_oxidase_subunit_II
napH	0,141	1,16E-36	ferredoxin-type_protein_NapH
ygcb	0,142	4,46E-34	CRISPR-associated_endonuclease/helicase_Cas3
flgG	0,145	2,91E-35	flagellar_basal-body_rod_protein_FlgG
flgH	0,145	3,81E-18	flagellar_L-ring_protein
fliI	0,145	2,20E-26	flagellum-specific_ATP_synthase_FliI
hypB	0,146	7,06E-05	hydrogenase_isoenzymes_nickel_incorporation_protein_HypB
nikD	0,149	7,04E-22	Ni(2+)_ABC_transporter_ATP_binding_subunit_NikD
cydX	0,152	1,42E-24	cytochrome_bd-I_ubiquinol_oxidase_subunit_CydX
rihC	0,154	1,96E-34	ribonucleoside_hydrolase_RihC

iraD	0,156	1,94E-27	anti-adaptor_protein_IraD,_inhibitor_of_sigma(S)_proteolysis
fucP	0,158	9,26E-27	L-fucose:H(+)_symporter
ydeN	0,158	1,19E-14	putative_sulfatase
ygcP	0,159	5,85E-47	putative_anti-terminator_regulatory_protein
glpQ	0,161	1,57E-57	glycerophosphoryl_diester_phosphodiesterase
yobD	0,161	1,36E-41	conserved_inner_membrane_protein_YobD
fliM	0,163	1,02E-22	flagellar_motor_switch_protein_FliM
melA	0,165	7,47E-29	alpha-galactosidase
hypE	0,166	9,10E-20	hydrogenase_maturation_protein,_carbamoyl_dehydratase
csrC	0,168	6,20E-64	small regulatory RNA
ygcO	0,168	1,44E-23	putative_4Fe-4S_cluster-containing_protein
ybiA	0,169	2,80E-29	N-glycosidase_YbiA
yjhP	0,169	5,92E-41	KpLE2_phage-like_element;_putative_methyltransferase_YjhP
hypA	0,17	0,00075605	hydrogenase_3_nickel_incorporation_protein_HypA
xylF	0,17	5,74E-30	xylose_ABC_transporter_periplasmic_binding_protein
fucI	0,171	2,51E-37	L-fucose_isomerase
ydhU	0,171	8,75E-39	putative_cytochrome_YdhU
cspD	0,173	9,56E-47	DNA_replication_inhibitor
fliG	0,174	2,06E-36	flagellar_motor_switch_protein_FliG
yccM	0,174	1,22E-19	putative_4Fe-4S_membrane_protein
fliN	0,175	1,07E-09	flagellar_motor_switch_protein_FliN
gpmM	0,175	1,82E-12	2,3-bisphosphoglycerate-independent_phosphoglycerate_mutase
nikE	0,175	1,43E-19	Ni(2(+))_ABC_transporter_ATP_binding_subunit_NikE
pgaC	0,175	4,48E-30	poly-N-acetyl-D-glucosamine_synthase_subunit_PgaC
aspA	0,176	7,42E-20	aspartate_ammonia-lyase
yidE	0,176	5,44E-50	putative_transport_protein_YidE
ycdT	0,178	9,04E-45	probable_diguanylate_cyclase_DgcT
uacT	0,179	1,08E-11	urate:H(+)_symporter
flgA	0,18	1,49E-43	flagellar_basal_body_P-ring_formation_protein_FlgA
yhaO	0,181	3,71E-36	cysteine detoxification protein CyuP
frwA	0,182	7,97E-23	putative PTS multiphosphoryl transfer protein PtsA
hdeB	0,183	7,54E-22	periplasmic_acid_stress_chaperone
nikC	0,183	1,72E-10	Ni(2(+))_ABC_transporter_membrane_subunit_NikC
nikB	0,184	1,23E-10	Ni(2(+))_ABC_transporter_membrane_subunit_NikB
ssnA	0,184	6,34E-24	putative_aminohydrolase
uspG	0,184	1,57E-23	universal_stress_protein_G
fucO	0,185	3,61E-21	L-1,2-propanediol_oxidoreductase
nrfE	0,186	1,43E-13	putative_cytochrome_c-type_biogenesis_protein_NrfE
katG	0,187	2,32E-24	hydroperoxidase_I
yjiK	0,187	6,77E-29	uncharacterized_protein_YjiK
zraS	0,19	9,89E-24	sensory_histidine_kinase_ZraS
glxA	0,191	1,89E-18	glutaminase_1
ghoT	0,192	5,11E-12	toxin_of_the_GhoTS_toxin-antitoxin_system
fliO	0,193	8,94E-10	flagellar_biosynthesis_protein_FliO
cydA	0,194	3,48E-10	cytochrome_bd-I_ubiquinol_oxidase_subunit_I
hdeA	0,194	3,99E-24	HdeA_monomer_chaperone_active_form
ygcN	0,195	9,35E-22	putative_oxidoreductase_with_FAD/NAD(P)-binding_domain
agp	0,196	5,68E-16	glucose-1-phosphatase
ykgF	0,196	7,01E-17	putative_amino_acid_dehydrogenase
ymgG	0,197	8,29E-08	PF13488_family_protein_YmgG
ykgE	0,198	3,46E-09	putative_lactate_utilization_oxidoreductase_YkgE
carB	0,199	8,14E-28	carbamoyl_phosphate_synthetase_subunit_beta
yjhQ	0,199	1,44E-25	putative_acetyltransferase_TopAI_antitoxin_YjhQ
fucK	0,2	6,79E-29	L-fuculokinase
napC	0,2	2,70E-22	periplasmic_nitrate_reductase_cytochrome_c_protein
carA	0,201	3,41E-11	carbamoyl_phosphate_synthetase_subunit_alpha
cdaR	0,202	3,21E-41	DNA-binding_transcriptional_activator_CdaR
ydhZ	0,202	2,51E-41	fumarase D
pepT	0,203	2,32E-11	peptidase_T
ydjY	0,205	1,28E-09	4Fe-4S_ferredoxin-type_domain-containing_protein_YdjY
yjhX	0,205	6,41E-33	toxin_of_the_TopAI-YjhQ_toxin-antitoxin_system
pyrI	0,206	1,98E-31	aspartate_carbamoyltransferase,_PyrI_subunit
yfcZ	0,208	7,03E-12	DUF406_domain-containing_protein_YfcZ

fliJ	0,209	1,59E-09	flagellar_biosynthesis_protein_FliJ
rzpD	0,209	1,25E-05	DLP12_prophage;_putative_prophage_endopeptidase_RzpD
fsaB	0,21	5,07E-21	fructose-6-phosphate_aldolase_2
glgS	0,212	2,36E-21	surface_composition_regulator
ravA	0,214	7,22E-12	regulatory_ATPase_RavA
frwC	0,216	2,78E-10	putative_PTS_enzyme_IIC_component_FrwC
viaA	0,219	1,76E-20	protein_ViaA
ysaA	0,219	1,05E-08	putative_electron_transport_protein_YsaA
pgaD	0,22	1,14E-10	poly-N-acetyl-D-glucosamine_synthase_subunit_PgaD
ydiV	0,22	2,12E-31	anti-FlhDC_factor
yahN	0,221	3,25E-12	putative_amino_acid_exporter
hybG	0,222	6,74E-20	hydrogenase_2_accessory_protein
mocA	0,222	2,72E-18	molybdenum_cofactor_cytidylyltransferase
ccmA	0,223	2,98E-21	heme_trafficking_system_ATP-binding_protein
mdtL	0,223	2,87E-26	efflux_pump_MdtL
ycjN	0,223	2,54E-07	putative_ABC_transporter_periplasmic_binding_protein_YcjN
ydfZ	0,224	7,35E-12	putative_selenoprotein_YdfZ
lrhA	0,225	1,07E-35	DNA-binding_transcriptional_dual_regulator_LrhA
yahE	0,226	0,00292973	DUF2877_domain-containing_protein_YahE
caiD	0,227	3,66E-06	crotonobetainyl-CoA_hydratase
cpdB	0,227	2,66E-53	2'3'_cyclic_nucleotide_phosphodiesterase/3'_nucleotidase
ccmC	0,228	8,92E-28	heme_trafficking_system_membrane_protein_CcmC
ulaA	0,228	9,15E-27	L-ascorbate_specific_PTS_enzyme_IIC_component
adiC	0,229	1,65E-16	arginine:agmatine_antipporter
bsmA	0,229	4,61E-09	DUF1471_domain-containing_putative_lipoprotein_BsmA
hmp	0,229	1,38E-26	nitric_oxide_dioxygenase
glpC	0,23	1,16E-14	anaerobic_glycerol-3-phosphate_dehydrogenase_subunit_C
ydjZ	0,23	4,26E-14	DedA_family_protein_YdjZ
yniA	0,23	7,23E-15	putative_kinase_YniA
nikA	0,231	1,34E-09	Ni(2+)_ABC_transporter_periplasmic_binding_protein
ucpA	0,231	1,39E-13	putative_oxidoreductase
atoS	0,232	4,51E-11	sensory_histidine_kinase_AtoS
insH1	0,233	1,39E-75	IS5 transposase and trans-activator
ykgG	0,233	1,07E-22	DUF162_domain-containing_lactate_utilization_protein_YkgG
atoC	0,236	1,51E-21	ornithine_decarboxylase_inhibitor_AtoC
ccmD	0,236	4,99E-07	heme_trafficking_system_membrane_protein_CcmD
araF	0,237	1,82E-27	arabinose_ABC_transporter_periplasmic_binding_protein
fucA	0,237	2,65E-22	L-fucose-phosphate_aldolase
dmlA	0,239	1,78E-25	D-malate/3-isopropylmalate_dehydrogenase
pka	0,24	8,94E-17	peptidyl-lysine_N-acetyltransferase_PatZ
csrB	0,244	3,07E-23	small regulatory RNA CsrB
yciF	0,244	2,02E-22	DUF892_domain-containing_protein_YciF
pflB	0,246	6,98E-11	pyruvate_formate-lyase
ybgE	0,246	1,33E-19	cyd_operon_protein_YbgE
ydch	0,246	1,93E-15	protein_Ydch
ccmB	0,247	2,87E-26	heme_trafficking_system_membrane_protein_CcmB
yiaM	0,247	0,00140709	2,3-diketo-L-gulonate:Na(+)_symporter_-_membrane_subunit
allS	0,248	1,08E-10	DNA-binding_transcriptional_activator_AllS
ccmE	0,248	1,45E-18	periplasmic_heme_chaperone
flgI	0,248	1,48E-13	flagellar_P-ring_protein
yjiH	0,248	1,93E-10	Gate_family_protein_YjiH
yjjP	0,248	5,91E-09	putative_succinate_exporter_YjjP
yecR	0,249	1,04E-14	lipoprotein_YecR
dctR	0,251	0,00025326	putative_DNA-binding_transcriptional_regulator_DctR
hdeD	0,252	2,01E-16	acid-resistance_membrane_protein
rhaR	0,252	4,13E-17	DNA-binding_transcriptional_activator_RhaR
hsdR	0,257	9,82E-22	type_I_restriction_enzyme_EcoKI_endonuclease_component
yfbS	0,258	2,59E-11	putative_transporter_YfbS
ompC	0,259	1,66E-48	outer_membrane_porin_C
uspA	0,259	8,45E-15	universal_stress_global_stress_response_regulator
ynjE	0,259	6,39E-18	molybdopterin_synthase_sulfurtransferase
yfeC	0,26	2,52E-22	putative_DNA-binding_transcriptional_regulator_YfeC
yjel	0,26	3,02E-33	DUF4156_domain-containing_lipoprotein_Yjel

malT	0,261	3,20E-19	DNA-binding_transcriptional_activator_MalT
quuD	0,261	8,48E-05	prophage_antitermination_protein_Q_homolog
ycjM	0,261	9,35E-19	glucosylglycerate_phosphorylase
ynhF	0,261	2,32E-26	stress_response_membrane_protein_YnhF
ydiL	0,262	7,82E-06	DUF1870_domain-containing_protein_YdiL
dtpB	0,264	1,98E-12	dipeptide/tripeptide:H(+)_symporter_DtpB
sslE	0,264	5,19E-37	putative_lipoprotein
ampC	0,265	3,84E-26	beta-lactamase
fixA	0,266	9,37E-09	putative_electron_transfer_flavoprotein_FixA
eptB	0,267	6,00E-44	Kdo2-lipid_A_phosphoethanolamine_7''-transferase
yidF	0,267	2,18E-14	uncharacterized_protein_YidF
gpr	0,268	3,90E-11	L-glyceraldehyde_3-phosphate_reductase
ulaC	0,268	2,67E-10	L-ascorbate_specific_PTS_enzyme_IIA_component
adhE	0,269	1,15E-22	aldehyde-alcohol_dehydrogenase
nrfG	0,269	2,94E-09	putative_formate-dependent_nitrite_reductase_complex_subunit
ypfM	0,272	0,01858095	uncharacterized_protein_YpfM
ygeY	0,273	3,67E-15	putative_peptidase_YgeY
yjfN	0,273	9,86E-07	protease_activator
fucU	0,274	6,85E-26	L-fucose_mutarotase
ygjR	0,274	3,45E-11	putative_oxidoreductase_YgjR
hyaA	0,278	1,70E-12	hydrogenase_1_small_subunit
ttdR	0,281	0,00013808	DNA-binding_transcriptional_activator_Dan
yrdF	0,281	8,68E-12	pseudogene
yhbS	0,282	6,20E-09	putative_acyltransferase_with_acyl-CoA_N-acyltransferase_domain
yjjB	0,282	1,59E-13	putative_succinate_exporter_YjjB
yijD	0,284	6,63E-31	conserved_inner_membrane_protein_YijD
ydeM	0,285	9,49E-06	putative_anaerobic_sulfatase_maturation_enzyme_YdeM
ccmH	0,286	1,85E-06	holocytochrome_c_synthetase_-_thiol:disulfide_oxidoreductase
fliK	0,286	6,81E-15	flagellar_hook-length_control_protein
raiA	0,286	2,86E-09	stationary_phase_translation_inhibitor_and_ribosome_stability_factor
ybcV	0,289	1,84E-07	DLP12_prophage;_protein_YbcV
cspC	0,29	7,79E-45	stress_protein,_member_of_the_CspA_family
yhbV	0,292	1,41E-06	putative_peptidase_YhbV
aphA	0,294	2,99E-16	acid_phosphatase/phosphotransferase
friA	0,295	1,93E-11	fructoselysine/psicoselysine_transporter
yfcC	0,296	1,19E-09	putative_transporter_YfcC
asnA	0,297	1,55E-09	asparagine_synthetase_A
ymgD	0,297	3,14E-11	PF16456_family_protein_YmgD
frwB	0,298	1,50E-12	putative_PTS_enzyme_IIB_component_FrwB
glmY	0,301	1,11E-15	small_regulatory_RNA_GlmY
hupB	0,302	2,17E-47	DNA-binding_protein_HU-beta
yhbU	0,302	9,99E-07	putative_peptidase_YhbU
nrfF	0,303	4,22E-05	putative_formate-dependent_nitrite_reductase_complex_subunit
yjiV	0,303	6,06E-23	putative_uncharacterized_protein
yqfG	0,303	0,04131362	uncharacterized_protein_YqfG
bglG	0,305	0,00016483	transcriptional_antiterminator_BglG
dmsD	0,305	8,97E-24	redox_enzyme_maturation_protein_DmsD
flhB	0,305	1,19E-07	flagellar_biosynthesis_protein_FlhB
ylcI	0,305	1,68E-07	DLP12_prophage;_DUF3950_domain-containing_protein_YlcI
yhfL	0,306	5,08E-05	DUF4223_domain-containing_lipoprotein_YhfL
rbbA	0,308	1,51E-23	ribosome-associated_ATPase
yihN	0,308	2,47E-19	putative_transporter_YihN
ymiA	0,31	2,06E-08	uncharacterized_protein_YmiA
agaV	0,311	3,99E-08	N-acetyl-D-galactosamine_specific_PTS_enzyme_IIB_component
yagJ	0,311	9,84E-19	CP4-6_prophage;_protein_YagJ
yhbT	0,311	2,61E-08	SCP2_domain-containing_protein_YhbT
ulaF	0,312	2,77E-14	L-ribose-5-phosphate_4-epimerase_UlaF
yoaE	0,312	5,32E-20	putative_inner_membrane_protein
yobF	0,312	1,93E-32	DUF2527_domain-containing_protein_YobF
pck	0,315	5,18E-29	phosphoenolpyruvate_carboxykinase_(ATP)
yihY	0,315	2,62E-33	putative_inner_membrane_protein
yqfA	0,315	2,79E-08	hemolysin-III_family_protein
bssR	0,317	6,97E-07	regulator_of_biofilm_formation

pfkA	0,317	6,81E-15	6-phosphofructokinase_I
dicF	0,318	0,04991216	small regulatory RNA DicF
yaeH	0,318	6,03E-14	DUF3461_domain-containing_protein_YaeH
flgJ	0,319	1,20E-06	putative_peptidoglycan_hydrolase_FlgJ
ynfO	0,324	0,00060749	Qin_prophage;_protein_YnfO
zraR	0,324	9,07E-12	DNA-binding_transcriptional_activator_ZraR
fliZ	0,326	2,25E-10	DNA-binding_transcriptional_regulator_FliZ
glpX	0,326	3,32E-27	fructose-1,6-bisphosphatase_2
hisL	0,326	4,35E-06	his_operon_leader_peptide
adeD	0,327	1,85E-24	adenine_deaminase
ybaV	0,327	4,35E-18	helix-hairpin-helix_3_family_protein
yhiD	0,327	0,00068206	inner_membrane_protein_YhiD
fucR	0,328	2,77E-16	DNA-binding_transcriptional_activator_FucR
yfeD	0,329	1,72E-14	putative_DNA-binding_transcriptional_regulator_YfeD
dcuR	0,33	8,11E-22	DNA-binding_transcriptional_activator_DcuR

Concluding Remarks

Fe-S clusters are essential cofactors for, except for a few exceptions, all living organisms. They require dedicated machineries for their assembly and their delivery to the Apo-proteins requiring them. The recent phylogenetic approaches suggest that Fe-S machineries were already present in the last universal common ancestor, LUCA. Since their discovery, identification and characterization of Fe-S proteins and the machineries responsible for their maturation, have been the subject of intensive research. Fe-S research is a very productive topic, every year new Fe-S proteins, new mechanisms of activity, and new insights on the machineries that synthesize them are discovered. In this manuscript I report the addition of a new member to the Fe-S biogenesis ISC machinery, ACP, as well as the characterization of the last unstudied Fe-S regulator in *E. coli*, YeiL. Although many discoveries have been made in the Fe-S field, many more are still to come.

The intriguing relationships between Fatty Acids and Fe-S biogenesis

The fact that ACP is involved in the ISC machinery is enigmatic and unexpected, as ACP is already known to be a central protein for fatty acid biosynthesis (FasII pathway). Moreover, the link between ACP and the ISC machinery is not restricted to *E. coli* since it has been shown that ACP participates in the biogenesis of Fe-S clusters in the mitochondria of humans and yeast. In eukaryotes ACP interacts with ISD11, the stabilizing protein of NFS1, whereas in *E. coli* ACP interacts with three proteins of the ISC machinery IscS, Fdx, and HscB. Therefore, the common feature between ACP's role in eukaryotes, regarding Fe-S biogenesis, and in prokaryotes seems to be its link with the cysteine desulfurase. This suggests that ACP role in Fe-S biogenesis might be tightly linked to the activity of the cysteine desulfurase.

Since the link between the FasII pathway and Fe-S cluster biogenesis is conserved between humans, yeasts, and *E. coli*, one might wonder if it is present in other organisms. Phylogenetic studies teach us that SUF rather than ISC is the most prevalent system in bacteria. Therefore, one crucial question arises: is there a link between fatty acids and Fe-S cluster biogenesis in the organisms lacking ISC. Our study suggested that ACP does not affect the biogenesis of Fe-S clusters by the SUF system, since there was no effect of ACP on a regulator matured by SUF nor any interaction between ACP and SufS, the cysteine desulfurase of the SUF system. We have however no information regarding the potential link between ACP and SUF in SUF only organisms.

Some bacteria possess more than one ACP, such is the case of *pseudomonas aeruginosa* that has three ACPs. All three of them can be phosphopantetheinylated and acylated but only one, ACP1, is involved in FasII pathway and is therefore essential (Ma *et al.* 2017). Since only the ISC system is present in *P. aeruginosa* it would be interesting to test if the ACP-IscS interaction is conserved and if so, which ACP is involved.

The most fascinating piece of information regarding ACP and Fe-S biogenesis comes from the study of the unusual mitochondria of *Plasmodium falciparum*. *P. falciparum* and other apicomplexan parasites have an atypical mitochondria that lost some major functions such as fatty acid biogenesis or lipoate synthesis. Interestingly, *P. falciparum* has conserved the interaction ACP-ISD11-NFS1. Moreover, the mitochondrial ACP seems to be crucial for Fe-S synthesis for this parasite as well (Falekun *et al.* 2021). These findings suggest that the evolutionary pressure in this parasite has led to the loss of ACP's main function in the mitochondria, the FasII pathway, but conserved its role in Fe-S cluster biogenesis. The question that naturally comes to mind is why would evolution maintain this interaction?

In *E. coli*, ACP is involved in at least six essential pathways. ACP is involved in fatty acids biosynthesis, membrane biosynthesis (lipopolysaccharides and phospholipids), vitamins biosynthesis (biotin and lipoate), stringent response, Fe-S cluster biogenesis and, possibly, structure of the chromosome. As for Fe-S clusters they are involved in a wide diversity of functions, such as respiration, genetic regulation, metabolite biogenesis, central metabolism and much more. Thus, we can speculate that ACP and ISC interaction has major consequences for the cell.

We propose here to use ACP involvement in the stringent response as a benchmark for ACPs role in Fe-S biogenesis. The stringent response or nutrient limitation stress is an adaptation of the cell to multiple stress related mainly to the availability of nutrients. The stringent response is activated when the level of 5'-(tri)diphosphate, 3'-diphosphate [(p)ppGpp], reaches a critical level. In *E. coli*, the level of (p)ppGpp alarmone in the cell, in any given moment, depends mainly on the activity of two proteins; RelA, a (p)ppGpp synthetase, and SpoT, a (p)ppGpp hydrolase and synthetase. It has been demonstrated that ACP interacts with the SpoT protein, and it has been proposed that ACP could modulate SpoT activity depending on the FasII activity. Once the stringent response is activated it would lead to a global gene regulation to induce cell arrest and the expression of resistance genes. We can speculate that by interacting with the ISC machinery, ACP provides the information regarding

the cell metabolic status. Similarly to ACP-SpoT interaction, ACP's effect on the ISC machinery can help to slow down the growth when in unfavorable conditions and then when the conditions are favorable again it can help the resume to a normal growth. We can imagine that this effect can be hastened Fe-S involvement in a plethora of functions.

YeiL, the last uncharacterized Fe-S regulator in *E. coli*

At the start of my thesis very little was known about YeiL, only one paper was published on the subject 23 years ago. Although we faced many challenges in the characterization of this regulator, we have at the end, provided much more information from what was initially known about YeiL.

We showed, by a transcriptomic approach, that YeiL affects the expression of hundreds of genes in the cell involved in various process amongst which, anaerobic respiration, sugar metabolism and nitric oxide (NO) stress response. By using a variant of YeiL that is unable to bind the cluster, YeiL*, we showed that the Apo-form of YeiL displays a strong regulatory activity. It is noteworthy to keep in mind that the overexpression of an Fe-S protein usually leads to the production of a mix of Holo- and Apo-forms, it is therefore too early to affirm whether both Apo-YeiL and Holo-YeiL are active or if it is only the Apo-form that is responsible for the regulation observed. In this study, we focused on one pathway regulated by both YeiL and YeiL*, the aldaric acid metabolism, and one pathway only regulated by YeiL*, the nitric oxide stress response.

We have shown that YeiL represses the expression of the aldaric metabolism genes as well as NO stress response genes. Moreover, YeiL potentially down-regulates these pathways in a similar fashion, *i.e.* competition with activators for the binding of promoter regions. Interestingly, aldaric acids are chemically synthesized by the NO-oxidation of simple sugars. Therefore, both pathways down-regulated by YeiL are linked to NO. However, the *yeiL* gene is very low expressed and our experimental data do not support a NO induction of *yeiL* expression nor an enhanced repressive activity in presence of NO. Therefore, it is possible that the role of YeiL is to down-regulate these pathways in absence of NO. Here, we propose a model in which YeiL role is to prevent inappropriate activation of these pathways in absence of NO.

The *hcp-hcr* operon expression is activated by SNO-OxyR. We propose that YeiL competes with OxyR for the binding of *hcp-hcr* promoter, therefore the following question

arises: in which conditions YeiL could outcompete OxyR for *hcp-hcr* promoter binding? OxyR is known for its role in induction of oxidative stress response and more particularly H₂O₂. OxyR has been well characterized regarding the activation of a whole set of genes involved in the response to oxidative stress. Those genes include the alkyl hydroperoxyde reductase AhpC, the catalase encoded by *katG*, as well as the *suf* operon. Activation of this regulon is done by the oxidized form of OxyR (Ox-OxyR) that is obtained through the sulfenylation of the Cys199 residue and the subsequent formation of a disulfide bond between the Cys199 and Cys208 residues (Lee *et al.* 2004). Interestingly it is the same residue that is nitrosylated by NO to generate SNO-OxyR, which controls the expression of genes involved in the response to NO, amongst which *hcp* (Seth *et al.* 2012). Although the overlap of the Ox-OxyR and SNO-OxyR regulons is very limited, it has been reported that some genes belonging to the Ox-OxyR regulon, like *katG* for instance, are slightly activated by SNO-OxyR as well (Seth *et al.* 2012). We therefore hypothesize that YeiL repression of *hcp* occurs in oxidative stress conditions and prevents *hcp* activation by Ox-OxyR (see the proposed model Fig. 1). We thus suggest that YeiL affinity for *hcp* promoter is higher than Ox-OxyR but lower than SNO-OxyR. We propose to test this hypothesis by studying the role of OxyR and YeiL in the expression of *hcp* under oxidative stress.

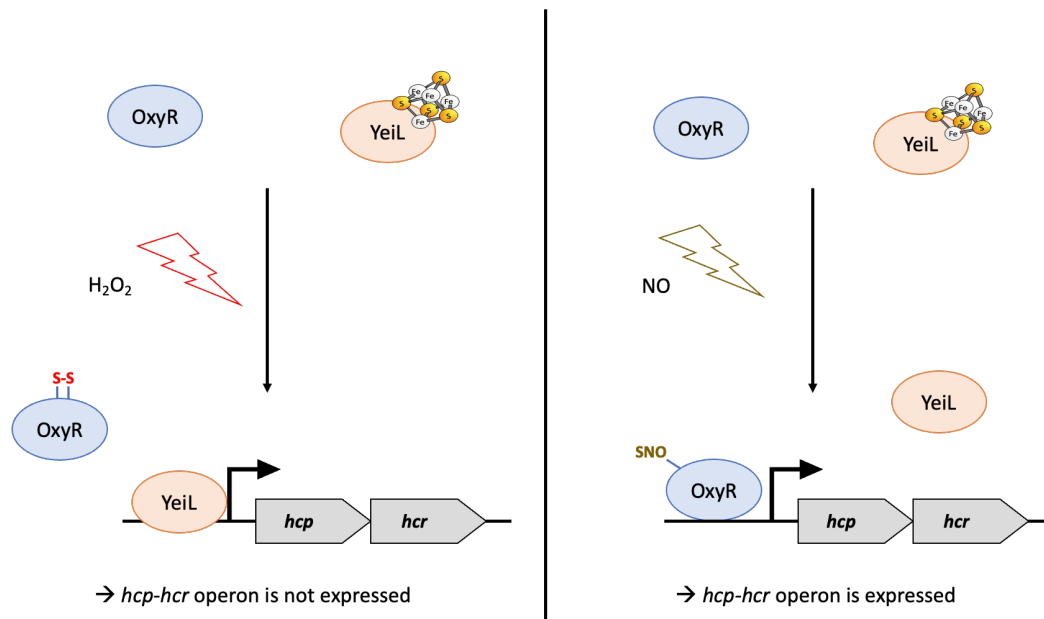


Figure 1. Proposed molecular mechanism for YeilL and OxyR regulation of *hcp-hcr* expression.

Exposure to H_2O_2 leads to the activation of OxyR, Ox-OxyR form, through the formation of a disulfide bond, and to the activation of YeilL by the loss of its cluster. In this condition Apo-YeilL affinity for *hcp* promoter is sufficient to prevent Ox-OxyR binding. Exposure to NO leads to the activation of OxyR, SNO-OxyR form, through nitrosylation, and to the activation of YeilL by the loss of its cluster. In this condition Apo-YeilL affinity for *hcp* promoter is not sufficient to prevent SNO-OxyR binding

As for the YeilL down-regulation of the aldaric acid pathway we have proposed that YeilL competes with the CdaR activator for the binding to the *cdaR* promoter region. However, the activity of CdaR in presence of other oxidized sugars has never been tested. Aldaric acids are obtained through the oxidation of simple sugars by NO. The reaction involves the oxidation of both ends of the aldose chain to form carboxylic groups (aldaric acids are also known as di-acid sugars) (Fig. 2 A). Simple sugars can also be oxidized by H_2O_2 and the product obtained are aldonic acids. The reaction involves the oxidation of only the aldehyde group into a carboxylic group (Fig 2 A). *E. coli* can metabolize aldonic acids thanks to genes encoded in the *gnt* operon (Coello *et al.* 1992). We propose here that YeilL prevents cross activation of the aldaric acid metabolism genes by aldonic acids through CdaR in order to prevent wasteful production of unwarranted proteins (see the proposed model Fig. 2 B). We propose to test this hypothesis by first studying the effect of aldonic acids on *cdaR* expression in a $\Delta yeiL$.

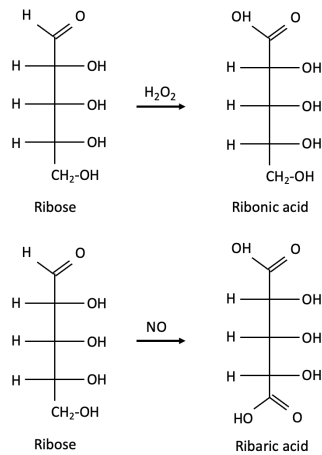
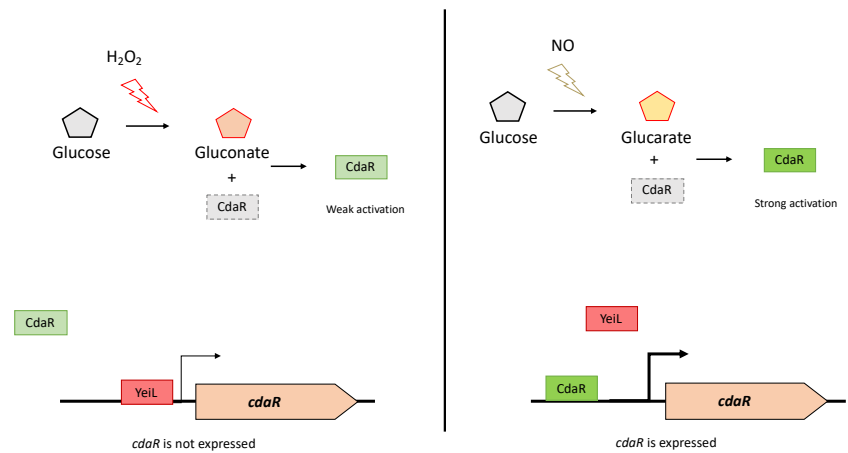
A)**B)**

Figure 2. Proposed mechanism for CdaR and YeiL regulation of *cdaR* expression. **A)** Oxidation of a ribose by H_2O_2 and NO . **B)** Exposure to aldonic acids leads to a weak activation of *CdaR* that is not sufficient to displace *YeiL* from *cdaR* promoter. Exposure to aldaric acids leads to the full activation of *CdaR*, which is sufficient to displace *YeiL* from *cdaR* promoter.

Based on our models for both NO stress response (*hcp-hcr* operon) and aldaric acids metabolism regulation (*cdaR* gene), it would be interesting to investigate *YeiL* role in H_2O_2 stress.

The study of the cross-talk between Fatty acid biogenesis and Fe-S cluster biogenesis, as well as the characterization of the *YeiL* regulator is a testimony for the all the discoveries that are still to be made on the Fe-S field. While we generally consider *E. coli* as the best characterized bacteria in biology, it is important to remember that we still know too little on the most fundamental functions of this bacteria.

Bibliography

- Altuvia, S., D. Weinstein-Fischer, A. Zhang, L. Postow and G. Storz (1997). "A small, stable RNA induced by oxidative stress: role as a pleiotropic regulator and antimutator." *Cell* **90**(1): 43-53.
- Anderson, M. S., C. E. Bulawa and C. R. Raetz (1985). "The biosynthesis of gram-negative endotoxin. Formation of lipid A precursors from UDP-GlcNAc in extracts of *Escherichia coli*." *J Biol Chem* **260**(29): 15536-15541.
- Anderson, M. S. and C. R. Raetz (1987). "Biosynthesis of lipid A precursors in *Escherichia coli*. A cytoplasmic acyltransferase that converts UDP-N-acetylglucosamine to UDP-3-O-(R-3-hydroxymyristoyl)-N-acetylglucosamine." *J Biol Chem* **262**(11): 5159-5169.
- Andreini, C., A. Rosato and L. Banci (2017). "The Relationship between Environmental Dioxygen and Iron-Sulfur Proteins Explored at the Genome Level." *PLoS One* **12**(1): e0171279.
- Angelini, S., L. My and E. Bouveret (2012). "Disrupting the Acyl Carrier Protein/SpoT interaction in vivo: identification of ACP residues involved in the interaction and consequence on growth." *PLoS One* **7**(4): e36111.
- Angerer, H. (2013). "The superfamily of mitochondrial Complex1_LYR motif-containing (LYRM) proteins." *Biochem Soc Trans* **41**(5): 1335-1341.
- Anjum, M. F., J. Green and J. R. Guest (2000). "YeiL, the third member of the CRP-FNR family in *Escherichia coli*." *Microbiology* **146 Pt 12**: 3157-3170.
- Ansari, A. Z., J. E. Bradner and T. V. O'Halloran (1995). "DNA-bend modulation in a repressor-to-activator switching mechanism." *Nature* **374**(6520): 371-375.
- Baba, T., T. Ara, M. Hasegawa, Y. Takai, Y. Okumura, M. Baba, K. A. Datsenko, M. Tomita, B. L. Wanner and H. Mori (2006). "Construction of *Escherichia coli* K-12 in-frame, single-gene knockout mutants: the Keio collection." *Mol Syst Biol* **2**: 2006 0008.
- Bak, D. W. and S. J. Elliott (2014). "Alternative FeS cluster ligands: tuning redox potentials and chemistry." *Curr Opin Chem Biol* **19**: 50-58.
- Barnard, A., A. Wolfe and S. Busby (2004). "Regulation at complex bacterial promoters: how bacteria use different promoter organizations to produce different regulatory outcomes." *Curr Opin Microbiol* **7**(2): 102-108.
- Bartberger, M. D., W. Liu, E. Ford, K. M. Miranda, C. Switzer, J. M. Fukuto, P. J. Farmer, D. A. Wink and K. N. Houk (2002). "The reduction potential of nitric oxide (NO) and its importance to NO biochemistry." *Proc Natl Acad Sci U S A* **99**(17): 10958-10963.
- Battesti, A., N. Majdalani and S. Gottesman (2015). "Stress sigma factor RpoS degradation and translation are sensitive to the state of central metabolism." *Proc Natl Acad Sci U S A* **112**(16): 5159-5164.
- Beinert, H., R. H. Holm and E. Munck (1997). "Iron-sulfur clusters: nature's modular, multipurpose structures." *Science* **277**(5326): 653-659.
- Beinert, H., M. C. Kennedy and C. D. Stout (1996). "Aconitase as Ironminus signSulfur Protein, Enzyme, and Iron-Regulatory Protein." *Chem Rev* **96**(7): 2335-2374.
- Beld, J., D. J. Lee and M. D. Burkart (2015). "Fatty acid biosynthesis revisited: structure elucidation and metabolic engineering." *Mol Biosyst* **11**(1): 38-59.
- Berks, B. C., S. J. Ferguson, J. W. Moir and D. J. Richardson (1995). "Enzymes and associated electron transport systems that catalyse the respiratory reduction of nitrogen oxides and oxyanions." *Biochim Biophys Acta* **1232**(3): 97-173.
- Boniecki, M. T., S. A. Freibert, U. Muhlenhoff, R. Lill and M. Cygler (2017). "Structure and functional dynamics of the mitochondrial Fe/S cluster synthesis complex." *Nat Commun* **8**(1): 1287.
- Bonomi, F., S. Iametti, A. Morleo, D. Ta and L. E. Vickery (2011). "Facilitated transfer of IscU-[2Fe2S] clusters by chaperone-mediated ligand exchange." *Biochemistry* **50**(44): 9641-9650.
- Borgaro, J. G., A. Chang, C. A. Machutta, X. Zhang and P. J. Tonge (2011). "Substrate recognition by beta-ketoacyl-ACP synthases." *Biochemistry* **50**(49): 10678-10686.

- Broussard, T. C., A. E. Price, S. M. Laborde and G. L. Waldrop (2013). "Complex formation and regulation of Escherichia coli acetyl-CoA carboxylase." *Biochemistry* **52**(19): 3346-3357.
- Brown, N. L., J. V. Stoyanov, S. P. Kidd and J. L. Hobman (2003). "The MerR family of transcriptional regulators." *FEMS Microbiol Rev* **27**(2-3): 145-163.
- Browning, D. F. and S. J. Busby (2004). "The regulation of bacterial transcription initiation." *Nat Rev Microbiol* **2**(1): 57-65.
- Bryant, J. A.F. C. MorrisT. J. KnowlesR. MaderbocusE. HeinzG. BoelterD. AlodainiA. ColyerP. J. WotherspoonK. A. StauntonM. JeevesD. F. BrowningY. R. SevastyanovichT. J. WellsA. E. RossiterV. N. BavroP. SridharD. G. WardZ. S. ChongE. C. GoodallC. IckeA. C. TeoS. S. ChngD. I. RoperT. LithgowA. F. CunninghamM. BanzhafM. OverduinI. R. Henderson (2020). "Structure of dual BOND-domain protein DolP identifies phospholipid binding as a new mechanism for protein localisation." *Elife* **9**.
- Bryant, P., G. Pozzati and A. Elofsson (2022). "Improved prediction of protein-protein interactions using AlphaFold2." *Nat Commun* **13**(1): 1265.
- Burmann, F., L. F. H. Funke, J. W. Chin and J. Lowe (2021). "Cryo-EM structure of MukBEF reveals DNA loop entrapment at chromosomal unloading sites." *Mol Cell* **81**(23): 4891-4906 e4898.
- Burschel, S., D. Kreuzer Decovic, F. Nuber, M. Stiller, M. Hofmann, A. Zupok, B. Siemiatkowska, M. Gorka, S. Leimkuhler and T. Friedrich (2019). "Iron-sulfur cluster carrier proteins involved in the assembly of Escherichia coli NADH:ubiquinone oxidoreductase (complex I)." *Mol Microbiol* **111**(1): 31-45.
- Calabrese, V., C. Mancuso, M. Calvani, E. Rizzarelli, D. A. Butterfield and A. M. Stella (2007). "Nitric oxide in the central nervous system: neuroprotection versus neurotoxicity." *Nat Rev Neurosci* **8**(10): 766-775.
- Calmels, S., H. Ohshima and H. Bartsch (1988). "Nitrosamine formation by denitrifying and non-denitrifying bacteria: implication of nitrite reductase and nitrate reductase in nitrosation catalysis." *J Gen Microbiol* **134**(1): 221-226.
- Chang, A. C. and S. N. Cohen (1978). "Construction and characterization of amplifiable multicopy DNA cloning vehicles derived from the P15A cryptic miniplasmid." *J Bacteriol* **134**(3): 1141-1156.
- Chatelet, C. and J. Meyer (1999). "The [2Fe-2S] protein I (Shetna protein I) from Azotobacter vinelandii is homologous to the [2Fe-2S] ferredoxin from Clostridium pasteurianum." *J Biol Inorg Chem* **4**(3): 311-317.
- Cherepanov, P. P. and W. Wackernagel (1995). "Gene disruption in Escherichia coli: TcR and KmR cassettes with the option of Flp-catalyzed excision of the antibiotic-resistance determinant." *Gene* **158**(1): 9-14.
- Chismon, D. L., D. F. Browning, G. K. Farrant and S. J. Busby (2010). "Unusual organization, complexity and redundancy at the Escherichia coli hcp-hcr operon promoter." *Biochem J* **430**(1): 61-68.
- Cho, H. J., E. Martin, Q. W. Xie, S. Sassa and C. Nathan (1995). "Inducible nitric oxide synthase: identification of amino acid residues essential for dimerization and binding of tetrahydrobiopterin." *Proc Natl Acad Sci U S A* **92**(25): 11514-11518.
- Cicchillo, R. M. and S. J. Booker (2005). "Mechanistic investigations of lipoic acid biosynthesis in Escherichia coli: both sulfur atoms in lipoic acid are contributed by the same lipoyl synthase polypeptide." *J Am Chem Soc* **127**(9): 2860-2861.
- Coello, N. B. and T. Isturiz (1992). "The metabolism of gluconate in Escherichia coli: a study in continuous culture." *J Basic Microbiol* **32**(5): 309-315.
- Constantinidou, C., J. L. Hobman, L. Griffiths, M. D. Patel, C. W. Penn, J. A. Cole and T. W. Overton (2006). "A reassessment of the FNR regulon and transcriptomic analysis of the effects of nitrate, nitrite, NarXL, and NarQP as Escherichia coli K12 adapts from aerobic to anaerobic growth." *J Biol Chem* **281**(8): 4802-4815.
- Corker, H. and R. K. Poole (2003). "Nitric oxide formation by Escherichia coli. Dependence on nitrite reductase, the NO-sensing regulator Fnr, and flavohemoglobin Hmp." *J Biol Chem* **278**(34): 31584-31592.

- Cory, S. A., J. G. Van Vranken, E. J. Brignole, S. Patra, D. R. Winge, C. L. Drennan, J. Rutter and D. P. Barondeau (2017). "Structure of human Fe-S assembly subcomplex reveals unexpected cysteine desulfurase architecture and acyl-ACP-ISD11 interactions." Proc Natl Acad Sci U S A **114**(27): E5325-E5334.
- Crack, J. C., B. K. Balasiny, S. P. Bennett, M. D. Rolfe, A. Froes, F. MacMillan, J. Green, J. A. Cole and N. E. Le Brun (2022). "The Di-Iron Protein YtfE Is a Nitric Oxide-Generating Nitrite Reductase Involved in the Management of Nitrosative Stress." J Am Chem Soc **144**(16): 7129-7145.
- Crack, J. C., J. Green, A. J. Thomson and N. E. Le Brun (2012). "Iron-sulfur cluster sensor-regulators." Curr Opin Chem Biol **16**(1-2): 35-44.
- Crack, J. C., J. Green, A. J. Thomson and N. E. Le Brun (2014). "Iron-sulfur clusters as biological sensors: the chemistry of reactions with molecular oxygen and nitric oxide." Acc Chem Res **47**(10): 3196-3205.
- Crack, J. C., C. J. Hamilton and N. E. Le Brun (2018). "Mass spectrometric detection of iron nitrosyls, sulfide oxidation and mycothiolation during nitrosylation of the NO sensor [4Fe-4S] NsrR." Chem Commun (Camb) **54**(47): 5992-5995.
- Crack, J. C. and N. E. Le Brun (2018). "Redox-Sensing Iron-Sulfur Cluster Regulators." Antioxid Redox Signal **29**(18): 1809-1829.
- Cronan, J. E. (2014). "The chain-flipping mechanism of ACP (acyl carrier protein)-dependent enzymes appears universal." Biochem J **460**(2): 157-163.
- Curatti, L., C. S. Brown, P. W. Ludden and L. M. Rubio (2005). "Genes required for rapid expression of nitrogenase activity in *Azotobacter vinelandii*." P Natl Acad Sci USA **102**(18): 6291-6296.
- D'Autreaux, B., D. Touati, B. Bersch, J. M. Latour and I. Michaud-Soret (2002). "Direct inhibition by nitric oxide of the transcriptional ferric uptake regulation protein via nitrosylation of the iron." Proc Natl Acad Sci U S A **99**(26): 16619-16624.
- D'Autreaux, B., N. Tucker, S. Spiro and R. Dixon (2008). "Characterization of the nitric oxide-reactive transcriptional activator NorR." Methods Enzymol **437**: 235-251.
- D'Autreaux, B., N. P. Tucker, R. Dixon and S. Spiro (2005). "A non-haem iron centre in the transcription factor NorR senses nitric oxide." Nature **437**(7059): 769-772.
- Datsenko, K. A. and B. L. Wanner (2000). "One-step inactivation of chromosomal genes in *Escherichia coli* K-12 using PCR products." Proc Natl Acad Sci U S A **97**(12): 6640-6645.
- Desai, J., Y. D. Wang, K. D. Wang, S. R. D. Malwal and E. Oldfield (2016). "Isoprenoid Biosynthesis Inhibitors Targeting Bacterial Cell Growth." ChemMedChem **11**(19): 2205-2215.
- Desnoyers, G., A. Morissette, K. Prevost and E. Masse (2009). "Small RNA-induced differential degradation of the polycistronic mRNA *iscRSUA*." EMBO J **28**(11): 1551-1561.
- Desvillechabrol, D., R. Legendre, C. Rioualen, C. Bouchier, J. van Helden, S. Kennedy and T. Cokelaer (2018). "Sequanix: a dynamic graphical interface for Snakemake workflows." Bioinformatics **34**(11): 1934-1936.
- Di Cara, F., P. Andreoletti, D. Trompier, A. Vejux, M. H. Bulow, J. Sellin, G. Lizard, M. Cherkaoui-Malki and S. Savary (2019). "Peroxisomes in Immune Response and Inflammation." Int J Mol Sci **20**(16).
- di Maio, D., B. Chandramouli, R. Yan, G. Brancato and A. Pastore (2017). "Understanding the role of dynamics in the iron sulfur cluster molecular machine." Biochim Biophys Acta Gen Subj **1861**(1 Pt A): 3154-3163.
- Dlouhy, A. C., H. Li, A. N. Albetel, B. Zhang, D. T. Mapolelo, S. Randeniya, A. A. Holland, M. K. Johnson and C. E. Outten (2016). "The *Escherichia coli* BOLA Protein IbaG Forms a Histidine-Ligated [2Fe-2S]-Bridged Complex with Grx4." Biochemistry **55**(49): 6869-6879.
- Dos Santos, P. C. and D. R. Dean (2017). FeS Cluster Assembly: NIF System in Nitrogen-Fixing Bacteria. Encyclopedia of Inorganic and Bioinorganic Chemistry, John Wiley & Sons.
- Dubrac, S., I. G. Boneca, O. Poupel and T. Msadek (2007). "New insights into the Walk/WalR (YycG/YycF) essential signal transduction pathway reveal a major role in controlling cell wall metabolism and biofilm formation in *Staphylococcus aureus*." Journal of Bacteriology **189**(22): 8257-8269.

- Edwards, P., J. S. Nelsen, J. G. Metz and K. Dehesh (1997). "Cloning of the *fabF* gene in an expression vector and in vitro characterization of recombinant *fabF* and *fabB* encoded enzymes from *Escherichia coli*." *FEBS Lett* **402**(1): 62-66.
- Emiola, A., J. George and S. S. Andrews (2014). "A Complete Pathway Model for Lipid A Biosynthesis in *Escherichia coli*." *PLoS One* **10**(4): e0121216.
- Esquilin-Lebron, K., S. Dubrac, F. Barras and J. M. Boyd (2021). "Bacterial Approaches for Assembling Iron-Sulfur Proteins." *mBio* **12**(6): e0242521.
- Even, S., P. Burguiere, S. Auger, O. Soutourina, A. Danchin and I. Martin-Verstraete (2006). "Global control of cysteine metabolism by *CymR* in *Bacillus subtilis*." *J Bacteriol* **188**(6): 2184-2197.
- Ezraty, B., A. Vergnes, M. Banzhaf, Y. Duverger, A. Huguenot, A. R. Brochado, S. Y. Su, L. Espinosa, L. Loiseau, B. Py, A. Typas and F. Barras (2013). "Fe-S cluster biosynthesis controls uptake of aminoglycosides in a ROS-less death pathway." *Science* **340**(6140): 1583-1587.
- Faber, F., L. Tran, M. X. Byndloss, C. A. Lopez, E. M. Velazquez, T. Kerrinnes, S. P. Nuccio, T. Wangdi, O. Fiehn, R. M. Tsolis and A. J. Baumler (2016). "Host-mediated sugar oxidation promotes post-antibiotic pathogen expansion." *Nature* **534**(7609): 697-699.
- Falekun, S., J. Sepulveda, Y. Jami-Alahmadi, H. Park, J. A. Wohlschlegel and P. A. Sigala (2021). "Divergent acyl carrier protein decouples mitochondrial Fe-S cluster biogenesis from fatty acid synthesis in malaria parasites." *Elife* **10**.
- Farhan, S. M., J. Wang, J. F. Robinson, P. Lahiry, V. M. Siu, C. Prasad, J. B. Kronick, D. A. Ramsay, C. A. Rupar and R. A. Hegele (2014). "Exome sequencing identifies *NFS1* deficiency in a novel Fe-S cluster disease, infantile mitochondrial complex II/III deficiency." *Mol Genet Genomic Med* **2**(1): 73-80.
- Filenko, N., S. Spiro, D. F. Browning, D. Squire, T. W. Overton, J. Cole and C. Constantinidou (2007). "The *NsrR* regulon of *Escherichia coli* K-12 includes genes encoding the hybrid cluster protein and the periplasmic, respiratory nitrite reductase." *J Bacteriol* **189**(12): 4410-4417.
- Filenko, N. A., D. F. Browning and J. A. Cole (2005). "Transcriptional regulation of a hybrid cluster (prismane) protein." *Biochem Soc Trans* **33**(Pt 1): 195-197.
- Fleischhacker, A. S., A. Stubna, K. L. Hsueh, Y. Guo, S. J. Teter, J. C. Rose, T. C. Brunold, J. L. Markley, E. Munck and P. J. Kiley (2012). "Characterization of the [2Fe-2S] cluster of *Escherichia coli* transcription factor *IscR*." *Biochemistry* **51**(22): 4453-4462.
- Flint, D. H. (1996). "*Escherichia coli* contains a protein that is homologous in function and N-terminal sequence to the protein encoded by the *nifS* gene of *Azotobacter vinelandii* and that can participate in the synthesis of the Fe-S cluster of dihydroxy-acid dehydratase." *J Biol Chem* **271**(27): 16068-16074.
- Fontecave, M., B. Py, S. Ollagnier de Choudens and F. Barras (2008). "From Iron and Cysteine to Iron-Sulfur Clusters: the Biogenesis Protein Machineries." *EcoSal Plus* **3**(1).
- Fox, N. G., X. Yu, X. Feng, H. J. Bailey, A. Martelli, J. F. Nabhan, C. Strain-Damerell, C. Bulawa, W. W. Yue and S. Han (2019). "Structure of the human frataxin-bound iron-sulfur cluster assembly complex provides insight into its activation mechanism." *Nat Commun* **10**(1): 2210.
- Galloway, S. M. and C. R. Raetz (1990). "A mutant of *Escherichia coli* defective in the first step of endotoxin biosynthesis." *J Biol Chem* **265**(11): 6394-6402.
- Gao, F. (2020). "Iron-Sulfur Cluster Biogenesis and Iron Homeostasis in Cyanobacteria." *Front Microbiol* **11**: 165.
- Garcia, P. S., F. D'Angelo, S. Ollagnier de Choudens, M. Dussouchaud, E. Bouveret, S. Gribaldo and F. Barras (2022). "An early origin of iron-sulfur cluster biosynthesis machineries before Earth oxygenation." *Nat Ecol Evol* **6**(10): 1564-1572.
- Garcia, P. S., S. Gribaldo, B. Py and F. Barras (2019). "The *SUF* system: an ABC ATPase-dependent protein complex with a role in Fe-S cluster biogenesis." *Res Microbiol* **170**(8): 426-434.
- Gardner, A. M. and P. R. Gardner (2002). "Flavohemoglobin detoxifies nitric oxide in aerobic, but not anaerobic, *Escherichia coli*. Evidence for a novel inducible anaerobic nitric oxide-scavenging activity." *J Biol Chem* **277**(10): 8166-8171.

- Gardner, P. R., A. M. Gardner, L. A. Martin and A. L. Salzman (1998). "Nitric oxide dioxygenase: an enzymic function for flavohemoglobin." Proc Natl Acad Sci U S A **95**(18): 10378-10383.
- Garwin, J. L., A. L. Klages and J. E. Cronan, Jr. (1980). "Structural, enzymatic, and genetic studies of beta-ketoacyl-acyl carrier protein synthases I and II of *Escherichia coli*." J Biol Chem **255**(24): 11949-11956.
- Gaudu, P., S. Dubrac and D. Touati (2000). "Activation of SoxR by overproduction of desulfoferrodoxin: Multiple ways to induce the soxRS regulon." Journal of Bacteriology **182**(6): 1761-1763.
- Gaudu, P., N. Moon and B. Weiss (1997). "Regulation of the soxRS oxidative stress regulon. Reversible oxidation of the Fe-S centers of SoxR in vivo." J Biol Chem **272**(8): 5082-5086.
- Gaudu, P. and B. Weiss (1996). "SoxR, a [2Fe-2S] transcription factor, is active only in its oxidized form." Proc Natl Acad Sci U S A **93**(19): 10094-10098.
- Gerstel, A., J. Zamarreno Beas, Y. Duverger, E. Bouveret, F. Barras and B. Py (2020). "Oxidative stress antagonizes fluoroquinolone drug sensitivity via the SoxR-SUF Fe-S cluster homeostatic axis." PLoS Genet **16**(11): e1009198.
- Giel, J. L., D. Rodionov, M. Liu, F. R. Blattner and P. J. Kiley (2006). "IscR-dependent gene expression links iron-sulphur cluster assembly to the control of O₂-regulated genes in *Escherichia coli*." Mol Microbiol **60**(4): 1058-1075.
- Gomes, C. M., A. Giuffre, E. Forte, J. B. Vicente, L. M. Saraiva, M. Brunori and M. Teixeira (2002). "A novel type of nitric-oxide reductase. *Escherichia coli* flavorubredoxin." J Biol Chem **277**(28): 25273-25276.
- Gomes, C. M., J. B. Vicente, A. Wasserfallen and M. Teixeira (2000). "Spectroscopic studies and characterization of a novel electron-transfer chain from *Escherichia coli* involving a flavorubredoxin and its flavoprotein reductase partner." Biochemistry **39**(51): 16230-16237.
- Greenberg, J. T., P. Monach, J. H. Chou, P. D. Josephy and B. Dimple (1990). "Positive control of a global antioxidant defense regulon activated by superoxide-generating agents in *Escherichia coli*." Proc Natl Acad Sci U S A **87**(16): 6181-6185.
- Gu, M. and J. A. Imlay (2011). "The SoxRS response of *Escherichia coli* is directly activated by redox-cycling drugs rather than by superoxide." Mol Microbiol **79**(5): 1136-1150.
- Gully, D. and E. Bouveret (2006). "A protein network for phospholipid synthesis uncovered by a variant of the tandem affinity purification method in *Escherichia coli*." Proteomics **6**(1): 282-293.
- Gully, D., D. Moinier, L. Loiseau and E. Bouveret (2003). "New partners of acyl carrier protein detected in *Escherichia coli* by tandem affinity purification." FEBS Letters **548**(1-3): 90-96.
- Gupta, K. J., J. K. Shah, Y. Brotman, K. Jahnke, L. Willmitzer, W. M. Kaiser, H. Bauwe and A. U. Igamberdiev (2012). "Inhibition of aconitase by nitric oxide leads to induction of the alternative oxidase and to a shift of metabolism towards biosynthesis of amino acids." J Exp Bot **63**(4): 1773-1784.
- Hagen, W. R. (2019). "EPR spectroscopy of putative enzyme intermediates in the NO reductase and the auto-nitrosylation reaction of *Desulfovibrio vulgaris* hybrid cluster protein." FEBS Lett **593**(21): 3075-3083.
- Harrop, T. C., Z. J. Tonzetich, E. Reisner and S. J. Lippard (2008). "Reactions of synthetic [2Fe-2S] and [4Fe-4S] clusters with nitric oxide and nitrosothiols." J Am Chem Soc **130**(46): 15602-15610.
- Hausladen, A., A. Gow and J. S. Stamler (2001). "Flavohemoglobin denitrosylase catalyzes the reaction of a nitroxyl equivalent with molecular oxygen." Proc Natl Acad Sci U S A **98**(18): 10108-10112.
- Heath, R. J. and C. O. Rock (1996). "Roles of the FabA and FabZ beta-hydroxyacyl-acyl carrier protein dehydratases in *Escherichia coli* fatty acid biosynthesis." J Biol Chem **271**(44): 27795-27801.
- Helander, I. M., B. Lindner, U. Seydel and M. Vaara (1993). "Defective biosynthesis of the lipid A component of temperature-sensitive *firA* (*omsA*) mutant of *Escherichia coli*." Eur J Biochem **212**(2): 363-369.
- Hernandez, V. J. and H. Bremer (1991). "*Escherichia coli* ppGpp synthetase II activity requires *spoT*." J Biol Chem **266**(9): 5991-5999.

- Herrera, M. G., M. F. Pignataro, M. E. Noguera, K. M. Cruz and J. Santos (2018). "Rescuing the Rescuer: On the Protein Complex between the Human Mitochondrial Acyl Carrier Protein and ISD11." ACS Chem Biol **13**(6): 1455-1462.
- Hidalgo, E. and B. Demple (1994). "An iron-sulfur center essential for transcriptional activation by the redox-sensing SoxR protein." EMBO J **13**(1): 138-146.
- Hidalgo, E., H. Ding and B. Demple (1997). "Redox signal transduction: mutations shifting [2Fe-2S] centers of the SoxR sensor-regulator to the oxidized form." Cell **88**(1): 121-129.
- Hughes, M. N. (2008). "Chemistry of nitric oxide and related species." Methods Enzymol **436**: 3-19.
- Imlay, J. A. (2006). "Iron-sulphur clusters and the problem with oxygen." Mol Microbiol **59**(4): 1073-1082.
- Ireland, W. T., S. M. Beeler, E. Flores-Bautista, N. S. McCarty, T. Roschinger, N. M. Belliveau, M. J. Sweredoski, A. Moradian, J. B. Kinney and R. Phillips (2020). "Deciphering the regulatory genome of Escherichia coli, one hundred promoters at a time." Elife **9**.
- Isabella, V. M., J. D. Lapek, Jr., E. M. Kennedy and V. L. Clark (2009). "Functional analysis of NsrR, a nitric oxide-sensing Rrf2 repressor in Neisseria gonorrhoeae." Mol Microbiol **71**(1): 227-239.
- Jakob, U., M. Eser and J. C. Bardwell (2000). "Redox switch of hsp33 has a novel zinc-binding motif." J Biol Chem **275**(49): 38302-38310.
- Jang, S. and J. A. Imlay (2010). "Hydrogen peroxide inactivates the Escherichia coli Isc iron-sulphur assembly system, and OxyR induces the Suf system to compensate." Mol Microbiol **78**(6): 1448-1467.
- Jarrett, J. T. (2003). "The generation of 5'-deoxyadenosyl radicals by adenosylmethionine-dependent radical enzymes." Curr Opin Chem Biol **7**(2): 174-182.
- Johnson, D. C., D. R. Dean, A. D. Smith and M. K. Johnson (2005). "Structure, function, and formation of biological iron-sulfur clusters." Annu Rev Biochem **74**: 247-281.
- Justino, M. C., C. C. Almeida, V. L. Goncalves, M. Teixeira and L. M. Saraiva (2006). "Escherichia coli YtfE is a di-iron protein with an important function in assembly of iron-sulphur clusters." FEMS Microbiol Lett **257**(2): 278-284.
- Justino, M. C., J. B. Vicente, M. Teixeira and L. M. Saraiva (2005). "New genes implicated in the protection of anaerobically grown Escherichia coli against nitric oxide." J Biol Chem **280**(4): 2636-2643.
- Kang, Y., K. D. Weber, Y. Qiu, P. J. Kiley and F. R. Blattner (2005). "Genome-wide expression analysis indicates that FNR of Escherichia coli K-12 regulates a large number of genes of unknown function." J Bacteriol **187**(3): 1135-1160.
- Karimova, G., J. Pidoux, A. Ullmann and D. Ladant (1998). "A bacterial two-hybrid system based on a reconstituted signal transduction pathway." Proc Natl Acad Sci U S A **95**(10): 5752-5756.
- Kelly, T. M., S. A. Stachula, C. R. Raetz and M. S. Anderson (1993). "The firA gene of Escherichia coli encodes UDP-3-O-(R-3-hydroxymyristoyl)-glucosamine N-acyltransferase. The third step of endotoxin biosynthesis." J Biol Chem **268**(26): 19866-19874.
- Kessels, J. M., H. Ousen and H. Van den Bosch (1983). "Facilitated utilization of endogenously synthesized lysophosphatidic acid by 1-acylglycerophosphate acyltransferase from Escherichia coli." Biochim Biophys Acta **753**(2): 227-235.
- Khoroshilova, N., C. Popescu, E. Munck, H. Beinert and P. J. Kiley (1997). "Iron-sulfur cluster disassembly in the FNR protein of Escherichia coli by O₂: [4Fe-4S] to [2Fe-2S] conversion with loss of biological activity." Proc Natl Acad Sci U S A **94**(12): 6087-6092.
- Kim, S. O., K. Merchant, R. Nudelman, W. F. Beyer, Jr., T. Keng, J. DeAngelo, A. Hausladen and J. S. Stamler (2002). "OxyR: a molecular code for redox-related signaling." Cell **109**(3): 383-396.
- Kim, S. O., Y. Orii, D. Lloyd, M. N. Hughes and R. K. Poole (1999). "Anoxic function for the Escherichia coli flavohaemoglobin (Hmp): reversible binding of nitric oxide and reduction to nitrous oxide." FEBS Lett **445**(2-3): 389-394.
- Koo, M. S., J. H. Lee, S. Y. Rah, W. S. Yeo, J. W. Lee, K. L. Lee, Y. S. Koh, S. O. Kang and J. H. Roe (2003). "A reducing system of the superoxide sensor SoxR in Escherichia coli." EMBO J **22**(11): 2614-2622.

- Korner, H., H. J. Sofia and W. G. Zumft (2003). "Phylogeny of the bacterial superfamily of Crp-Fnr transcription regulators: exploiting the metabolic spectrum by controlling alternative gene programs." *FEMS Microbiol Rev* **27**(5): 559-592.
- Krapp, A. R., M. V. Humbert and N. Carrillo (2011). "The soxRS response of *Escherichia coli* can be induced in the absence of oxidative stress and oxygen by modulation of NADPH content." *Microbiology (Reading)* **157**(Pt 4): 957-965.
- Lanz, N. D., M. E. Pandelia, E. S. Kakar, K. H. Lee, C. Krebs and S. J. Booker (2014). "Evidence for a catalytically and kinetically competent enzyme-substrate cross-linked intermediate in catalysis by lipoyl synthase." *Biochemistry* **53**(28): 4557-4572.
- Larson, M. H., L. A. Gilbert, X. Wang, W. A. Lim, J. S. Weissman and L. S. Qi (2013). "CRISPR interference (CRISPRi) for sequence-specific control of gene expression." *Nat Protoc* **8**(11): 2180-2196.
- Lazizzera, B. A., H. Beinert, N. Khoroshilova, M. C. Kennedy and P. J. Kiley (1996). "DNA binding and dimerization of the Fe-S-containing FNR protein from *Escherichia coli* are regulated by oxygen." *J Biol Chem* **271**(5): 2762-2768.
- Lee, C., S. M. Lee, P. Mukhopadhyay, S. J. Kim, S. C. Lee, W. S. Ahn, M. H. Yu, G. Storz and S. E. Ryu (2004). "Redox regulation of OxyR requires specific disulfide bond formation involving a rapid kinetic reaction path." *Nat Struct Mol Biol* **11**(12): 1179-1185.
- Lee, K. C., W. S. Yeo and J. H. Roe (2008). "Oxidant-responsive induction of the suf operon, encoding a Fe-S assembly system, through Fur and IscR in *Escherichia coli*." *J Bacteriol* **190**(24): 8244-8247.
- Leesong, M., B. S. Henderson, J. R. Gillig, J. M. Schwab and J. L. Smith (1996). "Structure of a dehydratase-isomerase from the bacterial pathway for biosynthesis of unsaturated fatty acids: two catalytic activities in one active site." *Structure* **4**(3): 253-264.
- Leipe, D. D., Y. I. Wolf, E. V. Koonin and L. Aravind (2002). "Classification and evolution of P-loop GTPases and related ATPases." *J Mol Biol* **317**(1): 41-72.
- Lenon, M., R. Arias-Cartin and F. Barras (2022). "The Fe-S proteome of *Escherichia coli*: prediction, function, and fate." *Metallomics* **14**(5).
- Li, H. and C. E. Outten (2012). "Monothiol CGFS glutaredoxins and BolA-like proteins: [2Fe-2S] binding partners in iron homeostasis." *Biochemistry* **51**(22): 4377-4389.
- Lim, S. C.M. FriemelJ. E. MarumE. J. TuckerD. L. BrunoL. G. RileyJ. ChristodoulouE. P. KirkA. BonehC. M. DeGennaroM. SpringerV. K. MoothaT. A. RouaultS. LeimkuhlerD. R. ThorburnA. G. Compton (2013). "Mutations in LYRM4, encoding iron-sulfur cluster biogenesis factor ISD11, cause deficiency of multiple respiratory chain complexes." *Hum Mol Genet* **22**(22): 4460-4473.
- Lin, S., R. E. Hanson and J. E. Cronan (2010). "Biotin synthesis begins by hijacking the fatty acid synthetic pathway." *Nat Chem Biol* **6**(9): 682-688.
- Livak, K. J. and T. D. Schmittgen (2001). "Analysis of relative gene expression data using real-time quantitative PCR and the 2^{-ΔΔC(T)} Method." *Methods* **25**(4): 402-408.
- Lo, F. C., C. C. Hsieh, M. Maestre-Reyna, C. Y. Chen, T. P. Ko, Y. C. Horng, Y. C. Lai, Y. W. Chiang, C. M. Chou, C. H. Chiang, W. N. Huang, Y. H. Lin, D. S. Bohle and W. F. Liaw (2016). "Crystal Structure Analysis of the Repair of Iron Centers Protein YtfE and Its Interaction with NO." *Chemistry* **22**(28): 9768-9776.
- Loiseau, L., C. Gerez, M. Bekker, S. Ollagnier-de Choudens, B. Py, Y. Sanakis, J. Teixeira de Mattos, M. Fontecave and F. Barras (2007). "ErpA, an iron sulfur (Fe S) protein of the A-type essential for respiratory metabolism in *Escherichia coli*." *Proc Natl Acad Sci U S A* **104**(34): 13626-13631.
- Loiseau, L., S. Ollagnier-de-Choudens, L. Nachin, M. Fontecave and F. Barras (2003). "Biogenesis of Fe-S cluster by the bacterial Suf system: SufS and SufE form a new type of cysteine desulfurase." *J Biol Chem* **278**(40): 38352-38359.
- Lonetto, M. A., V. Rhodius, K. Lamberg, P. Kiley, S. Busby and C. Gross (1998). "Identification of a contact site for different transcription activators in region 4 of the *Escherichia coli* RNA polymerase sigma70 subunit." *J Mol Biol* **284**(5): 1353-1365.

- Lu, P., C. Vogel, R. Wang, X. Yao and E. M. Marcotte (2007). "Absolute protein expression profiling estimates the relative contributions of transcriptional and translational regulation." Nat Biotechnol **25**(1): 117-124.
- Lundberg, J. O., E. Weitzberg, J. A. Cole and N. Benjamin (2004). "Nitrate, bacteria and human health." Nat Rev Microbiol **2**(7): 593-602.
- Ma, J. C., Y. Q. Wu, D. Cao, W. B. Zhang and H. H. Wang (2017). "Only Acyl Carrier Protein 1 (AcpP1) Functions in *Pseudomonas aeruginosa* Fatty Acid Synthesis." Front Microbiol **8**: 2186.
- MacMicking, J., Q. W. Xie and C. Nathan (1997). "Nitric oxide and macrophage function." Annu Rev Immunol **15**: 323-350.
- Magnuson, K., S. Jackowski, C. O. Rock and J. E. Cronan, Jr. (1993). "Regulation of fatty acid biosynthesis in *Escherichia coli*." Microbiol Rev **57**(3): 522-542.
- Maia, L. B. and J. J. Moura (2014). "How biology handles nitrite." Chem Rev **114**(10): 5273-5357.
- Martin, J. E. and J. A. Imlay (2011). "The alternative aerobic ribonucleotide reductase of *Escherichia coli*, NrdEF, is a manganese-dependent enzyme that enables cell replication during periods of iron starvation." Mol Microbiol **80**(2): 319-334.
- Masse, E. and S. Gottesman (2002). "A small RNA regulates the expression of genes involved in iron metabolism in *Escherichia coli*." Proc Natl Acad Sci U S A **99**(7): 4620-4625.
- McCarthy, E. L. and S. J. Booker (2017). "Destruction and reformation of an iron-sulfur cluster during catalysis by lipoyl synthase." Science **358**(6361): 373-377.
- Mehlretter, C. L., R. L. Mellies and et al. (1947). "Dimethylene-D-gluconic acid." J Am Chem Soc **69**(9): 2130.
- Mettert, E. L. and P. J. Kiley (2014). "Coordinate regulation of the Suf and Isc Fe-S cluster biogenesis pathways by IscR is essential for viability of *Escherichia coli*." J Bacteriol **196**(24): 4315-4323.
- Mettert, E. L. and P. J. Kiley (2018). "Reassessing the Structure and Function Relationship of the O(2) Sensing Transcription Factor FNR." Antioxid Redox Signal **29**(18): 1830-1840.
- Mettert, E. L., F. W. Outten, B. Wanta and P. J. Kiley (2008). "The impact of O(2) on the Fe-S cluster biogenesis requirements of *Escherichia coli* FNR." J Mol Biol **384**(4): 798-811.
- Meyer, J. (2008). "Iron-sulfur protein folds, iron-sulfur chemistry, and evolution." J Biol Inorg Chem **13**(2): 157-170.
- Miller, J. H. (1992). A short course in bacterial genetics : a laboratory manual and handbook for *Escherichia coli* and related bacteria. Plainview, N.Y., Cold Spring Harbor Laboratory Press.
- Moller, M. N., N. Rios, M. Trujillo, R. Radi, A. Denicola and B. Alvarez (2019). "Detection and quantification of nitric oxide-derived oxidants in biological systems." J Biol Chem **294**(40): 14776-14802.
- Monterrubio, R., L. Baldoma, N. Obradors, J. Aguilar and J. Badia (2000). "A common regulator for the operons encoding the enzymes involved in D-galactarate, D-glucarate, and D-glycerate utilization in *Escherichia coli*." J Bacteriol **182**(9): 2672-2674.
- Moreno-Vivian, C. and S. J. Ferguson (1998). "Definition and distinction between assimilatory, dissimilatory and respiratory pathways." Mol Microbiol **29**(2): 664-666.
- Myers, K. S., H. Yan, I. M. Ong, D. Chung, K. Liang, F. Tran, S. Keles, R. Landick and P. J. Kiley (2013). "Genome-scale analysis of *Escherichia coli* FNR reveals complex features of transcription factor binding." PLoS Genet **9**(6): e1003565.
- Nguyen, C., R. W. Haushalter, D. J. Lee, P. R. Markwick, J. Bruegger, G. Caldara-Festin, K. Finzel, D. R. Jackson, F. Ishikawa, B. O'Dowd, J. A. McCammon, S. J. Opella, S. C. Tsai and M. D. Burkart (2014). "Trapping the dynamic acyl carrier protein in fatty acid biosynthesis." Nature **505**(7483): 427-431.
- Nunoshiba, T., E. Hidalgo, C. F. Amabile Cuevas and B. Demple (1992). "Two-stage control of an oxidative stress regulon: the *Escherichia coli* SoxR protein triggers redox-inducible expression of the soxS regulatory gene." J Bacteriol **174**(19): 6054-6060.
- Oefner, C., H. Schulz, A. D'Arcy and G. E. Dale (2006). "Mapping the active site of *Escherichia coli* malonyl-CoA-acyl carrier protein transacylase (FabD) by protein crystallography." Acta Crystallogr D Biol Crystallogr **62**(Pt 6): 613-618.

- Ollagnier-De Choudens, S., Y. Sanakis, K. S. Hewitson, P. Roach, J. E. Baldwin, E. Munck and M. Fontecave (2000). "Iron-sulfur center of biotin synthase and lipoate synthase." Biochemistry **39**(14): 4165-4173.
- Ollagnier-de Choudens, S., Y. Sanakis, K. S. Hewitson, P. Roach, E. Munck and M. Fontecave (2002). "Reductive cleavage of S-adenosylmethionine by biotin synthase from *Escherichia coli*." J Biol Chem **277**(16): 13449-13454.
- Otsuka, Y., K. Miki, M. Koga, N. Katayama, W. Morimoto, Y. Takahashi and T. Yonesaki (2010). "IscR regulates RNase LS activity by repressing *rnlA* transcription." Genetics **185**(3): 823-830.
- Ouellette, R. A. and J. D. Rawn (2014). Carbohydrates. Organic Chemistry, Elsevier: 907-951.
- Outten, C. E., F. W. Outten and T. V. O'Halloran (1999). "DNA distortion mechanism for transcriptional activation by ZntR, a Zn(II)-responsive MerR homologue in *Escherichia coli*." J Biol Chem **274**(53): 37517-37524.
- Outten, F. W., O. Djaman and G. Storz (2004). "A *suf* operon requirement for Fe-S cluster assembly during iron starvation in *Escherichia coli*." Mol Microbiol **52**(3): 861-872.
- Outten, F. W., M. J. Wood, F. M. Munoz and G. Storz (2003). "The SufE protein and the SufBCD complex enhance SufS cysteine desulfurase activity as part of a sulfur transfer pathway for Fe-S cluster assembly in *Escherichia coli*." J Biol Chem **278**(46): 45713-45719.
- Padovani, D., F. Thomas, A. X. Trautwein, E. Mulliez and M. Fontecave (2001). "Activation of class III ribonucleotide reductase from *E. coli*. The electron transfer from the iron-sulfur center to S-adenosylmethionine." Biochemistry **40**(23): 6713-6719.
- Pao, G. M. and M. H. Saier, Jr. (1995). "Response regulators of bacterial signal transduction systems: selective domain shuffling during evolution." J Mol Evol **40**(2): 136-154.
- Parker, A., S. Cureoglu, N. De Lay, N. Majdalani and S. Gottesman (2017). "Alternative pathways for *Escherichia coli* biofilm formation revealed by sRNA overproduction." Mol Microbiol **105**(2): 309-325.
- Parris, K. D., L. Lin, A. Tam, R. Mathew, J. Hixon, M. Stahl, C. C. Fritz, J. Seehra and W. S. Somers (2000). "Crystal structures of substrate binding to *Bacillus subtilis* holo-(acyl carrier protein) synthase reveal a novel trimeric arrangement of molecules resulting in three active sites." Structure **8**(8): 883-895.
- Partridge, J. D., D. M. Bodenmiller, M. S. Humphrys and S. Spiro (2009). "NsrR targets in the *Escherichia coli* genome: new insights into DNA sequence requirements for binding and a role for NsrR in the regulation of motility." Mol Microbiol **73**(4): 680-694.
- Pereira, A. S., P. Tavares, C. Krebs, B. H. Huynh, F. Rusnak, I. Moura and J. J. Moura (1999). "Biochemical and spectroscopic characterization of overexpressed fuscodoxin from *Escherichia coli*." Biochem Biophys Res Commun **260**(1): 209-215.
- Petersen, C. and L. B. Moller (2001). "The RihA, RihB, and RihC ribonucleoside hydrolases of *Escherichia coli*. Substrate specificity, gene expression, and regulation." J Biol Chem **276**(2): 884-894.
- Pinilla-Redondo, R., L. Riber and S. J. Sorensen (2018). "Fluorescence Recovery Allows the Implementation of a Fluorescence Reporter Gene Platform Applicable for the Detection and Quantification of Horizontal Gene Transfer in Anoxic Environments." Appl Environ Microbiol **84**(6).
- Poole, R. K., M. F. Anjum, J. Membrillo-Hernandez, S. O. Kim, M. N. Hughes and V. Stewart (1996). "Nitric oxide, nitrite, and Fnr regulation of *hmp* (flavo-hemoglobin) gene expression in *Escherichia coli* K-12." J Bacteriol **178**(18): 5487-5492.
- Prince, J. P., J. R. Bolla, G. L. M. Fisher, J. Makela, M. Fournier, C. V. Robinson, L. K. Arciszewska and D. J. Sherratt (2021). "Acyl carrier protein promotes MukBEF action in *Escherichia coli* chromosome organization-segregation." Nat Commun **12**(1): 6721.
- Puglisi, R., R. Yan, S. Adinolfi and A. Pastore (2016). "A New Tessera into the Interactome of the *isc* Operon: A Novel Interaction between HscB and IscS." Front Mol Biosci **3**: 48.
- Py, B. and F. Barras (2010). "Building Fe-S proteins: bacterial strategies." Nat Rev Microbiol **8**(6): 436-446.

- Qi, L. S., M. H. Larson, L. A. Gilbert, J. A. Doudna, J. S. Weissman, A. P. Arkin and W. A. Lim (2013). "Repurposing CRISPR as an RNA-guided platform for sequence-specific control of gene expression." *Cell* **152**(5): 1173-1183.
- Rafi, S., P. Novichenok, S. Kolappan, C. F. Stratton, R. Rawat, C. Kisker, C. Simmerling and P. J. Tonge (2006). "Structure of acyl carrier protein bound to FabI, the FASII enoyl reductase from *Escherichia coli*." *J Biol Chem* **281**(51): 39285-39293.
- Rajagopalan, S., S. J. Teter, P. H. Zwart, R. G. Brennan, K. J. Phillips and P. J. Kiley (2013). "Studies of IscR reveal a unique mechanism for metal-dependent regulation of DNA binding specificity." *Nat Struct Mol Biol* **20**(6): 740-747.
- Ralt, D., J. S. Wishnok, R. Fitts and S. R. Tannenbaum (1988). "Bacterial catalysis of nitrosation: involvement of the nar operon of *Escherichia coli*." *J Bacteriol* **170**(1): 359-364.
- Ramachandran, R. A., C. Lupfer and H. Zaki (2018). "The Inflammasome: Regulation of Nitric Oxide and Antimicrobial Host Defence." *Adv Microb Physiol* **72**: 65-115.
- Raran-Kurussi, S., K. Keefe and D. S. Waugh (2015). "Positional effects of fusion partners on the yield and solubility of MBP fusion proteins." *Protein Expr Purif* **110**: 159-164.
- Reed, K. E. and J. E. Cronan, Jr. (1993). "Lipoic acid metabolism in *Escherichia coli*: sequencing and functional characterization of the lipA and lipB genes." *J Bacteriol* **175**(5): 1325-1336.
- Reinhart, F., S. Achebach, T. Koch and G. Uden (2008). "Reduced apo-fumarate nitrate reductase regulator (apoFNR) as the major form of FNR in aerobically growing *Escherichia coli*." *J Bacteriol* **190**(3): 879-886.
- Richards, T. A. and M. van der Giezen (2006). "Evolution of the Isd11-IscS complex reveals a single alpha-proteobacterial endosymbiosis for all eukaryotes." *Mol Biol Evol* **23**(7): 1341-1344.
- Richardson, D. J. (2000). "Bacterial respiration: a flexible process for a changing environment." *Microbiology (Reading)* **146 (Pt 3)**: 551-571.
- Rock, C. O., S. E. Goelz and J. E. Cronan, Jr. (1981). "Phospholipid synthesis in *Escherichia coli*. Characteristics of fatty acid transfer from acyl-acyl carrier protein to sn-glycerol 3-phosphate." *J Biol Chem* **256**(2): 736-742.
- Roos, V. and P. Klemm (2006). "Global gene expression profiling of the asymptomatic bacteriuria *Escherichia coli* strain 83972 in the human urinary tract." *Infect Immun* **74**(6): 3565-3575.
- Rowley, G., D. Hensen, H. Felgate, A. Arkenberg, C. Appia-Ayme, K. Prior, C. Harrington, S. J. Field, J. N. Butt, E. Baggs and D. J. Richardson (2012). "Resolving the contributions of the membrane-bound and periplasmic nitrate reductase systems to nitric oxide and nitrous oxide production in *Salmonella enterica* serovar Typhimurium." *Biochem J* **441**(2): 755-762.
- Ruan, J., Q. Xie, N. Hutchinson, H. Cho, G. C. Wolfe and C. Nathan (1996). "Inducible nitric oxide synthase requires both the canonical calmodulin-binding domain and additional sequences in order to bind calmodulin and produce nitric oxide in the absence of free Ca²⁺." *J Biol Chem* **271**(37): 22679-22686.
- Salas, A., J. J. Cabrera, A. Jimenez-Leiva, S. Mesa, E. J. Bedmar, D. J. Richardson, A. J. Gates and M. J. Delgado (2021). "Bacterial nitric oxide metabolism: Recent insights in rhizobia." *Adv Microb Physiol* **78**: 259-315.
- Salmon, K., S. P. Hung, K. Mekjian, P. Baldi, G. W. Hatfield and R. P. Gunsalus (2003). "Global gene expression profiling in *Escherichia coli* K12. The effects of oxygen availability and FNR." *J Biol Chem* **278**(32): 29837-29855.
- Sambrook, J., E. F. Fritsch and T. Maniatis (1989). *Molecular cloning : a laboratory manual, second edition*. Cold Spring Harbor, N. Y., Cold Spring Harbor Laboratory.
- Schwartz, C. J., J. L. Giel, T. Patschkowski, C. Luther, F. J. Ruzicka, H. Beinert and P. J. Kiley (2001). "IscR, an Fe-S cluster-containing transcription factor, represses expression of *Escherichia coli* genes encoding Fe-S cluster assembly proteins." *Proc Natl Acad Sci U S A* **98**(26): 14895-14900.
- Seo, S. W., D. Kim, R. Szubin and B. O. Palsson (2015). "Genome-wide Reconstruction of OxyR and SoxRS Transcriptional Regulatory Networks under Oxidative Stress in *Escherichia coli* K-12 MG1655." *Cell Rep* **12**(8): 1289-1299.

- Septer, A. N., J. L. Bose, A. K. Dunn and E. V. Stabb (2010). "FNR-mediated regulation of bioluminescence and anaerobic respiration in the light-organ symbiont *Vibrio fischeri*." FEMS Microbiol Lett **306**(1): 72-81.
- Seth, D., A. Hausladen, Y. J. Wang and J. S. Stamler (2012). "Endogenous protein S-Nitrosylation in *E. coli*: regulation by OxyR." Science **336**(6080): 470-473.
- Seth, D., D. T. Hess, A. Hausladen, L. Wang, Y. J. Wang and J. S. Stamler (2018). "A Multiplex Enzymatic Machinery for Cellular Protein S-nitrosylation." Mol Cell **69**(3): 451-464 e456.
- Shan, Y., Q. Pan, J. Liu, F. Huang, H. Sun, K. Nishino and A. Yan (2012). "Covalently linking the *Escherichia coli* global anaerobic regulator FNR in tandem allows it to function as an oxygen stable dimer." Biochem Biophys Res Commun **419**(1): 43-48.
- Shi, R., A. Proteau, M. Villarroya, I. Moukadiri, L. Zhang, J. F. Trempe, A. Matte, M. E. Armengod and M. Cygler (2010). "Structural basis for Fe-S cluster assembly and tRNA thiolation mediated by IscS protein-protein interactions." PLoS Biol **8**(4): e1000354.
- Siedler, S., G. Schendzielorz, S. Binder, L. Eggeling, S. Bringer and M. Bott (2014). "SoxR as a single-cell biosensor for NADPH-consuming enzymes in *Escherichia coli*." ACS Synth Biol **3**(1): 41-47.
- Silva, L. S. O., P. M. Matias, C. V. Romao and L. M. Saraiva (2021). "Structural Basis of RICs Iron Donation for Iron-Sulfur Cluster Biogenesis." Front Microbiol **12**: 670681.
- Simon, J. and M. G. Klotz (2013). "Diversity and evolution of bioenergetic systems involved in microbial nitrogen compound transformations." Biochim Biophys Acta **1827**(2): 114-135.
- Soppa, J. (2001). "Prokaryotic structural maintenance of chromosomes (SMC) proteins: distribution, phylogeny, and comparison with MukBs and additional prokaryotic and eukaryotic coiled-coil proteins." Gene **278**(1-2): 253-264.
- Stern, A. M. and J. Zhu (2014). "An introduction to nitric oxide sensing and response in bacteria." Adv Appl Microbiol **87**: 187-220.
- Stevanin, T. M., R. K. Poole, E. A. Demoncheaux and R. C. Read (2002). "Flavo-hemoglobin Hmp protects *Salmonella enterica* serovar typhimurium from nitric oxide-related killing by human macrophages." Infect Immun **70**(8): 4399-4405.
- Storz, G. and L. A. Tartaglia (1992). "OxyR: a regulator of antioxidant genes." J Nutr **122**(3 Suppl): 627-630.
- Sutton, V. R., A. Stubna, T. Patschkowski, E. Munck, H. Beinert and P. J. Kiley (2004). "Superoxide destroys the [2Fe-2S]²⁺ cluster of FNR from *Escherichia coli*." Biochemistry **43**(3): 791-798.
- Taber, H. W., J. P. Mueller, P. F. Miller and A. S. Arrow (1987). "Bacterial uptake of aminoglycoside antibiotics." Microbiol Rev **51**(4): 439-457.
- Thomas, J. and J. E. Cronan (2005). "The enigmatic acyl carrier protein phosphodiesterase of *Escherichia coli*: genetic and enzymological characterization." J Biol Chem **280**(41): 34675-34683.
- Thomason, M. K., T. Bischler, S. K. Eisenbart, K. U. Forstner, A. Zhang, A. Herbig, K. Nieselt, C. M. Sharma and G. Storz (2015). "Global transcriptional start site mapping using differential RNA sequencing reveals novel antisense RNAs in *Escherichia coli*." J Bacteriol **197**(1): 18-28.
- Toledo, J. C., Jr. and O. Augusto (2012). "Connecting the chemical and biological properties of nitric oxide." Chem Res Toxicol **25**(5): 975-989.
- Tonzetich, Z. J., H. Wang, D. Mitra, C. E. Tinberg, L. H. Do, F. E. Jenney, Jr., M. W. Adams, S. P. Cramer and S. J. Lippard (2010). "Identification of protein-bound dinitrosyl iron complexes by nuclear resonance vibrational spectroscopy." J Am Chem Soc **132**(20): 6914-6916.
- Tse Sum Bui, B., T. A. Mattioli, D. Florentin, G. Bolbach and A. Marquet (2006). "*Escherichia coli* biotin synthase produces selenobiotin. Further evidence of the involvement of the [2Fe-2S]²⁺ cluster in the sulfur insertion step." Biochemistry **45**(11): 3824-3834.
- Tucker, N. P., M. G. Hicks, T. A. Clarke, J. C. Crack, G. Chandra, N. E. Le Brun, R. Dixon and M. I. Hutchings (2008). "The transcriptional repressor protein NsrR senses nitric oxide directly via a [2Fe-2S] cluster." PLoS One **3**(11): e3623.
- Tucker, N. P., N. E. Le Brun, R. Dixon and M. I. Hutchings (2010). "There's NO stopping NsrR, a global regulator of the bacterial NO stress response." Trends Microbiol **18**(4): 149-156.

- Tyson, K. L., J. A. Cole and S. J. Busby (1994). "Nitrite and nitrate regulation at the promoters of two *Escherichia coli* operons encoding nitrite reductase: identification of common target heptamers for both NarP- and NarL-dependent regulation." *Mol Microbiol* **13**(6): 1045-1055.
- Uden, G. and J. Bongaerts (1997). "Alternative respiratory pathways of *Escherichia coli*: energetics and transcriptional regulation in response to electron acceptors." *Biochim Biophys Acta* **1320**(3): 217-234.
- van den Berg, W. A., W. R. Hagen and W. M. van Dongen (2000). "The hybrid-cluster protein ('prismane protein') from *Escherichia coli*. Characterization of the hybrid-cluster protein, redox properties of the [2Fe-2S] and [4Fe-2S-2O] clusters and identification of an associated NADH oxidoreductase containing FAD and [2Fe-2S]." *Eur J Biochem* **267**(3): 666-676.
- Van Vranken, J. G., M. Y. Jeong, P. Wei, Y. C. Chen, S. P. Gygi, D. R. Winge and J. Rutter (2016). "The mitochondrial acyl carrier protein (ACP) coordinates mitochondrial fatty acid synthesis with iron sulfur cluster biogenesis." *Elife* **5**.
- Varghese, S., Y. Tang and J. A. Imlay (2003). "Contrasting sensitivities of *Escherichia coli* aconitases A and B to oxidation and iron depletion." *J Bacteriol* **185**(1): 221-230.
- Vasil'eva, S. V., M. V. Stupakova, Lobysheva, II, V. D. Mikoyan and A. F. Vanin (2001). "Activation of the *Escherichia coli* SoxRS-regulon by nitric oxide and its physiological donors." *Biochemistry (Mosc)* **66**(9): 984-988.
- Vine, C. E. and J. A. Cole (2011). "Nitrosative stress in *Escherichia coli*: reduction of nitric oxide." *Biochem Soc Trans* **39**(1): 213-215.
- Vine, C. E., S. K. Purewal and J. A. Cole (2011). "NsrR-dependent method for detecting nitric oxide accumulation in the *Escherichia coli* cytoplasm and enzymes involved in NO production." *FEMS Microbiol Lett* **325**(2): 108-114.
- Vinella, D., C. Brochier-Armanet, L. Loiseau, E. Talla and F. Barras (2009). "Iron-sulfur (Fe/S) protein biogenesis: phylogenomic and genetic studies of A-type carriers." *PLoS Genet* **5**(5): e1000497.
- Vinella, D., L. Loiseau, S. Ollagnier de Choudens, M. Fontecave and F. Barras (2013). "In vivo [Fe-S] cluster acquisition by IscR and NsrR, two stress regulators in *Escherichia coli*." *Mol Microbiol* **87**(3): 493-508.
- Volbeda, A., C. Darnault, O. Renoux, Y. Nicolet and J. C. Fontecilla-Camps (2015). "The crystal structure of the global anaerobic transcriptional regulator FNR explains its extremely fine-tuned monomer-dimer equilibrium." *Sci Adv* **1**(11): e1501086.
- Volbeda, A., E. L. Dodd, C. Darnault, J. C. Crack, O. Renoux, M. I. Hutchings, N. E. Le Brun and J. C. Fontecilla-Camps (2017). "Crystal structures of the NO sensor NsrR reveal how its iron-sulfur cluster modulates DNA binding." *Nat Commun* **8**: 15052.
- Wachtershauser, G. (1992). "Groundworks for an evolutionary biochemistry: the iron-sulphur world." *Prog Biophys Mol Biol* **58**(2): 85-201.
- Wahl, A., L. My, R. Dumoulin, J. N. Sturgis and E. Bouveret (2011). "Antagonistic regulation of *dgkA* and *plsB* genes of phospholipid synthesis by multiple stress responses in *Escherichia coli*." *Mol Microbiol* **80**(5): 1260-1275.
- Wang, J., C. E. Vine, B. K. Balasany, J. Rizk, C. L. Bradley, M. Tinajero-Trejo, R. K. Poole, L. L. Bergaust, L. R. Bakken and J. A. Cole (2016). "The roles of the hybrid cluster protein, Hcp and its reductase, Hcr, in high affinity nitric oxide reduction that protects anaerobic cultures of *Escherichia coli* against nitrosative stress." *Mol Microbiol* **100**(5): 877-892.
- Wasserfallen, A., S. Ragetti, Y. Jouanneau and T. Leisinger (1998). "A family of flavoproteins in the domains Archaea and Bacteria." *Eur J Biochem* **254**(2): 325-332.
- Watanabe, S., A. Kita, K. Kobayashi and K. Miki (2008). "Crystal structure of the [2Fe-2S] oxidative-stress sensor SoxR bound to DNA." *Proc Natl Acad Sci U S A* **105**(11): 4121-4126.
- Wiedemann, N., E. Urzica, B. Guiard, H. Muller, C. Lohaus, H. E. Meyer, M. T. Ryan, C. Meisinger, U. Muhlenhoff, R. Lill and N. Pfanner (2006). "Essential role of Isd11 in mitochondrial iron-sulfur cluster synthesis on Isu scaffold proteins." *EMBO J* **25**(1): 184-195.

- Winter, S. E., C. A. Lopez and A. J. Baumler (2013). "The dynamics of gut-associated microbial communities during inflammation." *EMBO Rep* **14**(4): 319-327.
- Woodmansee, A. N. and J. A. Imlay (2003). "A mechanism by which nitric oxide accelerates the rate of oxidative DNA damage in *Escherichia coli*." *Mol Microbiol* **49**(1): 11-22.
- Wu, Y. and F. W. Outten (2009). "IscR controls iron-dependent biofilm formation in *Escherichia coli* by regulating type I fimbria expression." *J Bacteriol* **191**(4): 1248-1257.
- Xie, Q. W., H. J. Cho, J. Calaycay, R. A. Mumford, K. M. Swiderek, T. D. Lee, A. Ding, T. Troso and C. Nathan (1992). "Cloning and characterization of inducible nitric oxide synthase from mouse macrophages." *Science* **256**(5054): 225-228.
- Xie, Q. W., M. Leung, M. Fuortes, S. Sassa and C. Nathan (1996). "Complementation analysis of mutants of nitric oxide synthase reveals that the active site requires two hemes." *Proc Natl Acad Sci U S A* **93**(10): 4891-4896.
- Xue, Q., Y. Yan, R. Zhang and H. Xiong (2018). "Regulation of iNOS on Immune Cells and Its Role in Diseases." *Int J Mol Sci* **19**(12).
- Yao, J. and C. O. Rock (2017). "Exogenous fatty acid metabolism in bacteria." *Biochimie* **141**: 30-39.
- Yeo, W. S., J. H. Lee, K. C. Lee and J. H. Roe (2006). "IscR acts as an activator in response to oxidative stress for the *suf* operon encoding Fe-S assembly proteins." *Mol Microbiol* **61**(1): 206-218.
- Yukl, E. T., M. A. Elbaz, M. M. Nakano and P. Moenne-Loccoz (2008). "Transcription Factor NsrR from *Bacillus subtilis* Senses Nitric Oxide with a 4Fe-4S Cluster (dagger)." *Biochemistry* **47**(49): 13084-13092.
- Yuvaniyama, P., J. N. Agar, V. L. Cash, M. K. Johnson and D. R. Dean (2000). "NifS-directed assembly of a transient [2Fe-2S] cluster within the NifU protein." *Proc Natl Acad Sci U S A* **97**(2): 599-604.
- Zaslaver, A., A. Bren, M. Ronen, S. Itzkovitz, I. Kikoin, S. Shavit, W. Liebermeister, M. G. Surette and U. Alon (2006). "A comprehensive library of fluorescent transcriptional reporters for *Escherichia coli*." *Nat Methods* **3**(8): 623-628.
- Zeghouf, M., J. Li, G. Butland, A. Borkowska, V. Canadien, D. Richards, B. Beattie, A. Emili and J. F. Greenblatt (2004). "Sequential Peptide Affinity (SPA) system for the identification of mammalian and bacterial protein complexes." *J Proteome Res* **3**(3): 463-468.
- Zhang, L., A. K. Joshi and S. Smith (2003). "Cloning, expression, characterization, and interaction of two components of a human mitochondrial fatty acid synthase. Malonyltransferase and acyl carrier protein." *J Biol Chem* **278**(41): 40067-40074.
- Zheng, M., F. Aslund and G. Storz (1998). "Activation of the OxyR transcription factor by reversible disulfide bond formation." *Science* **279**(5357): 1718-1721.

Titre: Étude de la biogénèse des centres fer-Soufre en conditions de stress métaboliques et environnementaux

Résumé : Les centres fer-soufre (Fe-S) sont des cofacteurs métalliques essentiels dans la plupart des systèmes vivants. Chez *Escherichia coli*, les centres Fe-S sont impliqués dans l'activité de plus de 180 protéines tandis que chez l'Homme, des dysfonctionnements dans l'homéostasie des centres Fe-S sont à la base de nombreuses pathologies. Les protéines à centres Fe-S participent à des processus majeurs incluant la respiration, le métabolisme central, la réplication et la réparation de l'ADN. Chez *E. coli*, la biosynthèse des centres Fe-S est catalysée par l'activité de complexes multi-protéiques, ISC en conditions optimales, et SUF en conditions de stress (stress oxydant, faible biodisponibilité en fer). Mon projet de thèse s'est focalisé sur la relation entre le métabolisme des centres Fe-S et celui des acides gras, ainsi que sur la caractérisation d'un régulateur à centre Fe-S.

Un lien inattendu entre la biogénèse des acides gras et celle des centres Fe-S a été rapporté chez les eucaryotes. Le premier objectif de cette thèse a été de tester ce lien et d'étudier les mécanismes chez les procaryotes en étudiant *E. coli* comme modèle. Une approche de double hybride bactérien a montré des interactions spécifiques entre l'ACP (Acyl Carrier Protein) et trois membres de la voie ISC (IscS, Fdx, et HscB). Nous avons utilisé l'outil CRISPRi pour diminuer l'expression du gène essentiel *acpP* codant l'ACP. L'étude de l'effet de la diminution d'ACP dans la cellule sur différents rapporteurs, activité de régulateurs et d'enzymes à centres Fe-S, nous a permis de montrer que l'ACP a un effet positif sur la biogénèse ISC-dépendante des centres Fe-S.

Le second objectif de ma thèse a été la caractérisation d'un régulateur à centre Fe-S dont la fonction est encore inconnue, YeiL. L'expression de ce gène étant indétectable dans les conditions classiques testées, nous avons étudié l'effet de la surexpression de *yeiL* sous sa forme sauvage et sous une forme mutée ne pouvant plus lier le centre Fe-S. Une approche transcriptomique a montré que la production de ces deux formes modifie l'expression de centaines de gènes. L'analyse ontologique a révélé que la respiration anaérobie du nitrate, la réponse au stress nitrique, et l'utilisation de sucres oxydées, les acides aldariques, sont parmi les fonctions régulés par YeiL. De plus, ces trois fonctions ont comme point commun l'oxide nitrique, NO. Le NO est un produit de la respiration du nitrate, il induit une réponse adaptative spécifique, et favorise la formation d'acides aldariques. En étudiant les modalités d'expression de *hcp*, codant une NO réductase, nous avons montré un lien entre YeiL et OxyR, deux régulateurs transcriptionnels en compétition pour le contrôle de l'expression de *hcp*. L'étude de la voie de régulation des gènes du métabolisme des acides aldariques nous a permis de montrer que YeiL interfère avec la voie d'activation dédiée, via le régulateur CdaR. Il apparaît donc que dans les deux voies étudiées, YeiL régule l'expression de gènes par compétition avec d'autres régulateurs précédemment identifiés. Le NO est un effecteur de la réponse immunitaire innée, il a un effet bactéricide mais favorise aussi la formation d'acides aldariques. En utilisant un modèle de colonisation de l'intestin de souris, nous avons pu montrer que le régulateur YeiL a un effet positif sur la colonisation à long terme.

Mots-clés : Clusters Fer-Soufre, Acides gras, Régulation transcriptionnelle, Oxyde nitrique

Title: Study of Iron-sulfur cluster biogenesis in environmental and metabolic stress conditions

Abstract: Iron-sulfur (Fe-S) clusters are essential metallic cofactors present in most living organisms. In *Escherichia coli*, Fe-S clusters are involved in the activity of over 180 proteins, while in humans, dysfunctions in Fe-S cluster homeostasis are the root of many diseases. Fe-S cluster-containing proteins participate in major processes including respiration, central metabolism, DNA replication, and repair. In *E. coli*, Fe-S cluster biosynthesis is catalyzed by two multi-protein complexes, ISC under optimal conditions, and SUF under stress conditions (oxidative stress, low iron bioavailability). My PhD project focused on the relationship between Fe-S cluster metabolism and fatty acid metabolism, as well as the characterization of an Fe-S cluster regulator.

An unexpected link between fatty acid and Fe-S biogenesis has been reported in eukaryotes. The first objective of this thesis was to test this link and study the mechanisms in prokaryotes using *E. coli* as a model. A bacterial two-hybrid approach showed specific interactions between Acyl Carrier Protein (ACP) and three members of the ISC pathway (IscS, Fdx, and HscB). We used the CRISPRi tool to decrease the expression of the essential *acpP* gene encoding ACP. The study of the effect of ACP decrease on various Fe-S cluster reporters, regulators and enzymes activities, allowed us to show that ACP has a positive effect on the ISC-dependent Fe-S biogenesis.

The second objective of my thesis was to characterize an Fe-S cluster regulator whose function is still unknown, YeiL. As the expression of this gene was undetectable under tested conditions, we studied the effect of the overexpression of *yeiL*, both its wild-type form and a mutated form that cannot bind the Fe-S cluster. Transcriptomic analysis showed that the production of these two forms modifies the expression of hundreds of genes. Ontological analysis revealed that anaerobic nitrate respiration, nitric stress response, and the use of oxidized sugars, aldaric acids, are amongst the functions regulated by YeiL. Furthermore, these three functions are all related to nitric oxide, NO, which originates from nitrate respiration, induces a specific adaptive response, and promotes the formation of aldaric acids. By studying the expression of *hcp*, which encodes a NO reductase, we have shown a link between YeiL and OxyR, two transcriptional regulators in competition for the control of *hcp* expression. Our study of the transcriptional regulation of aldaric acids metabolism genes has allowed us to demonstrate that YeiL interferes with the dedicated activation pathway via the regulator CdaR. Thus, it appears that in both pathways studied, YeiL regulates gene expression by competing with other previously identified regulators. NO is an effector of the innate immune response, it displays a bactericidal effect but also promotes aldaric acids formation. Using a mice gut colonization model, we have shown that the YeiL regulator has a positive effect on long-term colonization.

Keywords: Iron-Sulfur clusters, Fatty acids, Transcriptional regulation, Nitric oxide